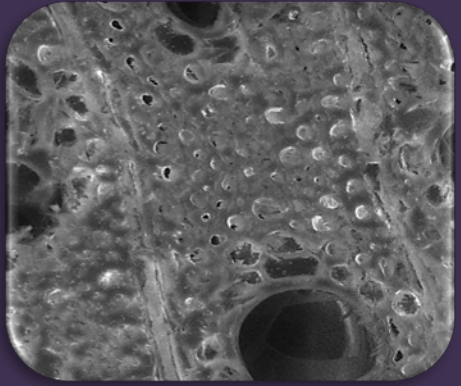
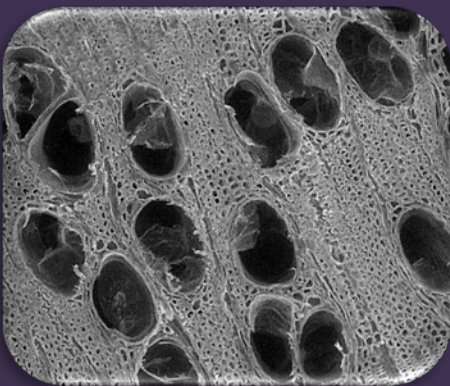
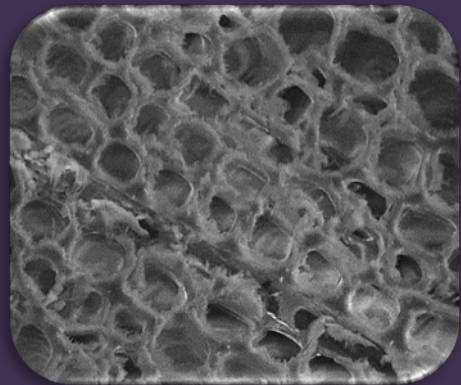
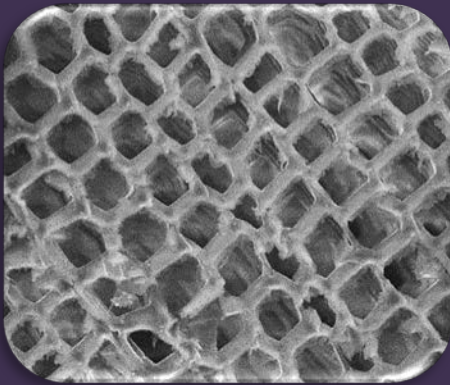


Doctoral dissertation

Industrial wood modification by heat treatments

René Herrera Díaz



eman ta zabal zazu

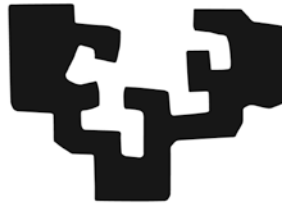


UPV EHU

Donostia-San Sebastián

2017

eman ta zabal zazu



Universidad
del País Vasco

Euskal Herriko
Unibertsitatea

Industrial wood modification by heat treatments

A dissertation presented by

René Herrera Díaz

In Fulfillment of the Requirements for the Degree Doctor of Philosophy in
Renewable Materials Engineering by the University of the Basque Country
UPV/EHU

Under the supervision of

Dr. Jalel Labidi

Dr. Rodrigo Llano-Ponte

Chemical and Environmental Engineering Department

Engineering School of Gipuzkoa

Donostia-San Sebastián

2017

PREFACE

The work reported in this thesis was mainly carried out in the Chemical Engineering Department at the University of the Basque Country (Donostia-San Sebastian, Spain) during 2014-2017. Significant contribution was also accomplished in Poland at the Poznan University of Life Sciences, in Italy at the Trees and Timber Institute CNR-IVALSA, and in Chile at the University of Bio-Bio.

I would like to express my gratitude to the Department of Economic Development and Competitiveness of the Basque Government for providing the financial support, which allowed me to work full time on the thesis for a period of four years. I would also like to thank the COST Action-1006, 1303 and 1407, as well as the Trees4Future program, for supporting my travels to many courses, conferences, and short-term scientific missions, which increased my knowledge in the field of biomaterials engineering and allowed me to contact with the international scientific community. I am grateful to the Spanish Company Torrebaso for providing most of the material used in this study under the name of termogenik treatment, and to the Chilean Company Bioforest S.A. for considering my assistance in the development of a heat-treated wood system.

My supervisors, Dr. Jalel Labidi and Dr. Rodrigo Llano-Ponte who allowed me to continue with the doctoral studies, and to be a part of his prestigious research group. Also for leaving me to work at my own pace and with my own ideas, for being always open to the possibility of performing a research abroad, and always seeking funding for my fellow doctoral students and doctors. Thank you very much! The professor Tomasz Krystofiak who helped me during my travels to his University and with the experiments and results. Ana and Kuba Sandak for introducing new and interesting branches of analysis of materials; professor Rubén A. Ananías for warm reception from him and from all the members of his research

group during my stay; Dra. Agnieszka Jankowska for SEM images of the cover. To each and every one of you, thank you very much for everything!

The working group of Biorefinery process laboratory, the colleagues who have left and the new ones, I am always willing to offer my collaboration as a basis for both academic and personal learning. The colleagues of other international institutions from Brazil, Tunisia, Italy, Lithuania, Poland, Portugal and anywhere in the world that has visited us, is always an opportunity to learn something new. My dearest friends at work, and people who have contributed in some way both personally and academically.

A big thank you to my family and especially to my mother who has been my source of inspiration and courage. To my friends, those who are present, those who left, the people who have accompanied me in this process at the beginning or those who have at the end, after all, the universe is made of stories, not atoms.

René Herrera Díaz.

Donostia-San Sebastian, December 2017

CONTENT

1 Introduction.....	1
1.1 Aim and research questions.....	1
1.2 Research objectives.....	2
1.3 Structure of the thesis.....	2
2 Background.....	4
2.1 Sustainable forestry.....	5
2.2 Wood processing industry.....	7
2.3 Cellular structure of wood.....	14
2.4. Molecular structure of wood.....	16
2.5 Cell wall chemistry.....	18
2.5 Wood-moisture relations.....	27
2.6 Surface properties in wood and adhesion.....	30
2.7 Durability and resistance of wood products.....	33
2.7.1 Wood and biotic factors.....	34
2.7.2 Wood and abiotic factors.....	37
2.7.3 Mechanical properties of wood.....	40
2.8 Chemical modification of solid wood.....	43
2.8.1 Acetylation treatment.....	44
2.8.2 DMDHEU treatment.....	45
2.8.3 Furfurylation treatment.....	46
2.8.4 Thermal treatment.....	48
2.9 Wood as a building material.....	49
3 Case study: Wood modification by heat treatments.....	52
3.1 Motivation.....	53
3.2 Experimental procedure.....	54
3.2.1 Wood material.....	54
3.2.2 Wood modification process.....	54

3.2.3 Characterization methods	55
3.3. Results and discussion	57
3.3.1 Chemical composition and structure of thermally modified wood.....	57
3.3.1.1 Chemical composition of wood	58
3.3.1.2 Soluble carbohydrates content	60
3.3.1.3 Wood chemical composition by Py-GC-MS	62
3.3.1.4 Wood chemical structure by FT-IR spectroscopy.....	67
3.1.3.5 Study on the thermal stability of modified wood	71
3.1.3.6 Acidity and pH of wood	74
3.1.3.7 Conclusions.....	75
3.3.2 Physical and mechanical properties of thermally modified wood	77
3.3.2.1 Changes in some physical properties of thermally modified wood.....	78
3.3.2.2 Surface wettability and liquid-solid interactions	80
3.3.2.3 Mechanical properties of thermally modified wood.....	81
3.3.2.4 Thermal resistance of thermally modified wood	85
3.2.2.5 Conclusions.....	87
3.3.3 Biological durability of thermally modified wood.....	88
3.3.3.1 Analysis of biological durability of basidiomycetes tests....	88
3.3.3.2 Chemical analysis of wood samples after durability tests...90	
3.3.3.3 Changes in soluble wood hydrolizates after durability tests	92
3.3.3.4 Hydrolytic enzymes activity during fungal degradation.....	96
3.3.3.5 Monitoring changes in chemical structure due to biodegradation	98
3.3.3.6 Conclusions.....	101
3.3.4. Weathering performance of thermally modified wood	102
3.3.4.1. Physical parameters after weathering tests.....	102

3.3.4.2. Evolution of mechanical properties after weathering test	104
3.3.4.3 Thermal performance of wood after weathering tests.....	108
3.3.4.4 Color changes of wood after weathering tests.....	109
3.3.4.5 Conclusions.....	112
3.3.5 Interactions of thermally modified wood with coating products	113
3.3.5.1 Preliminary identity test by NIR spectrometry.....	114
3.3.5.2 Wood finishes on thermally modified wood.....	115
3.3.5.3 Evaluation of coating-surface adhesion.....	116
3.3.5.4 Evaluation of properties in coated surfaces	118
3.3.5.5 Weathering resistance of coated heat-treated wood.....	122
3.3.5.5.1 Wood surface topography.....	122
3.3.5.5.2 Measurement of changes in the appearance of surface by hyperspectral images.....	125
3.3.5.5.3 Wettability, surface energy and work of adhesion after weathering	129
3.3.5.6. Conclusions.....	133
3.3.6. Environmental profile.....	134
3.3.6.1 The LCA study of thermally modified Pinus radiata boards	134
3.3.6.1.1 Life cycle impact assessment (LCIA)	138
3.3.6.1.2 Quantitative results.....	139
3.3.6.1.3. Sensitivity analysis.....	141
3.3.6.2 Characterization of residues generated during the industrial hydrothermal process	141
3.3.6.2.1 Thermogravimetric decomposition of extracts	142
3.3.6.2.2 Chemical structure of extracts by FTIR.....	144
3.3.6.2.3 Chemical composition of the residues generated	146
3.3.6.2.4 Potential use of residues generated during the industrial hydrothermal process.....	151

3.3.6.3 Conclusions.....	152
4 General conclusions, future research and published works	154
4.1 General conclusions.....	155
4.2 Future research	157
4.3 Published Works.....	158
4.3.1 Publications in scientific journals.....	158
4.3.2 Contributions in scientific conferences.....	160
4.3.3 Assistance to training related to the thesis.....	165
5 References.....	166
APPENDIX I: <u>Procedures</u>	185
APPENDIX II: <u>Techniques</u>	200
List of figures.....	210
List of tables.....	213

1

Introduction

1.1 Aim and research questions

The overall aim of the work carried out for this dissertation was to improve the properties of solid wood by heat treatments. The focus was to discover the specific changes that occurs in wood at chemical and physical level, as well as link these changes to the properties obtained and wood interactions. With this aim, the dissertation focused on the following six research questions:

- 1- How do different process temperatures (from 170°C to 210°C) affect the wood composition (structural, chemical and physical) and properties of thermally modified wood?
- 2- Which are the factors inherent to wood (density, moisture content, hygroscopicity, surface free energy) that influence the mechanical strength and dimensional stability of modified wood?
- 3- What are the reasons for the improved biological durability of modified wood and what is its evolution during its service life?
- 4- How is the response of the modified wood surface when coating products are applied to it?
- 5- Is it feasible to measure the environmental impacts of the modification treatment on an industrial scale and is it feasible to recover the residues generated?
- 6- How can the academy research help in the industrial development of products?

1.2 Research objectives

In order to achieve this aim, the following objectives were developed to address this research:

- 1- To determine the chemical changes that occurs in wood during the thermal modification and the main effects on the wood structure
- 2- To quantify the physical properties, mechanical strength and thermal resistance of the modified wood, as well as wood-water interactions.
- 3- To evaluate the biological durability of the thermally modified wood and to identify the action mechanisms in the wood of rot-fungi.
- 4- To determine the effects of biotic and abiotic factors on modified wood during its service life.
- 5- To examine the initial response of modified wood surfaces to finishing products and the response after weathering conditions.
- 6- To quantify the environmental impacts of the industrial process and to find added value to the residues generated.

1.3 Structure of the thesis

The dissertation begins by introducing the theoretical background of the wood processing industry, going through the wood structure and properties, to the modification methods to use as building material. Afterwards, the specific case of study of the thermal modification of wood in all aspects included in the objectives was summarized, analyzed and discussed. The experimental techniques and methods used are briefly summarized in this section and explained thoroughly in the appendix. The conclusions are drawn from the results and the suggestions for future research are included after the case of study. The publications that form the basis for this work are appended in the end.

2

Background

2.1 Sustainable forestry

Forests offer a wide range of products with value-added (wood and non-wood) in addition to intangible benefits (cultural and ecological considerations) that require sustainable forest management practices. Their sustainability demands the attention to forest degradation and deforestation by practicing a land management ethic which integrates reforestation, the managing, growing and harvesting of trees for useful products with the conservation of soil, carbon sequestration, water quality, biodiversity, recreation, and aesthetics^{1,2,3}. To summarize, it is necessary to meet the needs of the present without compromising the ability of future generations.

Wood is the main forest product used around the world, and it is calculated that the amount of wood on earth is about one trillion tons, with a growing rate of about 3% per year⁴. According to latest data from the FAO (Food and Agriculture Organization of the United Nations), 28.3% of the global sawn wood output, 24.1% of the artificial board output, 30.4% of wood pulp and 26.5% of the global wood and paper production were exported from wood producing countries. These recent data suggest a decline of global forest cover due to the increased volume of the global trade of wood products during the last decades⁵.

The fluctuations of global wood production and trade is linked with the reduction of deforestation in one country or region, which increases the pressure on forests in other locations. Generally, in case of shortages, the supply is carried out from tropical and subtropical countries, in which forests are still not managed sustainably, and any attempt to conserve native forests will be unsuccessful if consuming countries demand raw material^{6,7}.

Forests form part of the supply chain for the softwood and hardwood timbers used in the industry, in which the roundwood represent the first link or the raw material used for any purpose other than energy⁸. Figure I-1 shows the updated global production of industrial roundwood divided in coniferous and non-coniferous

species. The review of the global trade data for 2015 indicate that the Asia-Pacific is a net importer region of industrial roundwood (31 million m³ in 2015), and all other world regions are net exporters.

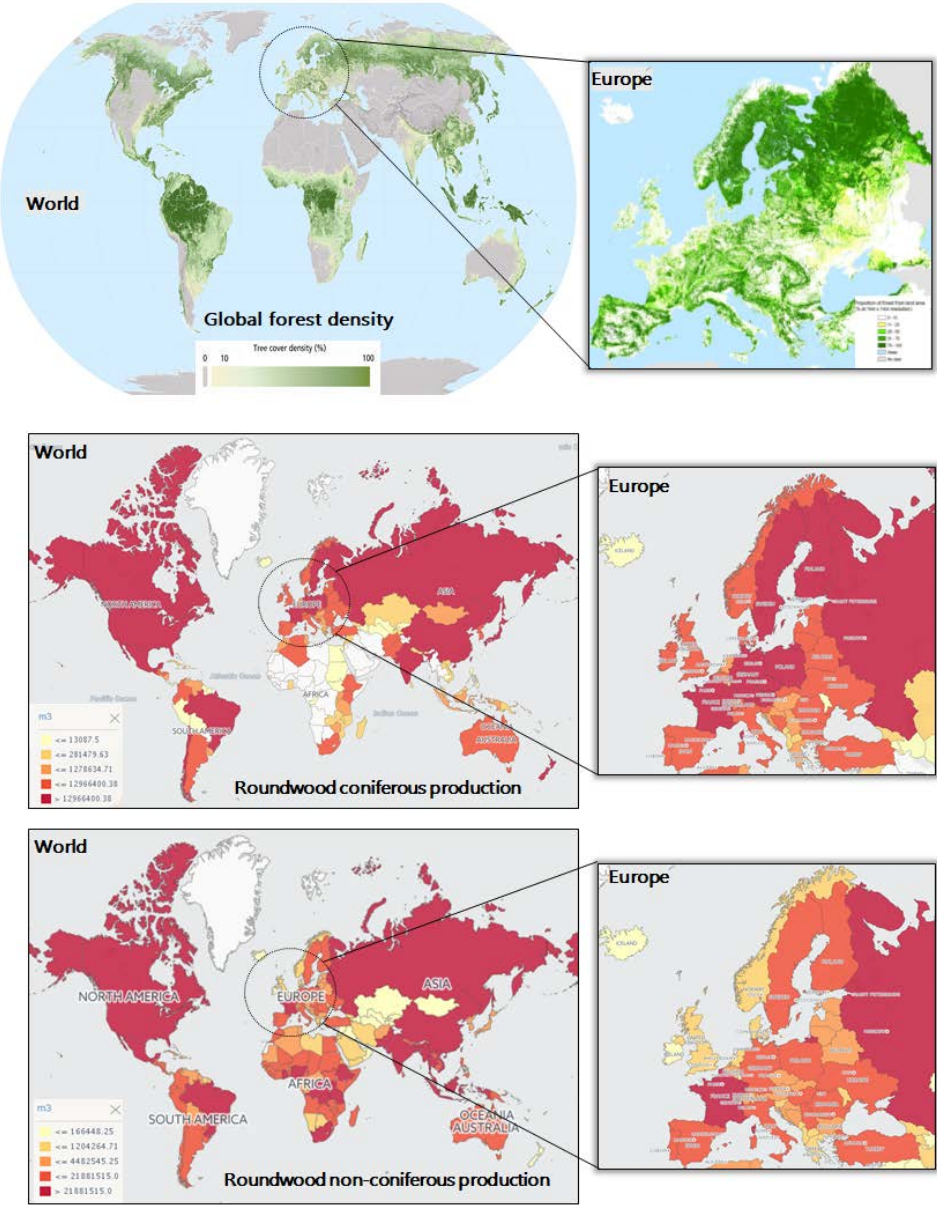


Figure I-1 Above: Global forest density; Center and below: production of industrial roundwood^{5, 9}.

The main net exporters of industrial roundwood in 2015 were Europe and Northern America (13 million m³ and 12 million m³, respectively). However, compared with the last decade, both exporting regions reported a considerable decline in net exports in 2015 of approximately 14% and 24%. The remaining world areas supply the industrial roundwood to the Asia-Pacific region⁵. These trends openly affect in many developing countries that have been replacing domestic wood production with imports of fast-growing species, and without a proper forest management, which further results in a negative effect on deforestation and forest degradation and the impact of the two on changing forest cover.

2.2 Wood processing industry

The development of forests management with the objective of wood production is terminated by harvesting operations, which from a technical point of view, are a sequence of cutting, processing and transporting of timber. Moreover, felled trees with branches removed and trunks cut to length for transportation are commonly referred to as roundwood, which is transported from the forest to the sawmill for further processing in order to remove bark and surface defects¹⁰.

The wood industrial sector practically uses the raw material in its integrality. Thus, during the processing of roundwood, approximately 50% is recovered as viable board and plank products, with the remaining wood waste, cutter shavings and fiber byproducts are typically used as biomass fuel or are mechanically milled to produce fibers or chips or chemically treated to prepare cellulose¹¹. The ensuing materials are used as the basis of boards and panels. Thus, this route prepares particleboard, oriented strandboard (OSB), hardboard and medium density fiberboard (MDF)⁴.

Nowadays, there is a growing attention in the European discussions on the use of wood in the future bioeconomy¹². Wood products are usually considered to have lower environmental impacts than equivalent products from nonrenewable raw materials. Woody biomass is when sustainably grown, a fully renewable resource

and a largely recyclable and reusable material, however, as a finite resource, its use and service life should be optimized. One way to achieve this target is through the multiple use of wood resources from trees by using residues, recycled (utilization in production) resources or recovered (collected after consumption) resources at least once or several times as a product before its end-of-life (energy use or landfill)^{13,14}, this concept is known as cascading use of wood products. Figure I-2 shows in the wood processing industry, the possible paths of the industrial by-products, residues as well as post-society used wood.

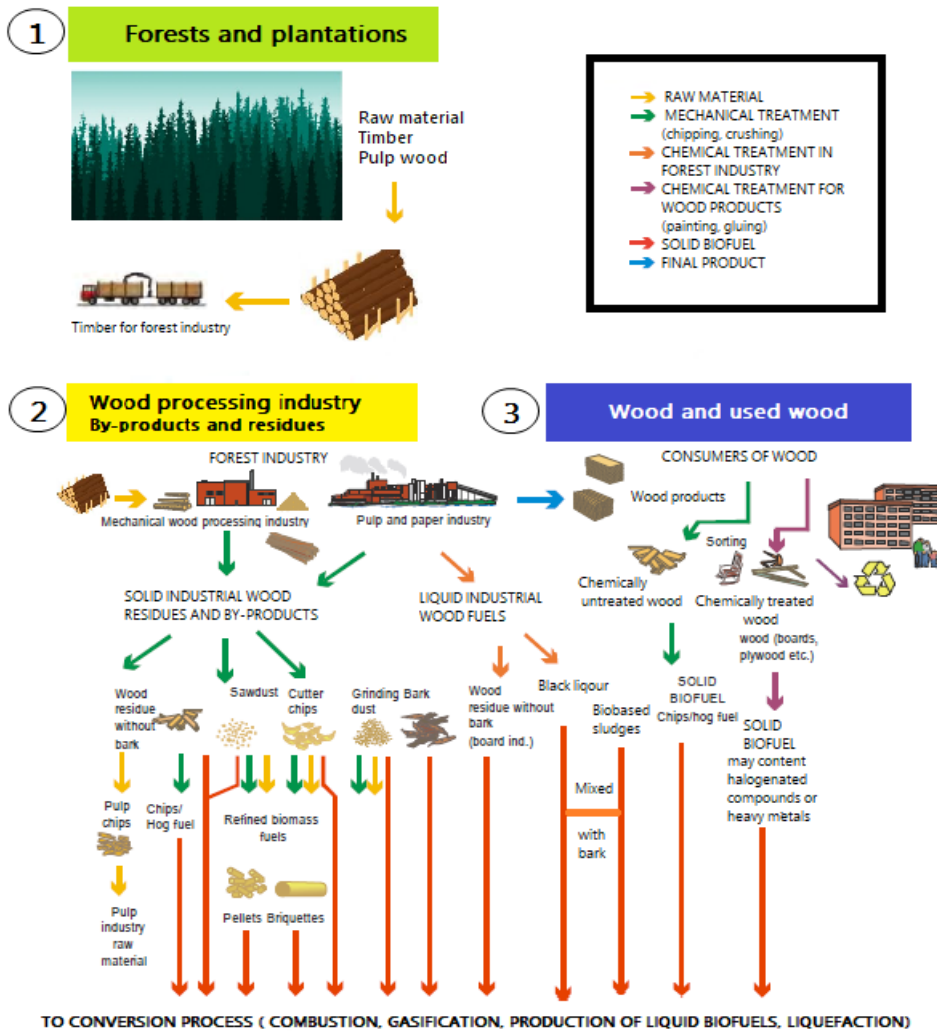


Figure I-2 Wood processing steps and possible paths of use of industrial byproducts, residues and used wood. Graphic adapted from Alakangas, 2015¹⁵.

Furthermore, the EU Forest Strategy (COM (2013)659) states that cascade use fulfils the criteria of resource-efficiency. Classes A, B, C and D for used wood, industrial wood residues and by-products were proposed in the guidelines. Wood categories A and B are specified according to EN ISO 17225-1–Solid biofuel standard and class C under EN 15359–Solid recovered fuels standard. Class D wood is treated with wood preservatives and is hazardous waste. Targets for reducing greenhouse gas emissions and a more resource-efficient society are expected to further increase the demand for wood as raw material in Europe during the next decades¹⁶.

Besides dimensional sawn timber, wood is also processed as engineered timber, which is structurally optimized in order to create wood composites manufactured from laminated timbers, adhesives and other materials used in the building industry. The benefits of these materials include increased dimensional stability, more homogenous mechanical properties and greater durability. After processing logs into sawnwood, the material is dried, planed and graded, to obtain timber of different quality as well as to manufacture different engineering wood composites. The most outstanding wood-based materials are schematized in Figure I-2 and briefly explained below:

- *Glue-laminated timber*. Also known as 'Glulam', is defined as a structural timber member composed by at least two essentially parallel laminations which may comprise of one or two boards side by side having finished thicknesses from 6 mm up to 45 mm [EN 14080:2013]. Glulam is typically used to fabricate curved and long beams.
- *Cross-Laminated Timber* (CLT): Timber panels that are made of a minimum of three layers of sawn softwood stacked on top of one another at right angles and glued to form a thickness in the range of 50– 500 mm suitable for floor, wall and roof elements of up to 13.5 m in length.¹⁷
- *Brettstapel*. Also known as 'dowellam', these solid wood panels are manufactured from softwood boards connected by hardwood dowels.

Hardwood dowels are driven into the panels at 8% MC. With the softwood boards at 12–15% MC the hardwood dowel swells to find equilibrium, fixing the panels tight without the need for glue¹⁸.

- *Stress-laminated-timber* (SLT): Timber laminations (boards of structural timber or glulam beams) are stacked side by side across the width of the deck. By applying pre-stressing rods through predrilled holes at regular intervals and applying the prestressing force, the assembled laminations will behave structurally like an orthotropic plate¹⁹.
- *Nail Laminated Timber* (NLT): Is created from dimensional lumber stacked on edge - 2x3, 2x4, 2x6, 2x8, 2x10, or 2x12 solid laminated and fastened together with nails. Plywood or OSB sheathing is often added to one side to provide a structural diaphragm²⁰.
- *Plywood*: A flat pressed multilayer wood panel composed of oriented wood veneers bonded by hot-pressing by using thermosetting adhesive resins. The veneers wood grain is oriented at 90 ° to each other in adjacent layers, yielding a particularly strong panel²¹.
- *Parallel strand lumber* (PSL): Also known as Parallam[®], is a beam made by a continuous manufacturing process composed of bigger size lumber needles reassembled with a structural exterior grade adhesive: when heat curing is isocyanates (pMDI) and PRFs when cold-curing²².
- *Laminated Veneer Lumber* (LVL): A flat pressed multilayer wood panel similar to plywood composed of oriented wood veneers, but differently from plywood, oriented all in the same direction in all the layers and bonded by hot-pressing by using thermosetting adhesive resins²³.
- *Oriented Strand Board* (OSB): A flat pressed three-layer wood composite panel composed of oriented wood wafers bonded by hot-pressing by using thermosetting adhesive resins. The very thin wafers are oriented in the same direction within the same layer and at 90° of each other in

adjacent layers, yielding a particularly strong panel very suitable for structural applications. It is the modern competitor of plywood²⁴.

- *I-Joists* (LSL): While these are more expensive and deeper than solid timber joists for an equivalent strength and stiffness, composite I-Joists are more dimensionally stable due to their homogeneous OSB web and the relatively small dimension of the solid timber or LVL²⁵.
- *Structural Insulating Panels* (SIPs): Structural prefabricated sandwich panels consisting of an insulation layer encased between two skins of fiber or oriented strand board¹⁰.
- *Medium Density Fiberboard* (MDF): A flat pressed wood composite panel composed of randomly oriented wood fibers obtained by thermomechanical wood pulping and bonded by hot-pressing by using thermosetting adhesive resins²⁴.

Although engineering wood products have superior structural properties as compared to dimensional timber, the use of adhesives has a negative impact on the primary energy consumed, associated with these binding products of non-renewable sources. Moreover, wood biomass is currently used in many different value chains, from wood-based products and materials to bio-chemicals and bioenergy, and in many different industrial sectors. According to the FAO statistics of global production and trade of forest products in 2015, the worldwide production in the UNECE region was relatively stable in 2015. With the exception of the paper and paperboard industry, consumption of all products increased by between 1.3% and 2.6% (See Table I-1)⁵.

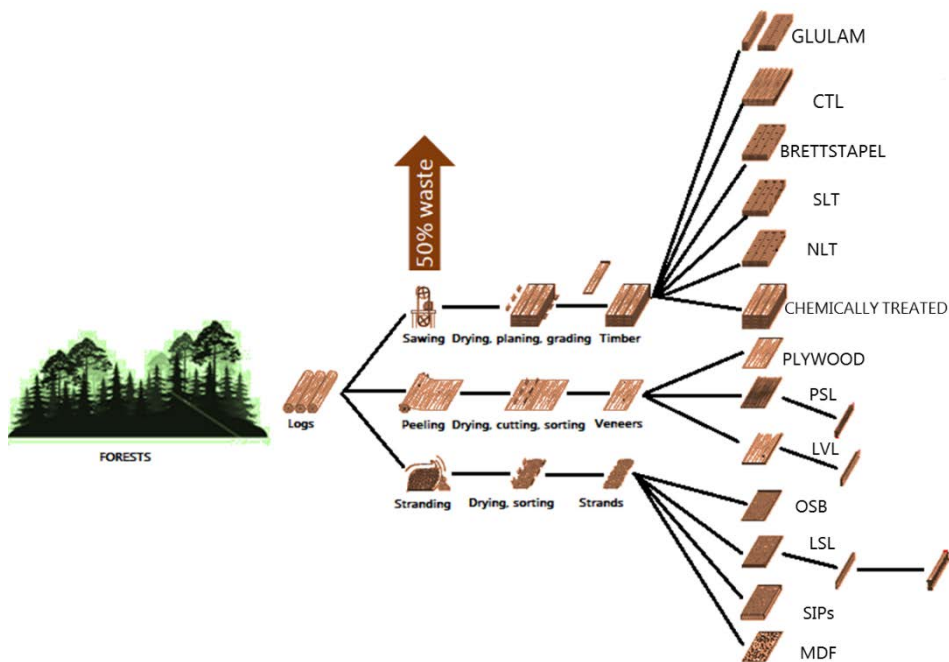










Figure I-3 Processing sequence of engineering wood products. Adapted from Ramage¹⁰.

The statistics show big differences between the diverse sub-regions; however, the total consumption of roundwood (including logs for industrial uses and fuel) in the UNECE region was increased 1.2% from 2014 and is the third consecutive year of growth. Total log usage reached its highest level in almost ten years in the UNECE region due to increased demand in the Asia-Pacific region. The concept of wood fuel is related to the roundwood that is used as fuel for cooking, heating or power production and it includes wood used to make charcoal. It contains wood harvested from main stems, branches and other parts of trees and wood chips to be used for fuel that is made directly from roundwood. The role of wood fuel in the energy system of the EU is of great importance²⁶. The recent dataset shows that the European wood fuel production has increased by 20%, although the global increase was only 2%. This is due to policies promoting bioenergy as well as the increase of the wood pellet production. In addition, by-products from wood processing are regularly used as bioenergy source, which represent up to 50% of the raw material.

Table I-1 Global production and trade of forest products in 2015⁵.

Product	Subproducts	Unit	Production				Exports			
			Change compared to:				Change compared to:			
			2015	2014	2000	1990	2015	2014	2000	1990
 Round wood	Total		3714	1	7	19	132	-7	12	40
	Wood fuel	1·10 ⁶ m ³	1866	0	5	11	9	0	158	-
	Industrial roundwood		1848	2	10	28	122	-8	7	31
 Wood pellets	Total	1·10 ⁶ t	28	8	-	-	16	7	-	-
 sawnwood	Total	1·10 ⁶ m ³	452	3	20	7	134	1	20	92
 Wood-based panels	Total		399	3	114	294	86	2	51	425
	Veneer and plywood	1·10 ⁶ m ³	171	6	157	290	33	2	50	425
	Particle/Fibre boards		228	1	91	297	53	1	51	538
 Woodpulp	Total	1·10 ⁶ t	176	0	3	40	59	2	54	179
 Other fiber pulp	Total		12	-6	-19	70	1	-2	55	142
 Recovery paper	Total	1·10 ⁶ t	225	1	57	345	57	3	130	930
 Paper & paperboard	Total		406	1	25	140	11	-1	13	217
Forest products value	Total	US\$ Billions	-	-	-	-	226	-11	56	298

2.3 Cellular structure of wood

The most peculiar characteristic of tree plants is the primary and secondary upward growth, the latter is not feasible in other types of vascular plants. This secondary growth is determined by the proliferative activity of vascular cambium, a group of dividing cells located between, and giving rise to xylem (water-conducting tissue located inside the cambium layer to the center of the tree) and to phloem (tissue responsible of the transfer of nutrients and located outside of the cambium). The secondary growth mechanisms cause that the oldest part of the tree is in the center of the trunk. The young xylem is the water-conducting tissue called sapwood, and if it dies and wood cells become empty it forms heartwood. Resinous materials and polyphenols successively protect these dead cells from fungal attack^{27,28}.

Wood properties are derived from the cell wall structures and wood polymer composition. Figure I-4 shows the representative anatomic sections of wood, which are not uniformly distributed between annual rings and the layers of heartwood and sapwood vary according to the environmental conditions of forests. Rapid growth during the spring produces less dense wood composed of large cells with thinner walls allowing the efficient water transport to support intense photosynthesis; this is known as earlywood. The following period of growth is slower and characterized by more densely packed and smaller cells, this is known as latewood^{10,29}.

Each annual ring consists of both early and latewood, and in softwoods, the transition can be gradual or diverse, but in hardwoods, vessels may have a different size in early and latewood, or more uniform. In the case of tropical trees, due to their constant growth may not produce annual growth rings or more than one growth ring per year. Despite the similar mode of growth, there are significant cellular differences between angiosperms (softwoods) and gymnosperms (hardwoods), which can be observed in the figure I-5. But in general, hardwoods are more complex than softwoods³⁰.

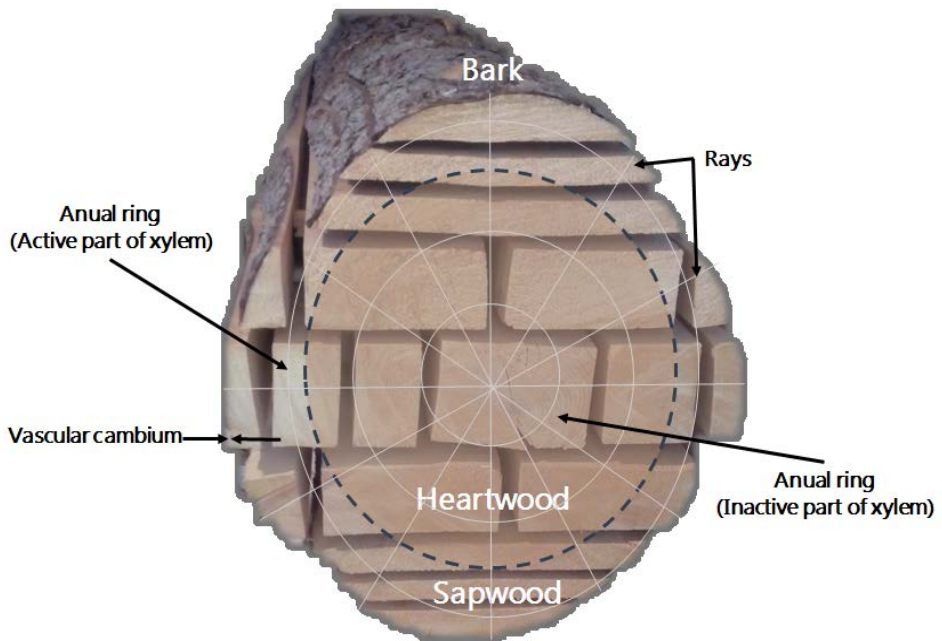


Figure I-4 Tree trunk cross-section anatomy with the characteristic parts.

On the one hand, in softwoods, tracheids are the predominant wood cell, which is longitudinally positioned within the trunk and are the major part of the woody mass. They are joined top-to-bottom via pits and their functions are both to conduct water and to provide structural support to the tree. The tracheids of softwoods are mostly or exclusively vertical. In some species a few tracheids may be placed horizontally in association with rays. Axial tracheids comprise 90 % or more of the volume of softwoods. The morphology of tracheids is different in the earlywood and latewood, and they are about 10 % longer in latewood than earlywood. The parenchymal cells are also presented, and are part of the rays, positioned radially within the trunk and could transport substances as resins; they make up approximately 6–10% wood volume. In general, parenchyma cells are smaller than other cells and has storage function in wood^{31, 32}.

On the other hand, in hardwoods, fibers are the predominant wood cell, which provide structural support and constituting 50% of the volume. Fibers are classified into fiber tracheids and libriform fibers. Fiber tracheids have border pits, while libriform fibers have simple pits. The other primary cell of the wood is the

water-conducting vessels, which represent 30% of wood, and are open-ended and stacked vertically to be later fused into long structures. Their joining points are called perforation plates, which allow high water conductance. The parenchymal cells are also presented in rays and with similar function as in softwoods^{10, 32}.

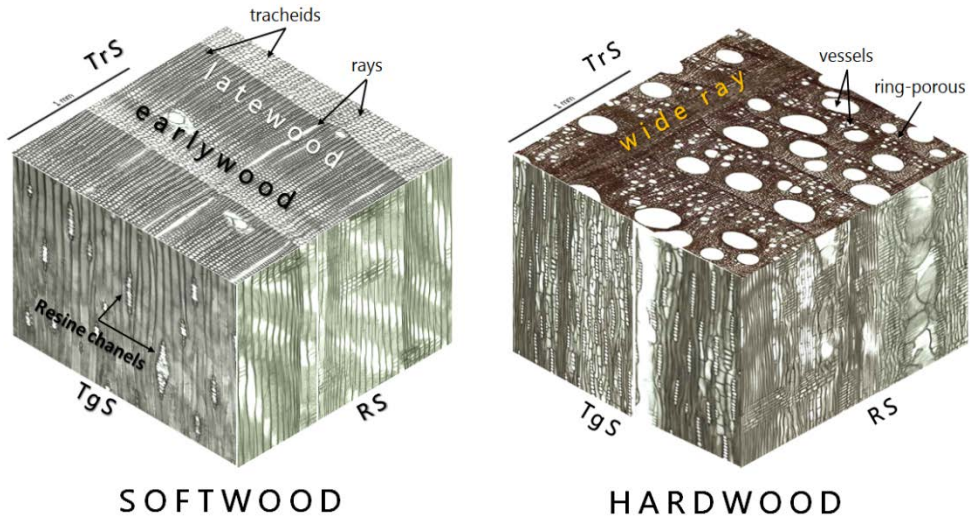
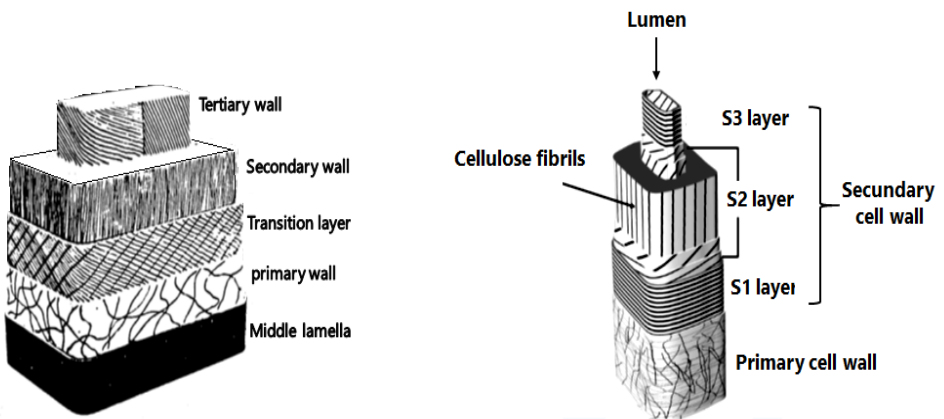


Figure I-5 Three-dimensional design of the wood microscopic structure (*Pinus sylvestris*, left; *Quercus robur*, right). Individual images of the Transverse Section (TrS), Radial Section (RS) and Tangential Section (TgS)³³.

2.4. Molecular structure of wood

The properties of wood originate from its cellular structure and wood polymer compositions. Therefore, the knowledge of the chemistry of basic polymers of wood is crucial for understanding the processes involved in their transformation. The cell wall structural features had been well studied, however some of the concepts have evolved. The first cell wall models were designed in the 50s based on light microscopy and on new findings by electron microscopy and the use of X-ray diffraction studies³⁴. Figure I-6 shows the cell wall sections and the modifications over time.

The cell wall is a multilayer composite in which the individual cell wall layers are distinguished one from another by the orientation of the crystalline cellulose microfibrils within each layer. The multilayer structure is the major determinant of strength and mechanical properties. In addition to the cell lumen, the xylem tracheids in softwoods or the fibers in hardwood cell wall present four different layers: primary and secondary, which in turn is subdivided into S1, S2 and S3. Next to two adjacent cells lies a region called the middle lamella, it is a lignin-pectin complex responsible for cementing the cell walls of two cells connected. The primary cell wall is a thin layer in which the microfibrils are randomly deposited. Both the middle lamella and primary walls are referred as the primary layer. The secondary layer in the cell wall within its subdivisions presents microfibrils closely packed and parallel to each other³⁵.



Old cell wall Model

Accepted cell wall Model

Figure I-6 Schematic diagram of cell wall structural models and its subdivisions^{36,35}.

The microfibril angle is the orientation between the cellulose microfibrils and the longitudinal cell axis. Such angle is a key factor in the mechanical behavior, and its variations in the particular layers provoke changes in stiffness of the overall cell, as follows: in S1 from 50° to 70°, in S2 from 5° to 15° and in S3 from 60° to 90°. The S2 is the thickest layer of the secondary cell wall covering 90% and is responsible for the high tensile strength and stiffness (due to the low microfibril angle) and low shrinkage of wood in the longitudinal direction. The layer S1 and

S3 are thinner and their microfibrils angle and thickness are responsible for the mechanical properties in the transverse direction³⁷.

2.5 Cell wall chemistry

In chemical terms, wood is best defined as a three-dimensional biopolymer composed of an interconnected network of cellulose, hemicelluloses, and lignin with minor amounts of extractives and inorganics (Figure I-7). The elemental composition of dry wood consist of 50% carbon, 6% hydrogen, 44% oxygen, and trace of inorganics compounds³⁸. There exists a huge variation between species, but in general, the proportions of the woody cell walls components are in softwoods 40–45% of cellulose content, 28–32% of lignin, 5-10% of xylans and 10-15% of mannan. In contrast, hardwoods species present 38–50% of cellulose, 20–22% of lignin, 10-35% of xylans and 3-5% of mannan³⁹.

Cellulose, as well as different types of hemicelluloses, belongs to the large group of biomolecules, the carbohydrates, which play central roles in all forms of life. The term 'sugar' is frequently applied to monosaccharides, disaccharides, and sometimes to short oligosaccharides. The classification depends on the carbon chains found in the structure, thus, a carbohydrate with a single carbon chain of three to six carbons atoms is a monosaccharide. Monosaccharides can couple to each other covalently by the hydroxyl groups, and if two are connected it is called disaccharide. Thereby, if three or more are connected are created trisaccharides, tetrasaccharides, etc. The oligosaccharide may contain from 3 up to approximately 10 monosaccharide units, and if it contains more monosaccharide units it is a polysaccharide^{38,40}.

The monosaccharides are defined according to the number of carbons, if they are aldoses or ketoses and to the orientation of the hydroxyl groups (Table I-2). Thereby, D-Mannose differs from glucose only in the orientation of hydroxyl on the C2; D Galactose differs from glucose in the orientation of the C4 hydroxyl; D-xylose is identical to glucose except that it does not have C6 hydroxyl; L-arabinose differs from xylose only in the orientation of the C3 hydroxyl⁴¹. Within the

monosaccharides D-Glucose is the most abundant, playing a crucial role in the plant cell wall constitution. Different types of modifications of the monosaccharides structure are very common; it is the case of the oxidized sugars, acetic acid and galacturonic acid. As for the disaccharides, they are presented as intermediates in enzymatic degradation of polysaccharides and are two monosaccharides linked by a glycosidic bond. The disaccharides are divided into reducing- and non-reducing sugars, where the latter lack a free anomeric carbon of aldose type (Table I-2)⁴⁰.

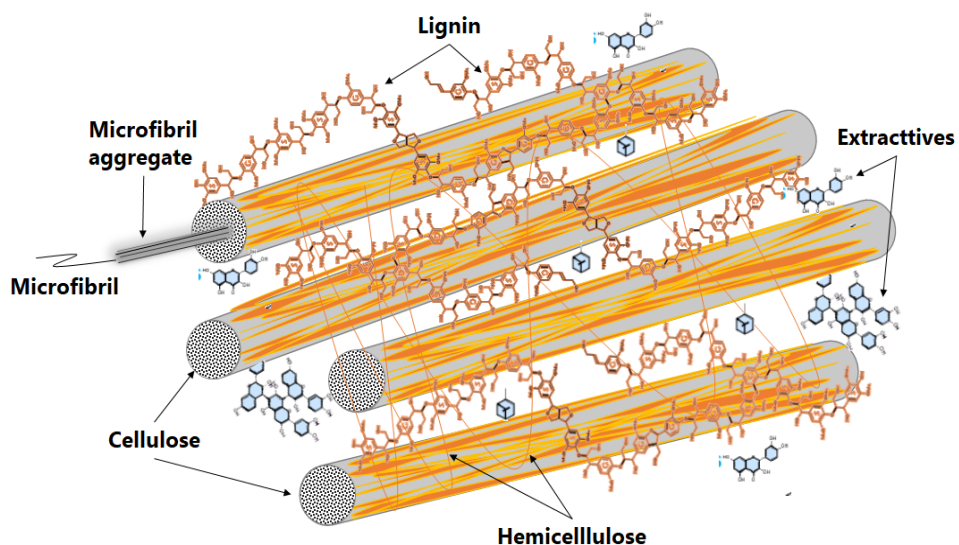


Figure I-7 Components and interactions of the wood polymer in its secondary cell wall.

The main polysaccharides have structural similarities, due to the fact that cellulose and most hemicelluloses are linked by β-1,4-glycosidic bonds. However, there are differences, as hemicelluloses are branched polysaccharides while cellulose is unbranched. Table I-3 shows the major polysaccharides present on the wood cell wall. The primary structure of cellulose is composed of very long linear chains of D- Glucose linked by β-1,4-glycosidic bonds, and the repeated unit in cellulose becomes a cellobiose unit rather than a glucose.

Table I-2 Common monosaccharides and disaccharides present in wood cell wall.

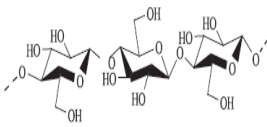
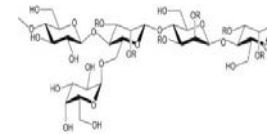
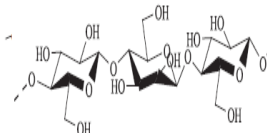
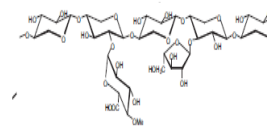
Monosaccharides			
Name	Composition	Structure	Ocurrence in wood
D-Glucose	Glc		Cellulose, glucomannan, xyloglucan
D-Manose	Man		Glucomannan
D-Xylose	Xyl		Xylan, xyloglucan
D-Galactosa	Gal		Glucomannan, pectin
L-Arabinose	Ara		Xylan, pectin
D-Galacturonic acid	GalUA		Pectin
Disaccharides			
Name	Composition	Structure	Ocurrence in wood
L-Rhamnose	Rha		Pectin, traces in xylan
Cellobiose	4-O(β-D-Glucopyranosyl)-D-Glucopyranose		Main product of enzymatic degradation of cellulose
Mannobiose	4-O(β-D-Mannopyranosyl)-D-Mannopyranose		Product of enzymatic degradation of hemicellulose
Xylobiose	4-O(β-D-Xylopyranosyl)-D-xylopyranose		Product of enzymatic degradation of hemicellulose

The degree of polymerization is often very high; values of 15 000 in one chain are reported making cellulose to one of the longest polysaccharides⁴⁰. The cellulose function in wood is always mechanical, working as reinforcing fiber, and these properties depending on its secondary structure. The glucan chains in cellulose are held together by hydrogen bonds to form cellulose microfibrils of a diameter of 3–5 nm ordered as 3-dimensional crystals. The first dimension is given by the covalent bonds along the cellulose chains, giving the final length of the fibril. The second dimension constitutes the hydrogen bonds, holding the cellulose chains together in sheets. The third dimension is given by the Van der Waals bonds and interaction bridging the cellulose sheets in fibrils form. The cellulose contains both highly ordered (crystalline) and less ordered (semi-crystalline or amorphous) structures. The location of the semi-crystalline or amorphous cellulose has been suggested that is either on the fibril surface, or in amorphous segments of fibrils cellulose^{41,42}.

Hemicelluloses are found in the matrix between cellulose fibrils in the cell wall. The components in lignocellulose are tightly associated and in several processes, it has been proved difficult to separate them from lignin and cellulose without modifying them. Hemicelluloses are one of the main constituents of wood, usually between 20 and 35 % of the dry mass, and have a degree of polymerization up to 200. Hemicelluloses from softwoods and hardwoods are not the same (Table I-3). In hardwoods, the predominant hemicellulose is a partially acetylated glucuronoxylan with a small proportion of glucomannan. In softwoods predominate acetylated galactoglucomannans and a small amount of arabinoglucuronoxylan³⁹. Acetyl groups are commonly a part of all hemicelluloses. The xylose based hemicelluloses in both softwoods and hardwoods are often simply called xylan³⁸. The reducing end group in xylan presents an irregular shape due to the insertion of specific sugar units, in hardwood xylans contain acetyl groups but softwood xylans contain L-arabinose side groups. The most abundant hemicellulose xylan in hardwoods is O-acetyl-4-O-methylglucuronoxylan or

glucuronoxylan. The glucuronoxylan is partially acetylated in its native state, and has an average molar masses of 5,600–40,000 and an average degree of polymerization of 100–220 in hardwood xylans^{39,43}.

Table I-3 Common polysaccharides present in the chemical structure of wood.

Polysaccharides			
Name	Composition	Structure	Ocurrence in wood
Cellulose	4-β-D-Glcp(1→4)-β-D-Glcp		Construction material of cell wall
Galactoglucomannan	β-D-Manp; β-D-Glcp; α-D-Galp; O-Acetyl		Softwood hemicellulose (5-8%)
Glucomannan	β-D-Manp; β-D-Glcp; α-D-Galp; O-Acetyl		Softwood hemicellulose (10-15%)
Arabinoglucuronoxylan	β-D-Xylp; 4OMe-α-D-GlcpA-α-L-Araf		Softwood hemicellulose (7-10%)

Regarding softwoods, arabinoglucuronoxylan is the most abundant xylan and contrary to hardwoods, no acetyl groups are found. The average molar masses of softwood xylans are slightly higher than hardwood xylans in the deacetylated form, and the average number of xylose units per xylan molecule is 90–120.

Mannans are also common in wood as galactoglucomannans and glucomannans but often the two forms are simply called glucomannan. In general three kinds of galactoglucomannans could be isolated from softwoods and hardwoods, and the lower degree of substitution with galactose units makes glucomannans less water soluble than galactoglucomannan⁴³. The native galactoglucomannans from

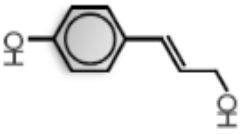
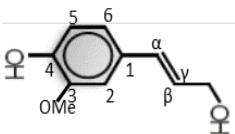
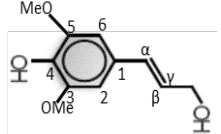
softwoods have O-acetyl groups primarily in the lignified secondary cell wall of softwoods. Molar mass parameters for galactoglucomannans indicate that the number of mannose and glucose units per galactoglucomannan molecule is 90-102⁴⁰. The galactoglucomannans appear to have a slightly higher polydispersity than the xylans.

Although it is unknown how different hemicelluloses provide properties to the cell walls, hemicelluloses are proposed to crosslink with cellulose by hydrogen bonds, which may influence the ability of the microfibrils to slip past one another⁴². In addition, during wood drying, the branched structure of hemicelluloses is responsible for the facility of attack by various chemical agents, including water. This explains, for example, the significant amounts of acetic acid found in condensates of wood driers⁴. Following the hydrolysis of the ester bonds of acetyl groups in xylans or in mannans, the acetic acid released increases the acidity of the medium, which supports degradations of pentoses to furfural and of hexoses to hydroxymethylfurfural⁴⁴.

Lignin plays a role in binding polymer constituents together in a wood composite system, linking the hemicelluloses through covalent bonds and providing the cell wall with rigidity and compressive strength. Lignins are polymerized mainly from three monomers called monolignols (p-coumaryl alcohol, coniferyl alcohol and sinapyl alcohol), which are propylphenol derivatives, with differences in the number of methoxy groups attached to the ring⁴⁰. Three main types of lignin are recognized according to their content of monolignols: Softwood lignin or guaiacyl lignin (G) consists almost exclusively of coniferyl alcohol and may contain small amounts of p-coumaryl alcohol, and few traces of sinapyl alcohol. In vessels and middle lamellas of hardwoods, a similar lignin is also found^{4,45}.

Hardwood lignin or syringyl-guaiacyl lignin, contains both coniferyl (G) and sinapyl alcohols (S) with proportions from approximately equal amounts, to three times higher levels of sinapyl alcohol. Some hardwood lignin may also contain small amounts of p-coumaryl alcohol (H)^{42,45}.

Table I-4 Composition of monolignols in different wood types.

Wood type	p-Coumaryl alcohol [%]	Coniferyl alcohol [%]	Sinapyl alcohol [%]
	H	G	S
			
Softwood	<5	>95	Trace
Hardwood	0-8	25-50	46-75

New information about lignin structures has been added, due to the progress of techniques such as NMR-analysis, which has led to a reconsideration of the covalent lignin pattern. Moreover, some new structures have been discovered, and the frequencies of some of the bonds have been reevaluated. Figure I-8 schematize the bonding types present on wood⁴⁶.

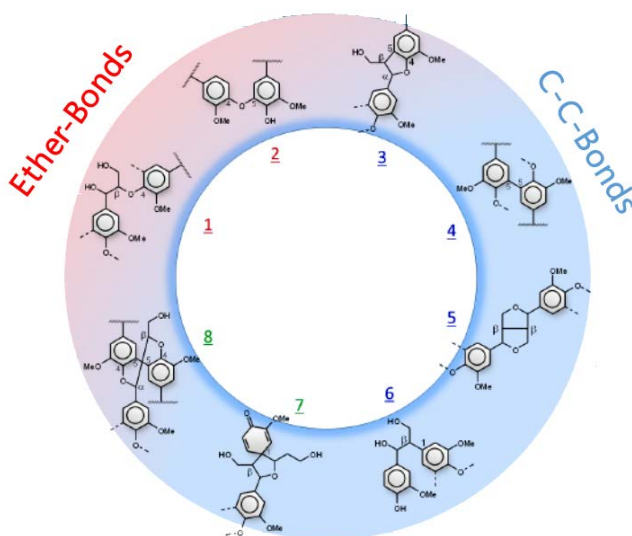


Figure I-8 Representation of bonding between monolignols of wood.

The most important bond between monolignols is the β -O-4 linkage. The chemical reactions in pulping, bleaching and biological lignin degradation, involve this bond. All β -O-4 inter-monomer bonds are relatively stable, but the carbon-carbon bonds (condensed bonds) are the most resistant, and these structures survive often chemical pulping⁴⁷. Recent data indicate that branch point α -O-4

bonds and γ -O-4 bonds does not exist in raw lignin, as well as α -carbonyls and vanillin structures do not seem to exist in newly synthesized lignin, but might be created during aging involving microbiological processes^{47,48}.


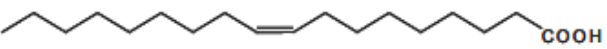


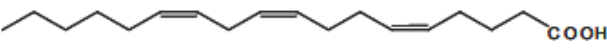
Other properties of lignin are concerning the cell wall hydrophobicity and the protection against the microbial degradation. On the one hand, the lignin inhibits swelling of the cell walls in water, and thereby that water leaks from a woody cell wall making the cell wall waterproof. On the other hand, the lignified woody tissue is basically compact and the polysaccharide-degrading proteins excreted by microorganisms cannot penetrate into the cell wall. Thus, it serves as a barrier against microorganisms⁴⁷.

Wood extractives are compounds with low molecular mass that are extractable from wood with various neutral solvents. In contrast to the structural polymers of wood, their composition varies considerably between tree families and species. Some extractives play a role in the metabolism of the living cells in the tree; others are produced to protect the tree against fungi and insects⁴⁹. The total amount of extractives is normally only a few percent of the wood, but it can be considerably higher in parts like bark and branches. The wood extracts are referred as the chemical compounds that are soluble in liquids of low polarity, that is, the lipophilic part of the wood extractives also named as wood resins. Wood extractives are chemically classified into different groups of compounds. The main constituents can be divided into aliphatic compounds, terpenes and phenolic compounds (not included as wood resin). The main aliphatic compounds are fatty acids and fatty alcohols, but hydrocarbons are also presented, such as n-alkanes⁴⁰. The fatty acids in most wood species have a chain length of 16 to 24 carbon atoms (C16; C18), but acids from C10 to C28 can also be found⁵⁰. Normally the unsaturated C18 acids, such as oleic, linoleic, and linolenic acid are the main constituents. In softwoods, an isomer to linolenic acid called pinolenic acid is one of the major fatty acids. As for unsaturated fatty acids, C18 acids linoleic, oleic and

linolenic constitutes between 75 and 85 % of them. However, the saturated acids have a wide range of proportions, depending on the wood species⁵¹.

Table I-5 Names and structures of the most common fatty acids present in wood³⁸.

SATURATED FATTY ACIDS		
Systematic name	Name	Formula
Dodecanoic acid	Lauryl acid	C ₁₁ H ₂₃ COOH
Tetradecanoic	Myristic	C ₁₃ H ₂₇ COOH
Hexadecanoic	Palmitic	C ₁₅ H ₃₁ COOH
Oktadecanoic	Stearic	C ₁₇ H ₃₅ COOH
14-methylhexadecanoic	Anteisoheptadecanoic	C ₁₆ H ₃₃ COOH
Eicosanoic	Arachinic	C ₁₉ H ₃₉ COOH
Docosanoic	Behenic	C ₂₁ H ₄₃ COOH
Tetracosanoic	Lignoceric	C ₂₃ H ₄₇ COOH
Hexacosanoic	Cerotic	C ₂₅ H ₅₁ COOH

UNSATURATED FATTY ACIDS	
Name	Representation
Palmitoleic acid-C16	
Oleic acid-C18	
Linoleic acid-C18	
Linolenic acid-C18	
Pinolenic acid-C18	

The terpenic composition of wood presents a clear distinction between hardwoods and softwoods; while in softwood include mono, sesqui, and diterpenes together with sterols, in hardwoods mainly contain sterols, triterpenoids and higher terpenes, such as polyprenoles⁵². The monoterpenes are especially volatile and together with the sesquiterpenes, they give the typical aroma of softwood resins. The sterols are closely related to the triterpenes, but they are found in both softwoods and hardwoods. The main wood sterol is sitosterol, very close to cholesterol, one of the main sterols in humans and animals, but also present in wood in low quantities⁴.

The phenolic extractive compounds are usually only found in the heartwood and in the bark, where they act as fungicides⁵³. Therefore, during heartwood formation, the parenchyma cells greatly increase their production of phenolic compounds, and in many species the heartwood can be visibly identified by a change in color, originating from polyphenols formed. Most of these compounds are water-soluble but they can be found also in acetone extractives⁵⁴.

2.5 Wood-moisture relations

The wood structure is formed in a state water-saturated keeping the wood elastic and able to withstand environmental stresses. The dimensional stability, as well as the mechanical, elastic, and thermal properties, depend on the moisture content³⁸. Moisture is presented in wood as free water (in the cell voids or lumens) and as bound water (in the cell wall). The wood in green state has the maximum moisture content with the total amount of free and bound water in the living tree⁵⁵. The moisture content of green wood varies between species and depends on the density¹¹. The wood volume does not change until it reaches the Fiber Saturation Point (FSP), which is defined as the moisture content of the cell wall when there is no free water in the voids and the cell walls are saturated with water⁴.

The average FSP ranges are from 20 to 50% depending on the wood species. Below the FSP the wood volume starts to shrink in different proportions due to their anisotropic properties (tangential shrinkage is about twice that of radial shrinkage and longitudinal is almost zero); however, only the cell wall shrinks beyond the fiber saturation point and the lumen stays the same size. Figure I-9 shows the water in wood at different drying states and its relation to the dimensional stability. The wood is in its Equilibrium Moisture Content (EMC) when it is in equilibrium with the surrounding relative humidity (RH). The moisture content of wood is a dynamic property that is constantly changing as the surrounding moisture content changes. Only when wood stays at one RH for long periods, the wood will reach an equilibrium moisture content^{11,38,55}.

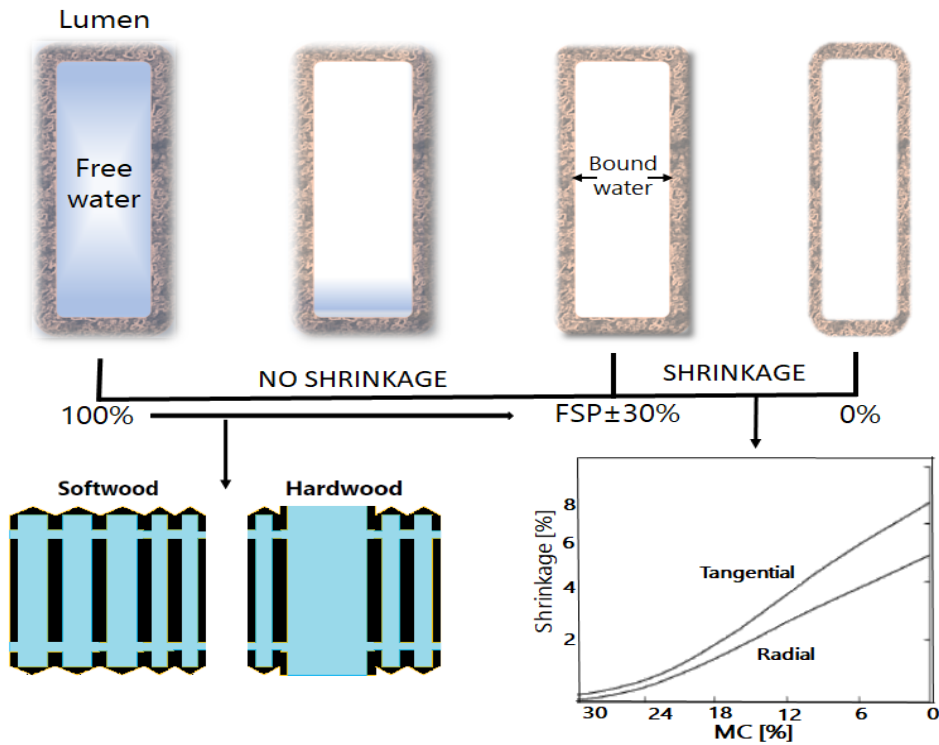


Figure I-9 Water in wood at different drying points and the relation between shrinkage and MC Adapted from USDA,2010¹¹.

Understanding the differences in moisture content from wet to dry and from dry to wet is very important to visualize the differences in the mechanical properties of wood. The adsorbing (A) curve is always lower than the desorbing (D) curve and the A/D ratio generally ranges between 0.8 and 0.9 depending on the relative humidity and wood species (Fig. I-10). The oven-dry wood (wood dried above 100 °C) presents the minimum MC in wood, which is less than one percent but not zero because there is a small amount of water that is so tightly bound to wood that it is impossible to remove.

For wood to swell from the dry state, water must enter the cell wall, and this penetration may result from mass flow followed by diffusion into the cell wall, which is a rapid process; or may enter from vapor-phase or bound-water diffusion entirely within the cell wall, which is a slow process. Wood is much more permeable in the longitudinal direction than in the radial or tangential directions (Fig. I-9). Because of this anisotropy, longitudinal flow paths are of major

importance in the wetting of wood exposed to the weather⁵⁶. Swelling of the wood continues until the cell reaches the FSP, and beyond the FSP, the remaining water is free water in the void structure and does not contribute to further swelling. This process is reversible, and wood shrinks as it loses moisture below the FSP. The Swelling-shrinkage process generates different curves called wood sorption hysteresis¹¹.

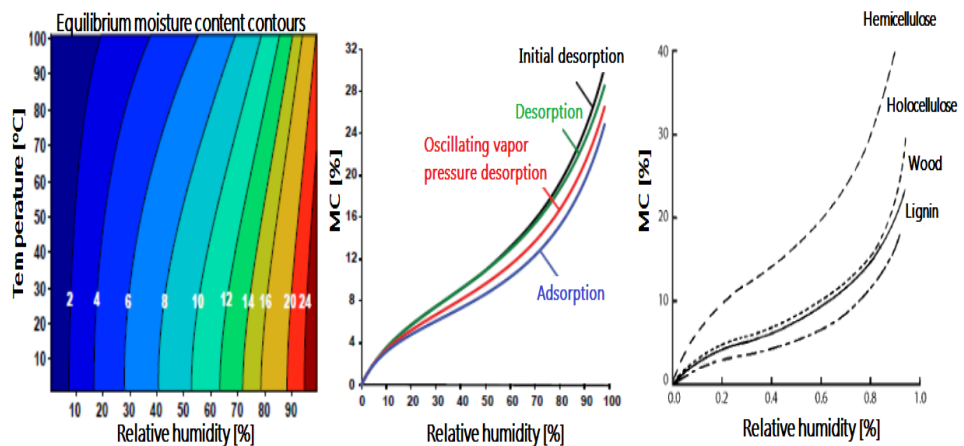


Figure I-10 Wood-water interactions. Left: EMC as function of RH-Temp. Center: MC-RH relations under adsorption and various desorption conditions. Right: Sorption isotherms for wood cell wall components Adapted from USDA, 2010¹¹.

As is shown in the sorption isotherms of wood components, all of the cell wall polymers (cellulose, hemicelluloses and lignin) are hygroscopic, and their order of hygroscopicity is as follows: hemicelluloses > cellulose > lignin. However, the sorption of moisture not only depends on its hydrophilic nature but also on the accessibility of water to the polymers hydroxyl groups. Thus, the hydroxyl sites in the hemicelluloses and lignin are accessible to moisture but only the non-crystalline portion of cellulose (approximately 40%) and the crystallite surfaces are accessible to moisture but not the crystalline portion of cellulose (approximately 60%)⁵⁷.

Regarding the effects of moisture on other wood properties, a brief resume is included in this section. The capacity of microorganisms to degrade wood is associated with the moisture content of the cell wall, and depending on the

microorganism, the values at or close to the FSP are the most critical points for attack¹⁰. The order of attack from higher to lower MC is as follows: soft-rot fungi > brown-rot fungi > white-rot fungi > microorganisms⁵⁸. The thermal and electrical conductivity is very low in dry wood, and increases with increasing MC. Heat transmission through dry wood is slow but heat transfer is much faster in moist wood using the water as the heat conductor. There is a strong correlation between mechanical properties and the MC of wood, changing drastically at MCs below the FSP and changing slightly at MCs above the FSP. European standards for structural timber specify an upper limit of 20% MC for dry graded timber in order for it to receive a defined strength grading. In addition, the dried timber anticipate the MC within a building environment prior its use and avoid excessive movement searching the equilibrium service condition⁴

2.6 Surface properties in wood and adhesion

The understanding of wood surface properties and adhesion have the potential to result in better adhesive systems and effective processing methods⁵⁹. The quality and durability of wood coatings are determined by the surface properties of the wood and the coating, while for wood applications, commodities and composite products, studying the mechanisms responsible for wood bonding is an important aspect⁴.

Wood surface properties and adhesion can be divided into physical and chemical properties. Physical properties include morphology, roughness, smoothness, specific surface area and permeability. Chemical properties include elemental and molecular, or functional, group composition. All together determine the thermodynamic characteristics of the wood surface, such as surface free energy and surface acid-base acceptor and donor numbers³⁸.

Wood depends on the interactions of interlocking and charges to create a proper adhesive bond. Mechanical interlocking occurs on the millimeter and micron-length scales, diffusion within the cell wall pores occurs on the nanoscale, and chemical charge interactions occur on the nanoscale or molecular level. The most

accepted models of wood adhesion are the mechanical interlocking, electronic or electrostatic theory, adsorption (thermodynamic) or wetting theory, diffusion theory, chemical or covalent bonding theory, acid-base theory and the theory of weak boundary layers⁴ (Figure I-11). It should be noted that these models are not mutually exclusive and several can act simultaneously depending on the particular conditions.

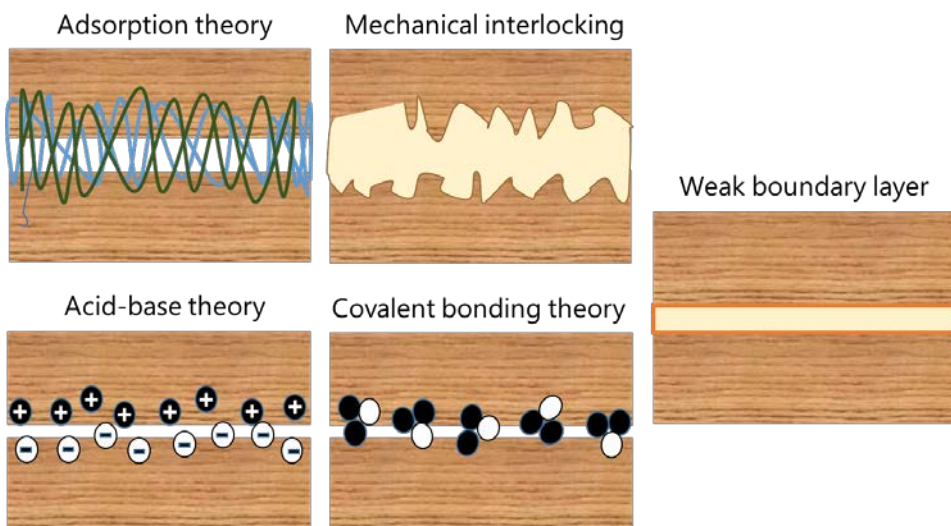


Figure I-11 Representation of accepted models of wood adhesion.

The mechanical interlocking theory is commonly used to describe wood bonding due to the microcellular characteristics of wood. The electronic or electrostatic theory is applied in finishing and coating operations, although needs more fundamental research. The adsorption or wetting theory has been comprehensively studied on wood over the past decades. The diffusion theory has received attention in the area of thermoplastic matrices used in wood plastic composites. The covalent bonding theory has been studied to understand durable wood bonding with thermosetting adhesives. The concept of acid-base theory has received significant attention regarding wood surfaces in recent years. The theory of weak boundary layers for wood is also a current focus of attention, mostly due to the impact of preparing wood surfaces for bonding and the effect of surface aging on inactivating wood surfaces^{4,60}.

An interphase includes the three-dimensional area of contacts (interface) between adhered substrates, and the region of some finite thickness extending on both sides of the interface, in that region the penetration of the adhesive occurs in the wood. The interphase possesses the properties of the lignocellulosic adherends and binder polymers (or adhesives), and an effective contact of adhesives on adherends is essential. The thermodynamic work of adhesion, which is calculated from the solid-liquid contact angle, is an indicator of the adhesion between adhesive and low-energy substrates. Minimized interfacial tension promotes an optimum adhesion strength, and this is possible when there are surface similarities or compatibilities between the two phases (adhesive and adherends), it usually occurs when both have similar solubility parameters, thereby decreasing the interfacial tension to the minimum^{4,60,61}.

The surface properties of wood can vary as a function of the mechanical surface pre-treatment: saw-milling, knife planned, blade cutting and sanding⁶². The dynamic wettability of different machined wood surfaces presents the fastest wetting of probe liquids on the sanded surfaces because of higher surface roughness and increased capillary forces as compared with the saw, knife planed and blade cutting surfaces. A smoother wood surface appears to provide better wetting and penetration properties for adhesives, which probably can be attributed to less entrapment of air between the product and the wood surface structure^{62,63}.

A recent review found that there are over 100 available analytical techniques to study material surfaces from the gross length scale down to the atomic level; however, only some are suitable for the surface analysis of wood materials³⁸. The most relevant methods used on wood can be divided into three broad categories: microscopic, spectroscopic, and thermodynamic. The microscopic methods provide information about surface morphology (optical and electron microscopy with energy dispersive X-ray (EDX)). The spectroscopic methods provide information about surface chemistry (inverse gas chromatography (IGC), Fourier

transform infrared (FTIR) and Raman spectroscopy). The thermodynamic methods provide information about the surface energy (contact angle analysis).

Table I-6 Most relevant analytic techniques used in wood surfaces⁶⁴.

Parameter	Microscopy	SEM	TEM	EDX	XPS	Contact angle	IGC	IR / Raman	AFM
Incident radiation	VIS,IR, UV	Electron	Electron	Electron	X-Ray	-	-	IR	-
Analysis Depth	48 μm	-	-	0.5-5 μm	0.5-10 nm	-	-	0.5-5 μm	-
Spatial Resolution	0.25 μm	10 nm	0.5 nm	0.5-5 μm	5-75 μm	70 μm -10 mm	-	30 μm	1 nm
Depth profile	yes	no	no	no	yes	no	no	no	no
Chemical information	-	no	no	no	yes	no	no	yes	no
Imaging	yes	yes	yes	no	yes	no	no	no	yes
Mapping	no	no	no	yes	yes	no	no	yes	yes
Surface energy	-	no	no	no	no	yes	yes	no	yes

The comparison table I-6 provides the particular attributes of each technique that is important to obtain information about surface properties of wood and fiber materials, including analysis depth, spatial resolution, chemical information, detectable elements, imaging/mapping capability, and depth profiling.

2.7 Durability and resistance of wood products

There are several factors affecting the durability and service life of wood and its products. The most significant factors that have a role in the durability of wood are the environmental factors, which are divided into biotic (insects, fungi, molds, marine borers and bacteria) and abiotic factors (UV-radiation, relative humidity and moisture content, temperature and exposure time), in addition to their physical-mechanical properties. Thus, the service life of wood materials in a structure depends primarily on the humidity conditions, the presence of wood attacking organisms, and the natural durability of wood (strength properties).

2.7.1 Wood and biotic factors

In trees, wood was designed to resist a wet environment and interact with several macro and microorganisms in ground or water contact. On the other hand, when wood is dried the new physical properties avoid the propagation of pathogenic organisms and prolong the service life of products. Therefore, the biological degradation is directly correlated with the wood moisture content and the abiotic conditions of the place where the material is exposed. Table I-7 shows the different organisms that interfere with the wood durability and figure I-12 presents some examples.

Table I-7 Biotic factor causing deterioration of wood^{65,66}.

Type of organism	Classification	Deteriorating agent	MC in wood
Macroorganisms	Insects	Termites	Green and dry wood
		Ants	Dry wood
		Beetles	Green and dry wood
	Crustaceans	Marine borers	Wet sea wood
Microorganisms	Fungus	Brown rot-fungi	Green and dry wood
		White rot-fungi	Green and dry wood
	Bacteria	Molds	Green and semidry
		Lignocellulosic bacteria	Green wood

Insects may damage wood and in many situations, they must be considered for protective measures. Termites are the major insect enemy of wood, but they are considered a less serious threat than fungi. Many types of termites attack wood, but the subterranean termites (Formosan termites) are specially consider, as they develop colonies in the ground and build tunnels to reach wood that they can use for food. Termites prefer the softer parts of the wood and attack springwood first. They are hierarchical species and those responsible for attacking wood are the worker termites while the male and female winged forms swarm from the new colonies. The Formosan termites can infest wood above ground and its attack is faster and more destructive as compared to other subterranean termites⁶⁷.

Other insects use wood for shelter and not for food, as is the case of carpenter ants, which prefer soft or decayed wood. They live in colonies and have several casts, attacking earlywood first and they only attack latewood to get to more earlywood. Moreover, some types of beetles and borers attack wood; the lygid beetles cause major damage to dry hardwoods, especially woods with large pores such as oak, affecting more the wood when the moisture content is between 10 and 20%, but can attack wood with up to 30% moisture content. Anobiid beetles are found in both hardwoods and softwoods and prefer the sapwood that is closest to the bark, requiring a moisture content about 15%. Long-horned beetles are extremely destructive to hardwoods, and attack both dying and living trees and bore into the heartwood, eventually killing the tree^{4,65}.

In wood that is in contact with salty or brackish water, there are some organisms called marine-borings, which cause extreme damage to wood structures in these waters all over the world. The most destructive marine borers are the shipworms, which are part of a group including *Teredo* and several species of *Bankia*. In their early stage, the young larva are very small and free-swimming organisms. When they find wood, they develop into a new form and penetrate into the wood with an entrance hole less than 2 mm in diameter. The shipworm then grows in length inside the wood and causes internal damage.⁶⁸

Fungi are the principal microorganisms that can degrade wood, either as food supply or as shelter. The growth of fungi depends on suitably mild temperatures, moisture, and air (oxygen). Decay fungi are multicellular filamentous organisms that are spread by the wind, insects or animals, to germinate on wood, where their hyphae secrete enzymes that attack the wood cells, resulting in wood decay⁶⁹.



Figure I-12 Representative samples of deteriorating agents.

Brown-rot, white-rot and soft-rot fungi all have enzymes that can degrade lignin, hemicellulose and cellulose^{69,70}. Brown-rot fungal degrades the carbohydrate polymers in the cell wall and the remaining lignin makes the wood look somewhat brown. The Brown-rot attack results in a high strength loss at a very low weight loss, but there is a large loss of molecular weight in the carbohydrate fraction. The most accepted theory of the brown-rot action mechanism divides the attack in an initial enzymatic degradation on the hemicelluloses that generates energy that is used to start the release of ferric ion and hydrogen peroxide to start degradation of the cell wall matrix, and thus, leading to strength losses at this early stage of attack. Then, the hyphae release enzymes type endo and exo-cellulases that start to degrade cellulose with very little attack on the lignin^{71,72}. As an example, at a general weight loss of 52%, the total carbohydrate loss is about 86%. Usually they attack softwood although there are reports of these organisms also degrading hardwood⁴.

Unlike the brown-rot, the white-rot fungi attack all cell wall components including lignin, which causes the wood to acquire whitish tones after attack. White-rot fungi mainly attack hardwoods but can also attack softwoods. Strength properties decrease gradually as decay progresses; however, toughness is reduced at early stages of attack⁷².

Molds are another type of fungi that live on plants or wood, with a large number of different species. They are filamentous organisms and the production of spores is characteristic of them. Unlike bacteria, molds are made of many cells and have branches and roots that are very thin threads. Molds are mainly on the surface of wood, and they require energy (food), oxygen and a suitable temperature and moisture content. Molds that grow on wood typically discolor the wood through the production of pigmented spores, but, it should be noted that stain fungi do not belong to this division and these can penetrate deeply into the wood structure. Molds are often found in combination with bacteria, but in general, bacteria in wood do not cause drastic effects. Some may cause strength losses over long periods of exposure, particularly in forest soils. They are found in waterlogged wood both in seawater and fresh water and above ground. Some bacteria can open up some closed pit structures making the wood more susceptible to attack by fungi⁶⁹.

2.7.2 Wood and abiotic factors

The abiotic factors are those environmental elements that affect wood when it is exposed to weather and in turn facilitates the attack of biological agents. The principal abiotic elements involved in the weathering of wood are the ultraviolet energy (UV), water (rain), oxygen and temperature⁷³. However, the ultraviolet (UV) portion of the solar spectrum initiates the weathering process by photo-oxidation or photochemical degradation of wood surfaces⁷⁴. As the weathering process occurs on the surface, the first indication is a change in wood color. The UV radiation has sufficient energy to chemically degrade wood structural components (lignin and carbohydrates), but its effect on the mechanical properties is minimum³⁸. The visible portion of the solar spectrum also causes minimal damage in surfaces at the short wavelengths, but the changes do not involve degradation of the wood structure.



Figure I-13 Wood color changes by UV degradation (Kulch, Austria).

The UV and visible radiation that reaches earth is limited to the range between 295-800 nm, while the infrared (IR) has wavelengths between 800-3000 nm. The photon energy is inversely proportional to the wavelength of the radiation, and this energy is very important because it can initiate the wood photochemical reactions. Table I-8 shows the bond energies and wavelengths for different types of bonds found in wood. In order for a photochemical reaction to occur, enough energy to disrupt a chemical bond must be absorbed by some chemical moiety in the wood⁷⁵. The absorption of energy in wood surface is a necessary condition to start a chemical degradation reaction.

One of the first cell wall polymers to be degraded by UV radiation is the lignin, causing bond dissociation of lignin moieties having α -carbonyl, biphenyl, or ring-conjugated double bond structures⁷⁶. Lignin absorbs UV radiation throughout the UV spectrum and in the UV-Vis light spectrum. However, absorption at 295 nm is the only one that is important for weathering of wood. The mechanism of lignin photodegradation is complex, with different pathways giving free phenoxy radicals leading to chain cleavage and yellowing. One of the main phenoxy radicals is a guaiacoxo radical, which undergo transformation into quinoid structures,

causing these the yellowing of the surface of the wood. Considering lignin as the key structure in wood photodegradation, Figure I-14 shows different pathways of the radical formation from lignin degradation, thus suggesting mechanisms for wood photodegradation.

Table I-8 Bond dissociation energies and radiation wavelength⁴.

Bond	Bond dissociation energy [Kcal/mol]	Wavelength [nm]
C-C (Aromatic)	124	231
C-H (Aromatic)	103	278
C-C (Methane)	102	280
O-H (Methanol)	100	286
C-O (Ethanol)	92	311
C-O (Methanol)	89	321
CH ₃ COO-C (Methyl ester)	86	333
C-C (Ethane)	84	340
C-COCH ₃ (Acetone)	79	362
C-O (Methyl ether)	76	376

The weathering stages start with the lignin degradation but the action of rain removes some of the holocelluloses along with the lignin. As the UV degradation and water washing continue, wood loses fibers and cracks appear due to the continuous swell-shrink dynamic. Color changes as a function of time, and a light colored wood starts to turn yellow in the early stages of weathering, but after about 1 year, the wood has turned to an orange hue, to finally turn in a silvery gray hue⁷⁶. Testing the weathering effects on wood may take several years and diverse results due to the specific conditions of the test location. One way to standardize the weathering effects is through accelerated artificial testing, which simulate natural weathering conditions in controlled cycles of UV radiation, light, water spray and heat. Even though the results of the artificial test are practical, they should be regarded only theoretically.

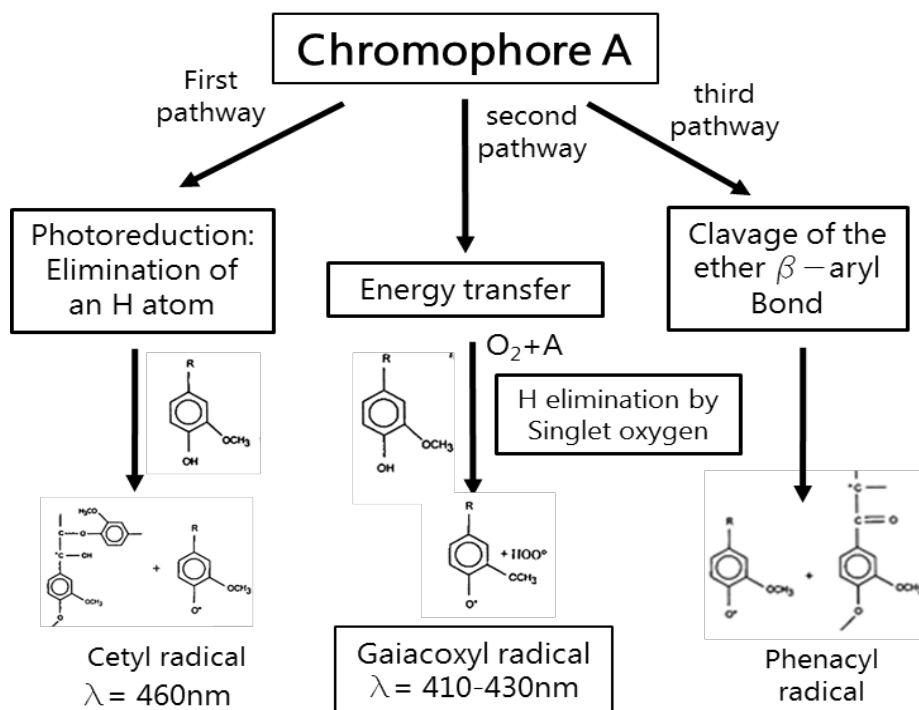


Figure I-14 Possible Mechanism of free radical formation from lignin degradation. Adapted from Gérardin, 2015.⁷⁶

2.7.3 Mechanical properties of wood

Wood is an orthotropic material; that is, it has unique and independent mechanical properties in the directions of three mutually perpendicular axes: longitudinal, radial, and tangential. The longitudinal axis L is parallel to the fiber (grain); the radial axis R is normal to the growth rings (perpendicular to the grain in the radial direction), and the tangential axis T is perpendicular to the grain but tangent to the growth rings (Figure I-15). This distinctive characteristic makes twelve constants necessary to describe the elastic behavior of wood: three modulus of elasticity (E), three modulus of rigidity (G), and six Poisson's ratios (μ) are needed (nine are independent)¹¹.

Elasticity means that deformations produced by stress are recoverable after loads are removed, so the property ends when a plastic deformation or failure occurs. The modulus of elasticity is usually obtained from compression tests but in general there is only available data from the longitudinal axis. Moreover, the ratio of the

transverse to axial strain is called Poisson's ratio, thus, when a sample is loaded axially, the deformation perpendicular to the direction of the load is proportional to the deformation parallel to the direction of the load.

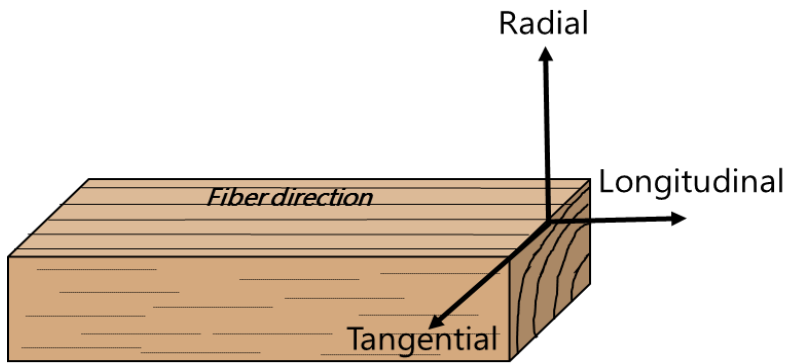


Figure I-15 Principal axes of wood with respect to fiber direction and growth rings.

The different directions of applied stress and the direction of the lateral deformation are denoted as follows: μ_{LR} , μ_{RL} , μ_{LT} , μ_{TL} , μ_{RT} , and μ_{TR} . Two of the Poisson's ratios (μ_{RL} and μ_{TL}) are very small and are less precisely determined than are those for other Poisson's ratios. The elastic ratios and the elastic constants vary between species and with the moisture content and specific gravity. The modulus of rigidity or shear modulus indicates the resistance to deflection caused by shear stresses. The three shear modulus are denoted by G_{LR} , G_{LT} , and G_{RT} . As with the modulus of elasticity, the shear modulus vary within and between species and with moisture content and specific gravity. The most common mechanical properties measured as strength properties for design, and to evaluate work at maximum load in bending, are briefly explained below¹¹:

- Modulus of rupture: Reflects the maximum load-carrying capacity of a sample in bending and is proportional to maximum moment tolerated by the specimen. This modulus is an accepted criterion of strength, although it is not a true stress because the formula used for calculations is valid only to the elastic limit.
- Work to maximum load in bending: Ability to absorb shock with some permanent deformation and more or less injury to a sample. This load is

a measure of the combined strength and toughness of wood under bending stresses.

- Compressive strength parallel to grain: Maximum stress sustained by a compression parallel-to-grain sample having a ratio of length to least dimension of less than 11.
- Compressive stress perpendicular to grain: Reported as stress at the proportional limit, but is not clearly defined such limit.
- Shear strength parallel to grain: Ability to resist internal slipping of one part upon another along the grain. Values presented are average strength in radial and tangential shear planes.
- Impact bending: A hammer with known weight is dropped upon a beam from successively increased heights until rupture occurs or the beam deflects 152 mm or more. The drop that causes failure is a comparative value that represents the ability of wood to absorb shocks that cause stresses beyond their proportional limit.
- Tensile strength perpendicular to grain: Resistance of wood to forces acting across the grain that tend to split a member.
- Hardness: Generally defined as resistance to indentation using a modified Janka hardness test, measured by the load required to embed a ball to one-half of its diameter.
- Tensile strength parallel to grain: Maximum tensile stress sustained in the direction parallel to the grain. Relatively few data are available on the tensile strength of various species

The variations in the hierarchical microstructure of plants provide a very wide range of mechanical properties, illustrated in figure I-16, which shows the average variations and differences values of strength versus Young's modulus, for three groups of plant materials: woods, parenchyma and palm stems⁷⁷.

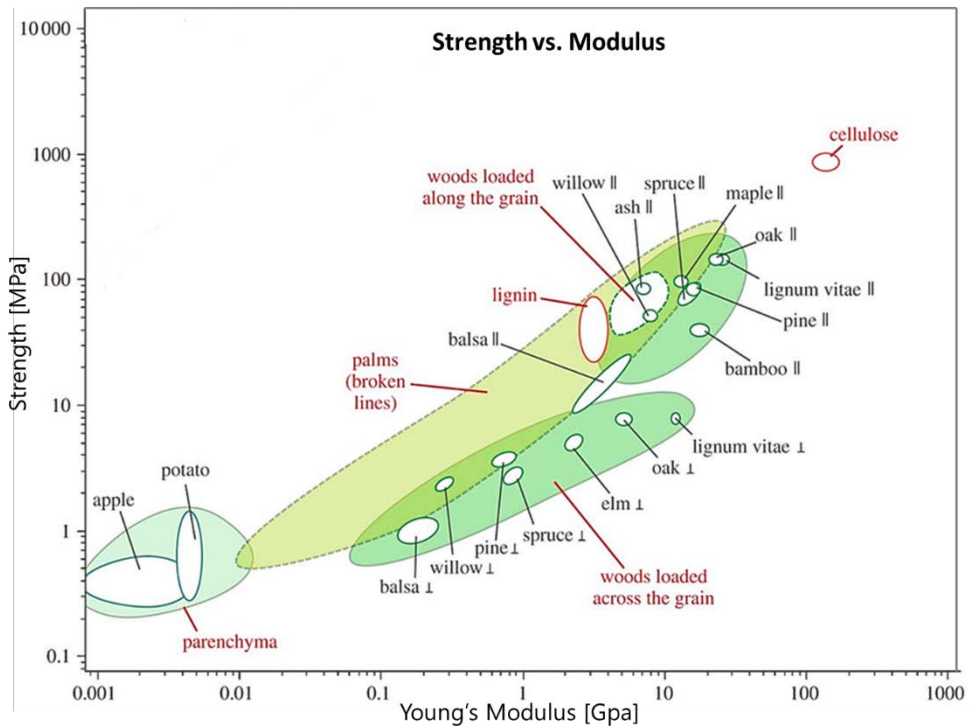


Figure I-16 Strength plotted against Young's modulus for selected plant materials. Adapted from L.J. Gibson⁷⁷.

Strength properties in wood include torsion, toughness, rolling shear, and fracture toughness, as well as properties involving time under load include creep, creep rupture or duration of load, and fatigue strength, are less commonly measured. In general, the variability of properties is important in both production and consumption of wood products.

2.8 Chemical modification of solid wood

The objective of the chemical modification of solid wood is generally to increase wood dimensional stability through reduction of its affinity to moisture, as well as to improve its resistance to biodegradation⁷⁸. The chemical modification is based on the reactions between hydroxyl and phenyl groups of the wood components and an external reagent applied. The external agent reacts with wood usually through esterification or alkylation reactions, but in the case of heat treatments, the wood is modified by hydrolysis reactions⁷⁹. The mechanism of stabilization

varies depending on the method used; in the case of the reactions involving modification of hydroxyl groups of wood, stabilization is due to the reduction of free sites able to bind water through hydrogen bonds, but also to the bulking effect of groups grafted onto wood⁷⁸. After modification, the cell wall is less available for water molecules, reducing the water absorption in the modified wood. This section briefly explains four methods that are the most used on an industrial scale.

2.8.1 Acetylation treatment

The acylation process of wood has been studied using a wide range of chemicals, among which are acid anhydride, acyl chloride, ketene or phthalic anhydride. However, only a few of them have been industrially developed, and the common reason is the difficulties to transfer and adapt the results obtained at laboratory scale to industrial scale. The most investigated acylation reaction is wood acetylation⁸⁰. The typical reagents used are acetic anhydride (liquid or vapor) or ketene, with the advantage that the modified wood is free of all byproducts or these products are easily removed by heating under vacuum (e.g. acetic acid formed during acetylation with acetic anhydride). The reaction of wood with acetic anhydride can be carried out with or without a catalyst in temperatures between 100 and 130 °C followed by a vacuum step to remove unreacted anhydride and acetic acid. This reaction involves the replacement of the hydrogen atom of a hydroxyl group with an acetyl group (CH₃CO) yielding an acetate ester and the corresponding carboxylic acid⁸¹.

The acetylation of wood results in a reduction of the moisture absorption of 50-80% in humid air hence increases the dimensional stability. Studies performed with different wood species indicated that equilibrium moisture content decreased as the degree of acetylation increased, while mechanical properties were not affected or just slightly. Other advantages of acetylation are the improved durability against termites and fungi (avoiding the use of preservation products and the

inhibition of photo discoloration and photo-yellowing (through reduction of the formation of colored chromophores on the wood surface)⁸².

In 2007, an industrial plant was established in the Netherlands for the commercial production of acetylated wood under the tradename Accoya[®]. This plant has a capacity of approximately 30,000 m³ per year using Radiata pine for treatment. The process is based on a vacuum/pressure impregnation of wood with acetic anhydride at approximately 120 °C for several hours, a vacuum stage at an elevated temperature and if necessary a drying process to evaporate acetic acid and unreacted acetic anhydride still present in wood after treatment. Possible markets include decking, flooring, doors, windows, furniture, cladding, veneer, panel products, civil engineering and waterworks. Worldwide, several projects have been realized but an interesting example of a civil engineering project is the Ark Encounter opened in 2016 in Cincinnati (USA), it features a full-size Noah's Ark, spanning 150 m long, 26 m wide, and 15 m high (Figure I-17).



Figure I-27 Acetylated wood used in a civil engineering project (Accoya[®]), Cincinnati (USA), 2016.

2.8.2 DMDHEU treatment

Another example of chemical modification at industrial scale is through N-methylol compounds, like 1,3-dimethylol-4,5-dihydroxyethyleneurea (DMDHEU), originally used as a wrinkle-resistant finish in the textile industry⁸³. In wood treatments, these compounds are used to enhance the resistance of wood to weathering because they can crosslink the cell wall occupying the void space and

reducing the pore size; this creates an effect of dimensional stability in the modified wood⁷⁸.

Other effects are the increase of the hydrophobic character of wood, which however, does not negatively affect the wetting of wood surface by waterborne coatings⁸⁴. The strength properties are not hardly affected, although the surface hardness shows a strong increase after DMDHEU treatment. The decay resistance is not improved with DMDHEU treatment, so it is not a biocidal alternative to classical preservation methods. However, with the addition of Boric acid and phenyl boronic acid, the decay resistance against brown- and white-rot fungi increased considerably.

Since 2006, the DMDHEU treatment is marketed by BASF in cooperation with the University of Gottingen under the tradename Belmadur[®] process. The treatment is carried out in two stages (Fig. I-28): the first stage includes vacuum pressure impregnation with a waterborne DMDHEU solution (including a catalyst) in a conventional vacuum-pressure vessel. The second stage consists on drying to a low moisture content and curing at a temperature between 100 °C and 150 °C for about 16 hours in a kiln. Several wood species are used and a wide range of applications has been suggested, such as parquet floors, stairs, window frames, doors, cladding, garage doors and decking.



Figure I-28 Stages of Belmadur process (BASF pilot plant, Gottingen, Germany). Adapted from H. Millitz presentations.

2.8.3 Furfurylation treatment

Wood modification with furfuryl alcohol is a nontoxic alternative to conventional preservation treatments. The furfurylation process is based on *in-situ* polymerization of furfuryl alcohol (at 100 °C to achieve polymerization) into the

cell walls of wood. The process includes vacuum (0.1 bar) for 45 minutes and pressure (8 bar) for 45 minutes, to then impregnate with a waterborne furfuryl alcohol solution prior to curing (at 100 °C) for 8 hours. According to the modification levels, a wide variety of properties like dimensional stability, hardness, MOR, MOE, and resistance to decay and insect attack were improved, these properties depend on the retention of grafted/polymerized furfuryl alcohol in the wood⁸⁵.

The use of furfuryl alcohol obtained from renewable hydrolyzed biomass waste and improvement of the polymerization process, have led to the development of commercial production according to the Kebony technology, and two main processes for production have been developed: Kebony® for hardwood modification and VisorWood® for softwood modification

Since 2008, a state-of-the-art plant is operative with a capacity of approximately 20,000 m³ of furfurylated wood per year. There are many constructions using furfurylated wood are worldwide (Fig. I-29), and the main markets are cladding, decking and roof boards, outdoor applications where durability against biological decay is required.



Figure I-29 The Biological House, Middelfart (Denmark), using Kebony® for the exterior cladding.

2.8.4 Thermal treatment

Although the thermal treatments are known since the 1950s⁸⁶, their industrial exploitation is still recent, and was favored by the environmental pressure on the use of biocides, leading to the progressive disappearance of some preservation products. Thermal modification is a physical process that chemically modifies the structure of wood cell wall polymers through different chemical reactions, conferring to the material new properties (hygroscopicity, dimensional stability, decay resistance, diffusibility and permeability), while its strength decreases more or less according to the treatment conditions⁸⁷. Due to the improvement of durability towards wood-rotting fungi, heat-treated wood is considered as a nonbiocidal alternative to classical wood preservatives for applications in hazard classes 2 and 3⁷⁸.

All these thermal modification technologies involve wood heat treatment at high temperature between 180 °C and 240 °C under oxygen-free atmosphere to avoid burning involving the use of either steam, nitrogen or oil. The main differences between the different industrial methods are based on the materials used (wood species, fresh or dried wood, moisture content, dimensions), process conditions applied (one or two process stages, wet or dry process, heating medium, oxygen or nitrogen as sheltering gas, heating and cooling-down velocity) and the equipment necessary for treatment (process vessel, kiln). The specifications of the various thermal modification methods are reported in several patents (EP0018446 1982, EP0612595 1994, EP0623433 1994, EP0622163 1994, EP0695408, EP0759137 1995, JP 3585492, US5678324, CA 2162374). Below in table I-9 is an overview of heat treatments that are commercially used in Europe:

Table I-9 Production of thermally modified wood in Europe (Adapted from Manninen, 2014⁸⁸).

Producer	Production 2008 [m³]	Capacity [m³]
Austria	12000	10000
Croatia	4800	8000
Estonia	1200	15000
Finland	95000	214000
Germany	13500	17700
Netherlands	7000	15000
Sweden	-	5000
Switzerland	3000	3500
Turkey	8400	9000
Total	156700	197200

The possible uses for thermally modified materials are in the building industry (flooring, cladding, bevel siding, salvages and sheds, doors, window frames and windows exterior), Civil engineering (decking, sound barriers) and garden wood (garden furniture, terrace and garden planking⁸⁹. In Spain, some building introduce thermally modified wood by Termogenik Treatment (Figure I-30):



Figure I-30 Thermally modified façades, Leioa and San Sebastian, Spain.

2.9 Wood as a building material

The three structural materials currently used in the construction of large structures are steel, reinforced concrete and the wood that could reduce the environmental impact of construction⁹⁰. The market share of wood construction in the house construction markets has remained at around 8–10 % in Europe on average over

the past decades⁹¹. However, it varies regionally, from approx. 80 % in the Nordic countries to close 0% in some Southern European countries. The wood as a building material is efficient in structures, or parts of structures, in which a high proportion of the load to be resisted is the self-weight of the structure (roofs, some bridges and the gravity load resisting system of tall buildings)⁹². Another positive point is related to the seismic forces, in which the force imposed on the structure by shaking depends strongly on its mass, and with lighter structures (like wood) experiences less impact⁹³. Regarding its mechanical properties, wood may be particularly efficient in certain structural forms such as shell structures; these are efficient for long-span roofs since they transfer loads purely in compression and shear in the plane of the shell. This form has been used to create very large structures without the need for the infrastructure associated with the production of large curved engineered wood products such as glulam.

In the last decade, engineers have started to look at the possibility of building much taller with wood⁹⁴. The complexity of the structure of a tall building increases with the height of the structure. In low-rise buildings, where the forces to be resisted are relatively low, it is possible to resist lateral loads by bending stresses in walls which form a vertical beam. This is the approach widely used in cross-laminated timber (CLT) construction in buildings⁹⁵. The use of wood as a structural material, however, often has the consequence of introducing other materials to achieve certain performance requirements: concrete is used to achieve acceptable floor vibration or thermal mass. Another point of view to consider is to compare the amount of wood used in a building to that which can be produced by a particular forest area. That means if the population of Europe (750 million) lived in wood buildings (Approx. 3 people per house), then approximately 40–50 million hectares of forest would be required to renew those buildings every 50 years¹⁰.



Figure I-31 Examples of tall wood buildings: (A) Kizhi Pogost-37.5m, Russia, 1862; (B) WIDC-30m, Vancouver, Canada, 2014; (C) Oakwood tower-300m, London, conceptual stage.

3

**Case study: Wood
modification by heat
treatments**

3.1 Motivation

The industrial application of new wood technologies will open the door to the development of a forest bioeconomy, especially in regions with this important resource. Currently in the Basque Country there is an industrial thermal treatment chamber to chemically modify wood using high temperatures, and to the best of our knowledge, is the only one operating in Spain. The heat treatments chemically modify wood and due to this modification, the wood properties are altered, changing the surface polarity, reducing the moisture content, and obtaining greater dimensional stability. In order to understand the changes that occur in wood it is necessary to explore its chemical composition via both wet chemistry and using analytic techniques. Simultaneously, the treated wood and wood-based products require to fulfill certain physical-mechanical and aesthetical characteristics, as well as biological protection, and to recognize the main material applications and its limitations. Once the characteristics of the treated products have been recognized, investigate the evolution of the material over time and the changes in its properties is a significant part of the comprehensive study of the material and its commercialization. Another important factor is the study of the surface properties and interactions with coatings and bonding products, necessary for different wood applications. Finally, assessing the environmental aspects and potential impacts associated with the production of thermally modified wood through an environmental and energetic profile may help to identify processes or stages in the wood chain with a high environmental impact. In addition, the study of the residues generated could add value to the integral process.

3.2 Experimental procedure

3.2.1 Wood material

The material analyzed in this study was the one used industrially for the thermal modification process. Mainly local sawnwood (Basque Country, Spain) was analyzed, although sawnwood from Poland, Finland and Chile were also used. The characterized wood species were the softwood specie *Pinus radiata* D. Don (Monterey pine) and the hardwoods species *Fraxinus excelsior* L. (European Ash) and *Quercus robur* L. (European Oak)

The wood industrial sector chooses these species among others due to their availability and low cost, and taking into account that the idea is to promote their use as an added-value product and to compete with timber of higher quality or with tropical wood.

3.2.2 Wood modification process

The whole process begin with the harvesting operations, in which the felled timber is cut to length for transportation from forest to sawmill, then debarked, and sawed processing, fulfilling the chain of custody according to the PEFC⁹⁶. In industry, the sawn timber is air-dried exposing by natural convection and then kiln drying at 100/70°C (temperature of dry bulb thermometer / temperature of wet bulb thermometer) with airflow speed of 6 m/s. The drying treatment is necessary to optimize the consequent thermal modification process by avoiding a water content above the fiber saturation point.

The thermal modification process is performed in an airtight reactor under inert N₂ atmosphere or in saturated steam atmosphere depending on the available industrial kiln. The modification process begins with a fast increase of temperature up to 100 °C, which allows the drying of the wood to 3–4% of moisture content. After drying, the wood specimens were heat-treated, under dry and atmospheric conditions, using superheated steam or nitrogen gas as a

sheltering gas to exclude oxygen and to avoid damage in wood. In this stage, the temperature is raised to its maximum level. Modification time and treatment temperatures are shown in Table II-1.

The last stage is the cooling down the reactor and stabilizing samples to atmospheric conditions. In order to avoid abrupt temperature and pressure fluctuations, this stage takes about 24 h at controlled release of pressure and relative humidity until room temperature. The temperature gradient between surface and inner site of the samples did not exceeds of 15–20 °C with the purpose of retain the wood quality.

Table II-1 Treatment temperatures, classes and wood species⁹⁷.

Wood specie	Reactor location	Total treatment time [h]	Temperature Dry bulb/Wet bulb [C°]	Treatment class
<i>Pinus radiata</i>	Spain	60	190/100	Thermo-S
		70	210/100	Thermo-D
<i>Quercus robur</i>	Spain	55	170/100	Thermo-S
	Poland	60	190/100	Thermo-S
<i>Fraxinus excelsior</i>	Finland	70	200/100	Thermo-D
	Spain	70	210/100	Thermo-D

The company that supply the treated wood was principally Torresar (Spain) and its modification process is patented as Termogenik. Wood from Thermo-Drewno (Poland) and Thermo-wood (Finland) processes were also used for several characterizations.

3.2.3 Characterization methods

The experimental work done as part of the doctoral thesis is summarized in the following diagram (Figure II-1), which is distributed in different thematic sections with their respective experimental procedures. The experimental procedures and

techniques are detailed in the appendices of the manuscript, and the results are presented in the following thematic blocks.

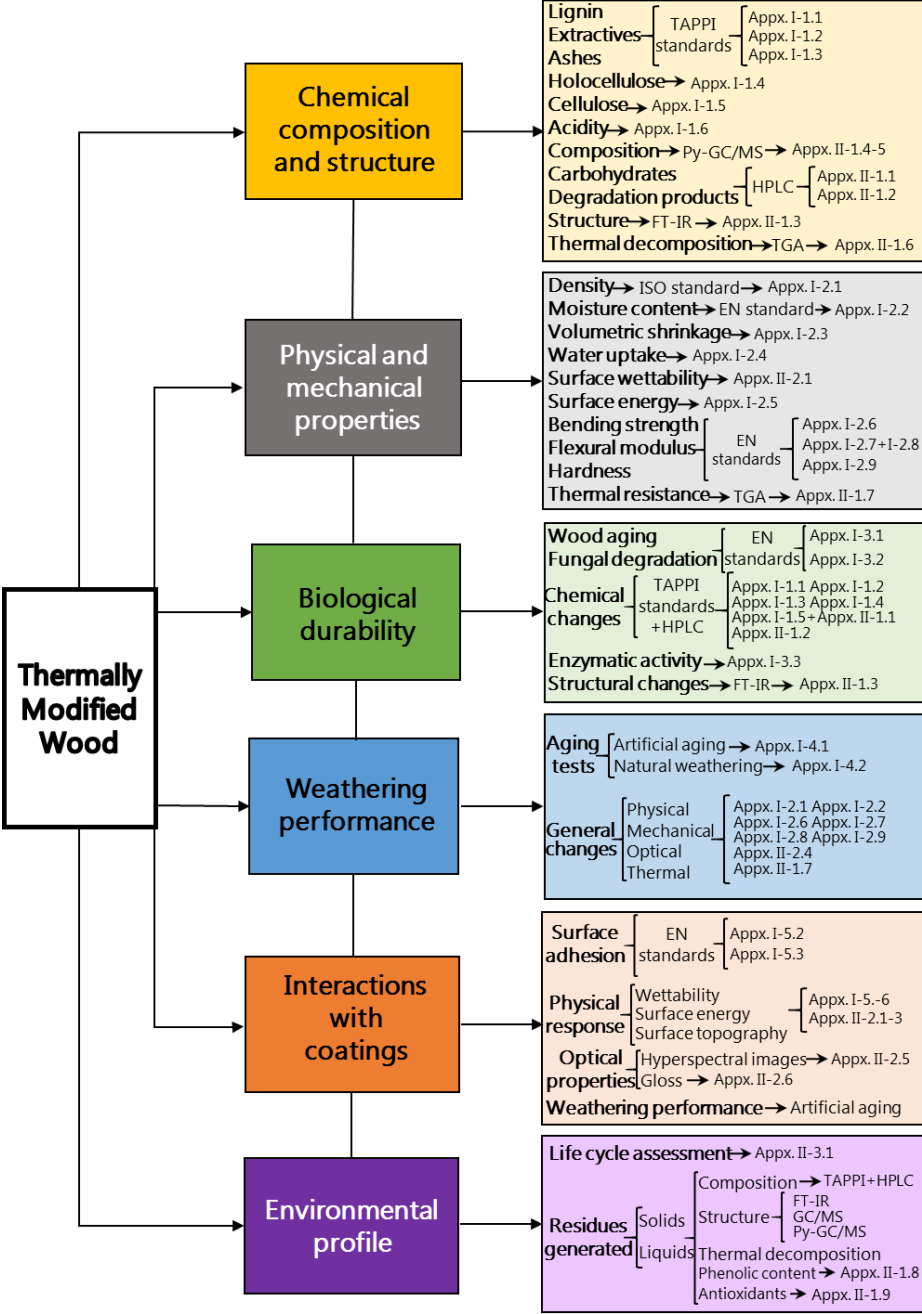


Figure II-1 Schematic of the different sections of study and the experimental procedures performed in each of them.

3.3. Results and discussion

3.3.1 Chemical composition and structure of thermally modified wood

The first section corresponding principally to the changes in chemical composition and structure of wood due to the thermal treatment. In this section were used three different wood species and three different temperatures of treatment. The first specimen was *Quercus robur* treated at 170 °C (T-Oak170), the second was *Pinus radiata* treated at 190 °C and 210 °C (T-Pine190, T-Pine210), and the third one was *Fraxinus excelsior* treated at 210 °C (T-Ash210). The experimental scheme is summarized in the Figure II-2 and the respective methods are explained in the appendices.

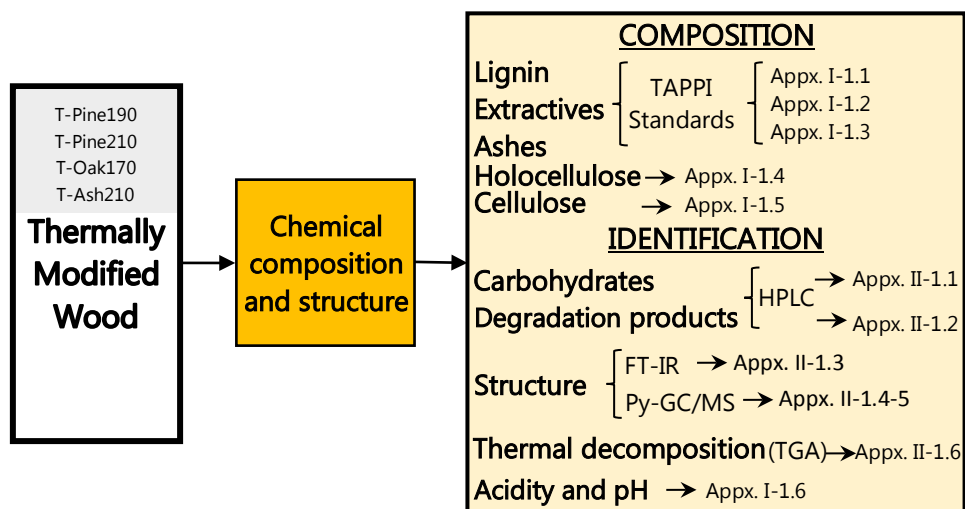


Figure II-2 Scheme of the chemical analysis performed on wood.

3.3.1.1 Chemical composition of wood

The results of wood chemical composition obtained by wet chemistry (Table II-2) shown that heat treatments modify the main constituents of *Pinus radiata*, *Quercus robur* and *Fraxinus excelsior*, due to the degradation of the cell wall components and the release of extractive compounds⁹⁸. The chemical analyses revealed that during the heat treatment the proportion of hemicelluloses decreased in a higher proportion compared to the other macrocomponents, being the first component to degrade due to treatment.

Table II-2 Changes in chemical composition after heat treatment of wood.

Analysis [%]	Hemi-cellulose	CR ¹	α-Cellulose	CR	Lignin	CR	Extracts	CR	Ash
<i>Pinus radiata</i>	23.61 ±0.87	-	45.15 ±1.15	-	27.65 ±0.68	-	2.85 ±0.06	-	0.27 ±0.01
<i>T-Pine190</i>	13.66 ±0.74	1.73	42.69 ±1.05	1.06	38.96 ±1.11	0.71	3.11 ±0.10	0.92	0.26 ±0.01
<i>T-Pine210</i>	12.89 ±0.49	1.83	41.48 ±1.01	1.09	40.20 ±1.08	0.71	4.77 ±0.79	0.60	0.26 ±0.01
<i>Quercus robur</i>	18.89 ±0.24	-	46.37 ±0.46	-	29.12 ±1.38	-	5.53 ±0.26	-	0.52 ±0.01
<i>T-Oak170</i>	9.89 ±0.43	1.91	49.39 ±0.85	0.93	31.64 ±0.91	0.92	6.28 ±0.13	0.88	0.70 ±0.01
<i>Fraxinus excelsior</i>	19.10 ±1.08	-	48.49 ±1.36	-	28.80 ±1.56	-	4.08 ±0.34	-	0.49 ±0.12
<i>T-Ash210</i>	12.12 ±1.36	1.58	40.33 ±1.69	1.20	37.39 ±1.87	0.77	6.90 ±0.82	0.59	1.06 ±0.10

¹CR= Change Ratio: control/T-sample

Hemicelluloses are found in the matrix between cellulose fibrils in the cell wall and are difficult to separate from lignin and cellulose without modifying it. In untreated wood, the percentage of hemicelluloses was between 19 and 24% of

the dry mass, and *Pinus radiata* presented a greater proportion than the studied hardwoods, although hemicelluloses from softwoods and hardwoods present different composition. All the thermally modified samples show a change ratio well above the unit (>1.58) compared to initial hemicellulose content. Remarkable the different behavior of hardwoods, while T-Oak170 present the maximum decrease of hemicelluloses at the lowest treatment temperature (170 °C), T-ash210 is the most stable at higher temperature of treatment (210 °C).

Several studies have shown that heat treatment causes significant degradation of wood constituents, resulting in a decrease of the hemicelluloses content^{87,99,100}. The degradation of hemicelluloses, involves dehydration reactions that reduce the hydroxyl groups (-OH), with a direct impact on the moisture content and the conformation of O-acetyl groups^{38,100}.

On the other hand, the cellulose content has a different response to the obtained for hemicelluloses; In T-Pine decrease with the treatment intensity but with slight changes ($1.06 \geq CR \leq 1.09$). The hardwoods have diverse behavior, and T-Oak170 remains stable with a proportional increase of cellulose content, but T-Ash210 shows the maximum decrease of cellulose content ($CR=1.20$) among all samples tested. Further studies indicated stability of the cellulose content after thermal treatments¹⁰¹; it could be due to the increase of cellulose crystalline proportion as the more unstable part of cellulose (amorphous cellulose fraction) had been degraded. This effect is more evident in T-Ash210 samples, where it appears that much of the amorphous cellulose has been degraded.

Regarding lignin content, there was a significant alteration in treatments above 190 °C, more pronounced in T-Pine samples than in T-Ash. On the other hand, in Oak (T-Oak170) the lignin content remained more stable with a $CR \approx 0.92$, showing a minimal effect when compared with samples of Ash and even lower compared to Pine. Therefore, treatments above 190 °C modify in the lignin

structure in greater intensity¹⁰². Several authors affirm that a greater amount of phenolic-OH groups are present in the lignin structure after heat treatments due to the demethoxylation of the methoxy groups of guaiacyl and syringyl, in addition to greater proportion of free ortho sites from the demethoxylation of the methoxy groups, basis of lignin^{103,104}. Such polycondensation reactions occur during at high temperatures (>180 °C) by increasing cross-linking with other components of the cell wall, like fragments of cellulose and hemicelluloses that degrade and easily connect with lignin. This effect generates the apparent increase of the lignin content^{105,106}.

Moreover, the concentration of extractives compounds experienced a considerable increase in all treated species regarding the treatment intensity, with change ratio from 0.92 in Thermo-S to 0.60 in T-pine210. Although most of the extractives compounds disappeared or degraded, particularly the most volatile, new compounds can emerge from wood with increasing the temperature of treatment due to the degradation of structural components of the cell wall. The increase of extractives compounds in softwood species was also reported by other authors, and is probably caused by degradation of polysaccharides during the depolymerization reactions, in which phenolic compounds can be formed in these reactions, also the extractives of the new matrix may be more easily soluble in the ethanol-toluene mixture used for this test^{107,108}.

3.3.1.2 Soluble carbohydrates content

A rapid analytical technique was used to hydrolyze wood in order to fractionate the carbohydrates content and to obtain quantitative data. The main results in Table II-3 showed that the hygrothermal treatments induce changes in the carbohydrates content of wood specimens. The most remarkable change was the quantitative increase of soluble glucans (including cellulose and glucose structural units of the hemicellulosic polymer), as consequence of thermal treatments in all specimens. On the other hand, the main components of

hemicelluloses decreased their proportion because of the treatment. The elevated stability of cellulose and the manifest decrease of hemicelluloses content were a direct consequence of the heat treatments, in which the stability of the glucose proportion (as cellulose constituent) and the diminishing of xylose and arabinose (main constituents of hemicelluloses) confirms that statement¹⁰⁹.

Table II-3 Carbohydrates content and changes after heat treatment of wood.

Compound	Concentration [%]						
	<i>Pinus radiata</i>	<i>T-Pine190</i>	<i>T-Pine210</i>	<i>Quercus robur</i>	<i>T-Oak170</i>	<i>F. excelsior</i>	<i>T-Ash210</i>
Glucan+ Hemicelluloses ^a	53.76	60.67	62.63	59.62	68.61	66.53	78.66
Anhydroxylose	23.12	19.92	18.68	29.63	28.46	30.92	20.44
Anhydrorabinose+ anhydrogalactose ^b	12.12	6.99	5.27	5.04	1.52	1.50	0.90
Anhydromannose	10.99	12.41	13.40	5.71	1.41	1.05	-
Yield of saccharides	69.21	63.49	62.61	77.03	71.16	79.61	74.32
Acetic acid	-	0.84	1.21	-	-	-	1.23

^a Glucan (including cellulose and glucose structural units of hemicellulosic polymers); ^b Amount corresponding to the sum of the compounds

Alterations of wood properties after heat treatment are mainly due to the thermal degradation of hemicelluloses^{87,110}, which are less noticeable in T-Oak170 (Thermo-S class) and are considerable in treatments with higher temperature as in T-Pine210 and T-Ash210 (Thermo-D class). The degradation appears at Thermo-S temperatures when wood is treated under steam atmosphere. According to Weiland *et al.*¹¹¹, wood heat treatment at temperatures comprised between 200 °C and 260 °C causes significant degradation of hemicelluloses with formation of acetic acid, as in the analyzed samples. Two main reactions occur during acid degradation of polysaccharides, and especially of hemicelluloses: rupture of the β -(1-4) linkage between the different sugar units (arabinose,

galactose, xylose and mannose) and dehydration reaction of the resulting monomeric sugars, leading to furfural or hydroxymethylfurfural, which can undergo further degradation (Figure II-3). Degradation of amorphous cellulose starts progressively with the increases of treatment temperature, changing the amorphous cellulose/crystalline cellulose ratio.

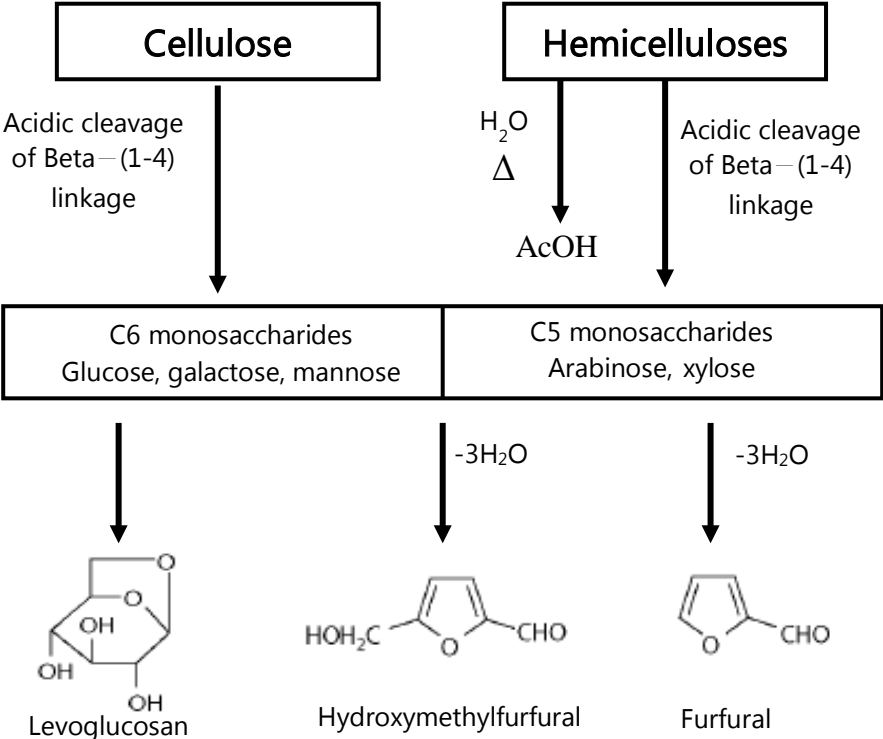


Figure II-3 Scheme of depolymerization and degradation of polysaccharides during wood modification.

3.3.1.3 Wood chemical composition by Py-GC-MS

Conventional analytical methods are principally based on the separation of different components to determine the chemical composition of wood. Pyrolysis-Gas Chromatography/Mass Spectrometry (Py-GC/MS) has been successfully used to determine the chemical composition of lignocelluloses and lignin for several decades. An analysis of the entire polymeric complex is advantageous for

understanding the performance of the thermally modified wood, complementary to wet chemical analyses. The test was carried out using a hardwood and a softwood in order to know the initial differences and the changes due to treatment. A small amount of sample (>400 µg) was used for test, and the results are shown with the corresponding chromatograms in Figure II-4. The identities of the twenty principal compounds released during the pyrolysis and their relative abundances are visible in Table II-4.

The Py-GC/MS technique reveals interesting information about the sequence and relative abundance of the compounds along thermal breakdown of wood components. Regarding the wood pyrograms, a wide range of compounds were reported, although some were predominate in the treated and reference samples, particularly palmitic and stearic acid, furfural and 4-vinylguaiacol. The control specimens (*Pinus radiata* and *Quercus robur*) maintained significant differences in the pyrolytic fingerprints (table II-4), caused by differences in their macromolecular structures¹¹². However, palmitic acid presented the largest area of the pyrolytic product found in both reference samples (peaks: 19 and 14 respectively) at similar retention time.

Moreover, other common saturated fatty acids were present: stearic acid listed as one of the most abundant compounds in reference samples (peaks: 20,15). Eicosadienoic acid, presented only in *Q. robur* sample (peak: 17), and dicarboxylic acid (fumaric acid) presented as a pyrolysis product of *P. radiata* (peak: 1). There was also a relatively high content of aliphatic carboxylic acids; most of them were presented in volatile phase of wood as fatty acids or as their esterified derivatives. Several reaction pathways formed these products, and certain higher-molecular-mass aliphatic hydrocarbons can be found¹¹³.

Table II-4 Peak assignment for the pyrograms obtained. Relative intensity of the products (%) and retention time (RT) are showed.

Compounds list	RT ¹ [min]	<i>Pinus radiata</i>		<i>T-Pine190</i>		<i>T-Pine210</i>		<i>Quercus robur</i>		<i>T-Oak170</i>	
		Peak	Area (%)	Peak	Area (%)	Peak	Area (%)	Peak	Area (%)	Peak	Area (%)
CPC-acid	4.01	-	-	-	-	-	-	1	1.47	-	-
Fumaric acid	4.44	1	1.12	-	-	-	-	-	-	-	-
Furfural	5.49	2	1.22	1	1.29	1	1.15	2	5.02	1	3.16
2-Pyrrolidinone	6.87	-	-	-	-	-	-	3	1.07	-	-
Cyclopentane-1,2-dione	7.78	3	1.93	2	1.68	2	1.55	-	-	-	-
Methylfurfural	8.88	-	-	-	-	-	-	-	-	2	1.01
Methyliminoperhydro-1,3-oxazine	9.88	-	-	-	-	3	1.08	-	-	-	-
Dihydropyrimidine dione	9.92	-	-	-	-	-	-	4	8.30	3	2.96
o-Guaiacol	12.60	4	3.62	3	2.51	4	2.14	-	-	4	1.00
2-Propenoic acid	15.43	-	-	-	-	5	1.12	-	-	-	-
5-Hydroxymaltol	15.44	-	-	-	-	-	-	-	-	5	1.41
4-Methylguaiacol	15.63	5	3.63	4	2.27	6	3.55	-	-	-	-
Catechol	15.75	6	1.45	5	1.19	7	1.14	-	-	-	-
HMF	16.69	7	1.35	6	1.11	8	1.59	-	-	6	2.68
Pyrocatechol	17.76	-	-	-	-	-	-	-	-	7	1.59
Thiocyanic acid	17.87	-	-	-	-	-	-	5	1.23	-	-
4-Heptanol	19.26	-	-	-	-	-	-	-	-	8	1.79
Ethylguaiacol	18.38	8	1.48	-	-	9	1.12	-	-	-	-
4-Vinylguaiacol	19.80	9	4.65	7	3.14	10	2.99	6	1.32	9	1.57
Syringol	21.55	-	-	-	-	-	-	7	1.50	10	2.07
Eugenol	21.83	10	1.57	8	1.17	-	-	-	-	-	-
Vanillin	23.61	11	1.67	9	1.34	11	1.18	-	-	-	-
Benzoic acid	25.48	-	-	-	-	-	-	8	2.14	11	2.39
Trans-iso-eugenol	25.55	12	4.82	10	3.06	12	2.60	-	-	-	-
Propyl guaiacol	25.93	13	1.14	-	-	-	-	-	-	-	-
Benzothiophene	26.48	-	-	11	1.14	-	-	-	-	-	-
Levoglucofan	26.81	-	-	12	1.88	13	1.36	-	-	-	-
Acetovanillone	26.82	14	1.34	13	1.42	14	1.62	-	-	-	-
D-Allose	27.22	-	-	-	-	-	-	-	-	12	1.23
Homovanillic alcohol	28.27	-	-	-	-	15	1.21	-	-	13	1.02
Anisole	29.31	-	-	-	-	-	-	9	3.61	14	3.81
Homovanillic acid	31.91	15	1.98	14	1.25	16	1.05	-	-	-	-
Syringaldehyde	31.92	-	-	-	-	-	-	10	1.22	-	-
Benzofuran	32.18	16	1.10	-	-	-	-	-	-	-	-
Methoxyeugenol	32.94	-	-	-	-	-	-	11	5.05	15	2.07
4-propyl-diphenyl	33.04	-	-	-	-	-	-	-	-	16	1.59
Myristic acid	34.25	-	-	15	1.48	-	-	-	-	-	-
Coniferyl aldehyde	34.44	17	2.34	16	1.50	17	1.48	12	2.31	17	1.8
Desaspidinol	34.62	-	-	-	-	-	-	13	1.47	-	-
Coniferyl alcohol	34.79	18	3.83	17	1.48	18	1.71	-	-	-	-
Undecanoic acid	36.48	-	-	-	-	-	-	-	-	18	1.02
Palmitic acid	38.65	19	4.72	18	17.25	19	10.11	14	9.83	19	8.99
Stearic acid	42.37	20	3.29	19	13.18	20	8.96	15	9.50	20	2.48
Oleamide	45.73	-	-	20	0.79	-	-	-	-	-	-
Cyclolanost	56.86	-	-	-	-	-	-	16	2.05	-	-
Eicosadienoic acid	57.10	-	-	-	-	-	-	17	1.62	-	-
Stigmastan	57.26	-	-	-	-	-	-	18	1.33	-	-
Cycloergost	58.28	-	-	-	-	-	-	19	4.01	-	-
Cycloheptane-4methylene	58.97	-	-	-	-	-	-	20	1.69	-	-

¹RT= Retention Time

Other extractives components were found in *Q. robur* specimen, among them the methoxy phenols, particularly abundant when the starting molecule contains the methoxy group, such as anisole (peak: 9) an important primary product. Other lipophilic compounds, such as steroid hydrocarbons (peak: 18), phenolic

extractives and other compounds (peaks: 1, 7, 16, 19) are significant pyrolysis constituents of hardwoods. Moreover, various compounds derived from the carbohydrate fractions were identified in reference woods, such as furfural (peak: 2), cycloalkane and furanic derivatives, in *P. radiata*, which possibly appear due to the thermal degradation of arabinose and xylose. In addition, 5-hydroxymethyl-2-furaldehyde was identified (peak: 7), which comes from the glucose units of cellulose¹¹⁴.

Concerning the lignin-derived compounds, their pyrolysis products are more easily identifiable than polysaccharides, showing volatile methoxyphenols molecules of guaiacyl-type and their oxidized-derivatives (peaks: 3, 6, 14, 19 *P. radiata*; 4, 2 *Q. robur*), and dimethoxyls of syringyl-type (Peaks: 17, 18 *P. radiata*; +10, 12 *Q. robur*). These compounds are mainly originated from the cleavage of β -O-4 and arylglycerol- β -arylether linkages^{115,116}. Hence thermal degradation of lignin leads to a broad variety of pyrolysis products interacting with other organic or inorganic wood constituents, as indicated above.

In the pyrograms of thermally modified samples, there are present some different degradation products derivate from treatment. In T-Pine190, fatty acids from extractives compounds (peaks: 18, 19) were identified and some products originating from carbohydrates such as levoglucosan (peak: 12), which is an anhydrosugar and the main thermal degradation product of cellulose (see Fig. II-4)¹¹⁶. The pyrolytic behavior in T-Pine210 was relatively similar to the reference wood but with a relative increase in the fatty acids proportion (peaks: 19, 20); also new pyrolytic products appeared from the carbohydrates fractions (peaks: 1, 3, 14). In addition, there was a slight decrease in the relative amount of lignin-derived compounds compared with *P. radiata* but a similar amount regarding T-Pine190.

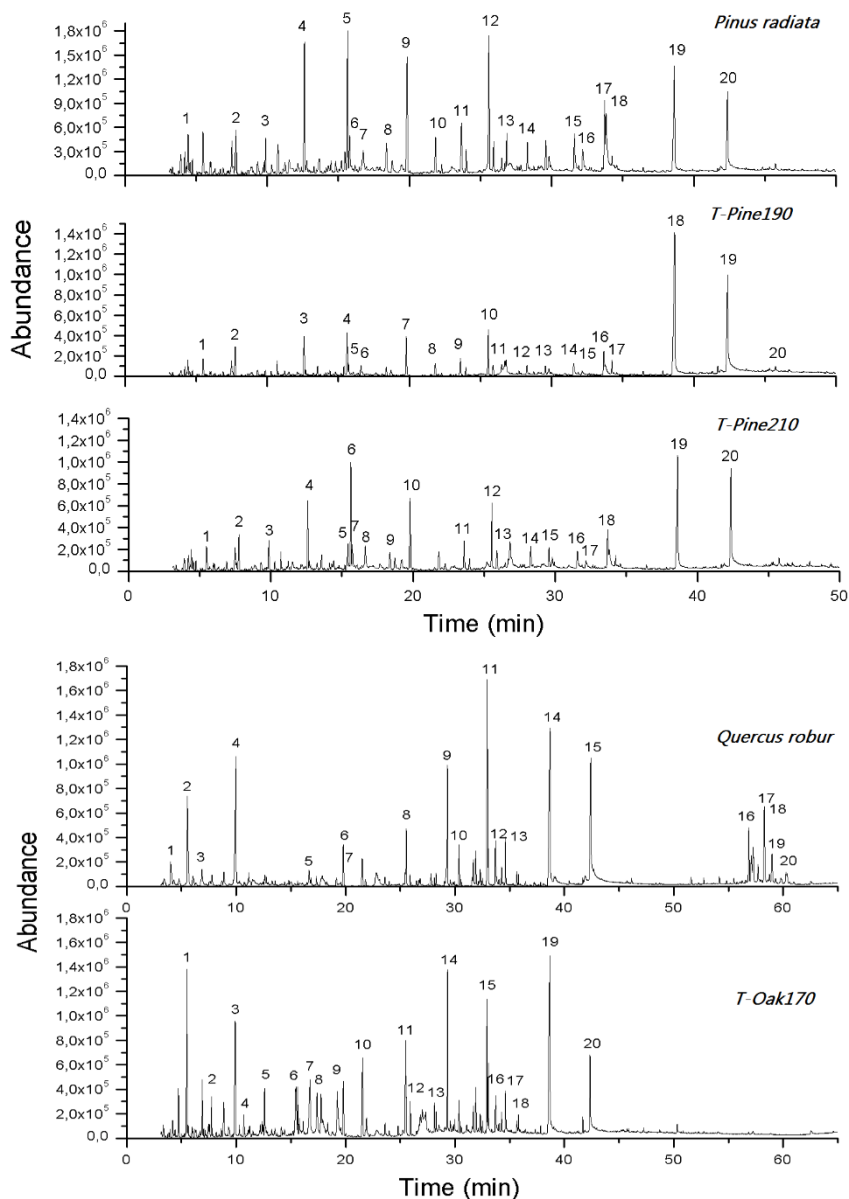


Figure II-4 Py-GC/MS chromatograms of modified and control specimens. Peak labels are listed in Table II-4.

Furthermore, the composition of pyrograms from T-Oak170 reveal significant differences compared to reference samples, some peaks were removed after treatment (peaks: 16-20) and others compounds present a decreasing relative proportion; these compounds are mainly derived from lipophilic extractives such

as fatty acids and others extractives²². On the other hand, fractions derived from carbohydrates increased (Peaks: 1, 2, 5, 6, 13) by releasing new compounds connected with sugar fractions. Although a relative amount of lignin derivatives remained stable, most of the released compounds underwent progressive rearrangements, which in turn are different from those released in *Q. robur*. Cellulose has a strong resistance to hydrothermal treatments, but at high temperatures can be degraded into levoglucosan. Proof of this is the presence of such compound in the pyrograms of T-Pine190 and T-Pine210 but not in the pyrograms of T-Oak170. This behavior could indicate that during thermal modification of *Quercus robur* cellulose was not degraded, because of the lower temperature of treatment. Therefore, cellulosic hydroxyl groups degraded slower than hydroxyl groups of polysaccharides, as demonstrate the carbohydrates analysis^{113,117}.

The pyrolytic products were released from multiple dehydrations and rearrangements at high temperature, and the main decomposed products were derived from carbohydrates (cellulose and hemicellulose destruction products) and lignin derivatives¹¹⁸. In addition, the acids content varied during the treatment, due to the cleavage of acetyl groups in hemicelluloses as well as to the oxidative process of the modification.

3.3.1.4 Wood chemical structure by FT-IR spectroscopy

The differences in chemical structure of wood were observed by FT-IR technique, with the aim of attributing the bands that could belong to carbohydrates and to lignin fraction, and in turn, to visualize all chemical changes that took place during the heat treatments. The common peaks of the spectra and their assignments are listed in the table II-5, and the comparison of all FT-IR spectra is presented in Figure II-5.

In general, the FT-IR spectra of modified samples was analogous to that found in reference but with minor differences. That differences indicating that some chemical modifications in the cell wall have occurred because of treatment. These differences are somewhat complex to interpret since there are several reactions occurring at the same time. However, there were some changes from the mildest treatment corresponding to T-Oak170. In this case a slight decrease in peak at 1734 cm^{-1} was noticeable, and this was assigned to functionality C=O of esters, ketones, aldehydes and acids. The lignin bonds are hampered and thus react with aldehydes groups due to the increase of reactivity, concentration of phenolic groups and its condensation¹¹⁹.

The FT-IR spectra of T-Pine190 and T-Pine210 showed a smoothing wave of the band at 3340 cm^{-1} corresponding to OH stretching vibration from carboxylic acids present in both hemicelluloses and lignin¹²⁰. Acetylation reduces the number of hydroxyl groups in wood, and therefore the intensity of the hydroxyl peak at 3350 cm^{-1} . The reduction of the intensity of the hydroxyl peak indicates that in the treated wood less hydroxyl groups are accessible to be acetylated¹⁰⁰.

Besides, the accessibility of hydroxyl groups for acetylation is highly correlated with the availability of water and leads to a drastic change of the hygroscopicity of wood. The band between 2900 cm^{-1} and 2800 cm^{-1} is composed of the overlapping of the stretch asymmetric and symmetric vibrations of methyl and methylene^{101,121}.

There was an apparent displacement of the CH band due to structural and relative composition changes, probably due to the changes in cellulose crystallinity, which influences the CH and OH stretch frequencies. The bond C=O in T-Pine190 and T-Pine210 showed a different behavior at 1734 cm^{-1} , this is probably due to changes in carbonyl groups of acetoxy xylans, besides, the band at 1716 cm^{-1} is associated with carboxylic groups; this band increases in T-Pine190 while in T-Pine210 was shifted to a flat wave. The increasing and flattening in thermally

modified specimens was described in other studies, and may be due to the increase of carbonyl or carboxyl groups in lignin caused by its oxidation¹²¹.

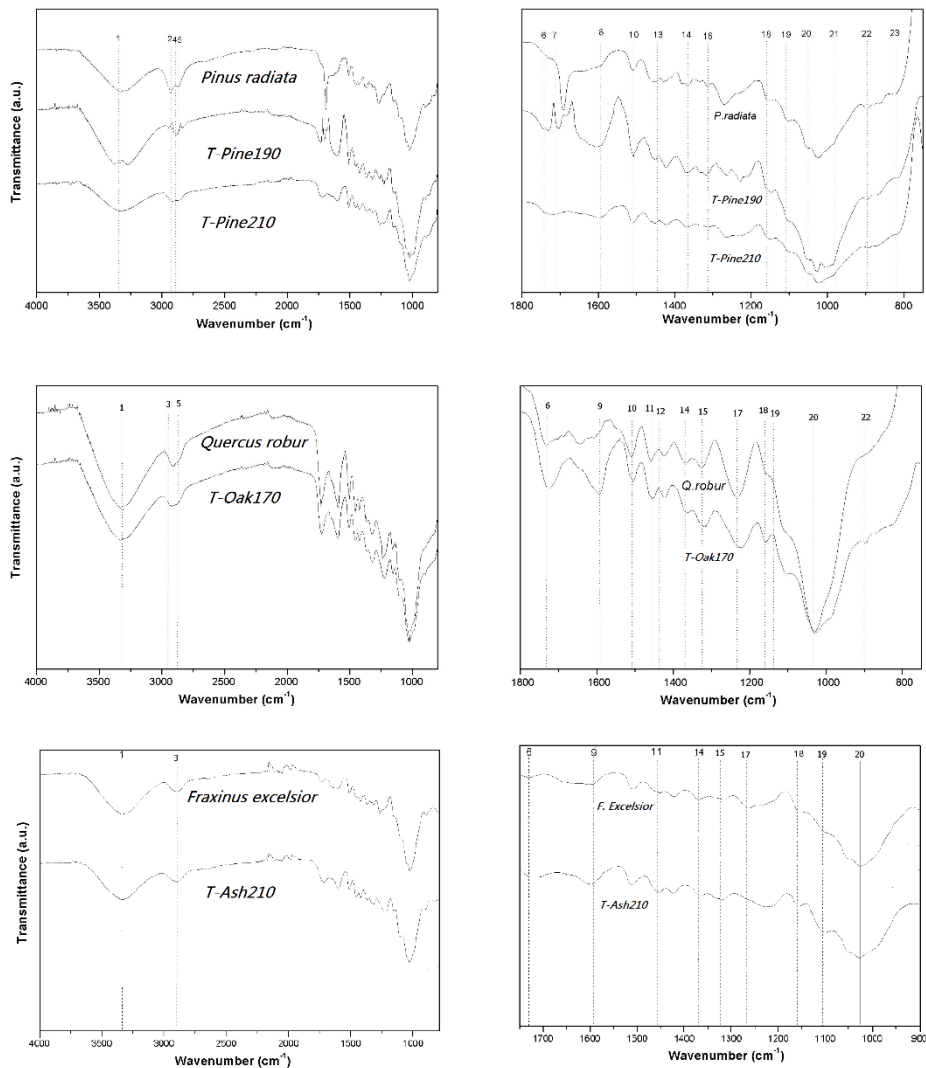


Figure II-5 FT-IR chromatograms of modified and control specimens. Peak labels are listed in Table II-5.

Moreover, the band at 1595 cm^{-1} in T-Oak170 was smoother than in *Q. robur*, and that corresponds to vibrations in the aromatic ring of lignin. Such smoothing effect suggests that there was a structural modification around the aromatic rings and increasing the percentage of lignin in treated wood. At approximately 1500 cm^{-1} is located a characteristic band of aromatic rings, corresponding mainly to

benzene ring over the lignin guaiacyl-syringyl matrix¹²². In *P. radiata* this band was located at 1509 cm⁻¹ and in *Q. robur* was located at 1504 cm⁻¹. However, no remarkable shifting was found in this band.

Table II-5 FT-IR bands present in wood and its assignment.

Wavenumber (cm ⁻¹)			Assignment ¹	Band number ²
<i>P.radiata</i>	<i>Q.robur</i>	<i>F.Excelsior</i>		
3340	3340	3340	OH ostretching (L)	1
2942	-	-	CH ₂ anti-symmetric stretching	2
-	2941	2910	CH stretching in CH ₂ and CH ₃	3
2897	-	-	CH stretching (C)	4
2873	2894	-	CH stretching (C;L)	5
1734	1734	1740	Bond C=O stretching , non-	6
1716	-	-	conjugated carboxylic groups	7
1605	-	-	Aromatic skeletal vibrations (L)	8
-	1595	1595	Aromatic skeletal vibrations (L)	9
1509	1504	-	Aromatic skeletal vibrations (L)	10
-	1456	1460	Anti-symmetric CH	11
-	1424	-	Aromatic skeletal vibrations (L)	12
1456	-	-	CH in plane bending (C;L)	13
1375	1375	1375	CH bending (C;H)	14
-	1327	1324	Syringyl ring breathing with C-	15
1317	-	-	CH ₂ wagging (C)	16
-	1240	1260	Syringyl ring breathing with C-	17
1165	1165	1158	Anti-symmetric bridge oxygen	18
1112	1122	1106	Anti-symmetric in-phase ring	19
1060	1060	1030	CO stretching (C)	20
983	-	-	CO stretching (C)	21
897	897	-	Aromatic CH group frequency	22
815	-	-	Aromatic CH out-of-plane	23

A peak in *P. radiata* was established at 1456 cm⁻¹, which corresponds with the asymmetric deformation of C-H bond of xylan, and according to several authors, this peak appears as effect of hygrothermal treatment^{100,119,120}. The band at 1375

cm^{-1} was different in treated samples, which may represent the relative decrease in the concentration of carbonyl groups due to reduction of wood density. Furthermore, the bands at 1327 cm^{-1} and at 1240 cm^{-1} represent the contributions of syringyl and guaiacyl lignin condensed units¹²².

The bands at 1112 cm^{-1} in *P. radiata* and 1122 cm^{-1} in *Q. robur* were assigned to characteristic CH, CO deformations or stretching vibrations in different groups of lignin and carbohydrates¹²¹. The bands at 1165 cm^{-1} and at 1060 cm^{-1} were assigned to characteristic CO stretching vibrations belonging to diverse groups of carbohydrates. In treated samples, the intensity of the band at 897 cm^{-1} seemed to increase comparing to reference samples, and this band is categorized as sugar ring tensions; the impact on polysaccharides during the treatment may be visualized by the increase of the intensity of this band¹²⁰.

3.1.3.5 Study on the thermal stability of modified wood

The chemical components inside wood are closely combined in each single cell, but the behavior during thermal degradation of the main compounds is diverse, and the components react separately according to temperature intensity. In figure II-6 are represented the thermo-gravimetric (TGA) curves and their derivate (DTG) of thermally modified wood and reference specimens.

The thermal analyses of wood and modified wood, bring an idea of the critical points in which the macro-compounds are degraded and thus, the principal changes that occurs during the treatment and at treatment temperatures. The first stage observed during the thermal degradation was the dehydration process from room temperature up to $130 \text{ }^\circ\text{C}$, where noncombustible products, traces of inorganic compounds and water vapor were produced. Such type of behavior is analogous in treated and reference samples. The mass loss during this phase is about 7-8% in reference specimens, and is gradually reduced with the increase of treatment temperature¹²³.

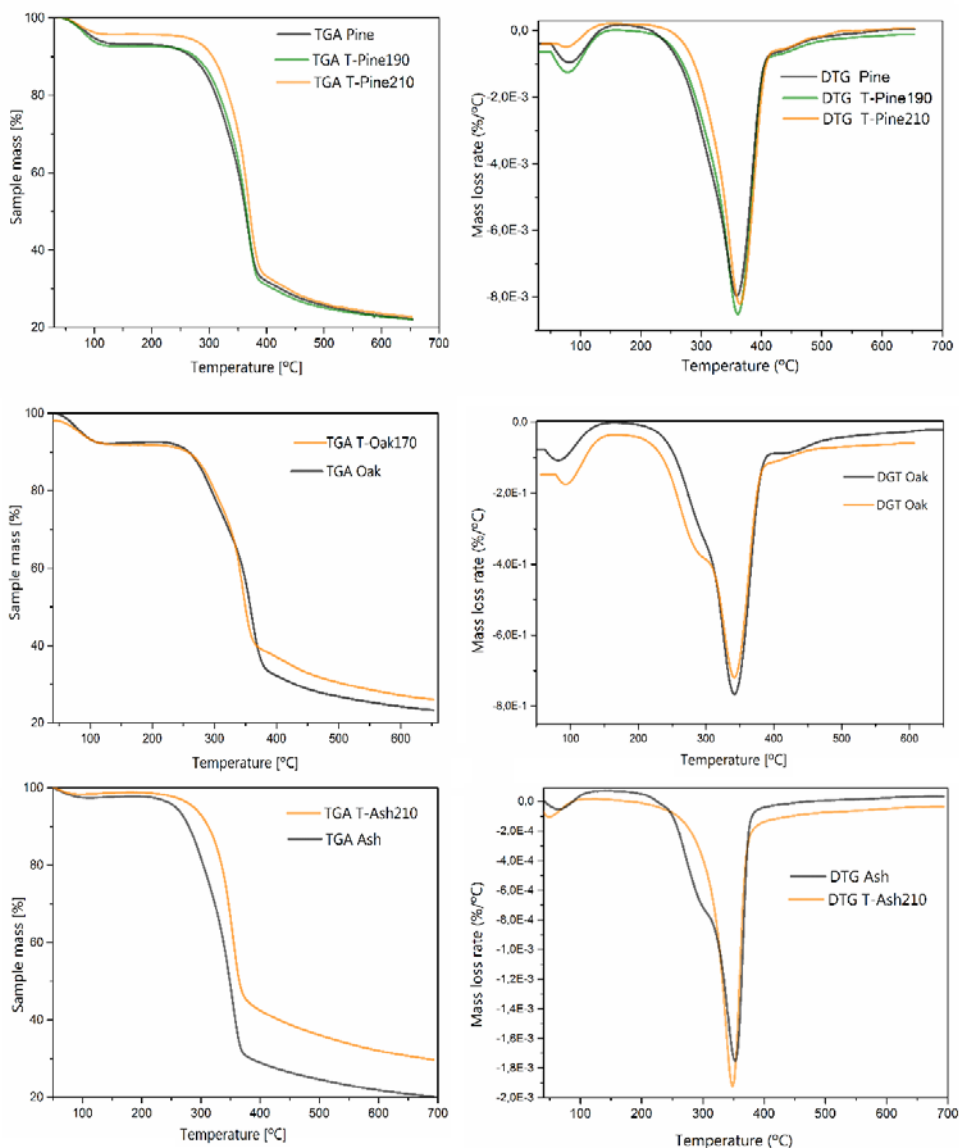
There was no apparent mass loss at the temperature range from 130 to 180 °C, however, degradation of hemicelluloses has already started below 170 °C (or before in T-Oak170), and some wood components began to break their bonds. These compounds mainly belong to lignin structures, which exhibit high structural diversity and their degradation starts gradually over a wider temperature range than carbohydrates. The thermal modification mainly affects the most hydrophilic compounds, principally those that belong to hemicelluloses, subjecting these to dehydration reactions with the consequent destruction of hydroxyl groups. As a result, the treated wood has a lower water affinity, and thus, improving its dimensional stability^{123,124}.

Moreover, the main loss of mass is observed at temperatures in range from 200 °C to 360 °C in *P. radiata* (T-Pine and reference), and from 180 °C to 350°C in *Q. robur* (T-Oak170 and reference). The mass reduction is higher in reference samples than in thermally treated samples, reaching the maximum difference in T-Pine210. On this thermal stage, the deterioration of hemicelluloses has already begun and the highest proportion of lignin degradation occurs. At temperatures about 300 °C, a crossing of thermograms (TGA –DGA) takes place, which is the thermal segment more critical for the degradation of hemicelluloses. In control samples and in the mild treatment T-Oak170, some of these compounds have already degraded (mainly lignin and amorphous cellulose), since the minimum temperature for the decomposition of cellulose crystals in inert atmosphere is about 300 °C and 360 °C¹²⁵.

The TG curves in *P. radiata* (treated and reference) showed a mass loss of around 60% in the range from 200 °C to 380 °C, while in *Q. robur* it was around 50% in the same range. This range is the most critical for the polymer degradation, where all the structural constituents undergo thermal breakdown, being steepest in hemicelluloses at lower temperatures, and in cellulose at temperatures higher than 300 °C. After 375 °C, the thermal decomposition was carried out slowly until

650 °C, wherein the degree of thermal decomposition of cellulose was about 80%. In general, the thermograms show higher thermal stability (>5-20%) and lower water content in heat-treated samples than reference samples, maybe due to cross-linking of wood polymers during treatment^{125,126}.

Figure II-6 Thermo-gravimetric curves and their derivatives (DTG) of Pine, Oak and Ash and modified samples.



3.1.3.6 Acidity and pH of wood

The results of this section are expressed in terms of pH and water-insoluble acidity, which are negatively correlated (Fig. II-7). The acidity of wood increases after heat-treatment of the softwood sample, as follows: Pine<T-Pine210<T-Pine190, this effect inversely proportional in the pH values. In the mild heat treatment of hardwood occurs the same tendency (T-Oak170). The increase in the acidity after modification may be attributed to the formation of carboxylic acids, such as acetic and formic acids. The formation of acetic acid already begins at temperatures lower than 200°C, and is caused by the cleavage of acetyl groups of hemicelluloses¹²⁷. Therefore, a high acidity is present after a mild treatment (170,190 °C), but a severe treatment (210°C) led to a lower acidity in T-Pine210 and much lower in T-Ash210.

Although carboxylic acids are also formed during the strong modification process, may be vaporized and emitted from the wood to treatment kiln at high temperatures⁹⁹. This could cause a greater release of organic acids as volatile organic compounds out of the kiln at higher temperature, resulting in the incorporation of the acids in the wastewater.

Table II-5 Acidity and pH values in modified and control samples.

Sample	<i>Pinus radiata</i>	T- Pine190	T- Pine210	<i>Quercus robur</i>	T- Oak170	<i>Fraxinus excelsior</i>	T- Ash210
Acidity [meq g ⁻¹ drywood]	1.93	3.45	2.51	1.15	3.81	2.81	1.59
pH	5.36 ±0.10	4.28 ±0.12	4.82 ±0.23	4.75 ±0.08	4.33 ±0.11	4.55 ±0.14	5.32 ±0.26

Average value of three measurements

The effect of pH regulation by the process conditions can help understanding the changes that occur in the chemical components of wood. Consequently, hemicelluloses will be hydrolyzed preferentially, in a mild heat treatment of wood in acid medium, and dehydration reactions during thermal treatments of

polysaccharides will cause a decomposition of hydrolyzed sugars. Pyranosidic ring structures will be dehydrated into hydroxymethylfurfural and furanosidic ring structures in furfural⁷³. Acidic extractives in some wood species interfere with the curing and hardening reactions of adhesive and coating systems and are associated with increased brittleness of the coating film, reduced adhesion strength, and peeling of the coating from the wood¹²⁸. Alternatively, the preferential removal of acidic extractives during the modification of T-Ash210 decreased its acidity, and in this case, could increase adhesion of a waterborne coating.

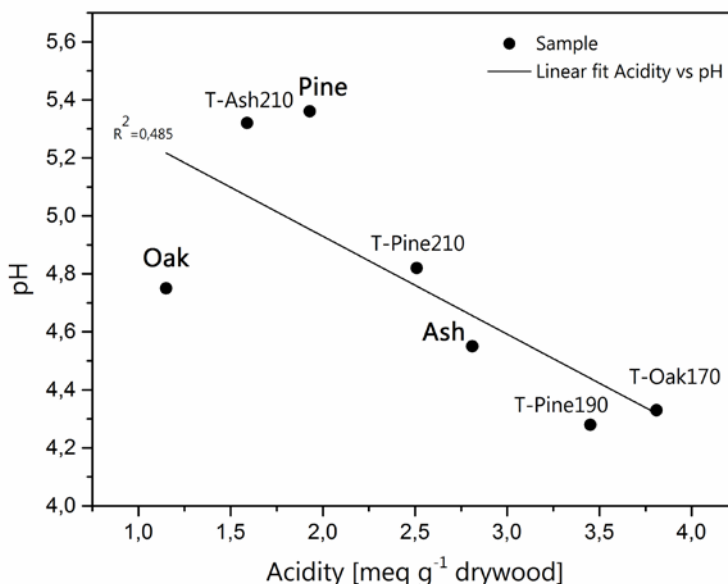


Figure II-7 Correlation between acidity and pH of wood samples.

3.1.3.7 Conclusions

The results of this extensive chemical analysis showed the changes that occurs during the thermal treatment and principally the effect of the hydro-thermolysis in the fractions of hemicelluloses. The most hydrophilic compounds were depolymerized, decreasing the availability of hydroxyl groups, in addition to the hydrolysis cleavage of acids mainly from acetyl groups. The changes are induced by different chemical reactions occurring simultaneously, and the presence of

water plays an important role in the catalyst (depolymerization) of carbohydrates (autocatalysis of the process). Moreover, polycondensation reactions occurred that contributed to the increase of the lignin content, resulting in a cross-linking of the lignin network. These findings contribute to a better understanding of the reaction mechanism of heat treatment process of wood and their effect in the dimensional stability and water affinity.

3.3.2 Physical and mechanical properties of thermally modified wood

The second section corresponding principally to the changes in physical and mechanical properties due to the thermal treatment. In this section were used two different wood species and three different temperatures of treatment. The first specimen was *Pinus radiata* treated at 190 °C and 210 °C (T-Pine190, T-Pine210), and the second one was *Fraxinus excelsior* treated at 210 °C (T-Ash210) for the study of physical properties, and at 190 and 200 °C (T-Ash190 and T-Ash200) for the study of surface wettability. The measurements of this section are summarized in the Figure II-8 and the respective methods are explained in the appendices.

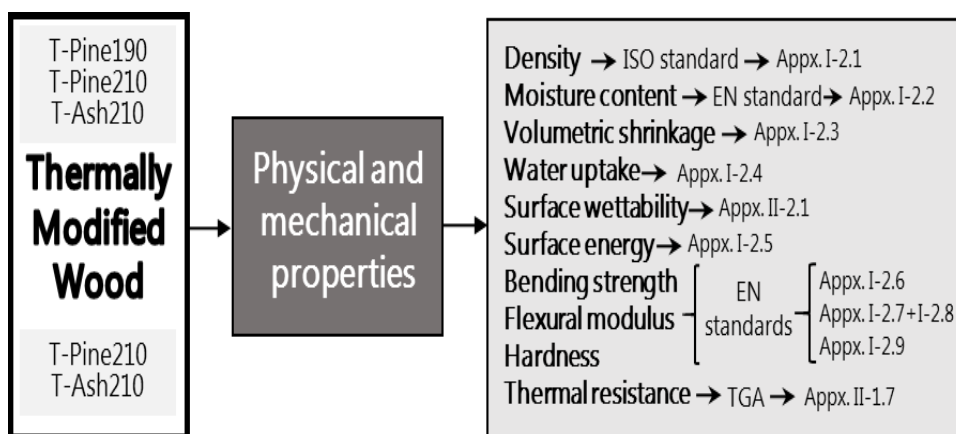


Figure II-8 Scheme of the physical and mechanical properties performed on wood.

3.3.2.1 Changes in some physical properties of thermally modified wood

The chemical analysis of the thermally modified wood showed the loss of hygroscopic hemicellulose polymers and consequently, an effect is the significant decrease of moisture content, and the decrease of wood density (Table II-6). However, there is not a clear MC-density relationship, and initial wood density possibly is not an influencing factor. Thus, the decrease of MC depends on other wood physical changes such as the cell wall thickness or microporosity^{87,129}. One important effect of heat-treatment was the reduction of the hygroscopicity, which in turn contributed to higher dimensional stability. The wood specimens presented a progressive recovery of the volumetric shrinkage of more than 70% comparing control with modified samples; finally, the values of dimensional change were close to 1%.

The influence of treatment in the wood hygroscopicity is a positive effect for outdoor applications where wood is exposed to weather variations¹³⁰. This effect is proportional to the decreasing number of accessible hydroxyls on the cellulose, hemicelluloses and lignin after treatment. All mean values were significantly different ($P < 0.05$) either in volumetric or single direction (longitudinal, tangential and radial).

Despite the fact that a substantial volumetric stability after heat treatment was achieved, the transversal to radial shrinkage ratio (Ψ) presented only a slight decrease towards the unity from control samples to heat-treated. The results showed that wood kept the same order of anisotropy at either high or low moisture content, but improving the dimensional stability after drying treatments (Fig. II-9). Therefore, the anatomical aspects that influenced the wood shrinkage, such as the tracheid structure, cell wall thickness, ray tissues, and the microfibril angles of the transversal directions, were not significantly affected by treatment.

Table II-6 Changes in physical properties of wood after modification.

Sample	<i>Pinus radiata</i>	T-Pine190	T-Pine210	<i>Fraxinus excelsior</i>	T-Ash210
Moisture content [%]	11.02 ±0.50 ^{***}	6.25 ±0.60 ^{***}	5.49 ±0.14 ^{***}	11.08 ±0.92 ^{***}	5.23 ±0.79 ^{***}
Density ¹ [kg/m ³]	454.98 ±45.85 ^{***}	437.88 ±42.18 ^{**}	412.62 ±7.09 ^{**}	670.53 ±32.16 ^{***}	468.14 ±10.78 ^{***}
WL [%]	-	3.76 ±1.58 ^{***}	9.31 ±0.24 ^{***}	-	30.18 ±3.25
WWA [%]	56.32 ±2.21 ^{***}	40.02 ±1.42 ^{***}	34.78 ±1.12 ^{***}	54.65 ±1.95 ^{***}	33.03 ±0.36 ^{***}
Volumetric shrinkage	4.41 ±0.42 ^{***}	1.37 ±0.33 [*]	1.12 ±0.23 [*]	4.32 ±0.92 ^{***}	1.28 ±0.16 ^{***}
Ψ [T/R]	1.47 ±0.33	1.37 ±0.27	1.34 ±0.21	1.43 ±0.20	1.31 ±0.19

¹ oven dry basis; WL:Weight loss; WWA:Weight of water absorbed; Ψ : Anisotropy coefficient; Significance of each set of values means (one-way ANOVA): (***) significantly different, P<0.001; (**) significantly different, P<0.01; (*)significantly different, P<0.05

Thermally modified samples (T-Pine190, T-Pine210, T-Ash210) showed a clear reduction of water uptake (%WWA) compared to unmodified wood. Anatomically, heat treatment degrades the tracheid walls during heat treatment, affecting the major components of the cellulose cell wall, responsible for the reductions in density, thickness swelling and modulus of rupture¹³¹. The lower water uptake in heat-treated wood compared to untreated wood, shows that the changes in

wood–water relationship are more affected by the chemical composition than its anatomical structure.

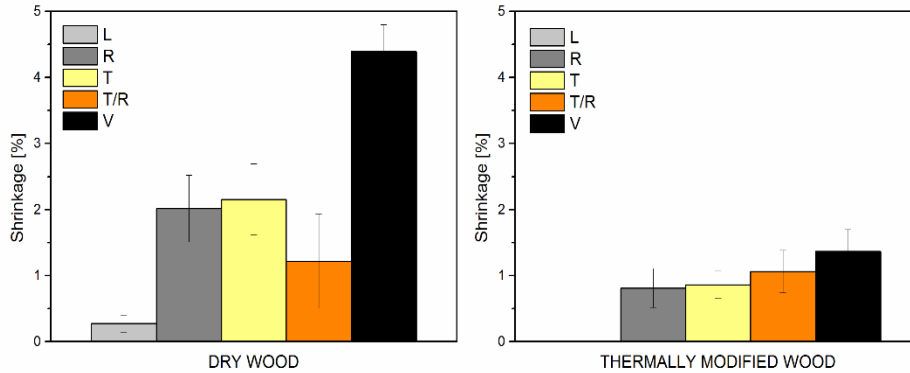


Figure II-9 Dimensional stability in dry wood and thermally modified wood.

3.3.2.2 Surface wettability and liquid-solid interactions

The evaluation of the modified wood surface wettability was performed according to the results of the equilibrium contact angle with three liquids of different polarity: water ($\gamma_{LV} = 72.8 \text{ mN/m}$; $\rho = 998 \text{ kg/m}^3$), ethylene glycol ($\gamma_{LV} = 47.7 \text{ mN/m}$; $\rho = 1113 \text{ kg/m}^3$) and methylene iodide ($\gamma_{LV} = 50.8 \text{ mN/m}$; $\rho = 3325 \text{ kg/m}^3$). In addition, the surface free energy was evaluated from the results of the three tested liquids, and the samples used for the evaluation were *Fraxinus excelsior* industrially treated at three different intensities: T-Ash190, T-Ash200 and T-Ash210. The results and calculations are presented in table II-7.

The interactions between reference liquids of different molecular properties and surfaces were assessed by measuring a sessile drop contact angles. The results reveal major differences between control and the modified woods (from mild to strong treatment), especially evident as increase of the contact angles for each liquid and principally water (θ_w). The migration of hydrophobic compounds and physical parameters variations, may promote the inactivated wood surface and the reduction of adhesive absorption into the wood, in addition to the molecular

reorientation of the surface functional groups and the cell micropores closure^{132,133}.

Table II-7 Liquid-solid interactions and values of work of cohesion.

Evaluation		<i>Fraxinus excelsior</i>	<i>T-Ash190</i>	<i>T-Ash200</i>	<i>T-Ash210</i>
Contact angle	ϑ_W	66.31	99.96	99.19	97.20
	ϑ_E	29.40	30.10	37.90	35.20
	ϑ_D	19.70	27.60	23.50	25.30
Surface free energy	γ_S^p	44.88	0.020	0.020	0.010
	γ_S^d	06.78	52.79	52.36	51.72
	γ_S^T	51.66	52.81	52.39	51.72
Work of cohesion	W_C	103.3	105.6	104.8	103.5

The surface free energies γ_S^T , was calculated as a superposition of its polar and disperse contributions, and was comparable between thermally treated and reference samples. However, the share of the polar-to-dispersive distributions changed remarkably, shifting from low to high disperse contribution (γ_S^d) in addition to strong reduction of γ_S^p . These effects are associated to the decrease of equilibrium moisture content occurring in modified samples leading to a non-polar character of the thermally treated wood¹³⁴. Other authors consider that the changes in polarity are caused by the removal of acid components during the acetylation in the modification process¹³⁵. The reduction of the acid-base component after thermal modification could be supported in this study by the decrease of acidity and the increase of pH especially in T-Ash 210.

3.3.2.3 Mechanical properties of thermally modified wood

Strength and stiffness in bending are generally expressed as modulus of rupture (MOR) and modulus of elasticity (MOE), respectively. These properties were determined by three-point bending, and two values of flexural modulus (MOE)

were calculated: Firstly, the standard MOE according to EN 408:2010+A1:2012 but correcting the effects of the equipment used. Secondly, the MOE was measured from five different spans considering the shear effect and local deformations, in order to create a linear regression model to finally indicate an adjusted value (Appendix I-2.6).

Heat-treated wood mechanical resistance, and particularly MOE and MOR in bending, decrease according to the treatment intensity (Table II-8). These results shown that wood stiffness in *Pinus radiata* was unaffected by treatment temperature, whereas the values were similar when modifying at 190 °C or at 210 °C. However, in *Fraxinus excelsior* the wood stiffness decreased significantly up to 40% of the initial value. This result indicated that in some case is necessary to adjust the treatment parameters such of temperature or schedule time, in order to an improvement in dimensional stability in treated *Fraxinus excelsior* wood, with a far less substantial loss of mechanical performance.

Table II-8 Changes in mechanical properties of thermally modified samples.

Properties	<i>Pinus radiata</i>	<i>T-Pine190</i>	<i>T-Pine210</i>	<i>Fraxinus excelsior</i>	<i>T-Ash210</i>
MOE ^a [MPa]	13597 ±1041.61	13850 ±1041.61	14220 ±1435.49	13546*** ±1704.02	8190*** ±1233.90
MOE ^b [MPa]	14720 ±802.78	13983.12 ±657.65	14102 ±1115.97	13689 ±1309.92	8338 ±977.39
MOR [MPa]	129.34 ±10.02***	101.29 ±4.80***	80.39 ±10.37*	138.39 ±20.53***	63.58 ±3.46***
HB [MPa]	3.75 ±0.37***	3.09 ±0.14***	2.44 ±0.43***	5.77 ±0.81***	5.02 ±0.63***

^a MOE from the linear regression model; ^b MOE calculated according to EN 408:2010+A1:2012

Regarding the bending strength (MOR), it is well known that thermal modification particularly affects this mechanical parameter, with values between 3 and 50% lower than unmodified softwoods or hardwoods, so it is generally qualified for non-structural elements such as cladding on wooden buildings^{88,136}. In this study, the modulus of rupture (MOR) significantly dropped up to 55% lower after thermal modification. The bending strength loss seems to be an effect of the degradation of the hemicelluloses fraction and structural changes, since this fraction is the most thermal-chemically sensitive. Above 180 °C some chemical reactions are produced which could even affect the cellulose fraction, increasing its crystalline proportion, and thus having a negative impact on MOR (Fig.II-10). This effect seems to be evident when using T-Ash samples (MOR<50%), and slighter on T-Pine samples (MOR<30%)

Concerning the surface hardness (refers to the Brinell hardness measured in tangential direction), the values were lower in modified wood than control as follows: Ash>T-Ash210>Pine>T-Pine190>T-Pine210; these differences are usually due to the type of wood (hardwoods or softwoods). However, the decrease was higher in treated hardwood (up to 35%) than in treated softwood (decrease of 12%). Several studies showed different effects on the hardness of wood, a decrease but also an increase has been noticed (depending on the wood species and treatment method)^{137,138}.

In this study, the hardness decreased to varying degrees, depending on the specie more than temperature. Thermally modified wood has growing market in outdoor applications, and the mechanical properties are important in service as for exterior applications, like exterior cladding, windows and door joinery, garden furniture, and decking. There are also many indoor applications, such as flooring, paneling, and kitchen furnishings and interiors of bathrooms and saunas^{139,140}. Because it loses strength, modified wood is not recommended for structural applications.

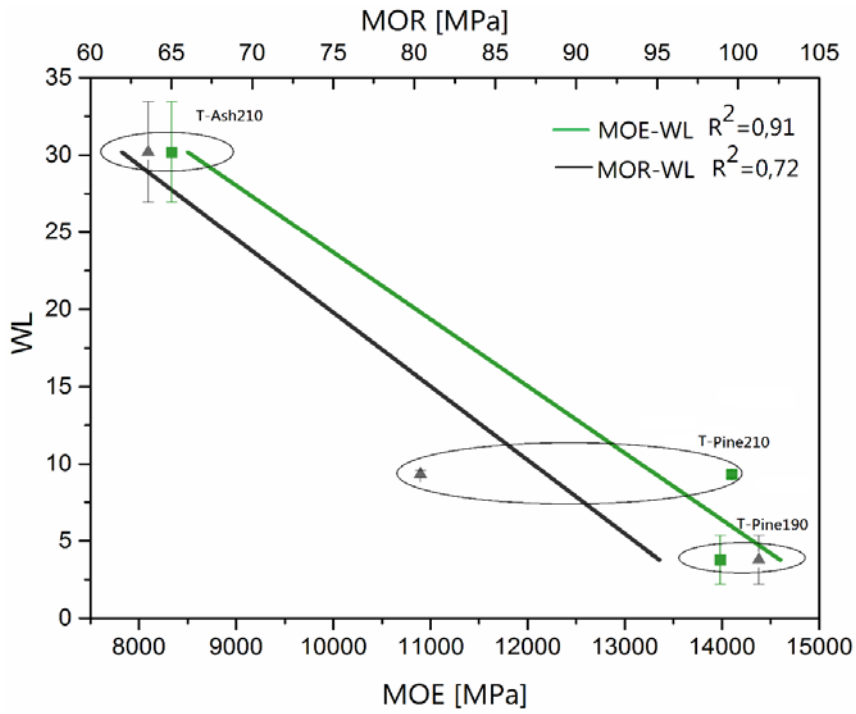


Figure II-10 Correlations between weight loss and MOR, MOE after heat-treatment.

3.3.2.4 Thermal resistance of thermally modified wood

In this section, the thermo-gravimetric analysis was performed to assess the thermal degradation of the wood samples (in O₂ atmosphere) and the influence that treatment had over the thermal behavior. The curves of the thermo-gravimetric analysis (TGA) include the performance of *Fraxinus excelsior* and *Pinus radiata* and their modifications T-Ash210 and T-Pine210 (Fig. II-11).

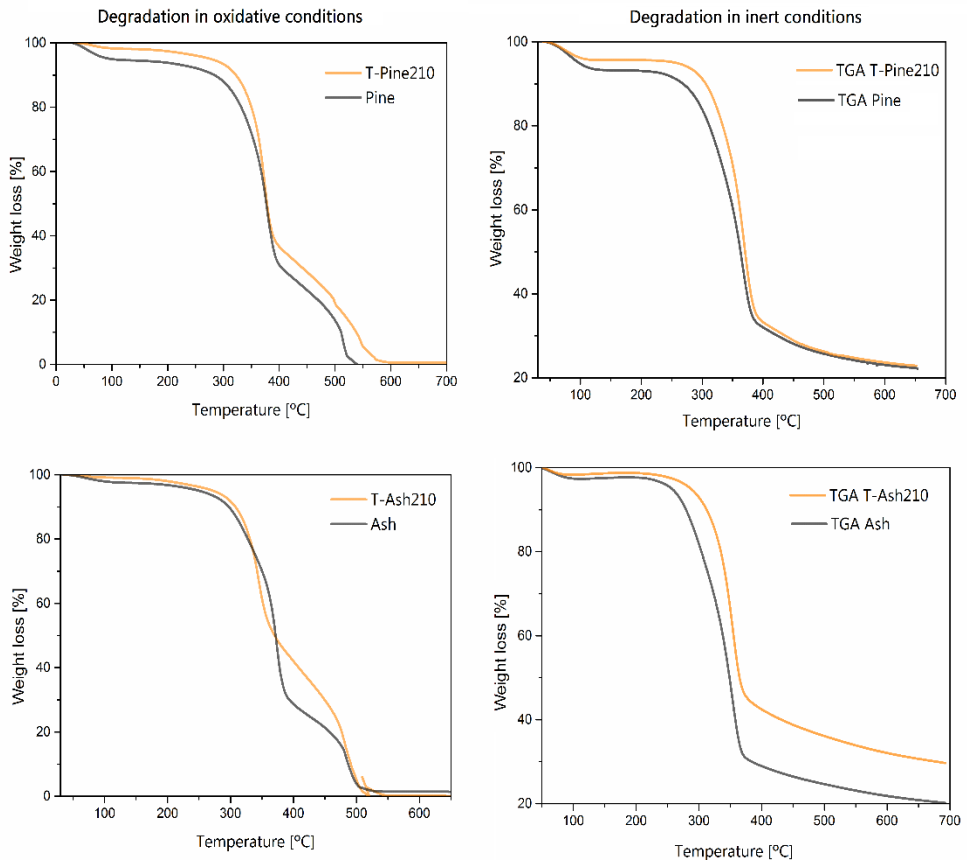


Figure II-11 Thermal degradation performance of wood in inert and oxidative conditions.

From this figure, it was observed that the thermal degradation of wood presented several stages; the temperatures when wood is degraded at 10, 50 and 100% were obtained from the first derivative of TG points (DTG) and expressed in Table II-8. Thermal analysis technology is useful for obtaining information about the

degradation of studied samples during the course of temperature change. The effectiveness of fire behavior on wood may be evaluated and the effect of volatiles formed with increasing temperature, which is related to amount of residue produced¹⁴¹. In addition, the thermo-oxidation during the process is observed with TG/DTA when comparing the degradation process in inert (N₂) and oxidative (O₂) environment, revealing the weight change process with relevant heat change⁴.

Table II-9 Ranges of thermal degradation of wood and their temperatures.

Sample	T _{10%}	T _{50%}	T _{max}
<i>P. radiata</i>	283.39	376.97	377.42
T-Pine210	322.20	378.15	373.83
<i>F. excelsior</i>	297.23	371.83	373.56
T-Ash210	307.91	371.00	345.14

The pyrolytic behavior of wood was quite complicated for its heterogeneous constitutes. Different thermal pyrolytic pathways competed with each other, and it was believed that the thermal degradation behavior could be altered in the modified wood matrix. Comparing to the untreated wood, there were differences for thermal degradation of modified wood through different pyrolytic pathways. After the slight weight loss around 100°C related to the vaporization of moisture, one difference between control and modified wood was the decrease of initial degradation temperature, more evident in Pine vs. T-pine thermograms. Then, another step was observed in the range 200-280°C with a mass loss around 5-10%. This step was associated to the dehydration and carbonization of hemicelluloses. The third step was observed in the range between 300-380°C and was related to the degradation of the cellulose polymer, since it is said to be stable to thermal degradation until 370°C. This stage represented the 50% of the mass loss, since the cellulose is the main component present in wood samples

(Table I-2). By the end of this step, the major part of the carbohydrate polymers were already degraded. Hence, the final stage was due to the degradation of the lignins, and the char formed from celluloses. This last stage in the range 400-525°C represented around the 20-25% of the mass loss. The samples were totally degraded and no residue was left when the temperature reached 600°C.

The major finding of TGA analysis is the slowing of degradation of thermally modified wood in the early stages of degradation, which corresponds to an increase in minimum energy required to start the active thermal decomposition in wood. The modified wood underwent thermal decomposition in temperature above 300 °C while in unmodified was in the range between 280-290 °C. The feasible reasons of this effect may be due to catalyzing dehydration, rearrangement, and carbonization of polysaccharides, reducing the formation of volatile flammable gas.

3.2.2.5 Conclusions

The results of physical properties, mechanical strength and wood-water interactions showed the effect of treatment on the cell wall constituents, in which tracheid's (softwood) or fibers (hardwood) degradation reduce the water uptake. In addition, the microfibrils proportion and their angle orientation are responsible for the reductions in density, thickness swelling but also for the lower modulus of rupture. The surface free energy of modified wood was similar to reference samples. Nevertheless, the polar-to-dispersive distribution shifts from low to high disperse contribution, leading the wood to a non-polar character. The mechanical resistance, and particularly MOE and MOR in bending decrease according to the treatment intensity, and above 180 °C, some chemical reactions could even affect the cellulose fraction, increasing its crystalline proportion, and thus having a negative impact on MOR and hardness.

3.3.3 Biological durability of thermally modified wood

The third section corresponding to the biological durability of thermally modified wood, specifically the resistance against wood-rotting basidiomycetes. In this section were used two different wood species *Fraxinus excelsior* and *Pinus radiata* heat-treated at 210 °C. After fungal exposure, the material was analyzed in order to find the chemical changes that occurs in wood after attack, as well as the action mechanism of rot-fungi and understand the reasons of the improved durability of thermally modified wood. The procedure and analyses of this section are summarized in the Figure II-12, and the respective methods are explained in the appendices.

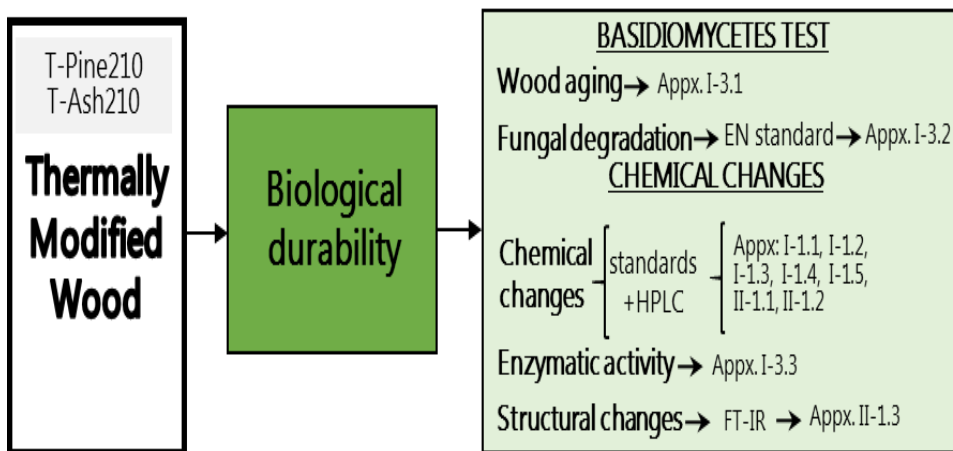


Figure II-12 Scheme of the experimental procedure and measurements of the section.

3.3.3.1 Analysis of biological durability of basidiomycetes tests

The results from wood durability standard tests against white rot and brown rot fungi were examined in order to quantify the changes in wood components, composition of the hydrolyzates, weight and moisture content after fungal decay test. From the set of 10 samples of each species and after eight and 24-week incubation, the mass loss (ML) was calculated following the criteria of EN

113:1996/A1:2004 standard, moisture content (MC) according to EN 13183-1/AC: 2004 and the durability class based on EN 350-1:2007 (results in table II-10).

The wood durability against basidiomycetes clearly differs between heat-treated wood (ML= up to 10% after 24 weeks) and untreated wood (ML= up to 32% after 24 weeks) showing an enhanced durability in modified samples, with durability class 1, 2, according to standard classification.

Table II-10 Results of biological durability test of thermally modified wood.

Sample	Incubation period [weeks]	Fungal strain	MC [%]	Mass loss [%]	x-value	Durability Class [EN 350-1]
<i>Pinus radiata</i>	8	Gt ^a	15.85±0.10	12.46±4.69	-	-
	24	Gt	16.02 ±0.35	28.51 ±8.56	-	-
T-Pine210	8	Gt	6.34 ±0.05	0.81 ±0.42	0.07	1
	24	Gt	6.49 ±0.07	10.28 ±2.36	0.36	3
<i>Fraxinus excelsior</i>	8	Tv ^b	14.18 ±0.14	15.63 ±5.19	-	-
	24	Tv	14.68 ±0.18	32.47 ±11.04	-	-
T-Ash210	8	Tv	5.89 ±0.17	1.23 ±1.17	0.08	1
	24	Tv	6.47 ±0.13	9.36 ±3.06	0.28	2

^a *Gloeophyllum trabeum*, ^b *Trametes versicolor*

The results showed an increase in mass loss over exposure time with both rot fungi and in all wood samples. In control samples from 8 to 24 weeks the mass loss varies about 16% and in treated samples about 8-9%. Moreover, there were no significant differences in samples degradation depending on fungi, providing according to EN 350-1 the durability class 1 in thermally modified samples in short exposition period (8 weeks) and decreasing to class 2-3 in extended period

of exposition (24 weeks). Following these gravimetric results, it is feasible to establish the grade of attack and somehow to predict the behavior through time (Fig. II-13). However, with the available information the reason of the improvement is interpreted only from the MC standpoint, which is quite lower in modified wood (below 6%), and apparently due to the reduced availability of water binding sites on wood surface⁸⁷.

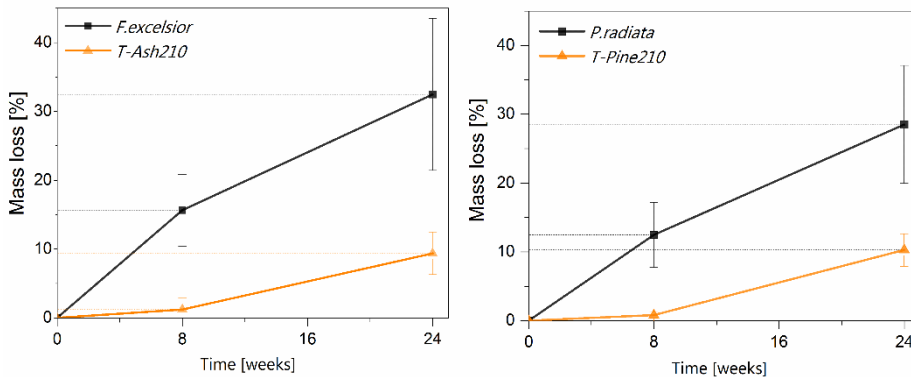


Fig. II-13 Performance over time of wood samples after fungal inoculation.

The changes in MC of modified wood probably reduce the microvoids network and as consequence, the access to interior cell wall or the processes involving surface reaction are delayed enhancing the durability against wood-rotting basidiomycetes¹⁴². However, the moisture content was increasing over time (up to 9-10%) favoring to gradual oxidative degradation and allowing an enzymatic action where mass loss start to be detected.

3.3.3.2 Chemical analysis of wood samples after durability tests

After 8 and 24-week exposure to wood-rotting basidiomycetes, the specimens were subjected to wet chemical analyzes in order to quantify their changes in chemical composition; these quantitative changes are shown in Table II-11. With respect to control samples, the chemical analysis revealed that during fungal exposition the hemicellulose, cellulose and lignin were gradually diminished in both wood species. A significantly higher change ratio in hemicellulose of *Pinus radiata* (CR = -14.91) compared with *Fraxinus excelsior* (CR = -6.23) was observed.

On the other hand, the extracts content decreased in *Fraxinus excelsior* (CR=-0.54), but increased in *Pinus radiata* (CR=+21.05). The degradation process by *G. trabeum* involves mechanism to produce oxidative residues, mainly low molecular size fragments, that may accumulated during the enzymatic degradation phase and cause an apparent increase in the extractives content of tested samples¹⁴³.

Table II-11 Changes in chemical composition of wood after durability test.

Sample	Hemicellulose (%)	CR ¹	α -Cellulose (%)	CR	Lignin (%)	CR	Extracts (%)	CR	Ash (%)
P.radiata	23.61 ±0.87	-	45.15 ±1.15	-	27.65 ±0.68	-	2.85 ±0.06	-	0.27 ±0.01
Pr-8^a	22.38 ±0.57	-5.21	44.42 ±0.69	-1.62	27.38 ±0.27	-0.98	3.14 ±0.11	+10.18	0.26 ±0.02
Pr-24^b	20.09 ±0.77	-14.91	44.15 ±1.03	-2.22	27.06 ±0.57	-2.13	3.45 ±0.06	+21.05	0.25 ±0.01
T-Pine210	12.89 ±0.49	-	41.48 ±1.01	-	40.20 ±1.11	-	4.77 ±0.79	-	0.26 ±0.01
T-Pine210-8	14.11 ±0.31	+9.47	41.99 ±0.75	+1.23	37.02 ±0.80	-7.91	4.48 ±0.14	-6.08	0.26 ±0.01
T-Pine210-24	18.20 ±0.74	+41.20	43.19 ±1.05	+4.12	32.38 ±1.11	-19.45	3.9 ±0.10	-18.24	0.26 ±0.01
F.excelsior	19.10 ±0.87	-	48.49 ±1.15	-	28.80 ±0.68	-	4.08 ±0.06	-	0.49 ±0.01
Fe-8	18.38 ±0.79	-3.77	47.89 ±0.63	-1.24	28.58 ±0.52	-0.76	3.66 ±0.15	-10.29	0.39 ±0.06
Fe-24	17.91 ±0.49	-6.23	47.22 ±1.01	-2.62	27.98 ±1.08	-2.85	3.65 ±0.09	-10.54	0.36 ±0.01
T-Ash210	12.12 ±0.24	-	40.33 ±0.46	-	37.39 ±1.08	-	5.90 ±0.26	-	1.06 ±0.01
T-Ash210-8	13.52 ±0.74	+11.55	41.31 ±1.06	+2.43	36.19 ±0.92	-3.21	5.16 ±0.09	-12.54	0.85 ±0.01
T-Ash210-24	15.18 ±0.71	+25.25	42.59 ±0.35	+5.60	34.64 ±1.38	-7.36	3.80 ±0.17	-35.59	0.72 ±0.01

¹ CR= Change Ratio; ^a 8=Samples after 8 weeks of decay; ^b 24=Samples after 24 weeks decay

The relative degradation of chemical components differs according to wood type and rot fungi. In *P. radiata* the brown rot fungus used (*G. trabeum*) mainly attacked polysaccharides whereas lignin has been slightly less affected and the extracts have

relatively increased¹⁴⁴. Moreover, degradation of the white rot fungus (*T. versicolor*) in *F. excelsior* was extended to all components with a less pronounced decline in the polysaccharides¹⁴⁵. The specimens T-Pine210 and T-Ash210 confirmed a high correlation between durability and degradation or transformation of some wood components. The apparently high content of lignin of modified samples could be interpreted as a reducing effect of the components rich in carboxylic acid into aliphatic carboxylic groups during the industrial treatment, which does not involve lignin formation but rather a cross-link of low molecular size fragments together with degradation of polysaccharides¹¹⁰. These added components are relatively more susceptible to an attack by rot fungi as shown by decreasing its content in these specimens. Besides, in the industrial hydrothermal wood a higher concentration of extractives was generated during heating mainly due to degradation of structural components and the subsequent arising of new compounds. This effect did not improve durability of heat-treated wood against fungi since relative content of extracts has been progressively decreased (CR = up to -18; -35), indicating that the extractives did not increase wood resistance neither acted as fungicides during decay test.

In summary, the high resistance of industrial heat-treated wood could focus on fungal degradative mechanisms from the early decay stages where fungal enzymatic mechanisms are unable to access into the wood cell wall and the non-enzymatic mechanisms should be involved. At early stages, modifications in wood polymer network and the lack of accessible nutrients from the polysaccharides are crucial aspects which delay the biodegradation process and the not recognition by rot fungal enzymes.

3.3.3.3 Changes in soluble wood hydrolizates after durability tests

The fractionation and measure of the wood content of soluble hydrolizates was performed by acid hydrolysis and then by using high performance liquid chromatography (HPLC). The quantitative and qualitative data was obtained to

determine the effects of rot fungi in wood during the decay. The main results are presented in Table II-12. After acid hydrolysis, the soluble fraction was quantified to obtain the total hydrolyzates content (THC), which was increasing gradually with the time of fungal exposition, but with greater intensity in control samples. These hydrolyzates arise from degradation products mainly fragments of polysaccharides, which are transformed into monosaccharides and these into decomposition products⁴⁰.

The relative concentration of released sugars and its qualitative fractionation in control samples (treated and untreated) shown a reduced depolymerization degree, with fractions from hemicellulosic sugars (glucose, xylose and arabinose) and cellulose (glucose). The main differences appeared in the modified wood with the formation of acetic acid ($\approx 1\%$; in T-Pine210 and T-Ash210), due to the cleavage of the acetyl groups of hemicelluloses, besides the total degradation of arabinose. After 8 weeks of colonization by rot fungi, in untreated samples the main fractions of sugars diminished relatively (Fig.II-14). In contrast, oxalic acid in *P. radiata* (3%) and *F. excelsior* (2%) was produced. The same trend occurred in the modified specimens (oxalic 2% in T-Pine210 and 5% in T-Ash210; acetic 1% in T-Pine210 and 2% T-Ash210), plus the formation of the organic acids. After 24 weeks of incubation, the maximum depolymerization grade was achieved, with a gradual relative decrease in the polysaccharides hydrolyzates of all samples (treated and untreated), and the increase of the degradation products.

Table II-12 Soluble carbohydrates released after acid hydrolysis (w/w).

Sample	THC ¹ [mg]	Glucose [%]	Arabinose [%]	Xylose [%]	Xylitol [%]	Oxalic acid [%]	Acetic acid [%]	Other acids [%]
P.radiata	99.31	66.26	2.64	31.73	-	-	-	-
	±4.32	±0.92	±0.17	±1.35	-	-	-	-
Pr-8	101.26	61.73	1.05	33.83	0.08	3.02	-	-
	±12.92	±1.15	±0.02	±0.14	±0.38	±0.65	-	-
Pr-24	107.16	54.06	0.61	35.49	0.21	7.52	2.69	0.92
	±13.19	±2.81	±0.52	±1.72	±0.02	±1.12	±0.45	±0.08
T-Pine210	83.01	67.89	-	31.10	-	-	1.12	-
	±2.92	±0.41	-	±0.67	-	-	±0.24	-
T-Pine210-8	83.84	66.80	-	30.80	0.12	2.04	1.21	-
	±2.45	±0.80	-	±0.14	±0.04	±0.94	±0.05	-
T-Pine210-24	86.25	62.42	-	30.02	0.16	5.24	1.46	0.81
	±2.97	±1.79	-	±0.86	±0.02	±2.94	±0.23	±0.02
F.excelsior	89.50	67.33	2.55	30.95	-	-	-	-
	±3.16	±0.25	±0.24	±0.04	-	-	-	-
Fe-8	92.05	66.88	1.95	27.67	-	2.12	2.21	-
	±4.65	±1.03	±0.03	±3.35	-	±0.65	±0.36	-
Fe-24	100.35	59.95	0.15	25.87	0.05	5.52	7.87	0.40
	±2.65	±3.45	±0.02	±2.13	±0.01	±1.12	±1.24	±0.01
T-Ash210	84.40	78.66	-	20.34	-	-	1.23	-
	±3.21	±0.06	-	±0.04	-	-	±0.16	-
T-Ash210-8	85.63	74.72	-	17.30	0.25	4.82	1.69	-
	±1.05	±2.41	-	±0.32	±0.12	±0.14	±0.41	-
T-Ash210-24	88.30	68.02	0.13	15.61	0.93	13.53	2.23	0.52
	±1.02	±1.63	±0.08	±1.16	±0.42	±1.63	±1.12	±0.04

¹ THC= Total Hydrolyzates Content

In summary, the results showed an increase of THC over time in all samples along with a relative decrease of polysaccharide fractions and a gradual bioconversion to products, mainly organic acids. Therefore, by correlating data of wood hydrolyzates together with durability test is reasonable assign the apparent lignin percentage (after modification) as a lignocellulosic cross-linking of low molecular size fragments with a small amount of fermentable sugars. The stages of wood colonization involve an initial non-enzymatic phase wherein degradation mechanisms run efficiently in control samples followed by an enzymatic depolymerization, with certain differences depending on the rot fungus and the

selected wood species¹⁴⁶. On the modified wood, the 'destructive' enzymatic phase takes part only after a long-lasting non-enzymatic phase, getting moderate mass losses. As an indicator of initial oxidative phase was the formation of oxalic acid and, in a lower level, acetic acid. These low molecular weight compounds, probably secreted by white and brown rot fungi, are crucial in early biodegradation mechanisms, acting as direct agents in oxidative process as well as mediators in the subsequent enzymatic decay¹⁴⁷.

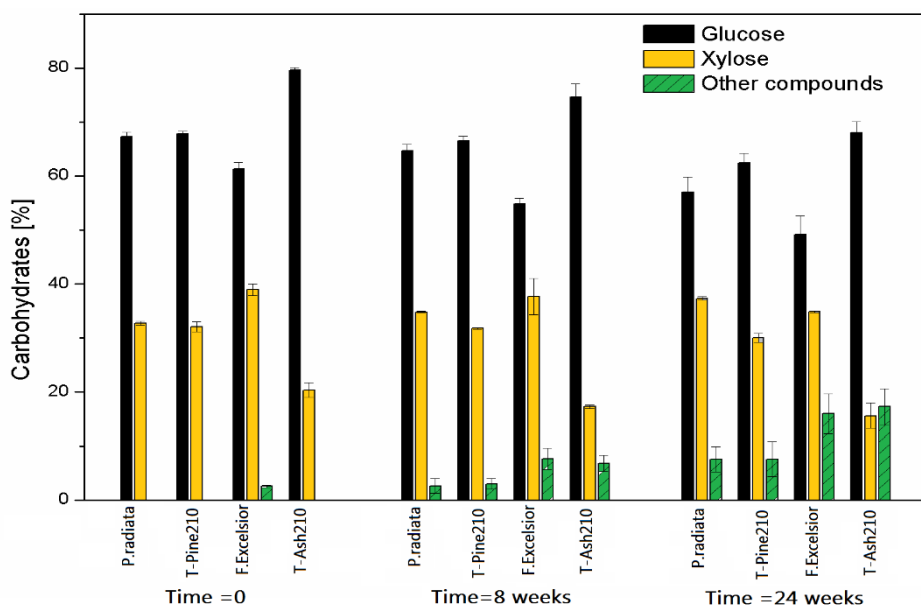


Figure II-14 Evolution of soluble carbohydrates in wood with rotting-fungi.

During the non-enzymatic biodegradation, oxalic acid was the main carboxylic acid released of wood-rot fungi interactions, which has the ability to be a strong chelator of Fe_3^+ and Fe_2^+ , with a large influence on Fenton chemistry as well as in redox properties of iron-oxalate complexes to iron solubilization. The basis of Fenton chemistry ($Fe_2^+ + H_2O_2 \rightarrow Fe_3^+ + OH + \cdot OH$), describes the use of iron present in wood, through its reduction to Fe^{2+} until react with hydrogen peroxide to generate the $\cdot OH$ radical (Fenton-based $\cdot OH$) during the first steps of fungal decay¹⁴⁸. Such radical is a strong oxidant probably depolymerize polysaccharides via hydrogen abstraction, being a possible interpretation to non-enzymatic mechanisms used by *G. trabeum* and *T. versicolor* wood-rotting fungi.

3.3.3.4 Hydrolytic enzymes activity during fungal degradation

The main purpose was to observe the degree of depolymerization of wood constituents due to enzymatic hydrolysis, and to analyze the composition of the degraded products, in order to verify the differences between samples over time and the enzymatic efficiency on thermally modified wood.

The enzymes cellulase and endo-1, 4- β -xylanase were used to perform enzymatic hydrolysis, taking into account the fact that the main fractions degraded in the fungal test were glucose and xylose. Thus, the samples were subjected to enzymatic hydrolysis for 72 h, successively was measured the degree of depolymerization according to weight loss as well as the released fractions by cellulase and xylanase enzymes^{149,150} (Table II-13).

With respect to control samples (without fungi), the depolymerization degree observed in untreated samples was quite higher with mass losses between 25% and 30% in unmodified samples and between 6% and 14% in thermally modified samples. This remarkable variation suggests that the distribution of modify wood chemical constituents positively influences durability against rot fungi reducing its enzymatic efficiency. The decreased content in polysaccharides and its cross-linking with fractions of lignin could limit the enzymatic recognition and delay enzymatic degradation.

At the same time, a gradual increase in depolymerization was observed in the durability test samples (decayed samples) with certain differences depending on the enzyme used. Thus, enzymatic degradation after exposure for 8 weeks was increased between 6% and 10% in modified samples while in untreated samples about 2%. In accordance with the results, the enzymatic mechanisms started gradually to depolymerize the samples, suggesting that during the fungal decay test non-enzymatic stages act by facilitating a subsequent enzymatic intracellular access¹⁵¹.

Table II-13 Soluble compounds released after enzymatic hydrolysis (w/w).

Sample	WL ¹ [%]	THC ² [mg]	Polysaccharides [%]	CR ³	OC ⁴ [%]	CR	Oxalic Acid [%]
PrX ^a	27.20 ±3.23	1.41 ±0.03	98.16 ±1.26	-	1.84 ±0.24	-	-
Pr-8X	32.89 ±2.36	23.65 ±3.69	94.52 ±9.65	-3.71	2.20 ±0.07	+19.56	3.64 ±0.08
Pr-24X	43.95 ±3.56	40.83 ±3.63	90.34 ±7.53	-7.97	5.95 ±0.44	>100	4.45 ±0.12
T-Pine210X	6.12 ±0.26	0.99 ±0.07	90.34 ±0.15	-	9.70 ±0.02	-	-
T-Pine210-8X	12.65 ±1.39	8.36 ±1.34	79.35 ±9.10	12.17	14.34 ±1.10	+47.84	11.96 ±0.47
T-Pine210-24X	31.83 ±4.81	21.50 ±2.67	78.50 ±2.68	13.11	12.98 ±1.20	+33.79	14.74 ±1.94
PrC ^b	25.13 ±1.91	45.11 ±4.01	86.43 ±4.17	-	13.29 ±1.53	-	-
Pr-8C	28.79 ±1.04	91.04 ±3.87	94.60 ±9.09	+9.45	4.98 ±1.03	-62.53	-
Pr-24C	36.67 ±2.64	168.64 ±4.46	94.98 ±12.48	+9.89	4.23 ±0.33	-68.17	0.79 ±0.12
T-Pine210C	11.15 ±1.02	3.22 ±0.14	92.05 ±2.97	-	7.95 ±1.15	-	-
T-Pine210-8C	18.16 ±3.78	45.42 ±2.12	88.38 ±3.65	-3.99	4.33 ±1.52	-45.53	6.72 ±1.88
T-Pine210-24C	32.83 ±3.94	119.41 ±3.32	89.40 ±3.17	-2.88	2.22 ±1.88	-72.08	8.39 ±1.94
FeX	25.49 ±1.02	8.36 ±0.12	92.09 ±4.45	-	7.90 ±1.02	-	-
Fe-8X	27.34 ±2.81	65.67 ±2.01	79.29 ±5.83	13.90	8.05 ±1.39	+1.89	12.65 ±1.36
Fe-24X	32.91 ±3.98	142.31 ±4.52	77.34 ±6.62	16.02	8.15 ±0.38	+3.16	14.05 ±1.10
T-Ash210X	12.80 ±0.85	0.85 ±0.03	87.58 ±1.98	-	12.42 ±1.00	-	-
T-Ash210-8X	16.23 ±3.03	8.69 ±2.32	81.70 ±3.13	-6.71	13.64 ±0.75	+9.82	4.65 ±0.39
T-Ash210-24X	26.31 ±3.54	26.54 ±2.10	72.97 ±4.75	16.68	20.68 ±1.02	+66.51	6.35 ±0.94
FeC	26.69 ±2.98	23.52 ±1.90	81.11 ±2.81	-	18.88 ±0.74	-	-
Fe-8C	32.65 ±4.25	200.15 ±9.98	90.91 ±7.55	12.08	9.45 ±0.38	-49.95	-
Fe-24C	40.18 ±2.79	348.61 ±6.56	90.68 ±4.87	11.80	9.26 ±0.89	-50.95	1.35 ±0.94
T-Ash210C	14.91 ±1.69	2.13 ±0.02	86.43 ±4.12	-	13.58 ±0.65	-	-
T-Ash210-8C	22.37 ±4.03	90.21 ±2.32	90.87 ±3.82	+5.14	9.04 ±0.57	-33.43	-
T-Ash210-24C	32.40 ±3.46	172.05 ±2.26	90.67 ±2.41	+4.91	8.53 ±0.96	-37.19	0.81 ±0.94

¹ WL=Weight Loss; ² THC=Total Hydrolyzates Content; ³ CR=Change Ratio; ⁴ OC=Other Compounds; ^a X= xylanase; ^b C=cellulase

At 24 weeks of fungal exposure, the hydrolyzates percentage continued to increase up to 26% in modify samples, whereas in untreated samples the percentage of depolymerization varies depending on the type of wood-enzyme with a degradation increase by cellulase up to 15% and by xylanase until 19%. In accordance with the results, the enzymatic hydrolysis after 24 weeks of fungal exposure was conducted satisfactorily in all samples (control and treated) and in the case of hydrothermal samples, the fungal exposure over time acts as a pretreatment allowing subsequent enzymatic hydrolysis. The distribution of enzymatic hydrolysis fragments is complex and affected by many factors. However, it is notable the appearance of oxalic acid in the wood degraded by fungi, indicating that this compound arose in the wood-fungi oxidative phases where apparently acted as oxidative agent and mediator of the subsequent enzymatic phases^{151,152}. Regardless of results, further experiments are required to explore the role of various enzymes in thermally treated wood degradation and understand the involved mechanisms.

3.3.3.5 Monitoring changes in chemical structure due to biodegradation

The chemical structure of wood has been characterized by FT-IR to inspect any possible structural change due to fungal attack in wood. The figure II-15 shows the spectra of all samples prior to and following to rot fungal exposure indicating the bands with variations to study the possible effect of exposure on the carbohydrates and lignin precursors.

Obviating the initial differences explained in a previous section, the spectra after the periods of fungal exposure are quite similar exhibiting the representative peaks of the wood structure and differ only in slight displacements and changes of intensity. However, alterations in spectra were perceptible particularly in *F. excelsior* exposed to *T. versicolor*, shifting or smoothing some bands corresponding to polysaccharides or lignin compounds¹²¹. The peak at 3340 cm^{-1} assigned to hydroxyl groups appears slightly shifted in *F. excelsior* samples, this change is probably due

to an acetylation reaction during the exposure to *T. versicolor* and this reaction is not evident in treated wood.

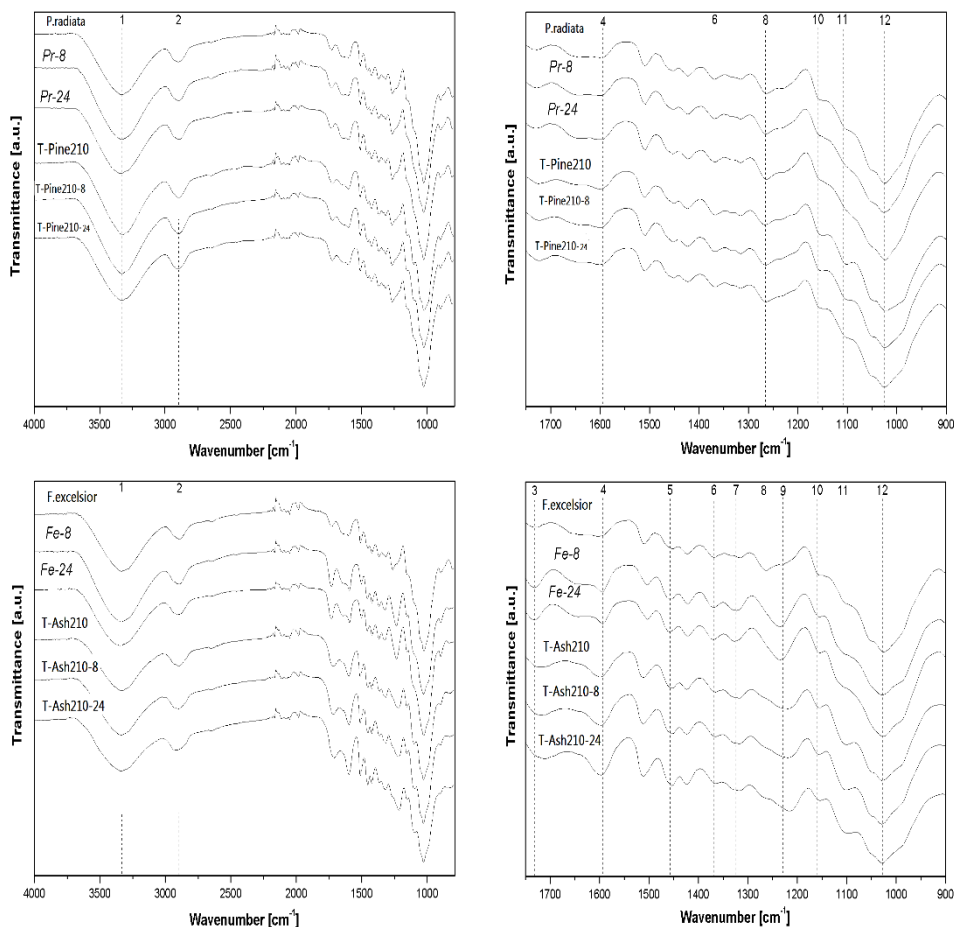


Figure II-15 FT-IR spectra of wood before 8 and 24 weeks of fungal attack.

The effect of acetylation of wood during fungal attack is correlated with the accessibility of water and hence the reduction of the number of hydroxyl groups in wood. In addition, the acetylation reaction is associated with the increased intensity of the carbonyl peak at 1740 cm^{-1} in *F. excelsior*, whereas, no variation was found in the hydroxyl peak of T-Ash210, indicating that fewer hydroxyl groups are accessible to be acetylated and is consistent with the higher protection against to rot fungi. A remarkable increase was observed at 1595 cm^{-1} in *F. excelsior* and slight in T-Ash210 exposed to *T. versicolor*, as occurred in the peak at 1740 cm^{-1} this could be referred

to the acetylation reaction associated to fungal exposure, which intensified carbonyl bands¹⁵³. Moreover, the lignin structures was not intensified in the referred peaks of *P. radiata* samples, indicating differences in the degradation mechanism of *G. trabeum*.

An additional peak was established at 1460 cm⁻¹ which corresponds with the asymmetric deformation of C-H bond of xylan. This peak appears in the modify wood spectra and the relative changes in elongation depend on the shifted spectrum of aromatic skeletal in lignin associated with the relative increase of carbohydrates after fungal exposure¹⁵³. In control samples, the fungal decay is focused on the polysaccharides and the progressive increase is associated with the variance resulting in lignin spectrum^{153,154}. The band at 1375 cm⁻¹ has a slight change in the relative intensities in untreated decayed species; the peak is assigned to the C-H deformation in cellulose and hemicelluloses which represent the relative decrease of polysaccharides in untreated samples and a shifted spectrum in treated samples due to the relative changes in components¹⁰⁰. The following band at 1324 cm⁻¹ remains stable almost absent in spectra; although shows a shoulder in decayed samples of *Fraxinus excelsior* where apparently the polysaccharides have been accumulated during selective decay stage of *T. versicolor*.

In *Fraxinus excelsior* the peak at 1260 cm⁻¹ may have been suppressed by a strong absorption at 1235 cm⁻¹, where was developed a shoulder possibly due to the degradation of xylan, since this band partially results from the C-O in xylan. The fingerprint region from 1200 cm⁻¹ to 800 cm⁻¹ include peaks characteristics of different groups from carbohydrates at 1158 cm⁻¹, 1106 cm⁻¹ and 1030 cm⁻¹ attributed to C-O-C, C-O and O-H deformation or stretching vibrations^{153,154}. In control samples the intensities of the indicated peaks decreased with the exposure time and the 1106 cm⁻¹ peak is almost absent after rot exposure. In contrast, the treated samples remain with a similar intensity in the indicated peaks, showing a reduction only after 24-weeks decay, fitting with the prolonged protection of the thermally modified wood.

3.3.3.6 Conclusions

The changes of cell wall structure and porosity in heat-treated wood enhances the durability against wood-rotting basidiomycetes, where degradation is only noticeable after an extended period. Degradation was probably a consequence of moisture increase producing an acetylation effect in wood during fungal exposure, associated with a higher intensity of carbonyl bands according to FT-IR spectra of control samples. In contrast, minor variations in the hydroxyl bands of modified wood indicate that is less accessible to acetylation, consistent with the higher protection against rot fungi. The fungal colonization mechanisms by rot basidiomycetes in wood involve an initial non-enzymatic oxidative phase followed by weak enzymatic depolymerization. In the initial phase was formed oxalic acid, probably secreted either by white or brown rot fungi which acts as direct agent in the oxidative process via Fenton chemistry, facilitating a subsequent enzymatic intracellular. Enzymatic mechanisms in basidiomycetes started gradually to depolymerize the modified wood only after a long period of fungal colonization. The enzymatic hydrolytic activities increased the kinetics reaction of the selective lignocellulosic enzymes achieving a moderate degradation of thermally modified wood over time.

3.3.4. Weathering performance of thermally modified wood

The fourth section aims to determine the effects of biotic and abiotic factors on thermally modified wood (T-Ash210 and T-Pine210) during its service life. To achieve this goal, samples were submitted to a natural aging and artificial weathering test. Then, physical-mechanical, thermal and optical properties were measured in order to know the response of the material and have an idea about its prospects of use as building material in façade systems compared to unmodified timber. The procedure of weathering test and the analyses of the general changes are summarized in the Figure II-16. The natural and artificial aging procedure are explained in the appendices.

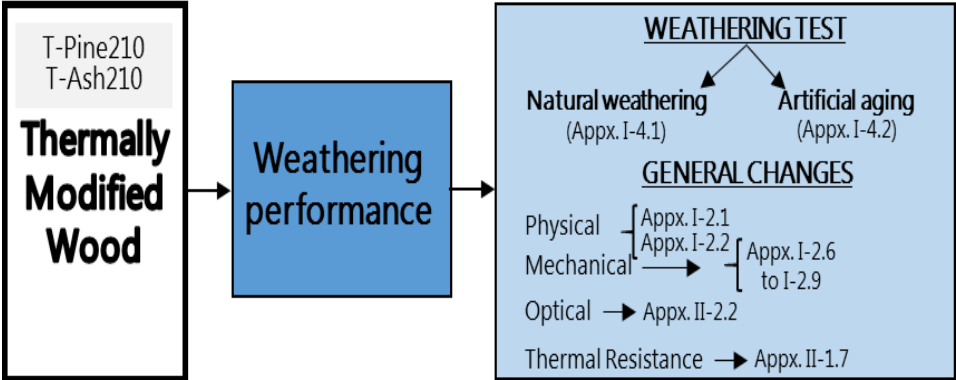


Figure II-16 Schematic of weathering tests on wood and properties analyzed.

3.3.4.1. Physical parameters after weathering tests

Two different tests were performed to measure the evolution of thermally modified wood against weathering factors. On the one hand, wood was exposed twelve months to natural weathering in a location with oceanic climate (San Sebastian, Spain: 43°18'33.054"Latitude N; 2°0'34.817"Length W) facing south direction at 45 degrees of inclination. On the other hand, wood was subjected to accelerated aging cycles based on a modified EN 927-6:2007, in which samples were exposed to intervals of heat, water and UV-A light (80 cycles, 2120 hours).

After weathering tests, a divergent tendency on wood-water interactions was found (Fig. II-17), while the ratio initial/ weathered was higher than one in both untreated species (with greater differences in *F. excelsior* wood), the ratio was lower than one in both T-samples (with greater differences in T-pine210), although with lower MC values than the unmodified ones (results in Table II-13). The results showed the influence of chemical changes during treatment on the sorption phenomenon, inclined to reach higher equilibrium moisture probably by the binding of water molecules with the cellulose content¹⁵⁵. Opposite is the effect that appears on control samples, in which hydroxyl groups of cellulose and lignin tend to satisfy the water needs at certain point, and thus not taking up water¹⁵⁶.

Table II-13 Changes of physical properties after weathering tests.

Sample	Properties	Initial	Natural weathering ratio [I/Nw] ^a	Artificial weathering ratio [I/Aw] ^b
<i>Fraxinus excelsior</i>	MC [%]	11.08±0.92	1.21	1.18
	ρ [Kg m ⁻³]	670.53±12.16	1.12	1.10
T-Ash210	MC [%]	5.23±0.79	0.95	0.80
	ρ [Kg m ⁻³]	468.14±10.78	1.14	1.10
Pinus radiata	MC [%]	11.02±0.10	1.09	1.10
	ρ [Kg m ⁻³]	602.13±18.36	1.10	1.10
T-Pine210	MC [%]	6.07±0.21	0.64	0.66
	ρ [Kg m ⁻³]	534.93±12.36	1.08	1.02

^aInitial/Natural weathered; ^b Initial/Artificial weathered

Regarding the weathering method used, the natural exposition had a more prominent effect on the MC with greater differences from the initial values, however, only statistically differentiated in T-Pine210 (P<0.05, BSD). The higher ratio in natural weathering may be due to the biotic factors that start to develop

during the exposure, although not clearly visible and with values below 15% MC where the critical point for treated wood begins.

All samples showed a decreasing density after weathering tests, with a similar initial/ weathered ratio in *F. excelsior* and T-Ash210 ($P < 0.001$, BSD), but higher on *P. radiata* ($P < 0.001$, BSD) than T-Pine210 (without statistical differences). The decrease in density after weathering could be correlated to the wood degradation phases: First, a slow structural change is presented, and then a rapid erosion rate of lignin and cellulose take place, resulting in mass loss¹⁵⁶. Water plays a crucial role during weathering, washing the degradation products from the surface as well as leaching hemicelluloses, abrading the surface, and finally causing checking and raised grain^{156,157}.

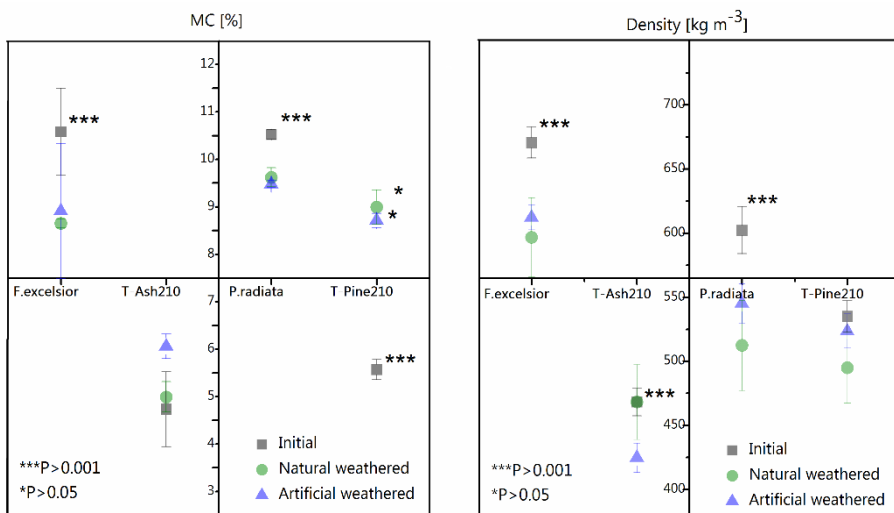


Figure II-17 Variations on density and moisture content after natural or artificial weathering test.

3.3.4.2. Evolution of mechanical properties after weathering test

Two values of flexural modulus (MOE) were calculated: Firstly, the standard MOE according to EN 408:2010+A1:2012 but correcting the effects of the equipment used. Secondly, the MOE was measured from five different spans considering the shear effect and local deformations, in order to create a linear regression model to finally indicate an adjusted value. Although both MOE values are different, the

trends after weathering tests are similar (Table II-14), and the proportions between untreated-treated samples are comparable to that found in other studies with thermally modified wood^{158,159,160}.

Table II-14 Changes in mechanical properties after weathering tests.

Sample	Properties [Mpa]	Initial	After artificial weathering	After natural weathering
<i>F.excelisior</i>	MOE ^a	13546±1704.02	13023±1275.98	11932±1136.45
	MOE ^b	13689±1309.92	13551±962.11	9688±174.10***
	MOR	138.39±20.53	130.40±19.91	105.50±12.50**
	HB	5.77±0.81***	2.08±0.61*	1.94±0.12*
T-Ash210	MOE ^a	8190±1233.90	7015±986.21	7515±1148.17
	MOE ^b	8338±977.39	7318±1624.29	8031±650.46
	MOR	63.58±3.46	56.10±2.50	50.70±5.20*
	HB	5.02±0.63***	1.10±0.24***	0.78±0.10***
<i>P.radiata</i>	MOE ^a	13597±1041.61	12361±1100.11	11741±1126.21
	MOE ^b	14720±802.78	13190±1695.48	10668±926.66*
	MOR	129.34±10.02***	94.20±14.76	91.40±18.20
	HB	3.75±0.37***	1.40±0.21	1.34±0.24
T-Pine210	MOE ^a	14220±1435.49	12078±1068.22	13902±1256.74
	MOE ^b	14102±1115.97	12324±2259.64	14070±1031.50
	MOR	80.39±10.37*	65.53±14.91	63.50±5.30
	HB	2.44±0.43***	1.2±0.26	1.24±0.29

^a MOE from the linear regression model; ^b MOE calculated according to EN 408:2010+A1:2012

The highest losses in MOE were found in untreated samples (both, *Fraxinus* and Pine) exposed to natural aging, with reductions from 12 to 29% (Fig. II-18). Conversely, thermally modified samples were quite stable during natural aging with a reduction below 8% in T-Ash210 and stable values in T-Pine210. However, the artificial weathering test caused a greater reduction of MOE in T-Ash210 in comparison to *F. excelisior*, although with reductions below 15%; moreover, the

values were stable in T-Pine with lower reduction than in *P. radiata*. The results show that the biotic factors inherent to natural weathering conditions affect to a greater extent untreated wood; therefore, chemical changes occurring on T-samples stabilize the MOE when exposed to outdoor conditions, providing an extended service life of modified products.

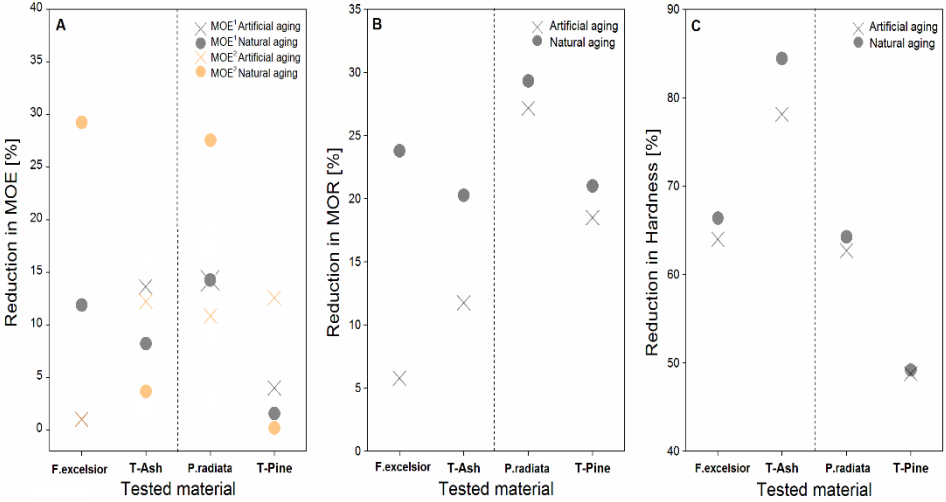


Figure II-18 Reduction of mechanical properties after weathering tests.

Regarding the bending strength (MOR), it is well known that thermal modification particularly affects this mechanical parameter, with values between 3 and 50% lower than unmodified hardwoods or softwoods, so it is generally qualified for non-structural elements such as cladding on wooden buildings^{160,161}. In spite of this fact, the reduction in MOR could be correlated with the decreased density after weathering ($R^2= 0.832$). In Figure II-19, a well-defined distribution in four groups was observed, corresponding to each group of samples. In addition, the modified samples present a lower reduction rate of MOR, since the distribution of the weathered values was narrower than control. The wide reduction in unmodified wood means that is more susceptible to chemical leaching during weathering conditions, therefore, with higher lignin depolymerization and extractive release that contribute to the microstructural breakdown¹⁶². The

average range of losses in MOE and MOR of this study is comparable to those found by other authors^{38,162}.

Concerning the surface hardness, the initial values were lower in modified wood than control as follows: *F. excelsior* > T-Ash210 > *P. radiata* > T-Pine210; these differences are usually due to the type of wood (hardwoods or softwoods). However, after natural or artificial aging test the hardness values showed the following rate of reduction: T-Ash210 > *F. excelsior* > *P. radiata* > T-Pine210, in which T-Pine210 has presented similar values to control pine and T-Ash210 has decreased dramatically (Fig. II-18). These results suggest that T-Pine210 is more resistance to surface stress than untreated Pine, an important property in service as floors or for exterior applications¹⁶³.

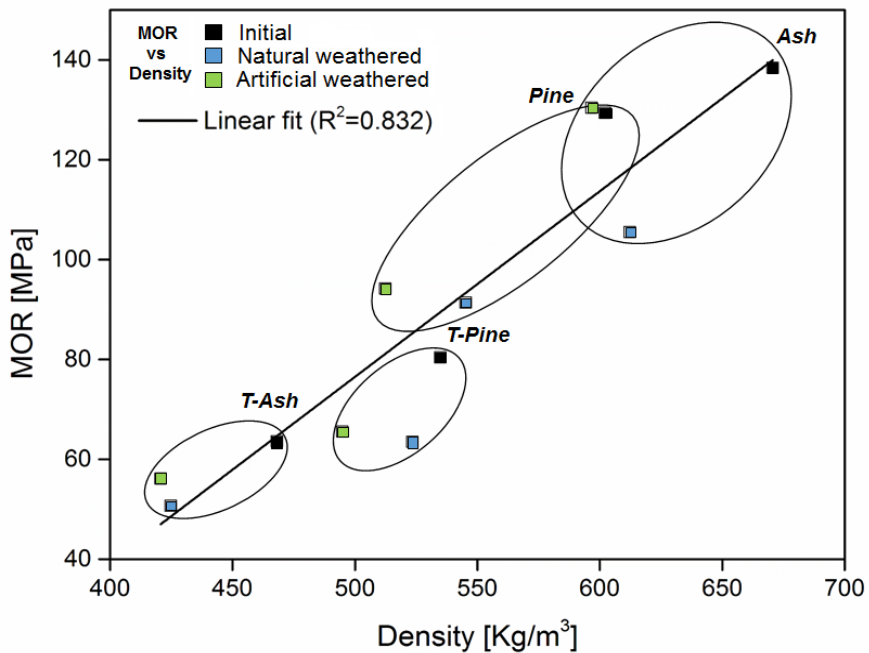


Figure II-19. Correlation between MOR-density and wood groups association.

3.3.4.3 Thermal performance of wood after weathering tests

Thermo-gravimetric analysis was performed to assess the thermal degradation of the wood samples and the influence that the weathering and aging had over the thermal behavior. The curves of the thermo-gravimetric analysis (TGA) are shown in figure II-20, and the critical degradation points obtained from the first derivative (DTG) are presented in Table II-8.

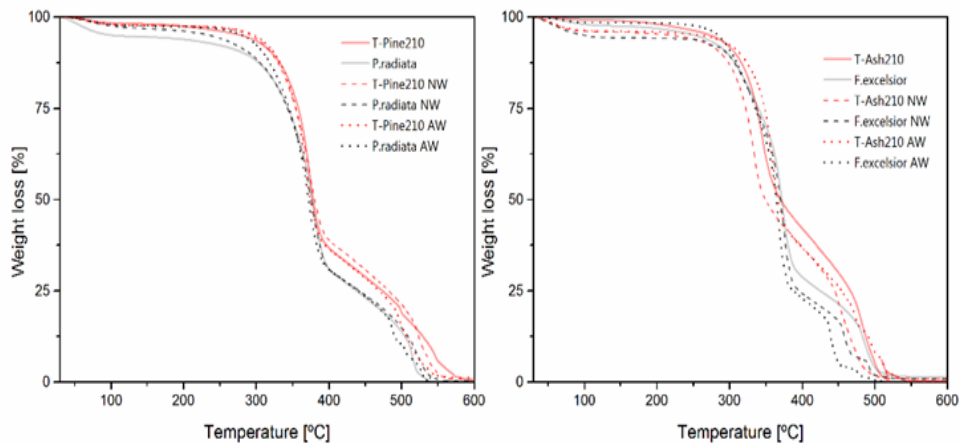


Figure II-20. Thermo-gravimetric curves of unweathered and weathered wood.

The thermal degradation of wood presented several stages already explained in section 3.3.2.4, and from the table II-8 is possible to see the specific differences between the T-Samples and untreated samples regarding the effect of weathering and aging. At the beginning, when only the 10% of the mass was lost, the thermal treatment increased or stabilized the temperature needed for that degradation, and the same tendency occurs with the temperature needed to degrade 50% of mass. Since the weight loss is directly related to the wood flammability, the previous results pointed out the slight reduction of the combustion capacity of thermally modified wood compared to the untreated. These results may be due to the fact that modified wood contain less volatile flammable compounds, and therefore the possibility of igniting and consequently combusting is diminished¹⁶⁴. Regarding the natural and artificial weathering of the samples, a clear tendency towards the reduction of the temperatures of degradation was

observed. This tendency was more marked in the *F. excelsior* samples than in the *P. radiata* ones. Nevertheless, the diminution of the degradation temperatures in the weathered samples occurred mostly in a small range.

Table II-15 Thermal degradation parameters extracted from the TG analysis.

Sample	Degradation % ¹	Unweathered [°C]	Artificial weathered [°C]	Natural weathered [°C]
<i>F.excelsior</i>	T _{10%}	297.23	303.19	296.54
	T _{50%}	371.83	364.39	369.78
	T _{MAX}	373.56	367.97	369.49
T-Ash210	T _{10%}	307.91	313.88	288.26
	T _{50%}	370.10	366.06	349.05
	T _{MAX}	345.14	359.81	333.48
<i>P.radiata</i>	T _{10%}	283.40	306.51	290.85
	T _{50%}	376.97	371.92	375.41
	T _{MAX}	377.42	372.60	376.79
T-Pine210	T _{10%}	322.20	324.96	321.33
	T _{50%}	378.15	374.26	380.23
	T _{MAX}	373.83	369.16	371.85

¹ Percentage of degradation:10%,50% and maximum degradation of samples

3.3.4.4 Color changes of wood after weathering tests

Visual appearance is one of the most important attributes of wood products when expose e.g. for external cladding, since wood colors fade down naturally in direct sun over time and can also turn grey or fade¹⁶⁵. The initial lightness values (L*) in T-Ash210 and T-Pine210 were significantly lower than *F. excelsior* and *P. radiata* (Table II-16), and colors of domestic thermally modified wood resemble tropical wood species. The total color differences (ΔE^*) after twelve months and/or 80

artificial cycles were quite evident in control Pine and Ash wood compared to the changes in T-Ash210 and T-Pine210, being generally a positive outcome when used as building material, adding advantages in terms of durability and aesthetic effect.

Table II-16 Changes in optical parameters after weathering tests.

Sample	Parameters [D65]	Initial	Δ Artificial aging	Δ Natural weathering	ΔE* Evaluation
<i>F.excelsior</i>	L	80.32±1.26			
	a	4.37±0.92	ΔE*= 8.65	ΔE*= 8.39	High color changes
	b	8.35±0.53			
	h	62.35±0.71	0.89	0.49	
	C	9.43±0.44	-3.65	-2.76	
<hr/>					
T-Ash210	L	65.07±0.36			
	a	0.80±0.10	ΔE*=1.59	ΔE*=0.66	Small difference
	b	-0.97±0.11			
	h	- 50.49±0.10	1.27	0.66	
	C	1.27±0.16	0.41	0.57	
<hr/>					
<i>P.radiata</i>	L	82.74±2.78			
	a	4.67±0.62	ΔE*=9.31	ΔE*=10.19	High color changes
	b	11.53±0.84			
	h	67.95±0.39	0.59	0.74	
	C	11.53±0.44	-3.12	-3.27	
<hr/>					
T-Pine210	L	67.67±1.25			
	a	2.76±0.49	ΔE*=0.88	ΔE*=1.61	Small difference
	b	2.12±0.11			
	h	37.58±3.37	0.25	0.37	
	C	3.48±0.15	-0.58	-1.34	

The Fig. II-21 shows the percentage of variation of the color parameters L^* , a^* , b^* after weathering tests, in addition to the optical appearance of the aged samples. The variation of the parameters in the untreated wood is significant and negative, although there are no clear differences between artificial or natural test. The parameters L^* and b^* of untreated wood decreased during the weathering tests, indicating that *F. excelsior* and *P. radiata* became darker, and are moving towards grayish tones. The L^* changes point out that UV light degrades rapidly the extractives in untreated wood followed by oxidation of the degradation products; thus, results in this considerable decrease in lightness¹⁶⁶. Both untreated samples initially tends to yellowing coloration, however in Ash wood the parameter a^* decreased toward greener tones after weathering tests^{167,168}. The overall color changes are associated to the chemical breakdown of lignin and extractives, and probably all wood surfaces will eventually turn silver-gray color after long-terms of natural light and UV exposition.

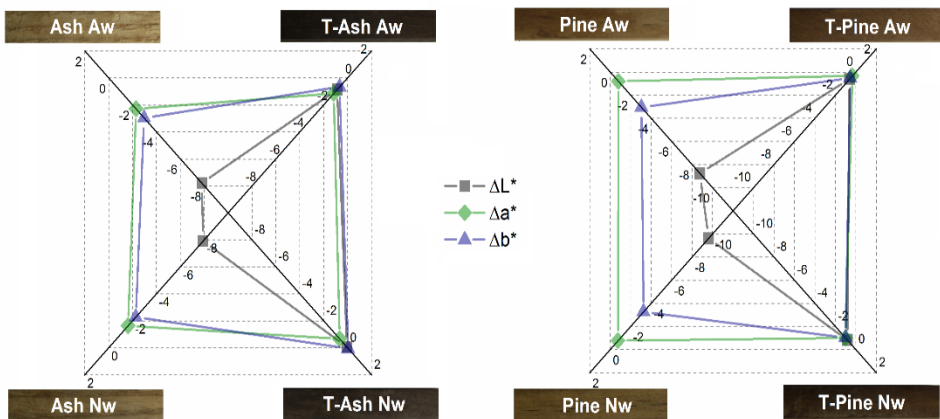


Figure II-21 Percentage of variations in parameters L^* , a^* , b^* after artificial (Aw) or natural weathering (Nw).

After weathering tests, the color parameters in T-samples were more stable than control, with negative variations ($<2\%$) and lower chromatic strength (ΔC^*), classified as samples with small differences. The lower values of hue and chroma of T-samples are connected with the color saturation caused by some fractions of lignin and hemicelluloses during treatment, which produce strongly colored

byproducts¹⁶⁹. The color stability of T-samples after weathering tests could be due to their altered chemical composition. Particularly, the rearranged lignin proportion contains molecules which protecting wood from UV radiation^{170,171}. On the other hand, after a long-term weathering conditions, the color changes could become similar to that found in control samples, and will require some surface protection, which is mandatory for many high value exterior wood end uses, such as window joinery and cladding, however, within an extended protection time than in untreated wood^{10,171}.

3.3.4.5 Conclusions

The implementation of thermally modified wood in industrial applications requires studies of the product performance under weathering conditions. The results show that natural weathering conditions had a more prominent effect on the properties of untreated wood, with greater differences in MC, MOE and MOR than in thermally modified wood; these results may be due to the influence of the biotic factors inherent to outdoor exposition. All samples showed a decreasing density after weathering tests, concluding that weathered samples were in the first phase of degradation with slow structural erosion denoted by the mass loss. The most stable values of MOE and hardness after weathering tests was in T-Pine²¹⁰, suggesting more resistant to surface stress than Pine. Moreover, the weathering tests did not compromise significantly the thermal degradation of the modified wood. The optical parameters in T-Samples were similar before and after weathering test, and thus classified as samples with small differences. The overall properties values after weathering tests provide favorable perspectives of service life in products made of thermally modified wood.

3.3.5 Interactions of thermally modified wood with coating products

To preserve surfaces of thermally modified products during outdoor exposure it is necessary to protect it against natural weathering factors, and thus to avoid surface degradation and changing tones. The fifth section, samples of *Fraxinus excelsior* were thermally modified at 192, 202 and 212°C and coated using with water or solvent products, followed by the assessment of adhesion and physical response in order to understand the performance and differences between treated surfaces. The second part of this study was to examine their response to artificial weathering test. The challenge was to understand changes to the physical and surface properties along the weathering duration in order to identify optimal process conditions and to find appropriate markets for the end-uses products. The surface properties analyzed before and after weathering test are summarized in the Figure II-22.

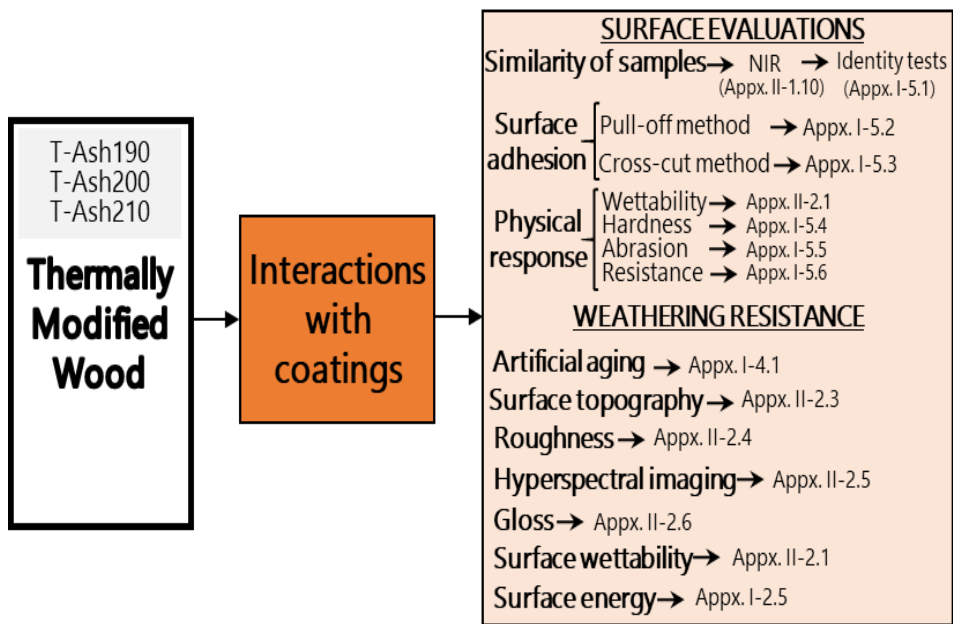


Figure II-22 Schematic of tests on coated surfaces of thermally modified wood.

3.3.5.1 Preliminary identity test by NIR spectrometry

In order to visualize the differences between samples due to thermal treatment, samples of their near-infrared spectra were taken and data set processed to present its heterogeneity or homogeneity using algorithms for clustering data and by principal component analysis (PCA) to reduce the dimension of the data set. The absorption bands in the NIR region (Appendix II-1.10) arise from overtones and combination bands caused by vibrations of C-O, O-H, C-H, and N-H groups, which have their fundamental molecular vibrations in the MIR region^{172,173}. As in various cases, the chemical information is barely selective within the typically broad and extensively overlapping bands of NIR spectra (Fig. II-23).

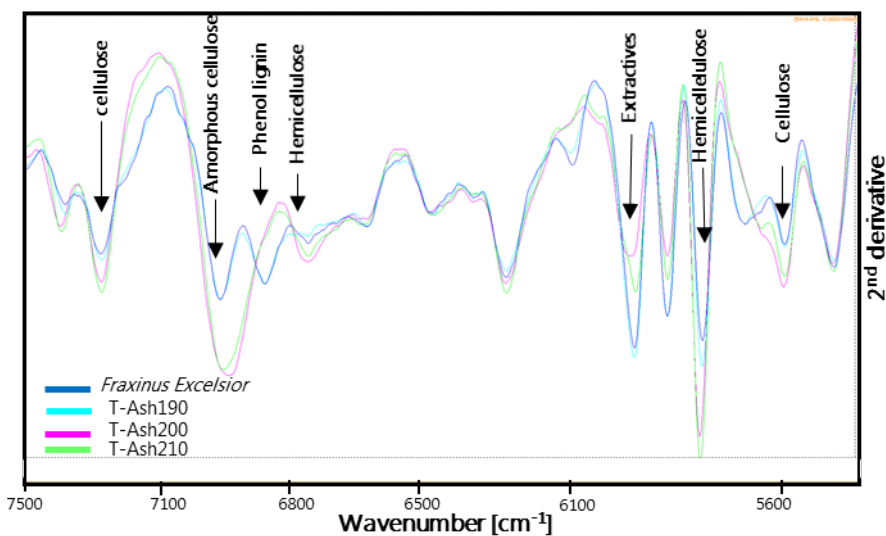


Figure I-23 NIR band assignments for wood and its components.

However, using multivariate analysis techniques is feasible to address variability on the obtained spectra through a spatial model, and visualize the relative distance between treatments. The cluster analysis (Fig. I-24 A) divided NIR data as a dendrogram in four main classes (without supervised statistical algorithms)^{174,175}. Then, the PCA decomposed highly correlated data in four defined groups corresponding to the treatments (T-Ash190, T-Ash200 and T-Ash210) and control samples (Fig. I-24 B), proving the capability of NIR measurement system to discriminate samples without overlapping clusters. In

conclusion, these results are a simple visualization but it is the basis of a predictive analysis, which allows beginning the study of surfaces treatments with the certainty that there are initial differences between samples.

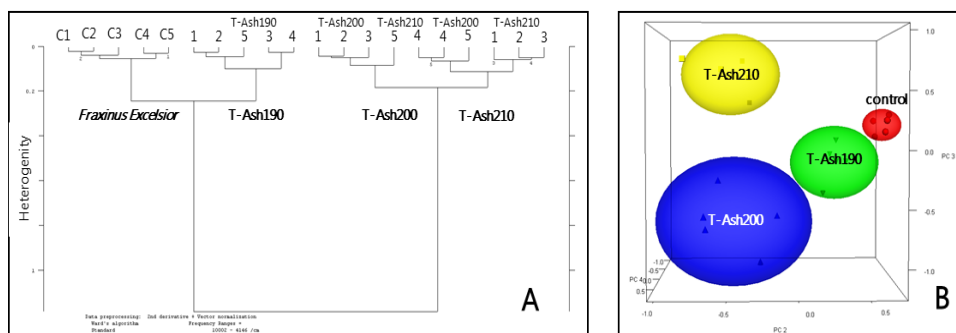


Figure I-24 Cluster analysis (A) and PCA scores discrimination (B) of samples.

3.3.5.2 Wood finishes on thermally modified wood

For the wood finishing (modified and unmodified) the surface was prepared by sanding with an orbital sander (320 grit) and then two coatings systems were applied to one lateral face: UV-curable coatings using industrial rollers in a hybrid line mix of LED and arc lamps (in Sherwin-Williams Company) and waterborne coatings using brush in laboratory conditions. The details of the coating application are summarized in the Table II-17.

Table II-17 Technical details of finishing process on wood.

Coating system	Process	Layer/ thickness ¹ [μm]	ρ [g cm ⁻³]	Amount [g m ⁻²]	Drying			Curing	
					Temp [°C]	RH ² [%]	Time [h]	UV [nm]	dose Speed [W [m cm ⁻²] min ⁻²]
100% UV- curable	Roller machine	1 st -Sealer / 50	1.12	20	-	-	-	Hg 280-320	80 10
		2 nd -Clear coat / 10	1.18	20	-	-	-	Hg 280-320	80 10
		3 rd -Topcoat / 5	1.19	10	-	-	-	Ga 390-450	12 0 15
Waterborne	Brush	1 st -Primer / 90	0,88	100	20	5 0	18	-	- -
		2 nd -Topcoat / 60	1,04	100	20	5 0	5-6	-	- -
		3 rd -Topcoat / 50	1.04	100	20	5 0	200	-	- -

¹ Theoretical thickness value provided by producers; ² RH= Relative Humidity

Wood coating systems were applied according to supplier's recommendations (e.g., quantities, layers, time), and then the coated samples were stored at 23±2°C and 60±5 % relative humidity to further experiments. Details concerning the applied coating systems are listed below.

Table II-18 Chemical composition and features of wood coatings systems.

Coating System	Product name - Target	Main components	Chemical composition		Quantity [%]
<i>100% UV-curable</i>	1.Beckry Seal - Clear sealer	Acrylate monomers;	TMPTA	C ₁₅ H ₂₀ O ₆	12.5-15
	2.Beckry Clear I - Clear coat	Acrylate oligomers; Urethanes; Photo initiator;	Acrylate oligomers EO-TMPTA	- C ₂₁ H ₃₂ O ₉	14-35 7-20
	3.Beckry Clear II - Topcoat	Resins; Additives	HMPP	C ₁₀ H ₁₂ O ₂	2.5-5
			Benzophenone (<i>Photoinitiator</i>)	C ₁₃ H ₁₀ O	1-2.5
<i>Waterborne</i>	1.Oli-KS - Primer	Ketones; Alcohols; Aromatic mixtures; Resins; Additives	Naphtha MEKO	- C ₄ H ₉ NO	50-55 0.1-0.9
	2.Oli -Aqua Top - Topcoat	Alkyd resin; PU disperser; Water; Additives	2- Ethylhexanol Water-based PUs	C ₈ H ₁₈ O - C ₈ H ₁₈ O ₃ C ₇ H ₅ NOS	32-55 1-5 1-3
	3.Oli-Aqua Härter - Hardener	Curing agents; Alkyl ethers; Isocyanates; Aromatic hydrocarbons	Blocked Isocyanate Xylene	- C ₈ H ₁₀	10-15 5-10
			EB	C ₆ H ₅ CH ₂ CH ₃	1-3
			MIT	C ₄ H ₅ NOS	0.1-0.9
			MPA	C ₆ H ₁₂ O ₃	25-35
			IPDI	C ₁₂ H ₁₈ N ₂ O ₂	20-25
			HDI	C ₈ H ₁₂ N ₂ O ₂	20-25

3.3.5.3 Evaluation of coating-surface adhesion

The influence of thermally modified wood on coating adherence was determined with the pull-off method and the adhesion values were classified according to cross-cut test, the results are shown in Table II-19 and Figure II-23. Finishing of modified wood presented improved adherence (with both coatings) compared

with unmodified wood, although strength values in general were low compared with other studies^{176,177}. The *100% UV-curable* product showed higher adherence values, and according to standards are classified as good or very good. Analyzing the reverse side of the detached films and dollies, control samples showed an adhesive fracture that apparently was shifting in the modified wood to a cohesive fracture (Fig. II-23). This effect is difficult to interpret because the cohesive failure could occur in the coating, glue or wood and is often combined within a fractured surface⁸⁹. Furthermore, the measured force could be influenced by the stress-distribution under the dolly stamp and the cut of the coating around the dolly. On the other hand, *waterborne* product presented lower adhesion values in all samples but with a significant improvement in T-Ash210 samples, varying the standard classification from bad adhesion (in control samples) to good adhesion. The adhesive fracture between priming and adhesive was predominant in control samples and T-Ash190 but was shifting to adhesive fracture between topcoat and intermediate coat in T-Ash200 and finally was more pronounced the cohesive failure in T-Ash210.

Table II-19 Coating adhesion on wood by pull-off test.

Sample	Finishes type	Adherence ¹					Classification ²	
		σ [MPa]	A	A/B	-/Y	Y		Y/Z
<i>F.excellsiior</i>		0.87±0.09	-	-	62.5	2.5	35	1
T-Ash192	UV-curable	1.02±0.07	24.29	3.57	15.71	9.29	47.14	0
T-Ash202		1.02±0.09	30.71	-	-	7.86	61.43	1
T-Ash212		1.06±0.09	37.86	-	-	5	57.14	1
<i>F.excellsiior</i>		0.77±0.10	10	-	90	-	-	5
T-Ash192	Waterborne	0.88±0.06	7.14	2.86	90	-	-	3
T-Ash202		0.87±0.05	20	75.71	4.29	-	-	4
T-Ash212		0.96±0.06	57.14	24.29	15.71	-	20	2

¹ Classification pull-off test [EN 4624]: A= adhesive fracture; A/B= adhesive failure substrate-coat; -/Y= cohesive failure from bond line; Y= cohesive fracture; Y/Z= cohesive failure bond line-stamp

² [EN ISO 2409] From 0 = very good adhesion to 5 = weak adhesion.

The most probably arguments of lower adhesion and failure changes with *waterborne* coating could be ascribed to the application and drying process. In

these steps, surface is more vulnerable to be contaminated by low molecular weight impurities of various origins including water. Thus, changing the nature of surface and undermining an improved adhesion^{178,179}. The differences in adhesion between the coatings (*100% UV-curable* and *waterborne*) are not correlated with differences in interfacial adhesion but are connected with the grade of surface modification in each treatment temperature. To improve the coating-wood adhesion of thermally modified samples is necessary a sanding pretreatment, which is relatively non-destructive and improve the surface flatness since wood is naturally rough on a scale relative to the molecule, besides, thermally modified surfaces present higher roughness than in unmodified samples^{180,181}.

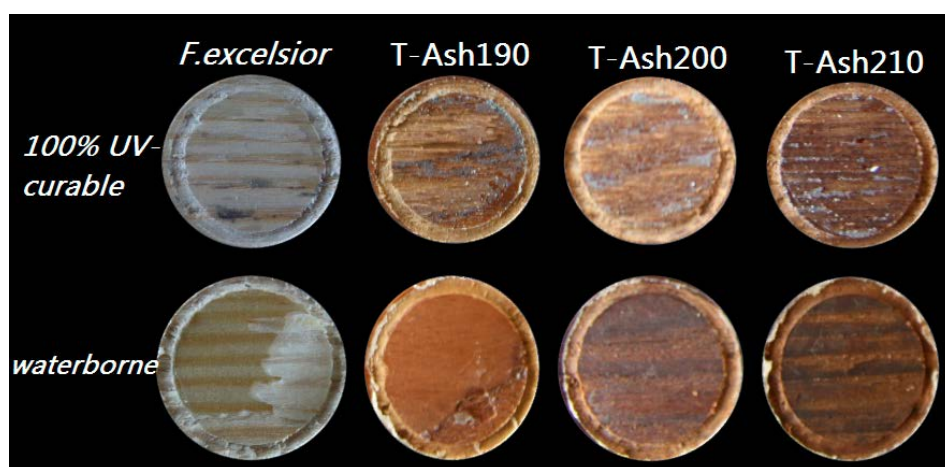


Figure II-25 Appearance of wood surfaces after pull-off test.

3.3.5.4 Evaluation of properties in coated surfaces

Some surface characterizations were performed to state the adequate uses of the modified material and to find differences between modified samples and performance of coating products. Tables II-20 and II-21 show the assessment of properties. The interactions between reference liquids and coated surfaces were assessed by measuring a sessile drop contact angles. Three liquids of different molecular properties were used in order to determine the thermodynamic state of each sample configuration. The results reveal differences between control and thermally modified wood in *100%UV-curable* coating surfaces, with higher contact angles for each liquid and principally water (θ_w). On the other hand, the

waterborne coating did not presented a clear trend regarding surfaces-tested liquids, except the wettability, which increased with the treatment intensity. Thus, the wettability is influenced by the nature of the substrate and coating, where pH, acidity and polarity are key factors in the wetting phenomena¹⁸².

Table II-20 Values of contact angle, surface energy and work of adhesion and cohesion of coated surfaces.

Coating product	Evaluation ¹	<i>F.excelior</i>	<i>T-Ash190</i>	<i>T-Ash200</i>	<i>T-Aash210</i>
100% UV-curable	θ_W	72.12	96.38	75.88	81.89
	θ_E	52.56	62.84	57.89	60.49
	θ_D	48.57	41.88	40.64	43.75
	γ_{SZ}^P	31.40	38.25	34.50	34.12
	γ_{SZ}^d	7.64	0.21	4.89	3.16
	γ_{SZ}^T	39.05	38.47	39.39	37.29
	W_a^P	29.18	89.87	85.00	84.02
	W_a^d	37.03	0.13	0.63	0.11
	W_a^T	66.21	90.00	85.63	84.13
	W_C	78.10	76.94	78.78	74.58
waterborne	θ_W	104.39	98.04	96.49	92.09
	θ_E	65.70	64.22	69.09	66.75
	θ_D	61.23	55.87	56.11	54.20
	γ_{SZ}^P	0.16	0.02	0.19	0.42
	γ_{SZ}^d	30.25	42.66	49.54	60.13
	γ_{SZ}^T	30.41	42.69	49.73	60.55
	W_a^P	2.08	2.05	6.31	9.32
	W_a^d	73.69	1.85	1.99	0.49
	W_a^T	75.77	3.90	8.30	9.81
	W_C	60.82	85.38	99.46	121.1

¹ Contact angles of water (θ_W), ethylene glycol (θ_E), didiiomethane (θ_D). Surface energy (γ_S), work of adhesion (W_a), work of cohesion (W_C)

The surface free energies γ_{SZ}^T , calculated as a superposition of its polar and disperse contributions, and the share of the polar-to-dispersive distributions

changed remarkably, shifting from low to high disperse contribution (γ_{s2}^d) in addition to strong reduction of γ_{s2}^p . These effects are associated to the decrease of equilibrium moisture content occurring in modified samples leading to a non-polar character of the thermally treated wood. The values of surface tension (γ_{s2}) obtained in modified samples should be considered satisfactory taking in to account that values should be higher at least 10 mJ/m² than the coating values¹⁸³. The hardness was measured counting the oscillation times of an instrument based on the principle that the harder film–substrate surface, the greater the amplitude time of oscillation; this parameter is important in the woodworking industry. The results show different trends of the films coated on the substrates; with higher values in all samples finish with *100%UV-curable* (25-29) comparing with *waterborne* finishes (15-17). According to results, surfaces coated with *100%UV-curable* products presented a positive effect with higher hardness values with increasing treatment temperature. This effect did not occur with *waterborne* products, which remained stable at different treatment temperatures.

Table II-21 Measurements of wood surface-coating resistance.

Sample	Coating product	Hardness [sec]	Wear-index ¹ [mg/1000 cycle]	Weight fall ² [mm]					Scratch load [g]	
				10	25	50	100	200		400
<i>F.excelsior</i>		25.58±0.12	101.71	5	4	2	2	1	1	1600
T-Ash190	<i>100% UV-curable</i>	26.55±0.36	74.75	5	4	4	3	1	1	1800
T-Ash200		28.08±0.12	83.67	5	4	3	2	1	1	1600
T-Ash210		28.94±0.39	71.25	5	4	2	2	1	1	1400
<i>F.excelsior</i>		17.56±0.39	60.51	5	5	3	2	1	1	2000
T-Ash190	<i>Waterborne</i>	15.50±0.12	64.25	5	4	2	2	1	1	1800
T-Ash200		15.92±0.39	52.52	5	4	3	2	1	1	1400
T-Ash210		16.00±0.12	40.05	5	4	3	2	1	1	1400

¹ Abrasive resistance measurement; ² Surface impact measurement

The abrasive resistance of the coated surface was measured by the wear index rate (WIR) indicating the weight loss in milligrams per thousand cycles of abrasion. The lower the wear index the better the abrasion resistance of tested surface¹⁸⁴. The results showed higher resistance to abrasion in thermally modified wood compared with unmodified wood when applied both coating systems. In

the case of *100%UV-curable* product was achieved a resistance 30 % higher on modified wood and the *waterborne* finishing showed a resistance 33% higher than control samples. The highest resistance values were obtained on T-Ash210. The analysis of surface impact by falling-weight test showed similar mean failure-energy values between modified and unmodified samples with the applied coating systems. Overall, finished samples exhibit good impact resistance up to 50 mm of drop ball heights and poor impact resistance from 200 to 400 mm of drop height for both coating variants (*100%UV-curable* and *waterborne*). These results indicate that thermal modification of wood did not influence negatively on the elastic properties of the substrate and thus allows this material to be used in the same conditions and range of applications such as unmodified wood¹⁸⁵. The results of scratch test revealed higher peel strength on T-Ash190 with both coating systems, decreasing with increasing of treatment temperature. Regarding to finishing techniques, the results suggest that on *waterborne* surfaces the scratch resistance was sensitive to the coat thickness with worse strength on samples with smaller coat thickness (T-Ash200 and T-Ash210). However, on *100%UV-curable* surfaces the coat thickness was thin and homogenous so probably the applied strength passes through the coating and penetrates the wood surface, being peel strength lower than when it just scratches the coating.

3.3.5.5 Weathering resistance of coated heat-treated wood

After an exhaustive analysis of the properties of the coated surfaces, it is necessary to analyze their behavior when the material is exposed to outdoor conditions, in this case emulating those conditions by an accelerated weathering test. The challenge of this section was to understand changes to the physical and surface properties along the weathering duration in order to identify optimal process conditions and to find appropriate markets for the end-uses products.

3.3.5.5.1 Wood surface topography

The surface geometry was reconstructed as a 3D model to assist the visual assessment of weathering effect on the surface texture (Fig. II-26-27). In addition, a stylus profilometer was used to measure the extent of irregularities expressed as Rz roughness parameter. Rz is most suitable for characterizing wood-based surfaces, as it is more sensitive to the topography changes such as cracks, shrinkage or blistering^{184,186}. The influence of weathering on the surface topography of thermally modified samples finished with *100%UV-curable* coating was not substantial, showing relatively small differences between untreated and thermally modified samples.

In the first case, the surface remains homogeneous and only the standard deviation of Rz increased due to weathering. Indeed, all the thermally treated samples before weathering presented similar Rz values, possessing higher standard deviation when compared to untreated wood. Nevertheless, weathering of T-Ash190 and T-Ash200 resulted in smoother surfaces as revealed by decreasing of roughness values for 20% and 32%, respectively. The same effect was not observed in case of weathered T-Ash210 with values of Rz and its standard deviation similar to control samples *F. excelsior* (Fig. II-26).

Surfaces with 100%UV-curable product

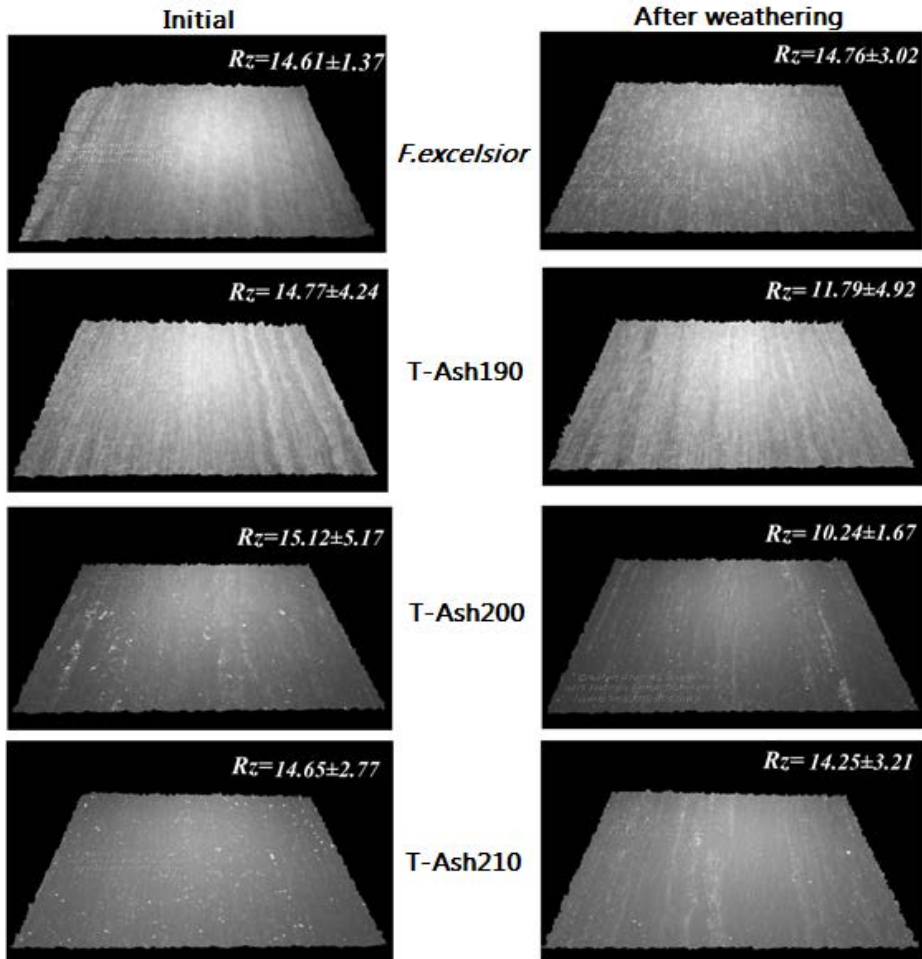


Figure II-26 3D surface topography maps and roughness (R_z) values of wood coated with *100%UV-curable* coating before and after aging test.

The effect of weathering was slightly different in the case of surfaces finished with *waterborne*. The initial surface roughness (R_z) of heat-treated samples was considerably higher than the reference samples, increasing more than double in T-Ash190 and T-Ash200. Nevertheless, all the *waterborne* surfaces were much smoother than samples finished with *100%UV-curable* system. R_z of reference samples increased slightly (~13%) after weathering, with constant standard deviations. On the contrary, the surface roughness of the heat-treated samples decreased after weathering tests from 30% (T-Ash190 and T-Ash210) to 50% (T-

Ash200). Such particular performance of the heat-treated surfaces could be related to the reduction of free hydroxyl groups in modified samples, effect which interferes during the curing. The treatment itself affects the coating-surface interaction by decreasing the penetration of coating, and therefore are more susceptible to weathering^{128,187}.

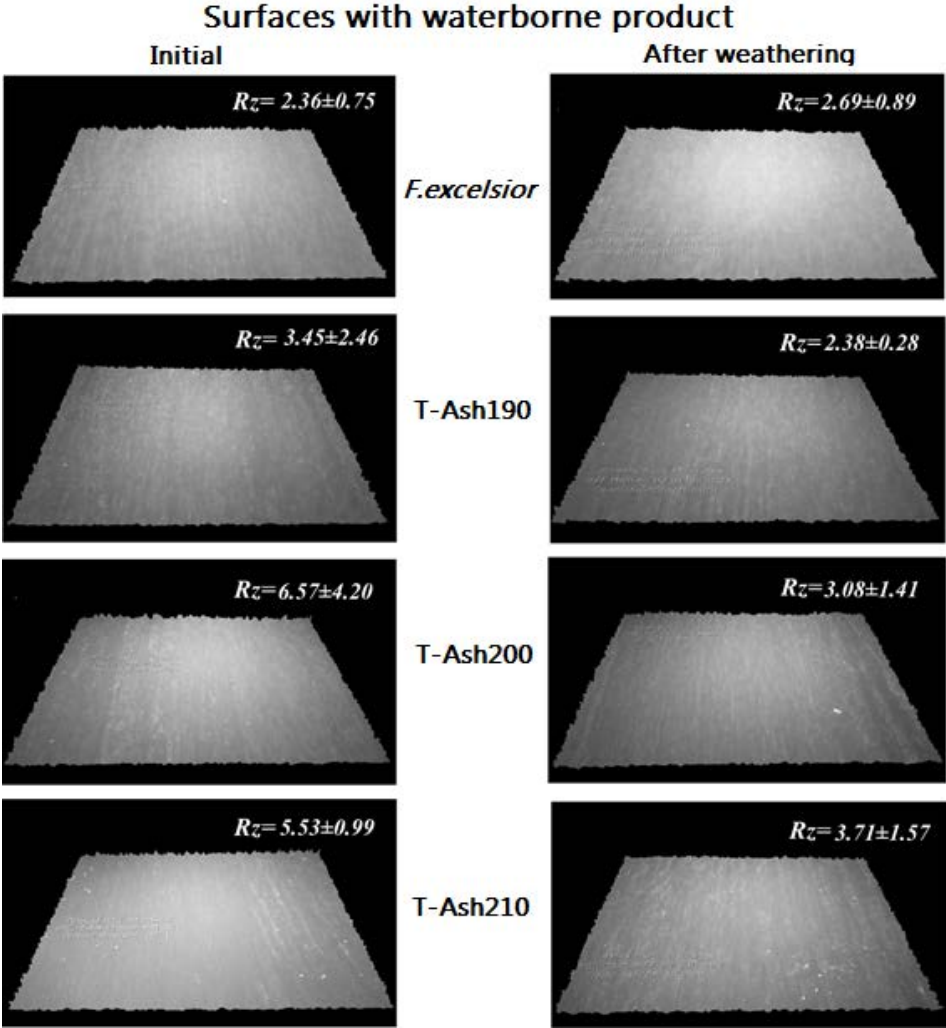


Figure II-27 3D surface topography maps and roughness (R_z) values of wood coated with *waterborne* coating before and after aging test.

3.3.5.5.2 Measurement of changes in the appearance of surface by hyperspectral images

Visual appearance is one of the most important attributes of wood products. Diverse coatings are designed for that reason to preserve the color stability avoiding dramatic changes to the surface outlook during service life¹⁸⁸ (Fig. II-26). The usual procedure of the surface color measurement is with color-meters, which is very limited as provides as a result an averaged value over the limited area. It is not enough information to properly define the fine variations of the wood surface pattern, including differences due to wood anatomy, staining, decay or surface finish applied.

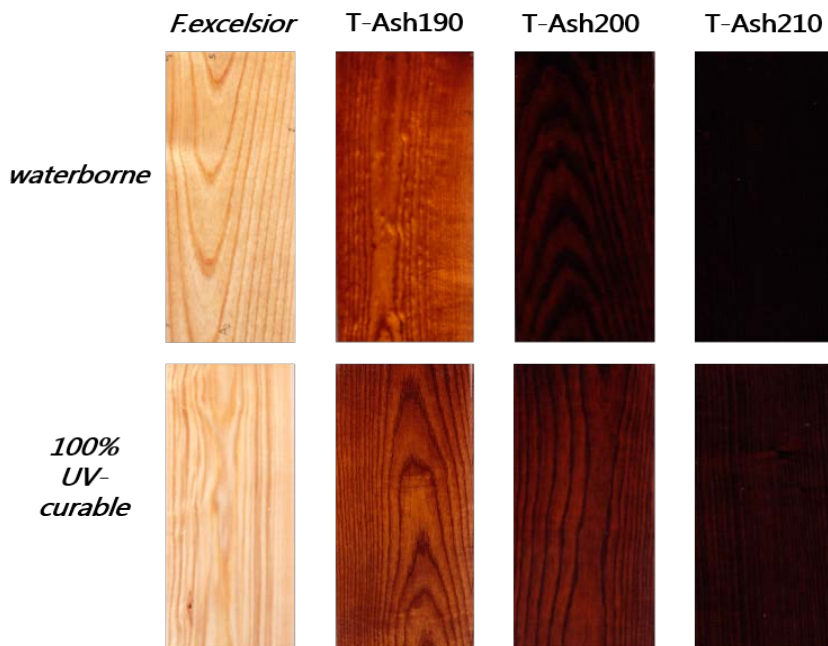


Figure II-28 Scanned images of wood with coating product.

An alternative approach for determining range of wood colors appearing on the exposed surface was adopted for the needs of this research. It is possible to scrutinize the whole range of color parameters, separate for each wood component, by assessing the surface with hyperspectral imaging. Such an approach facilitates the tracking and understanding of the optical changes due to weathering process with a fine resolution of a single pixel. Figure II-27 presents

a resulting series of CIE $L^*a^*b^*$ histograms obtained for both coating systems investigated, before and after artificial weathering.

The heat-treated samples coated with *100%UV-curable* coating did not present substantial differences caused by the exposure to weathering. All the distributions of the color parameters CIE L^* , a^* , b^* measured before and after weathering matched each other. The unique exception was observed in sample T-Ash200 where a shift of the a^* and b^* histograms is evident in non-weathered samples.

The weathering effect on the coated wood surface color was slightly more pronounced in a case of samples coated with *waterborne*. The trend of shifting the histogram of lightness L^* toward darker values was noticed in a case of T-Ash190 and T-Ash210, where differences reached ~18%. The gap between weathered (and not) samples was highest for sample T-Ash200 where medians were diverse more than 55%. Similarly, the range of the parameter a^* was shifted slightly toward greenish color in all heat-treated samples with exception of T-Ash200 where the difference reached ~26%.

Even if detailed numerical analysis of histograms provides evidences of minor changes due to the surface weathering, the visual assessment confirms minor deterioration. All the characterized samples were considered, therefore, as resistant to the artificial weathering. Complementary parameters were extracted from the median values of hyperspectral histograms to summarize in Table II-22 the overall color variation (ΔE) as well as to quantify the chromatic strength (C^*) and hue angle (h^*).

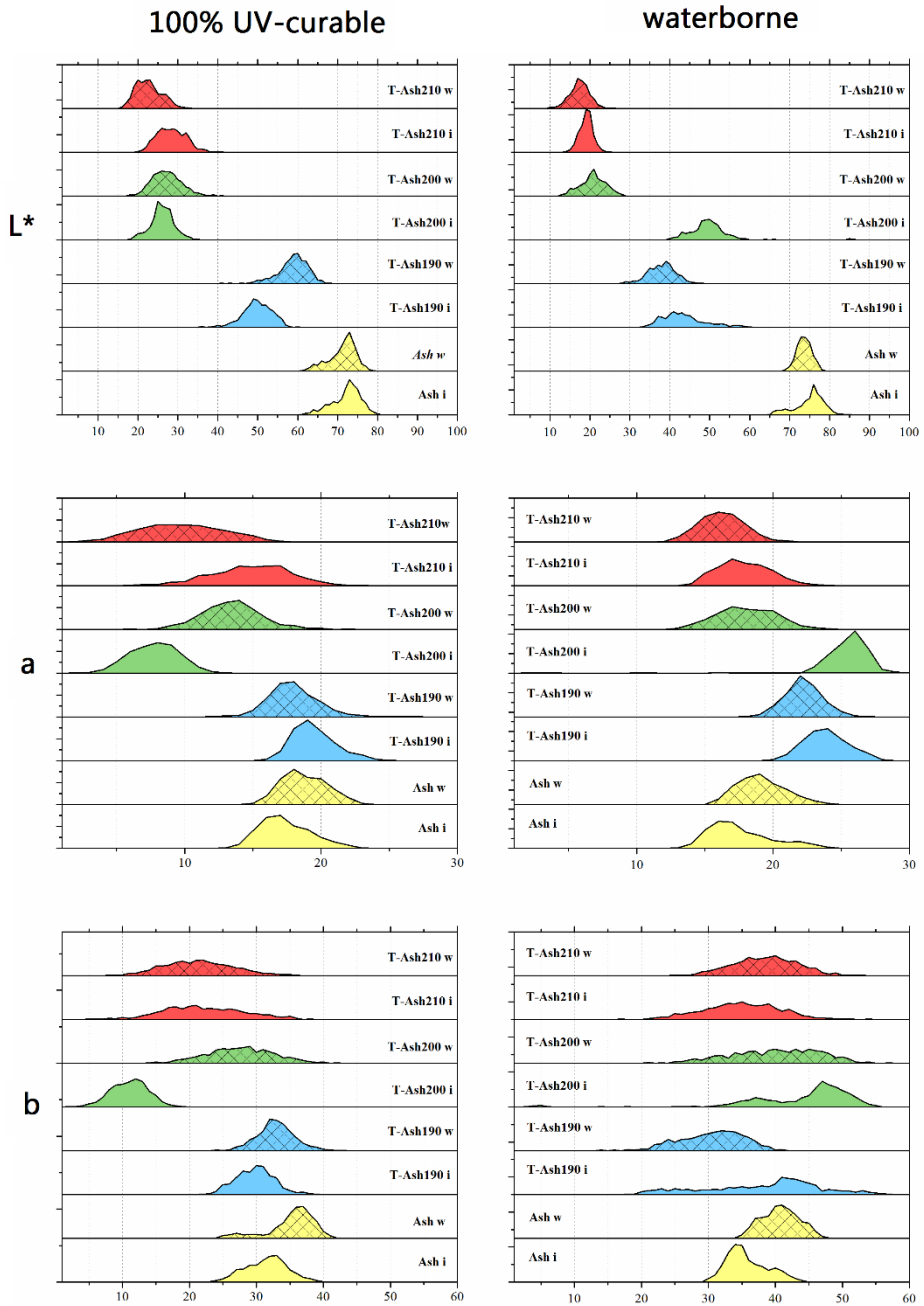


Figure II-29 Histograms of CIE $L^*a^*b^*$ color parameters after (a) and before (b) artificial weathering test obtained by hyperspectral image. T-Ash: (190,200,210). Control: C0.

The analysis of ΔE revealed a peculiar trend, in which the color stability varied according to the following sequence: *F. excelsior* > T-Ash210 > T-Ash190 > T-

Ash200. The development was similar either in *waterborne* or in *100%UV-curable* coatings. It is clear that the most intensively treatment (T-Ash210) presented an overall color variation change comparable with reference samples. It corresponded to the slight differences of the treatment processes implemented in different locations but follows results of the former studies as reported for the *waterborne* coatings. The change of the overall color ΔE was slightly higher in the case of T-Ash210 with *100%UV-curable* coating (55% higher than control) compare to T-Ash210 coated with *waterborne* coating (only 3.6% greater than control).

Table II-22 Changes in optical parameters after weathering test.

Product	<i>F.excellisor</i>			T-Ash190			T-Ash200			T-Ash210		
	b	Δ	a	b	Δ	a	b	Δ	a	b	Δ	a
<i>100%UV-curable</i>												
ΔE		4.76			9.64			17.48			7.41	
C^*	71.78	75.80		58.4	71.46		48.14	51.73		34.5	38.57	
h^*	18.19	25.96		13.33	13.48		11.72	11.88		6.64	6.12	
<i>Gloss</i>	26.79	31.28		28.58	27.92		15.32	15.72		7.91	9.34	
<i>waterborne</i>	i	Δ	w	i	Δ	w	i	Δ	w	i	Δ	w
ΔE		4.44			12.81			25.15			4.60	
C^*	32.59	33.98		34.19	30.82		16.15	16.6		13.1	16.54	
h^*	77.5	79.01		60.06	60.88		40.06	45.5		36.36	46.27	
<i>Gloss</i>	37.87	37.3		35.75	30.47		32.04	26.28		25.3	21.70	

b=initial; a=weathered, Δ =overall color difference

The chromatic strength (C^*) of heat-treated samples coated with *100%UV-curable* product had similar values to the reference samples, with exception of sample T-Ash190 where changes were noticeable. Values of C^* before weathering were lowest for *waterborne* coated samples due to an effect of the higher film thickness formed with this product. The variation of C^* values after weathering experiment were also relatively low (changes < 4%) in *waterborne* coated samples.

The hue angle (h^*) decreased inversely to the treatment intensity from control to T-Ash20, similarly in both researched coating systems. This is correlated with the visual perception of the color darkening at different levels of heat-treatment. The hue angle was constant after weathering test in all samples with *100%UV-curable* product. Though, h^* gradually increased from T-Ash190 to T-Ash210 when coated with *waterborne* product.

Both coating systems adopted for the needs of this research differed in term of the surface gloss. The *waterborne* finish is a shiny product with a major contribution of the light reflected from the surface in a specular mode. *100%UV-curable* is in contrast, applied as a semi-matt coating reflecting light with Lambertian scatter. The gloss retention on thermally modified samples coated with *100%UV-curable* product increased after accelerated weathering, with changes less than or equal to control ($\Delta gloss \leq 16\%$). The gloss of samples coated with *waterborne* product was lower than control, decreasing from 14 % to 18% when compared to non-weathered samples. The reduction of the gloss value is usually associated with the surface (micro) roughness evolution. Some authors consider the gloss-roughness progress as a usable indicator of the surface state in degradation process that could be also implemented for the service life length prediction^{189,190}. *100%UV-curable* surfaces of all investigated samples were rougher than *waterborne* coatings, even that were more stable along weathering. It was also noticed that even if initially shiny, *waterborne* surfaces were highly susceptible to the gloss reduction.

3.3.5.5.3 Wettability, surface energy and work of adhesion after weathering

The interactions between reference liquids and coated surfaces were assessed by measuring a sessile drop contact angles as was explained in section 3.3.5.3. An effect of the surface weathering on the wood-coating interactions was assessed following the same procedure and calculating three contact angles followed by solving the share contributions¹⁹¹. All the contact angles in no-treated samples

coated with both products were higher than in control wood, as presented in Table II-23. It is related to the presence of surfactants and/or additives in the formulation introduced to the coating in order to prolong the service life^{188,192}. Accordingly, the total surface energy of *waterborne* coatings (γ_S^T) increased following the treatment temperature (Control < T-Ash190 < T-Ash200 < T-Ash210). The overall alteration (~10%) was lower than in uncoated samples, with exception of T-Ash210, where $\gamma_{SZ} > \gamma_{SZ}$. Diverse trend was noticed for *100%UV-curable* coated samples, where the surface free energy γ_{SZ}^T was similar to that of uncoated control samples (γ_{SZ}^T), what was confirmed by the observations of other researchers^{128,193,194}. Contact angles on coated surfaces decreased after weathering test, making the surface less hydrophobic.

Table II-23 Liquid-solid interactions before and after weathering test.

Coating product	Evaluation ¹	<i>F.excelisior</i>		<i>T-Ash190</i>		<i>T-Ash200</i>		<i>T-Aash210</i>	
		<i>initial</i>	<i>weathered</i>	<i>initial</i>	<i>weathered</i>	<i>initial</i>	<i>weathered</i>	<i>initial</i>	<i>weathered</i>
<i>100% UV-curable</i>	θ_W	72.12	64.80	96.38	95.41	75.88	70.40	81.89	73.30
	θ_E	52.56	49.87	62.84	56.32	57.89	53.87	60.49	59.45
	θ_D	48.57	47.10	41.88	41.86	40.64	47.40	43.75	46.80
	γ_{SZ}^P	31.40	10.99	38.25	0.31	34.50	8.23	34.12	6.76
	γ_{SZ}^d	7.64	30.90	0.21	39.70	4.89	31.22	3.16	30.91
	γ_{SZ}^T	39.05	41.90	38.47	40.01	39.39	39.45	37.29	37.67
<i>waterborne</i>	θ_W	104.39	99.28	98.04	86.93	96.49	78.95	92.09	88.48
	θ_E	65.70	55.03	64.22	52.00	69.09	61.13	66.75	62.53
	θ_D	61.23	54.23	55.87	53.75	56.11	54.08	54.20	41.00
	γ_{SZ}^P	0.16	0.37	0.02	2.78	0.19	5.53	0.42	1.27
	γ_{SZ}^d	30.25	35.12	42.66	32.82	49.54	28.63	60.13	36.53
	γ_{SZ}^T	30.41	35.49	42.69	35.60	49.73	34.16	60.55	37.80

¹ Contact angles of water (θ_W), ethylene glycol (θ_E), didiomethane (θ_D); Surface energy(γ_S)

The surface free energy γ_{s2}^T of *waterborne* samples gradually decreased with increase of the treatment intensity (~38% from T-Ash190 to T-Ash210). Conversely, the γ_{s2}^T of *100%UV-curable* coating was relatively stable and not affected by the deterioration due to weathering. The share of dispersive component increased remarkably in *100%UV-curable* surfaces after weathering process, while in *waterborne* surfaces the disperse component was rather stable and dominant.

The surface free energy at the phase boundary of wood-solid coating (γ_{s1s2}) was determined separately for total, dispersive and polar components. Consequently, the theoretical work of adhesion (W_a) across an interface between wood and coating system as well as the cohesion work (W_c) of a solid coating to wood were calculated according to equations in appendix. As can be noticed in Table II-24, an increase of the coating adhesion to the substrate due to weathering leads to decreasing values of free surface energy at the phase boundary with wood (γ_{s1s2}^T)¹⁹⁵. This statement was confirmed in no-treated ash samples (weathered and control) coated with either *waterborne* or *100%UV-curable* products. In that case, obtained γ_{s1s2}^T was minor after weathering, without predominant polar or dispersive component. The total surface free energy γ_{s1s2}^T increased in thermally modified wood samples coated with *100%UV-curable* product. It implies a probable loss of adhesion occurring in the system due to weathering process. Relatively high γ_{s1s2}^T values were recorded in thermally modified wood coated with *waterborne*, due to the specific nature of the coating. However, the surface free energy decreased considerably after weathering, weakening the boundary layer.

The predicted work of adhesion (W_a) emphasized important differences between thermodynamic properties of applied coating products and its responses to weathering, especially considering thermal modification of the substrate bulk. The relatively low W_a noticed in *waterborne* coated samples increased considerably after weathering. It was explained by the fact that surfactants or

remaining solvents were removed from the coating by the surface washing¹⁹⁶. On the other hand, thermally modified samples finished with *100%UV-curable* coating possessed highest W_a values after curing, that dramatically decreased due to artificial weathering. This effect is related to the formation of weak boundary layers due to the accumulation of binders, or to the presence of water in the S_1S_2 interface that could influence the adhesion itself^{107,196}.

Table II-24. Surface free energy, work of adhesion and work of cohesion at the boundary phase of wood-solid coating.

Coating product	Evaluation ¹	Ash		ThA-192		ThA-202		ThA-212	
		initial	weathered	initial	weathered	initial	weathered	initial	weathered
Control	W_{C1}	103.31		105.63		104.77		103.45	-
	γ_{S1S2}^P	9.00	0.51	1.17	45.01	1.86	19.07	1.82	21.08
	γ_{S1S2}^d	15.48	1.30	0.10	37.94	4.28	29.66	3.05	30.56
	γ_{S1S2}^T	24.48	1.81	1.27	82.95	6.14	48.73	4.87	51.64
	W_a^P	29.18	17.26	89.87	8.09	85.00	41.52	84.02	37.40
	W_a^d	37.03	74.48	0.13	1.78	0.63	1.58	0.11	0.35
	W_a^T	66.21	91.74	90.00	9.87	85.63	43.10	84.13	37.75
	W_{C2}	78.10	83.80	76.94	80.02	78.78	78.90	74.58	75.34
100%UV-curable	γ_{S1S2}^P	5.01	3.98	50.76	31.34	46.24	23.85	42.82	36.78
	γ_{S1S2}^d	1.42	0.60	40.83	31.22	47.57	27.14	59.64	36.15
	γ_{S1S2}^T	6.43	4.58	91.59	62.56	93.81	50.99	102.46	72.93
	W_a^P	2.08	3.17	2.05	24.23	6.31	34.04	9.32	16.21
	W_a^d	73.69	79.40	1.85	1.62	1.99	1.51	0.49	0.38
	W_a^T	75.77	82.57	3.90	25.85	8.30	35.55	9.81	16.59
	W_{C2}	60.82	70.98	85.38	71.2	99.46	68.32	121.1	75.60
	waterborne	γ_{S1S2}^P	5.01	3.98	50.76	31.34	46.24	23.85	42.82
γ_{S1S2}^d		1.42	0.60	40.83	31.22	47.57	27.14	59.64	36.15
γ_{S1S2}^T		6.43	4.58	91.59	62.56	93.81	50.99	102.46	72.93
W_a^P		2.08	3.17	2.05	24.23	6.31	34.04	9.32	16.21
W_a^d		73.69	79.40	1.85	1.62	1.99	1.51	0.49	0.38
W_a^T		75.77	82.57	3.90	25.85	8.30	35.55	9.81	16.59
W_{C2}		60.82	70.98	85.38	71.2	99.46	68.32	121.1	75.60

¹ Surface energy free surface energy at the phase boundary with wood (γ_{S1S2}), work of adhesion (W_a), work of cohesion (W_c)

The overall stability of the wood-coating arrangement depends on the cohesion forces W_c within individual system components as well as on the W_a at the boundary phase¹⁹⁶. The coating was the weakest component¹⁹⁶ of the system in the thermally modified ash samples coated with *100%UV-curable* product, as $W_{C1} >$

$W_a > W_{C2}$. Nevertheless, the expected failure zone of the coating changed after weathering to the boundary phase, due to reduction of the work of adhesion W_a value. Analogous trend of the interface weakening was noticed for thermally treated coated with *waterborne* products. However, a major decrease in the W_a was noticed when comparing to weathered *100%UV-curable* samples.

3.3.5.6. Conclusions

The practical conclusion of the research presented confirmed highest suitability of the thermally modified wood for applications requiring elevated resistance for the surface weathering. Both tested coating configurations demonstrated superior performance with only small differences between products. The surface adherence is not significantly different from that of unmodified wood, thus, the reduced acidity and water uptake of modified wood did not negatively influenced the finishing of the modified surfaces. Both tested coating configurations demonstrated superior performance with only small differences between products. Thermally modified wood is suitable for high demanding surface finishing, even if further independent studies in the natural weathering arrangements are indispensable for the product quality assurance.

3.3.6. Environmental profile

The last section of this chapter deals with the environmental impacts and energy used for producing thermally modified wood, as well as the characterization of the liquid and solid residues generated during the industrial heat-treatment. On the one hand, the quantification of the environmental impacts and energy used for the production of one cubic meter of T-Pine, was elaborated using the LCA methodology. On the other hand, the residual fractions generated during industrial treatment were characterized in order to find possible uses, such as chemical or antioxidant products. The methodology used and the experimental process is summarized in the Figure II-28.

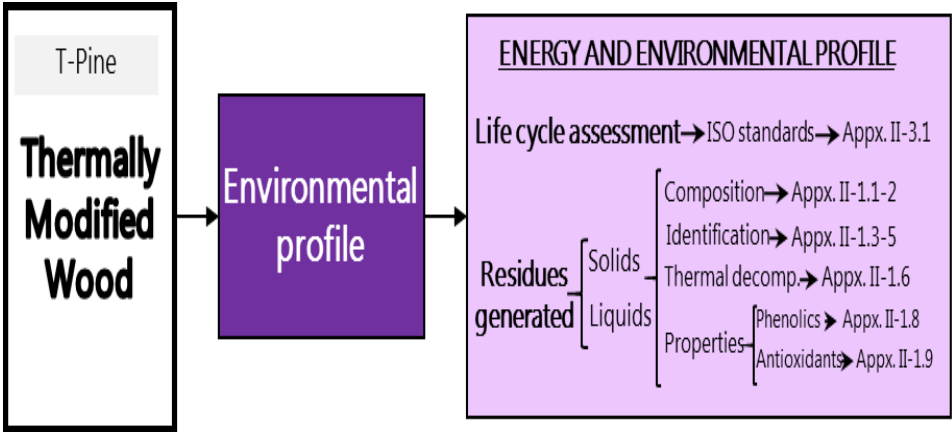


Figure II-30 Schematic of methodology used and experimental process for the analysis of residues generated.

3.3.6.1 The LCA study of thermally modified Pinus radiata boards

The LCA study of thermally modified boards was performed based on ISO 14040 (ISO 2006a) and ISO 14044 (ISO 2006b) standards. The potential life cycle environmental impacts associated with the production of thermally modified wood allows to the companies’ decision makers to be informed of the LCA study (cradle-to-gate) results, in order to have better opportunities to improve its environmental impacts. The principal parameters are listed as follows:

-Functional unit: The functional unit was defined as 1 m³ of thermally modified *Pinus radiata* boards. The choice of this functional unit is in agreement with other thermally modified products systems also assessed from an LCA perspective^{197,198}.

-System boundary: The system boundary for the product system in study is represented in a simplified way in Figure II-29. The modules included inside the boundaries are: raw material extraction and processing, processing of secondary material input (e.g. recycling processes); transport to the manufacturer; heat production; and manufacturing. The Spanish company of this example uses only natural gas for heat production.

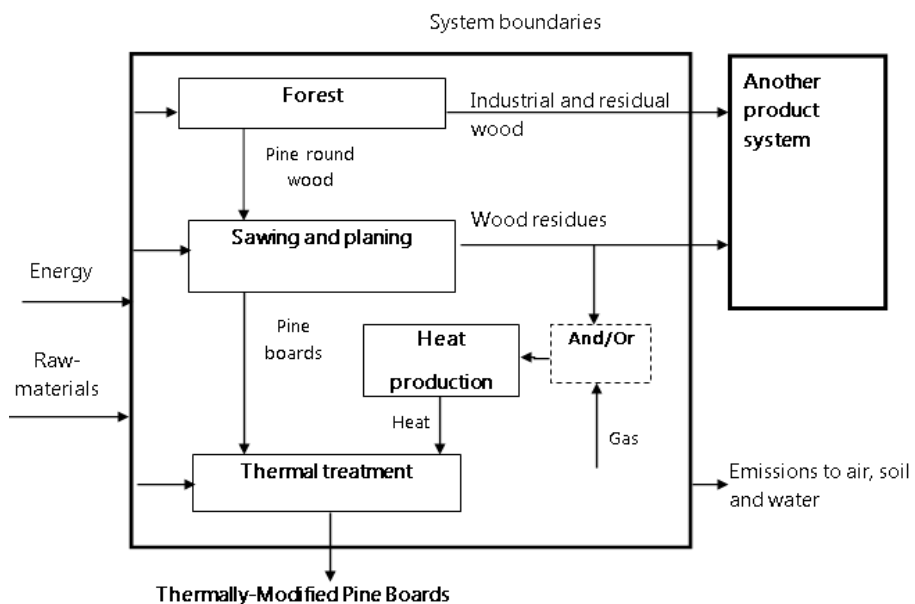


Figure II-31 System boundary for the product system.

-Allocation procedure: The forest process delivers the pine round wood as a product and industrial and residual wood as co-products. The sawing and planning process of the product system delivers the product, pine boards, and the following co-products: bark, sawdust and chips that can be used as raw material for other product systems (i.e. particle board, energy etc.). In order to solve this allocation problem, the environmental burdens are allocated to both product and co-products based on its economic value. This is in agreement with other forest-related LCA studies, in which stated that the economic allocation

could not respect the mass and energy balance of the products, correcting modules are defined in order to add or subtract the CO₂ uptake. Inputs that can be clearly attributed to specific products (e. g. gas is used only in thermal treatment) are allocated exclusively to them¹⁹⁹.

As the allocation approach can have a strong effect on the results a sensitivity analysis was also proposed considering both volume and economic allocations between the product and co-products, in order to identify differences on the environmental profiles.

-Inventory analysis: The impact analysis was performed using the LCA software SimaPro 8.1.0.60 (PRé 2015) and associated databases and methods.

-Data type/data collection: The dataset for the product and process included in the system boundary is the companies' data and is presented in Table II-25. The thermo-treatment used is Thermo-D (intense treatment) to reach a durability level that complies with the requirements for durability class 3.2 according to EN335-1-2006 standard, to use in construction of exterior decks or cladding. The data is from 2014 and all the wood comes from forests in the region where the facilities are located. All the materials and energy used for the production of the functional unit were accounted for it.

The case study was based on flat boards of radiata pine with the following dimensions: thickness = 21 mm; width = 90 mm; length = 2400 mm. The total 220 wood boards have 1m³. The average moisture content and density of wood varies from the moisture content ($u > 70\%$) and density ($\rho = 1250 \text{ kg/m}^3$) "green wood" to ($u = 11\%$) and ($\rho = 590 \text{ Kg/m}^3$) "dry wood". Regarding power sources used for electricity consumption, they were named as Endesa mix (26.5% renewables (pure + hybrid), 0.1% high efficiency cogeneration, 10.3% cogeneration, 12.9% natural gas combined cycles, 20% coal, 2.9% fuel/gas, 25.3% nuclear and 2% others). Since Endesa's electricity provided to the factory and its electricity mix is different from the Spanish average mix mentioned in the CNMC 2016.

Table II-25 Datasets for production of 1 m³ of Spanish thermally treated radiata pine boards.

Process	Inputs	Outputs
Forest		Pine round wood 1.86 m ³
Sawing and planning	Round wood (<i>Pinus radiata</i>) 1.86 m ³	Wood boards 1.09 m³
	Electricity 28.28 KWh	Wood residues (out) 0.77 m ³
	Round pine wood transport 35 t.Km	
Thermal treatment	Wood boards 1.09 m ³	Thermally modified pine boards 1 m ³
	Rope 0.02 Kg	Water 0.004 m ³
	Electricity 24 KWh	Rope 0.02 Kg
	Heat from natural gas 1465 MJ	
	Wood boards transport 22 t.Km	
	Water 0.004 m ³	

As the thermal treatment includes kiln drying of wet wood (u=70%) down to (u=12%), a shrinkage of 9% (in volume) was considered. Air emissions released from the wood are not accounted because it was considered the same emissions that would occur in wood without treatment. The following assumptions were made from datasets:

- The infrastructure of modified board production facilities was not taken into account as it has been assumed that its contribution to the overall impact is negligible²⁰⁰.
- The inventory datasets for the background system (such as electricity) were obtained and adapted as necessary from databases presented in SimaPro 8.1.0.60 software and other sources as presented in Table II-26. Whenever possible, the Ecoinvent unit process V2.2 was used, otherwise another database was chosen to model the system, like in the process, "heat from LPG" and "natural gas", where Franklin USA 98 database was used.

Table II-26 Datasets for the background system.

Process	Equivalent process	Source
Round wood	Round wood, softwood, under bark, $u=70\%$ at forest road/RER U	Ecoinvent database V 2.2
Electricity	Electricity, low voltage, at grid/ENDESA 2014 U	Ecoinvent database V 2.2 (adapted according to electricity source of ENDESA 2014)
Rope	Yarn, jute (GLO), market for Conseq	Ecoinvent 3
Heat from natural gas	Heat from nat. gas FAL	Franklin USA 98 database
Transport of round wood or wood boards	Transport, lorry >16 t, fleet average/RER U	Ecoinvent database V 2.2

3.3.6.1.1 Life cycle impact assessment (LCIA)

The method chosen for environmental impact assessment was ReCiPe Midpoint and Endpoint (H), version V1.12 / Europe ReCIPE H/A and for energy use was the Cumulative Energy Demand V1.09 (Pré 2015).

At the midpoint level, 18 impact categories are addressed in ReCiPe: climate change (CC), ozone depletion (OD), terrestrial acidification (TA), freshwater eutrophication (FE), marine eutrophication (ME), human toxicity (HT), photochemical oxidant formation (POF), particulate matter formation (PMF), terrestrial ecotoxicity (TET), freshwater ecotoxicity (FET), marine ecotoxicity (MET), ionizing radiation (IR), agricultural land occupation (ALO), urban land occupation ULO), natural land transformation (NLT), water depletion (WD), metal depletion (MD) and fossil depletion (FD).

At the endpoint level, most of these midpoint impact categories are multiplied by damage factors, and aggregated into three endpoint categories: Human health, Ecosystems and Resource. In Cumulative Energy Demand method, energy resources are divided in 5 impact categories: nonrenewable, fossil; nonrenewable, nuclear; renewable, biomass; renewable, wind, solar, geothermal; and renewable, water.

3.3.6.1.2 Quantitative results

The results show that to produce 1 m³ of thermally modified pine timber the Spanish company used a total of 17.55 GJ of cumulative energy demand of which 2.52 GJ was non renewable and 15.46 GJ renewable. The Table II-27 shows the contributions, to the impact categories considered in ReCiPe Midpoint method, for 1 m³ of thermally modified pine boards production by the Spanish company.

Table II-27 Impact assessment results associated with the production of 1 m³ of thermally modified pine boards.

Impact category	Unit	Spanish company (1m ³)
CC	kg CO ₂ eq	1.31E ²
OD	kg CFC-11 eq	4.77E ⁻⁶
TA	kg SO ₂ eq	1.71
FE	kg P eq	9.54E ⁻³
ME	kg N eq	3.24E ⁻²
HT	kg 1.4-DB eq	1.24E ¹
POF	kg NMVOC	1.39
PMF	kg PM10 eq	4.52E ⁻¹
TET	kg 1.4-DB eq	6.89E ⁻³
FET	kg 1.4-DB eq	2,34E ⁻¹
MET	kg 1.4-DB eq	2.45E ⁻¹
IR	kBq U235 eq	1.94E ¹
ALO	m ² a	1.90E ³
ULO	m ² a	1.92E ¹
NLT	m ²	1.74E ⁻¹
WD	m ³	1.05
MD	kg Fe eq	2.27
FD	kg oil eq	5.43E ¹

Acronyms: CC (climate change), OD (ozone depletion), TA (terrestrial acidification), FE (freshwater eutrophication), ME (marine eutrophication), HT (human toxicity), POF (photochemical oxidant formation), PMF (particulate matter formation), TET (terrestrial ecotoxicity), FET (freshwater ecotoxicity), MET (marine ecotoxicity), IR (ionising radiation), ALO (agricultural land occupation), ULO (urban land occupation), NLT (natural land transformation), WD (water depletion), MD (metal depletion) and FD (fossil depletion)

The results from the processes included in Spanish product system boundary, shown that electricity process is the main responsible for human toxicity (71%), ecotoxicity (freshwater 73% and marine 71%), ionising radiation (89%), water

depletion (70%) and metal depletion (54%). Heat production from natural gas is the main responsible by climate change (67%), terrestrial acidification (82%), photochemical oxidant formation (51%), particulate matter formation (69%) and fossil depletion (74%). Fossil fuel burned to harvesting round wood is the main responsible by ozone depletion (55%), marine eutrophication (48%), terrestrial ecotoxicity (76%), land occupation (agricultural almost 100% and urban 99%) and natural land transformation (97%). The contribution of transport process for the environmental profile is unrepresentative (varies from 0 to 10%) for the most indicators except for ozone depletion (22%) and metal depletion (15%). Technical wood drying infrastructure contribute with less than 1% for all impact categories. For related impact, categories considered in Environmental Product Declaration (EPD) the following comments can be addressed:

-Terrestrial Acidification (TA): The main source of this indicator is energy production with approximately 90 % of total (82 % is due to heat from natural gas).

-Freshwater Eutrophication: Freshwater eutrophication is mainly due to electricity production, representing 80 % of total. Other important source is fossil fuel burned in harvesting pine round wood process representing almost 14% of this indicator.

-Global warming (Climate change): Approximately 81% of this indicator value applies to energy for production of treated boards, and heat from gas is responsibly of the 67% of it.

-Photochemical oxidant formation: The main source of this indicator is energy for production of treated boards with 57% of total. However, another 39% applies to fossil fuel burned in the harvesting pine round wood process.

-Ozone layer depletion (ODP): Fossil fuel burned in harvesting pine round wood is still the process that most contributes to this indicator with 55% of total. Electricity and transport are other processes with a significant contribution of 13% and 22%, respectively.

-Fossil depletion: Heat from gas is the main source of this indicator with 74% of total.

3.3.6.1.3. Sensitivity analysis

The sensitivity analysis was done to determine the effects of different assumptions on LCA results, based on the using volume or economic allocations between the product and co-products. Factors allocation for products and co-products are presented in Table II-28. If mass allocation is considered instead economic allocation, the environmental profiles of thermally treated boards will be better. Thus, the indicators decrease between 4% for terrestrial acidification up to 29% for land occupation and transformation.

Table II-28 Mass allocation results of thermally treated boards.

Allocation Factors	Spanish thermally treated boards (1m ³)	
	Economic allocation	Mass allocation
Wood boards	0.79	0.56
Wood residues	0.21	0.44

3.3.6.2 Characterization of residues generated during the industrial hydrothermal process

The present section aimed to characterize the wood residual extracts generated during the industrial hydrothermal treatment of *Pinus radiata* (T-Pine210); besides, its physical properties were evaluated, in order to define the possible uses for the residual fractions such as natural antioxidants and chemical products from renewable materials.

Once heat treatment stages have been completed, inside the industrial drying chamber two types of residues are found: on the one hand, the volatile condensate which was retained in the aqueous phase; on the other hand, the solid residues (SRE) found in the lower part of the chamber (Fig. II-30). The extracts found within the aqueous phase (LRE) were necessary to separate them from the

water by a liquid-liquid extraction, in order to obtain a fraction (fLE) easier to characterize.

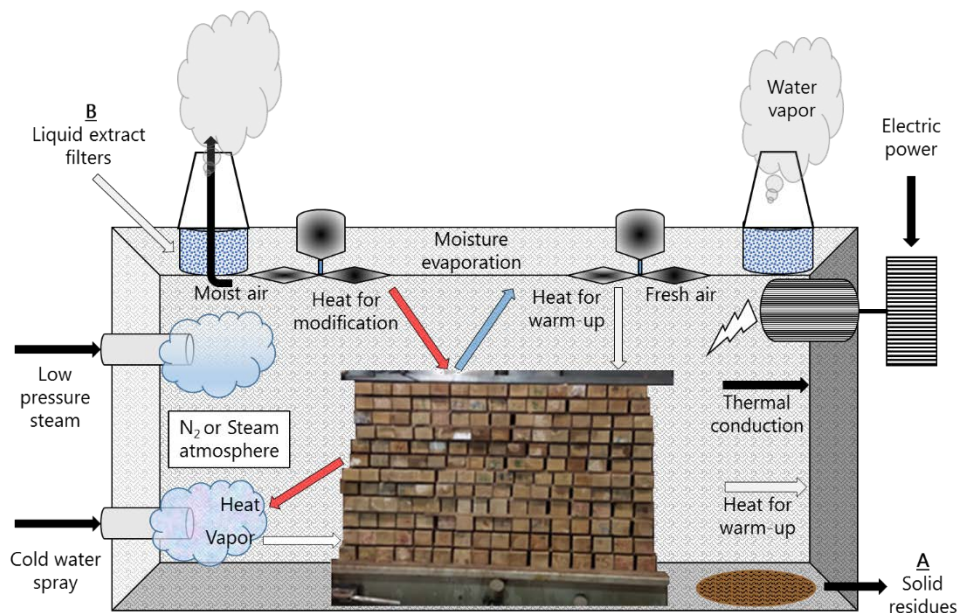


Figure II-32 Prototype of industrial thermal treatment kiln and location of solid (A) and liquid (B) residues.

3.3.6.2.1 Thermogravimetric decomposition of extracts

The thermal stability of wood residual extracts was determined with TGA, which measures the decomposition curve of the samples with increasing temperature, as shown in Figure II-31. Firstly, the analysis was carried out with LRE and SRE, but decomposition on LRE arise about 100 °C and no other shoulders in TGA curve neither mass residue above this point were detected. Thereby, the fractionated liquid extract (fLE) was evaluated instead of LRE.

The thermal profiles of SRE and fLE presented significant differences in the decomposition curves. An initial peak of first derivative curve in SRE (T_0) appeared about 92 °C and it represent approx. 14% of sample weight loss, corroborating the moisture by oven-drying method (about 13%), this loss could be attributed to evaporated water from sample. Likewise, the peak T_0 was not detected in fLE as expected, due to the liquid-liquid extraction method in which water is removed from sample.

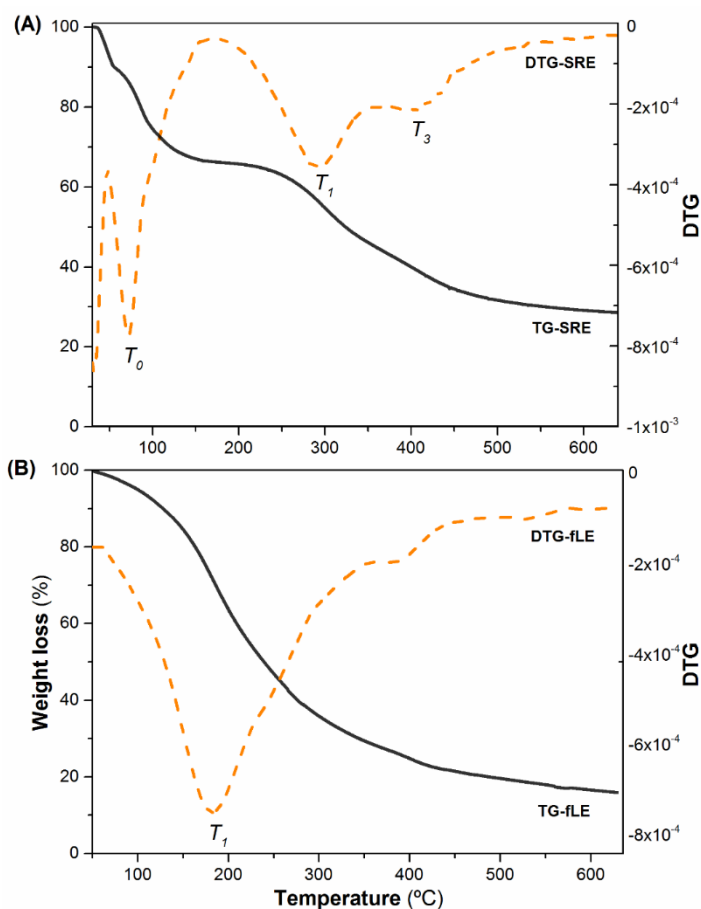


Figure II-33 TGA/DTG profiles of wood solid (A) and liquid (B) residual extracts of heat treatment of *Pinus radiata*.

Decomposition temperatures appear as shoulders in the TGA that are more easily observed in the DTG as peaks. In the case of SRE two turning points were presented, the first T_1 appears at 300.11 °C which means that 56.48% of sample was degraded up to this point, second T_2 appears at 443.62 °C with a 16.53% of sample degradation; finally, the sample has been decomposed approximately 73% at 700 °C. On the other hand, the DTG curve of fLE only showed a peak T_1 at 187 °C with a 30% of sample degradation and a residual mass of 14.31% at 700 °C.

The wood extractives start to decompose at lower temperatures than hemicelluloses and appear to protect them²⁰¹. In addition, the decomposition of

these extractives occurs in two stages with a wide temperature range between 200-550 °C. This aspect could overlap the curves of decomposition of polysaccharides and lignin, having an influence on the thermal stability of wood²⁰².

The first degradation in SRE (T_1) can be attributed to decomposition of hemicelluloses and the slower decomposition of lignin²⁰³. The second degradation step (T_2) could mean lignin and cellulose transformation or the mentioned overlapping of the released compounds^{202,204}.

With regard to fLE, some wood macromolecules start to decompose at low rate of temperature, such as fractions of lignin and non-cellulosic polysaccharides, but phenols, acids, aldehydes, ketones, furan derivative begin to be extracted at lower temperatures and are probably the main compounds of this fraction²⁰⁵. Taking into account the TG/DTG results above, it was confirmed that the SRE presents more thermal stability due to higher amount of cellulose and lignin residues²⁰³.

3.3.6.2.2 Chemical structure of extracts by FTIR

In order to represent and understand the chemical structure of residues generated during the heat-treatment of *Pinus radiata*, FTIR technique was used and the peaks found have been assigned to functional groups particularly in the fingerprint region. The absorption peaks were marked in Figure II-31 and their assignments were described in Table II-29

The main difference between fLE and SRE concerning FTIR analysis was attributed to volatile compounds generated during treatment within steam and condensed in the LRE. The most characteristic bands found in both residues correspond to a weak stretching of hydroxyl groups at 3350 cm^{-1} and strong methylene/methyl vibration at 2942 cm^{-1} and 2854 cm^{-1} ; these bands probably correspond to fractions of polysaccharides and lignin detached during thermolysis. On the group frequency region, the only difference was found at 3240 cm^{-1} in fLE, suggesting the existence of amine group. This group could be generated from

the thermal degradation of wood nitrogen derivatives such as proteins and aminoacids²⁰⁶.

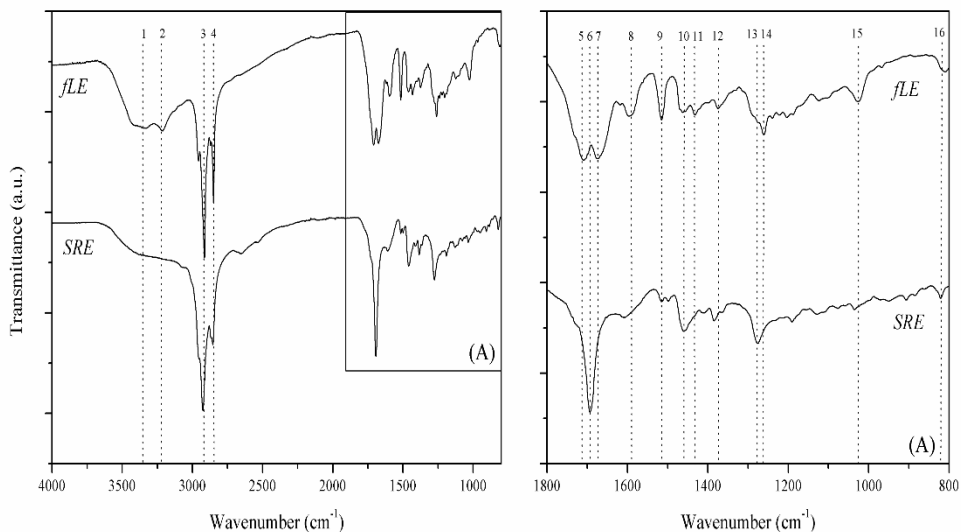


Figure II-34 FTIR spectra of wood residual extracts of heat treatment of *Pinus radiata*. Peak numbers were classified according to Table II-29.

The absorption bands in the fingerprint region are shown in Figure II-31(A), and the relevant changes were pointed out; however, are more complex and difficult to assign. In SRE an intense band at 1697 cm^{-1} was found and assigned to carbonyl stretch, but in fLE the same band was separated in two peaks, at 1734 cm^{-1} and 1680 cm^{-1} , that could be arises from saturated fatty acids, esters and aldehydes²⁰⁷.

The bands between 1600 cm^{-1} and 1400 cm^{-1} mostly represent substances of aromatic nature as shown by the predominance of ring vibrations in the spectrum. Due to low molecular weight of the aromatic compounds in fLE, the peaks 8, 9, 11 were detected (Figure II-31A). These substances are easily extracted from wood by heat steam and are soluble in water as expected. Moreover, in SRE a peak at 1456 cm^{-1} was detected, which corresponds with the asymmetric deformation of CH bond of xylan resulting from the degradation of hemicelluloses due to the thermal reaction²⁰⁸.

Table II-29 Peaks and assignments of FTIR spectra from residues generated during heat treatment of pine.

Wavenumber (cm ⁻¹)		Assignment	Peak number ^a
SRE	fLE		
-	3340	Intermolecular OH stretching	1
-	3240	N-H vibration	2
2942	2942	CH ₂ asymmetrical stretching vibration	3
2854	2854	CH ₂ /CH symmetrical stretching vibration	4
-	1734	Ester bond C=O stretching in saturated aliphatic acids	5
1697	-	C=O stretching vibration	6
-	1680	C=C aromatic skeletal vibration	7
-	1595	Within-ring skeletal bands	8
1510	1510	Aromatic C-C stretching vibration	9
1456	-	Asymmetrical CH deformation	10
-	1424	Aromatic skeletal vibration	11
1375	1375	CH in-plane bending in primary and secondary alcohols	12
1280	-	Carbon single-bonded oxygen in carboxylic acid	13
-	1260	Carbon single-bonded oxygen in carboxylic acid	14
-	1080	C-O asymmetrical stretching from ethers	15
815	813	Aromatic CH out-of-plane bending vibration	16

^a Peak number refers to the assignments in Fig. II-31

The intensity of peaks 12, 13, 14 vary from samples and are probably due to the production of new carboxylic acid, ester or anhydrides under the effect of steam and heat of wood treatment²⁰⁹. This fact indicates that the treatment temperature would promote degradation of extracts and polysaccharides to generate new compounds, which can arise from wood during the process.

3.3.6.2.3 Chemical composition of the residues generated

In order to track the source of the residual compounds generated during the thermal-treatment, *Pinus radiata* wood (untreated and heat-treated) was analyzed along with the residues by HPLC technique. The identification of detected products and its estimated concentrations are shown in Table II-30. Coinciding with TGA and FTIR results, the abundance of low-molecular substances such as phenolic compounds in LRE was confirmed. Moreover, the thermal

degradation of SRE in the range of polysaccharides was verified by the presence of its derived compounds and glucose moieties.

Thereby, the steam leachate was formed mainly by degraded products from the lignin and polyoses, and can vary due to evaporation and ventilation during the heat-treatment¹⁶⁹. The most abundant products concentrated in LRE were low-molecular organic acids such as acetic and formic acid. Acetic acid is already generated in the thermal modified *Pinus radiata*, and probably arise from the cleaving of acetyl-groups from polyoses and then captured in the residual aqueous phase²⁰⁹. In addition, formic acid could be generated by the degradation of hexoses of side chain that can give formic acid as by-products, as well as furfural-containing compounds²¹⁰.

In addition, other organic acids, such as galacturonic and lactic acid were generated during the thermolysis of wood, and were detected in both residual extracts. The polyoses found in *Pinus radiata* (before and after HT) were mainly galactoglucomannan (galactose, mannose and glucose) and in a minor proportion xylose, results that are in concordance with other related studies^{211,212}. The generation of xylitol in the LRE and SRE indicates an easy degradation of the units of xylose²¹². In spite of the fact that cellulose is less affected by heat treatment^{87,211}, the main compound found in SRE was glucan, that includes glucose structural units of hemicellulosic polymers and cellulose from its amorphous fraction, probably acidified with the organic acids generated¹⁶⁹.

Simultaneously, the volatile compounds of SRE and fLE were analyzed by Py-CG-MS and GC-MS techniques, respectively, and its chemical profiles are shown in Figure II-32. The volatile compounds found in the residues were classified in four main groups: sugars derived, lignin derived, nitrogen derived compounds and fatty/resin acids; and are summarized in Table II-31. The compounds derived from sugars were mainly identified in the fLE (29.40%) and in minor amounts in SRE (8.67%). The furans were probably originated from polyoses (5-

hydroxymethy-2-furaldehyde; 2-butyltetrahydrofuran; 2, 5 furandicarbaldehyde); moreover, maltol and butyrolactone are moieties that probably were arising from cellulose fraction^{213,214}.

Table II-30 Relative amounts of monosaccharides and degradation products in *Pinus radiata* (untreated and heat-treated) and in the residues generated during treatment.

Type of product	Compound	Concentration [%]			
		<i>Pinus radiata</i>	T-Pine210	LRE	SRE
Polysaccharides	Glucan + Hemicelluloses ^a	53.86	63.62	-	0.10
	Anhydroxylose	23.12	18.68	-	-
	Anhydrosabinose + Anhydrogalactose ^b	12.12	5.27	-	-
	Anhydromannose	10.99	13.40	-	-
	Yiel of saccaharides	62.21	62.61	-	-
	Thermal degradation products	Galacturonic acid	-	-	1.01
Xylitol		-	-	3.28	2.45
Lactic acid		-	-	5.01	4.87
Formic acid		-	-	24.5	-
Acetic acid		-	1.21	26.29	-
HMF ^c		-	-	1.24	-

^a Glucan (including cellulose and glucose structural units of hemicellulosic polymers); ^b Amount corresponding to the sum of the compounds ^c Hydroxymethylfurfural

Moreover, the aromatic hydrocarbons that have emerged from lignin transformation represent between 33-40% of the compounds found in fLE and SRE. The thermal degradation of lignin has produced guaiacol and syringol that are also converted in phenolic aldehydes (vanillin, coniferyl aldehyde), ketones (guaiacylacetone, acetoguaiacone), and others phenolic compounds such as E-isoeugenol, 2-hydroxy-1-(4-hydroxy-3-methoxyphenyl) ethanone, 2-methoxy-4-

vinylphenol and vinylacetylene^{213,215,216,217}. All these mentioned compounds were detected in both residual extracts.

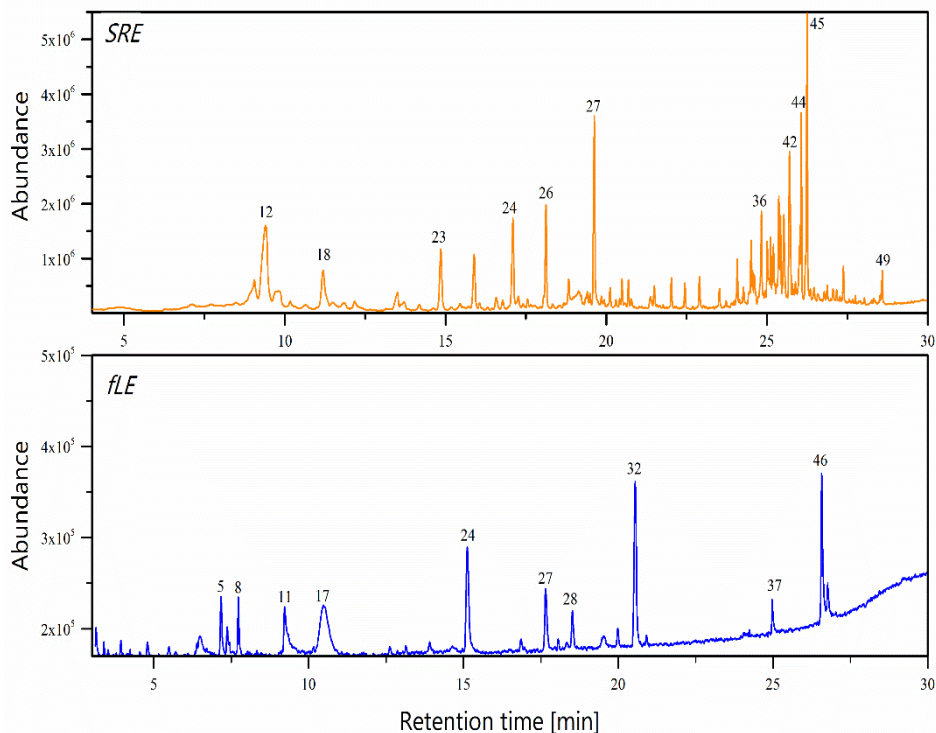


Figure II-35 Chromatograms obtained by Py-GC-MS (SRE) and GC-MS (fLE). Peak labels are listed in Table II-31.

Fatty acids are primarily produced as free acids in softwood and hardwood species, and the presence of methyl esters in the analyzed residues could be partially attributed to the methylation of these acids during pyrolysis²¹⁸. Moreover, resin acids have various structural isomers that when are submitted to pyrolysis treatment can appear like resins of abietic-type (dehydroabietic acid methyl ester)²¹⁹. Other authors found fatty and resin acids and their esterified derivatives in softwood and in forestry residues, such as hexadecanoic acid methyl ester and α -pimaric acid^{218,220}.

Table II-31 Chemical composition of the residues generated.

No.	Compound	RT ^a (min)	R. amount (%) ^b	
			fLE ^c	SRE ^d
<i>Sugar derived compounds</i>				
2	5-Methylfurfural	5.5	0.84	-
3	Furfuryl alcohol	6.5	2.83	-
4	2-Furanocarboxaldehyde-5-methyl	7.1	-	1.07
5	2,5-Furandicarbaldehyde	7.2	3.97	-
8	Maltol	7.7	3.36	-
10	2-Butyltetrahydrofuran	9.1	-	3.20
14	Furan α -carboxylic acid, methyl ester	9.8	-	0.91
15	5-Acetoxymethyl-2-furaldehyde	10.2	0.73	-
17	5-Hydroxymethyl-2-furaldehyde (HMF)	10.5	16.02	-
18	3(2H)-Furanone, dihydro-5-isopropyl	11.2	-	2.80
29	D-Allose	19.1	-	1.59
31	Phenylacetyl formic acid, 4 hydroxy-5-methoxy	20.0	1.11	-
	Sub-total		29.40	8.67
<i>Lignin derived compounds</i>				
6	Guaiaicol	7.4	1.59	-
12	Vinylacetylene	9.4	-	7.93
19	Cathecol	11.5	-	0.69
22	Syringol	13.9-15.9	0.75	1.91
23	2-Methoxy-4-vinylphenol	14.9	-	2.25
24	Vanillin	15.1-17.1	9.65	2.86
25	Acetoguaiacone	16.9-18.8	0.95	1.00
26	<i>E</i> -Isoeugenol	18.1	-	2.23
27	Guaiaicylacetone	17.7-19.6	5.04	4.49
28	2-Hydroxy-1-(4-hydroxy-3-methoxyphenyl) ethanone	18.6	2.74	-
32	Coniferyl aldehyde	20.6	12.50	-
36	Phenol,4'4-(1-methylethylidene)-bis [2-methyl]	24.8	-	2.25
38	Benzene, 1,1'-(1-methylethylidene)bis [4-methoxy]	25.0	-	1.66
39	Benzene, 1,3-diethyl-5-methyl	25.1	-	1.17
40	Benzaldehyde,3-[4,(1,1-dimethylethyl) phenoxy]	25.4	-	2.28
41	Cembrene	25.4	-	1.47
43	1-Heptene, 1,1-diphenyl	26.0	-	1.27
45	Benzylidenecamphor	26.2	-	5.68
	Sub-total		33.22	39.14
<i>Nitrogen-containing compounds</i>				
11	1-Butylimidazole	9.2	6.98	-
13	1H-Imidazole-4-carboxylic acid, methyl ester	9.7	-	0.93
16	2(1H)-Pyridinone, 3-methyl	10.2	-	0.86
33	2,5-Pyridinedicarboxylic acid, 2-methyl ester	24.1	-	0.90
37	Palmitic amide	25.0	1.87	-
42	Dehydroabietylamine	25.7	-	3.69
46	Oleamide	26.6	8.79	-
47	Stearic amide	26.8	2.83	-
	Sub-total		20.47	6.38
<i>Fatty/resin acids and others</i>				
7	Glutaric acid anhydrid	7.7	-	1.02
9	2-Pentenoic acid, 2-methyl	8.5	-	0.90
34	Hexadenoic acid, methyl ester	24.5	-	1.02
35	α -Pimaric acid	24.6	-	0.78
44	Phosphetane,2,2,3,4,4-pentamethyl-1-phenoxy-, 1-oxide	26.1	-	3.23
49	Dehydroabietic acid methyl ester	28.5	-	2.33
	Sub-total		-	9.28
	Total identified compounds		83.09	63.37

^a Retention time; ^b Percentage of peaks calculated by the area normalization method; Compounds measured by ^c GC-MS and ^d Py-GC-MS

In addition, some nitrogen-containing products were identified in SRE and fLE, which probably have been formed in the treatment chamber during the thermolysis process under the inert N₂ atmosphere, which could react with fatty and resin acids by generating new structural rearrangements (oleamide, palmitic amide, dehydroabietylamine, stearic amide). Besides, compounds constituted by NH₂ groups (1-butylimidazole) could be generated from fraction of proteins and aminoacids naturally present in wood²²¹.

3.3.6.2.4 Potential use of residues generated during the industrial hydrothermal process

Taking into account the results of the previous characterizations of the residues carried out, it was determined that the extracted products may have antioxidant capacity due to their composition and may also be a source of phenolic compounds useful in fine chemistry. To know that potential, DPPH free radical scavenging activity and total phenolic content (TPC) were used as determination techniques^{213,222,223}. The results of the phenolic content and antioxidant activity found in fLE and SRE are expressed in Table II-32.

The results indicate low values of TPC in the SRE fraction, in concordance with the results of chemical characterizations, where a large number of non-volatile compounds were found. In contrast, a higher concentration of gallic acid equivalent was measured in fLE, reaching up 95.15 g kg⁻¹ of extract. Moreover, this fraction presented a satisfactory scavenging activity (antioxidant activity) of 53.40% of DPPH free radical and the positive control obtained a value of 89.05%.

Table II-32 Phenolic content and antioxidant activity of the residues generated during the heat-treatment.

Sample	Total phenolic content [g kg ⁻¹]	DPPH radical inhibition [%]
fLE	95.12±0.24	53.40±3.12
SRE	40.72±1.29	15.29±0.38
Trolox	-	89.05±0.07

These promising results in fLE could be assigned to its high phenolic content, an important point for improve the profitability of the integral industrial process. In addition, synthetic antioxidants such as BHT (butylated hydroxyanisole) and BHA (butylated hydroxytoluene) have been restricted due to potential carcinogenic effects, thus promoting new organic alternatives²²⁴. However, these results are a preliminary screening and subsequent tests are necessary to monitoring the entire kinetics and stoichiometry of the reaction, such as azo-compound methods, which show a direct evidence of the ability of tested compounds to act as antioxidants, or methods based on the metal chelating activity against redox-active metals such as iron and copper^{218,220,224}.

3.3.6.3 Conclusions

The environmental products performance has become a growing concern, due to the increasing restrictive legislation and to a greater collective awareness of environmental problems. LCA may identify processes or stages in the wood chain with a high environmental impact and highlight areas where environmental information is unknown. Although the amount of energy necessary for the thermal treatment is much higher than that used in wood processing, the modified wood prolongs the service life of the product (3 or 4 times) without the use of chemical during the heat treatment process, promoting a sustainable development. However, there is a very low proportion of LCA in biomaterials including wood, which makes it difficult to compare with other products and to improve methods. Here some methodical approaches were proposed regarding the harmonization of system boundaries, functional units, considered processes, and allocation.

Another environmental aspect is the use of the residues generated during industrial hydrothermal treatment, and in this study, significant results were provided for a possible utilization of such biomass residues. The liquid residue (LRE) mainly presents low-molecular organic acids compounds and it showed a decomposition at lower temperature than the solid residue (SRE), which is composed by sugar derivatives. The preliminary evaluation confirmed the antioxidant capacity of the LRE, which could generate remarkable benefits in the integral process of industrial wood modification. However, subsequent tests are necessary to confirm these results.

4

**General conclusions,
future research and
published works**

4.1 General conclusions

The most relevant characteristic of modified wood by heat treatments is the fact that it is a physical process, which chemically modify the cell wall structure avoiding the use of chemicals during the process, thus promoting a sustainable development of new wood-based materials for industrial applications. The polycondensation reactions that occurs in the wood matrix, resulting in a cross-linking of the lignin network and in the depolymerization of the most hydrophilic compounds. In general, all changes are induced by different chemical reactions occurring simultaneously, which are intensified with the treatment temperature (from Thermo-S to Thermo-D) but also depending on the wood specie. However, is not feasible to predict the effect of treatment only by means of modification temperature, because some species like *Quercus robur* are more sensitive even at mild conditions and others like *Pinus radiata* are chemically resistant. The use of chemical information obtained by experimental and analytic methods, could be used to create predictive models that quickly provide information on presumably properties obtained and therefore, optimizing the appropriate treatment for each specific specie, saving time and chemical consumables.

During the heat treatment, modifications in the cell wall layers, such as degradation of fibers or tracheid's and changes in the microfibrils angles, are mainly responsible for the reduction in density and swelling, as well as for their improved dimensional stability. On the other hand, a negative effect is on the bending strength, which decreases after modification, having more impact at higher intensity of treatment. The wood properties after weathering conditions vary moderately in thermally modified wood, finding the greater differences in MC, MOE and MOR in the untreated wood; these results demonstrate the reduced influence of the factors inherent to outdoor exposition after modify wood, finding the most stable properties in pine samples treated at 210 °C (T-Pine210).

The effect of the physical-chemical changes in the modify wood enhances the durability against wood-rot basidiomycetes and their attack is only noticeable

after an extended period, considering heat treated wood as an alternative to conventional wood preservatives for applications in hazard classes 2 and 3. The mechanisms of colonization by fungi are altered in modified wood, in which the initial fungal oxidative process is less accessible to acetylation, and thus the enzymatic depolymerization begin only after an extended period of fungal colonization.

The components of the surface free energy were redistributed from polar-to-dispersive character changing the polarity of wood, as well as reducing acidity and the water uptake. This altered polarity do not significantly change the surface adherence from that found in the unmodified surfaces, and in general, the finishing process of the modified surfaces was not influenced negatively. Thermally modified wood is suitable for high demanding surface finishing and their performance after artificial weathering test provide favorable service life perspectives of the products made from this material.

The sustainability of thermally modified products requires prolonged lifespan and the possibility of reuse before their end of life. The first step is to identify processes or stages in the wood chain with a high environmental impact trying to harmonize the boundary systems, functional units, processes and allocation. Moreover, the surface preservation of modified wood products with adequate protective products provide an extended service life before its reuse according to the cascade principle for wood-based products. However, it is difficult to compare with other products due to the very low proportion of LCA concerning bio-based products. Another environmental aspect is the waste management of the residues generated during industrial hydrothermal treatment, in which the possible use as add-value products or as chemical feedstock could generate remarkable benefits in the integral process of industrial wood modification.

4.2 Future research

- Optimization of the modification process to obtain products with high quality by means of statistical projections from characterizations data. The use of chemometrics tools could speed up the process of quality control by extracting useful information from non-destructive techniques and simplifying the interpretation of results, without the excessive use of chemical consumables.
- General approach in the study of protective products specifically for thermally modified products, focused in the UV protection and fire resistance. In addition, testing the most typical wood products used in buildings and their interaction with adhesives and glues is an important point for future researches.
- Monitoring the application of environmental issues in the whole chain of custody of thermally modified products is a researcher key for future documents. The application of the cascading principles and the deepening in residual products of high added value, can be considered for future research.
- Chemical modification processes of wood at laboratory scale, including products such as lignins and fatty acids or natural extracts to improve the UV resistances, wettability and mechanical properties is one of the main goals for future research within the biorefinery processes group.

4.3 Published Works

4.3.1 Publications in scientific journals

During this doctoral thesis, the following publications in scientific journals related to the case study have been written:

- I. **Authors:** Herrera Rene, Erdocia Xabier, Llano-Ponte Rodrigo, Labidi Jalel
Title: Characterization of hydrothermally treated wood in relation to changes on its chemical composition and physical properties
Journal: Journal of Analytical and Applied Pyrolysis
DOI: 10.1016/j.jaap.2014.03.010
Volume: 107
Pages: 256-266
Year: 2014

- II. **Authors:** Herrera Rene, Erdocia Xabier, Llano-Ponte Rodrigo, Labidi Jalel
Title: Chemical analysis of industrial-scale hydrothermal wood degraded by wood-rotting basidiomycetes and its action mechanisms
Journal: Polymer Degradation and Stability
DOI: 10.1016/j.polymdegradstab.2015.03.013
Volume: 117
Pages: 37- 45
Year: 2015

- III. **Authors:** Herrera Rene, Muszyńska Monika, Krystofiak Tomasz, Labidi Jalel
Title: Comparative evaluation of different thermally modified wood samples finishing with UV-curable and waterborne coatings
Journal: Applied Surface Science
DOI: 10.1016/j.apsusc.2015.09.259
Volume: 357
Pages: 1444-1453
Year: 2015

- IV. **Authors:** Herrera Rene, Labidi Jalel, Krystofiak Tomasz, Llano-Ponte Rodrigo
Title: Characterization of thermally modified wood at different industrial conditions

Journal: Drewno
DOI: 10.12841/wood.1644-3985.C05.15
Volume: 59
Pages: 151-164
Year: 2016

- V. **Authors:** Herrera Rene, da Silva Daniela, Llano-Ponte Rodrigo, Labidi Jalel
Title: Characterization of pine wood liquid and solid residues generated during industrial hydrothermal treatment
Journal: Biomass and Bioenergy
DOI: 10.1016/j.biombioe.2016.10.006
Volume: 95
Pages: 174-181
Year: 2016
- VI. **Authors:** Herrera Rene, Sepúlveda Víctor, Perez Natalia, Salvo Linette, Salinas Carlos, Llano-Ponte Rodrigo, Ananías Rubén
Title: Effect of wood drying and heat modification on some physical and mechanical properties of radiata pine
Journal: Drying Technology
DOI: 10.1080/07373937.2017.1342094
Volume: 35
Pages: 1-8
Year: 2017
- VII. **Authors:** Ferreira Jose, Herrera Rene, Jalel Labidi, Esteves Bruno, Domingos Adalina
Title: Energy and environmental profile comparison of TMT production from two different companies - a Spanish/Portuguese case study
Journal: iForest
DOI:
Volume: 10
Pages:
Year: 2017
- VIII. **Authors:** Herrera Rene, Sandak Jakub, Robles Eduardo, Krystofiak Tomasz, Labidi Jalel
Title: Weathering resistance of heat-treated wood finished with coatings of diverse formulations
Journal: Progress in Organics Coatings
DOI: Submitted
Volume:
Pages:

Year: 2017

- IX.** **Authors:** Herrera Rene, Arrese Ainhoa, de Hoyos-Martinez Pedro L., Labidi Jalel, Llano-Ponte Rodrigo
Title: Evolution of thermally modified wood properties exposed to natural and artificial weathering and its perspectives as building material
Journal: Construction and building materials
DOI: Submitted
Volume:
Pages:
Year: 2017

Moreover, the following publications in scientific journals related to wood modification have been written:

- I.** **Authors:** da Silva Daniela, Herrera Rene, Batista Bibiana, Heinzmann Berta, Labidi Jalel
Title: Physicochemical characterization of leaf extracts from *Ocotea lancifolia* and its effect against wood-rot fungi
Journal: International Biodeterioration and Biodegradation
DOI: 10.1016/j.ibiod.2016.12.007
Volume: 117
Pages: 158-170
Year: 2017
- II.** **Authors:** Gordobil Oihana, Herrera Rene, Llano-Ponte Rodrigo, Labidi Jalel
Title: Esterified organosolv lignin as hydrophobic agent for use on wood products
Journal: Progress in Organic Coatings
DOI: 10.1016/j.porgcoat.2016.10.030
Volume: 103
Pages: 143-151
Year: 2017

4.3.2 Contributions in scientific conferences

The following works related to this doctoral thesis were presented in international scientific conferences and workshops:

- I.** **Authors:** Pedro G. De Cademartori, René Herrera, Luis Serrano, Jalel Labidi, Darci A. Gatto
Title: Influence of thermal treatment on the chemical composition and wettability of *Eucalyptus cloeziana* wood

Conference: Technical workshop: Bringing new functions to wood through surface modification, European cooperation in science and technology

Presentation: Oral

Place: Ghent University, Ghent, Belgium

Date: 17-19 April 2013

- II. **Authors:** René Herrera, Xabier Erdocia, Jalel Labidi
Title: Changes in chemical composition occurring in wood during the hydrothermal treatment process
Conference: Technical workshop: Characterization of modified wood in relation to wood bonding and coating performance, European cooperation in science and technology
Presentation: Poster
Place: Rogla, Slovenia
Date: 16-18 October 2013
- III. **Authors:** René Herrera, Xabier Erdocia, Jalel Labidi
Title: Chemical and enzymatic aspects of durability against white and brown rot fungi of industrial-scale hydrothermal wood
Conference: Seventh European Conference on Wood Modification, ECWM7
Presentation: Poster
Place: Lisbon, Portugal
Date: 10-12 March 2014
- IV. **Authors:** René Herrera
Title: Finishing process of thermally modified wood and resistance of coatings.
Conference: Report, Short-term scientific mission, European cooperation in science and technology
Presentation: Online: <http://cost-fp1006.fh-salzburg.ac.at>
Place: Poznan, Poland
Date: June 2014
- V. **Authors:** René Herrera, Monika Muszyńska, Tomasz Krystofiak, Jalel Labidi
Title: Surface finishing of thermally modified wood and resistance of coatings
Conference: Technical workshop: Advances in modified and functional bio-based surfaces, European cooperation in science and technology
Presentation: Oral
Place: Aristotle University of Thessaloniki, Greece

Date: 7-9 April 2015

- VI. Authors:** Rodrigo Llano-Ponte, René Herrera, Jalel Labidi
Title: La madera termo-tratada como material compuesto. Relación propiedades mecánicas estructura
Conference: Materiales compuestos 15
Presentation: Oral
Place: Madrid, Spain
Date: 6-8 July 2015
- VII. Authors:** Daniela T. Silva, René Herrera, Berta M. Heinzmann, Jalel Labidi
Title: Decay resistance and physicochemical properties of wood preservatives based on *Ocotea Acutifolia* leaves
Conference: Technical workshop: Life Cycle Assessment, EPDs and modified Wood, European cooperation in science and technology
Presentation: Poster
Place: University of Primorska, Koper, Slovenia
Date: 25-26 August 2015
- VIII. Authors:** René Herrera, Tomasz Krystofiak, Jalel Labidi
Title: Characterization of thermally modified wood at different industrial conditions
Conference: Wood-Science-Economy WSE
Presentation: Oral
Place: Poznan, Poland
Date: 5-6 October 2015
- IX. Authors:** René Herrera, Tomasz Krystofiak, Jalel Labidi
Title: Accelerated Weathering of Thermally Modified Wood Finishing with Waterborne and UV-curable Coatings
Conference: European Conference on Wood Modification, ECWM8
Presentation: Oral
Place: Helsinki, Finland
Date: 26-27 October 2015
- X. Authors:** René Herrera, Ana Sandak, Jalel Labidi
Title: Monitoring thermally modified wood performance by NIR. Case study: surface treatment
Conference: Application of NIR spectroscopy for wood science and technology research - NIR & WOOD – SOUNDS GOOD!
Presentation: Oral
Place: CNR-IVALSA, San Michele all'Adige, Italy

Date: 19-21 April 2016

- XI. Authors:** René Herrera, Daniela Thomas da Silva, Rodrigo Llano-Ponte, Jalel Labidi
Title: Characterization of waste from *Pinus radiata* generated during industrial thermal-treatment
Conference: 47th Annual Meeting of the International Research Group on Wood Protection
Presentation: Oral
Place: LNEC, Lisbon, Portugal
Date: 15-19 May 2016
- XII. Authors:** René Herrera, Ainhoa Arrese, Jalel Labidi, Rodrigo Llano-Ponte
Title: Dynamic evolution of physical-mechanical properties of heat-treated wood exposed to weathering conditions
Conference: World Conference on Timber Engineering, WCTE
Presentation: Oral
Place: Vienna University of Technology, Vienna, Austria
Date: 22-25 August 2016
- XIII. Authors:** René Herrera, Oihana Gordobil, Jalel Labidi
Title: Esterified lignin as hydrophobic agent for use on wood products
Conference: Technical workshop: innovative production technologies, increased wood products recycling, and reuse, European cooperation in science and technology
Presentation: Oral
Place: Brno, Czech Republic
Date: 29-30 September 2016
- XIV. Authors:** Eduardo Robles, René Herrera, Oihana Gordobil, Jalel Labidi
Title: Bio-cascading of heat-treated wood after service life to obtain lignocellulosic derivatives
Conference: Technical workshop: innovative production technologies, increased wood products recycling, and reuse, European cooperation in science and technology
Presentation: Oral
Place: Brno, Czech Republic
Date: 29-30 September 2016
- XV. Authors:** René Herrera, Oihana Gordobil, Jalel Labidi

Title: Esterified lignin as hydrophobic agent for use on wood products

Conference: 13th Pacific Rim Bio-Based Composite Symposium

Presentation: Oral

Place: Concepción, Chile

Date: 13-15 November 2016

- XVI.** **Authors:** René Herrera, Daniela Thomas da Silva, Jalel Labidi
Title: Potential use of plant extracts for protection of wood veneers
Conference: Technical workshop: Design, Application and Aesthetics of biobased building materials, European cooperation in science and technology
Presentation: Oral
Place: Sofia, Bulgaria
Date: 28-1 March 2017
- XVII.** **Authors:** René Herrera, Jakub Sandak, Eduardo Robles, Jalel Labidi
Title: Aesthetic changes of coated thermally modified wood after artificial weathering
Conference: 48th Annual Meeting of the International Research Group on Wood Protection
Presentation: Oral
Place: Ghent University, Ghent, Belgium
Date: 4-8 June 2017
- XVIII.** **Authors:** René Herrera
Title: Nuevas funcionalidades para la madera
Conference: Summer courses UPV/EHU, Bioeconomía forestal: Química verde
Presentation: Oral
Place: Donostia-San Sebastian, Spain
Date: 15-16 June 2017
- XIX.** **Authors:** René Herrera, Jalel Labidi, Rodrigo Llano-Ponte, Rubén Ananías
Title: The effect of wood drying and heat modification on some physical and mechanical properties of radiata pine
Conference: Technical workshop: Wood modification research and applications, European cooperation in science and technology
Presentation: Oral
Place: Salzburg University of applied sciences, Kulch, Austria
Date: 14-15 September 2017

4.3.3 Assistance to training related to the thesis

I have attended the following courses related to this doctoral thesis subject:

- I. **Title:** Finishing of the surface of thermally modified wood with UV lacquer products - theory and practice
Place: Poznan University of Life Sciences, Poznan, Poland
Date: 6-8 March 2013
- II. **Title:** X-ray tomography and service life prediction
Place: Ghent University, Ghent, Belgium
Date: 15-16 April 2013
- III. **Title:** Chemical and property changes in wood during THM-treatment
Place: Aalto University, Espoo, Finland
Date: 20-22 May 2013
- IV. **Title:** Production and Characterization of Decorative Laminates
Place: Porto and Viseu Universities, Porto and Viseu, Portugal
Date: 5-7 March 2014
- V. **Title:** Surface Characterization of Wood using Microtensile Testing
Place: Zagreb University, Zagreb, Croatia
Date: 2-4 July 2014
- VI. **Title:** Mould fungi - Evaluation of mould risk
Place: Bangor University, Bangor, UK
Date: 8-10 June 2015
- VII. **Title:** LCA of wood modification processes: where are the weaknesses in inventories?
Place: ETHZ, Zurich, Switzerland
Date: 3-4 December 2015
- VIII. **Title:** Think outside of the wooden box! PhD Workshop
Place: Hamburg University, Hamburg, Germany
Date: 3-5 July 2017

5

References

1. UNESE - Food and Agriculture Organization of United Nations Forest Products. *Forest Products Annual Market Review 2015-2016*. (2016). doi:ISBN 978-92-1-058365-7
2. Verma, M. Framework for forest resource accounting: factoring in the intangibles. *Int. For. Rev.* **10**, 362–375 (2008).
3. Gane, M. *Forest strategy : strategic management and sustainable development for the forest sector*. (Springer, 2007).
4. Belgacem, M. N. & Pizzi, A. *Lignocellulosic Fibers and Wood Handbook: Renewable Materials for Today's Environment*. *Lignocellulosic Fibers and Wood Handbook: Renewable Materials for Today's Environment* (2016). doi:10.1002/9781118773727
5. UNECE/FAO. *Forest Products. Annual Market Review 2015-2016*. (2016).
6. Plieninger, T. *et al.* The role of cultural ecosystem services in landscape management and planning. *Curr. Opin. Environ. Sustain.* **14**, 28–33 (2015).
7. Popp, J., Lakner, Z., Harangi-Rákos, M. & Fári, M. The effect of bioenergy expansion: Food, energy, and environment. *Renew. Sustain. Energy Rev.* **32**, 559–578 (2014).
8. Peck, T. . & Ottitsch, A. The European forest as source of industrial raw materials. *Land use policy* **17**, 209–219 (2000).
9. Keenan, R. J. *et al.* Dynamics of global forest area: Results from the FAO Global Forest Resources Assessment 2015. *Forest Ecology and Management* **352**, 9–20 (2015).
10. Ramage, M. H. *et al.* The wood from the trees: The use of timber in construction. *Renew. Sustain. Energy Rev.* **68**, 333–359 (2017).
11. Forest Products Laboratory - USDA. *Wood Handbook: Wood as an Engineering Material*. USDA - General Technical Report **General Te**, (2010).
12. EUROPEAN COMMISSION & Directorate-General for Research and Innovation. *Where next for the European bioeconomy?* (2014). doi:10.2777/95624
13. Sokka, L., Koponen, K. & Keränen, J. T. Cascading use of wood in Finland – with comparison to selected EU countries. *Res. Rep. VTT* 25 (2014).
14. Teuber, L., Osburg, V. S., Toporowski, W., Militz, H. & Krause, A. Wood polymer composites and their contribution to cascading utilisation. *J. Clean. Prod.* **110**, 9–15 (2016).
15. Alakangas, E., Koponen, K., Sokka, L. & Keränen, J. Classification of used wood to biomass fuel or solid recycled fuel and cascading use in Finland.

16. Commission, E. Communication From the Commission To the European Parliament, the Council, the European Economic and Social Committee and the Committee of the Regions. *Tak. Stock Eur. 2020 Strateg. Smart, Sustain. Incl. Growth* 21 (2014).
17. Ansell, M. P. *Wood Composites. Wood Composites* (2015). doi:10.1016/B978-1-78242-454-3.00015-9
18. Lyons, A. *Materials for architects and builders. Igarss 2014* (2014). doi:10.1007/s13398-014-0173-7.2
19. Freedman, G. & Kermani, A. Stress-laminated arches: a stronger case for timber bridges. *Civ. Eng.* **157**, 172–178 (2004).
20. Mongiardini, M. *et al.* Design and Testing of Two Bridge Railings for Transverse Nail-Laminated Timber Deck Bridges. *Transp. Res. Rec. J. Transp. Res. Board* **2262**, 119–130 (2011).
21. Levy, S. M. Plywood, Composite Wood Products, High-Pressure Laminates. *Constr. Build. Envel. Inter. Finish. Datab.* (2001).
22. Clouston, P. Characterization and strength modeling of parallel-strand lumber. in *Holzforschung* **61**, 394–399 (2007).
23. Sasaki, H. & Abdullahi, A. A. Lumber: Laminated Veneer. in *Reference Module in Materials Science and Materials Engineering* (2016). doi:10.1016/B978-0-12-803581-8.01989-5
24. Chapman, K. M. Wood-based panels: Particleboard, fibreboards and oriented strand board. in *Primary Wood Processing: Principles and Practice* 427–475 (2006). doi:10.1007/1-4020-4393-7_12
25. Leichti, R. J., Falk, R. H. & Laufenberg, T. L. prefabricated wood composite I-beams: a literature review. *Wood Fiber Sci.* **2**, 62–79 (1989).
26. European Union. Sustainable, secure and affordable energy for Europeans. *Sustain. Secur. Afford. energy Eur.* **1**, 14 (2012).
27. Miyashima, S., Sebastian, J., Lee, J.-Y. & Helariutta, Y. Stem cell function during plant vascular development. *EMBO J.* **32**, 178–193 (2013).
28. Blanchette, R. a & Biggs, a R. *Defense mechanisms of woody plants against fungi. Springer series in wood science* (1992).
29. Savidge, R. A. 'Annual Rings' in Temperate Zone Trees – Research Needs. in *Future od Dendrochronology - Trees RIngs and People* (2001).
30. von Arx, G., Crivellaro, A., Prendin, A. L., Čufar, K. & Carrer, M. Quantitative Wood Anatomy—Practical Guidelines. *Front. Plant Sci.* **7**, (2016).
31. Munster, S. & Andres, R. Internet bidez ordaindu izanaren agiria Justificante de pago de recibo por Internet. 9050794 (2014).

32. Thomas, P. *Trees : their natural history*. (Cambridge University Press, 2014).
33. Schoch, W., Heller, I., Schweingruber, F. H., Kienast, F. Microscopic Wood Anatomy. (2004). Available at: www.woodanatomy.ch. (Accessed: 30th November 2017)
34. Jarvis, M. C. & McCann, M. C. Macromolecular biophysics of the plant cell wall: Concepts and methodology. *Plant Physiol. Biochem.* **38**, 1–13 (2000).
35. Brandstrom, J. Morphology of Norway spruce tracheids with emphasis on cell wall organisation. *Department of Wood Science PhD*, 39 (2002).
36. Liese, W. Tertiary wall and warty layer in wood cells. *J. Polym. Sci. Part C Polym. Symp.* **2**, 213–229 (1993).
37. Chaffey, N. Microfibril orientation in wood cells: New angles on an old topic. in *Trends in Plant Science* **5**, 360–362 (2000).
38. Rowell, R. *Handbook of Wood Chemistry and Wood Composites, Second Edition*. (CRC Press, 2012). doi:10.1201/b12487
39. Laine, C. STRUCTURES OF HEMICELLULOSES AND PECTINS IN WOOD AND PULP. (Helsinki University of Technology, 2005).
40. Gellerstedt, G., Ek, M. & Henriksson, G. *Wood Chemistry and Wood Biotechnology. Wood Chemistry and Biotechnology* **1**, (2009).
41. Berg, J. M. (Jeremy M., Tymoczko, J. L., Stryer, L. & Stryer, L. *Biochemistry*. (W.H. Freeman, 2002).
42. Chen, H. Chemical Composition and Structure of Natural Lignocellulose. in *Biotechnology of Lignocellulose* 25–71 (Springer Netherlands, 2014). doi:10.1007/978-94-007-6898-7_2
43. Fry, S. C. CELL WALLS AND FIBERS | Cell Walls. in *Encyclopedia of Applied Plant Sciences* 75–87 (Elsevier, 2003). doi:10.1016/B0-12-227050-9/00014-4
44. Alberts, B. *et al.* The Plant Cell Wall. (2002). Available at: <https://www.ncbi.nlm.nih.gov/books/NBK26928/>. (Accessed: 1st December 2017)
45. Christiernin, M. Composition of Lignin in Outer Cell-Wall Layers. (Royal Institute of Technology, KTH, 2006).
46. Ralph, J. *et al.* Lignification: Are Lignins Biosynthesized via simple Combinatorial Chemistry or via Proteinaceous Control and Template Replication? in *Recent Advances in Polyphenol Research* **1**, 36–66 (2009).
47. Heitner, C., Dimmel, D. & Schmidt, J. *Lignin and Lignans: Advances in chemistry*. CRC Press Taylor & Francis Group (2010). doi:10.1016/0076-

6879(88)61028-7

48. Larisa Lvova, Dmitry Kirsanov, Audrey Legin, C. D. N. Lignin Applications in Chemical Sensing | Multisensor Systems for Chemical Analysis | Taylor & Francis Group. in *Multisensor Systems for Chemical Analysis* (ed. Pan Stanford) 30 (Taylor & Francis Group, 2014).
49. Hart, J. H. The Role of Wood Exudates and Extractives in Protecting Wood from Decay. in 861–880 (Springer, Berlin, Heidelberg, 1989). doi:10.1007/978-3-642-74075-6_22
50. Velíšek, J. & Cejpek, K. Biosynthesis of food constituents: Lipids. 1. Fatty acids and derived compounds - A review. *Czech Journal of Food Sciences* **24**, 193–216 (2006).
51. Rustan, A. C. & Drevon, C. A. Fatty Acids: Structures and Properties. in *Encyclopedia of Life Sciences* (2005). doi:10.1038/npg.els.0003894
52. Ek, M., Gellerstedt, G. & Henriksson, G. *Pulp and paper chemistry and technology. Volume 1, Wood chemistry and wood biotechnology*. (Walter de Gruyter, 2009).
53. S., M., D. Santana, A. L. B., A., C., S., L. & Bieber, L. Phenolic Extractives and Natural Resistance of Wood. in *Biodegradation - Life of Science* (InTech, 2013). doi:10.5772/56358
54. Wenjuan, C. Extraction of Scots Pine with Non-polar solvents. *Bachelor Thesis* (2013).
55. Gezici-Koç, Ö., Erich, S. J. F., Huinink, H. P., van der Ven, L. G. J. & Adan, O. C. G. Bound and free water distribution in wood during water uptake and drying as measured by 1D magnetic resonance imaging. *Cellulose* **24**, 535–553 (2017).
56. Engelund, E. T., Thygesen, L. G., Svensson, S. & Hill, C. A. S. A critical discussion of the physics of wood-water interactions. *Wood Sci. Technol.* **47**, 141–161 (2013).
57. Mohanty, A. K., Misra, M. & Drzal, L. T. (Lawrence T. *Natural fibers, biopolymers, and biocomposites*. (Taylor & Francis, 2005).
58. Reeb, J. E. & Reeb, J. E. Wood and Moisture Relationships. *Rehabilitation* 1–8 (1995).
59. Marra, A. A. *Technology of wood bonding : principles in practice*. (Van Nostrand Reinhold, 1992).
60. Stokke, D. D. & Groom, L. H. *Characterization of the Cellulosic Cell Wall. Characterization of the Cellulosic Cell Wall* (2008). doi:10.1002/9780470999714

61. Pizzi, A., Mittal, K. L., Dekker, M., New, E. R. & Basel, Y. *Handbook of Adhesive Technology*. (Taylor & Francis Group, 2003).
62. Stanzl-Tschegg, S.E. Gindl, M. S. G. Proceedings of the 2nd International Symposium on Wood Machining. in *2nd International Symposium on Wood Machining* (eds. tefanie Stanzl-Tschegg & Milojka Gindl, and G. S.) 514 (BOKU – Institute of Physics and Materials Science, 2004).
63. Obersriebnig, M., Konnerth, J. & Gindl-Altmatter, W. Evaluating fundamental position-dependent differences in wood cell wall adhesion using nanoindentation. *Int. J. Adhes. Adhes.* **40**, 129 (2013).
64. Conners, T. E. & Banerjee, S. *Surface analysis of paper*. (CRC Press, 1995).
65. Kirker, G. & Winandy, J. Above Ground Deterioration of Wood and Wood-Based Materials. in 113–129 (2014). doi:10.1021/bk-2014-1158.ch006
66. Reinprecht, L. Biological Degradation of Wood. in *Wood Deterioration, Protection and Maintenance* 62–125 (John Wiley & Sons, Ltd, 2016). doi:10.1002/9781119106500.ch3
67. Ewart, D. & Cookson, L. J. Termites and timber. *ACS Symp. Ser.* **1158**, 159–181 (2014).
68. Lopez-Anido, R., Michael, A. P., Goodell, B. & Sandford, T. C. Assessment of wood pile deterioration due to marine organisms. *J. Waterw. Port Coast. Ocean Eng.* **130**, 70–76 (2004).
69. Daniel, G. Fungal and bacterial biodegradation: White rots, brown rots, soft rots, and bacteria. *ACS Symp. Ser.* **1158**, 23–58 (2014).
70. Goodell, B., Qian, Y. & Jellison, J. Fungal Decay of Wood: Soft Rot—Brown Rot—White Rot. in 9–31 (2008). doi:10.1021/bk-2008-0982.ch002
71. Arantes, V. & Goodell, B. Current understanding of brown-rot fungal biodegradation mechanisms: A review. *ACS Symp. Ser.* **1158**, 3–21 (2014).
72. Niemenmaa, O., Professor Leif Jönsson Biochemistry, R. & Anne-Christine Ritschkoff VTT Espoo, P. Monitoring of Fungal Growth and Degradation of Wood. (University of Helsinki, 2008).
73. Fengel, D. & Wegener, G. *Wood: chemistry, ultrastructure, reactions. Wood: chemistry, ultrastructure, reactions.* (1989). doi:10.1007/BF02608943
74. Jirous-Rajkovic, V., Turkulin, H. & Miller, E. R. Depth profile of UV-induced wood surface degradation. *Surf. coatings Int. part B coatings Trans.* **87**, 241–247 (2004).
75. Yousif, E. & Haddad, R. Photodegradation and photostabilization of polymers, especially polystyrene: review. *Springerplus* **2**, 398 (2013).

76. Teacă, C.-A. & Bodîrlău, R. Photochemical Behavior of Wood Based Materials. in *Photochemical Behavior of Multicomponent Polymeric-based Materials* (ed. Rosu D., V. P. M.) 91–107 (Springer, Cham, 2016). doi:10.1007/978-3-319-25196-7_4
77. Gibson, L. J. The hierarchical structure and mechanics of plant materials. *J. R. Soc. Interface* **9**, 2749–66 (2012).
78. Gérardin, P. New alternatives for wood preservation based on thermal and chemical modification of wood— a review. *Ann. For. Sci.* doi:10.1007/s13595-015-0531-4
79. Candelier, K. *et al.* Control of wood thermal treatment and its effects on decay resistance: a review. *Ann. For. Sci.* **73**, 571–583 (2016).
80. Hill, C. *Wood modifications: Chemical, Thermal, and other Processes.* (2006). doi:10.1002/0470021748.fmatter
81. Rowell, R. M. Acetylation of wood: journey from analytical technique to commercial reality. *For. Prod. J.* **56**, 4–12 (2006).
82. Pu, Y. & Ragauskas, A. J. Structural analysis of acetylated hardwood lignins and their photoyellowing properties. *Science (80-.)*. **2139**, 2132–2139 (2006).
83. Abhyankar, P. N., Beck, K. R., Ladisch, C. M. & Frick, J. G. Effect of Different Catalysts on the DMDHEU-Cotton Cellulose Reaction. *Text. Res. J.* **56**, 551–555 (1986).
84. Xie, Y., Krause, A., Militz, H. & Mai, C. Coating performance of finishes on wood modified with an N-methylol compound. *Prog. Org. Coatings* **57**, 291–300 (2006).
85. Lande, S., Eikenes, M., Westin, M. & Schneider, M. H. Furfurylation of wood: Chemistry, properties, and commercialization. in *ACS Symposium Series* **982**, 337–355 (2008).
86. Stamm, A. J. Dimensional stabilization of wood by thermal reactions and formaldehyde cross-linking. *Tappi* **42**, 39–44 (1959).
87. Esteves, B. M. & Pereira, H. M. Wood modification by heat treatment: A review. *BioResources* **4**, 370–404 (2009).
88. Manninen, H., Hetemäki, L. & Hurmekoski, E. *Long-term outlook for engineered wood products in Europe Long-term outlook for engineered wood products in Europe Heikki Manninen.* (2014).
89. Yan-jun, X., Yi-xing, L. & Yao-xing, S. Heat-treated wood and its development in Europe. *J. For. Res.* **13**, 224–230 (2002).
90. Zabalza Bribián, I., Valero Capilla, A. & Aranda Usón, A. Life cycle

- assessment of building materials: Comparative analysis of energy and environmental impacts and evaluation of the eco-efficiency improvement potential. *Build. Environ.* **46**, 1133–1140 (2011).
91. Hurmekoski, E., Jonsson, R. & Nord, T. Context, drivers, and future potential for wood-frame multi-story construction in Europe. *Technol. Forecast. Soc. Change* **99**, 181–196 (2015).
 92. Hurmekoski, E., Hetemäki, L. & Linden, M. Factors affecting sawnwood consumption in Europe. *For. Policy Econ.* **50**, 236–248 (2015).
 93. Filiatrault, A. & Folz, B. Performance-Based Seismic Design of Wood Framed Buildings. *J. Struct. Eng.* **128**, 39–47 (2002).
 94. Parker, D. (Journalist), Wood, A. & Council on Tall Buildings and Urban Habitat. *The tall buildings reference book*. (Routledge, Taylor & Francis Group, 2013).
 95. Kuilen, J. W. G. V. De, Ceccotti, A., Xia, Z. & He, M. Very Tall Wooden Buildings with Cross Laminated Timber. *Procedia Eng.* **14**, 1621–1628 (2011).
 96. PEFC Council. *Chain of Custody of Forest Based Products - Requirements*. (2015).
 97. Finforest. *Thermowood technical manual*. (2005).
 98. Windeisen, E., Strobel, C. & Wegener, G. Chemical changes during the production of thermo-treated beech wood. *Wood Sci. Technol.* **41**, 523–536 (2007).
 99. Boonstra, M. *A two-stage thermal modification of wood*. (2008).
 100. Kocafe, D., Poncsak, S. & Boluk, Y. Effect of thermal treatment on the chemical composition and mechanical properties of birch and aspen. *BioResources* **3**, 517–537 (2008).
 101. Yildiz, S. & Gümüşkaya, E. The effects of thermal modification on crystalline structure of cellulose in soft and hardwood. *Build. Environ.* **42**, 62–67 (2007).
 102. Funaoka, M., Kako, T. & Abe, I. Condensation of lignin during heating of wood. *Wood Sci. Technol.* **24**, 277–288 (1990).
 103. Priadi, T. & Hiziroglu, S. Characterization of heat treated wood species. *Mater. Des.* **49**, 575–582 (2013).
 104. Kocafe, D., Huang, X., Kocafe, Y. & Boluk, Y. Quantitative characterization of chemical degradation of heat-treated wood surfaces during artificial weathering using XPS. *Surf. Interface Anal.* **45**, 639–649 (2013).

105. Kamdem, D. P., Pizzi, A. & Jermannaud, A. Durability of heat-treated wood. *Holz als Roh - und Werkst.* **60**, 1–6 (2002).
106. Uribe, B. E. B. & Ayala, O. A. Characterization of three wood species (Oak, Teak and Chanul) before and after heat treatment. *J. Indian Acad. Wood Sci.* **12**, 54–62 (2015).
107. Nuopponen, M., Vuorinen, T., Jämsä, S. & Viitaniemi, P. The effects of a heat treatment on the behaviour of extractives in softwood studied by FTIR spectroscopic methods. *Wood Sci. Technol.* **37**, 109–115 (2003).
108. Zhou Yuanlin. EXTRACTION OF SCOTS PINE BY POLAR SOLVENT. (Saimaa University of Applied Sciences, 2011).
109. Wikberg, H. & Maunu, S. L. Characterisation of thermally modified hard- And softwoods by¹³C CPMAS NMR. *Carbohydr. Polym.* **58**, 461–466 (2004).
110. Tumen, I., Aydemir, D., Gunduz, G., Uner, B. & Cetin, H. Changes in the chemical structure of thermally treated wood. *BioResources* **5**, 1936–1944 (2010).
111. Weiland, J. J. & Guyonnet, R. Study of chemical modifications and fungi degradation of thermally modified wood using DRIFT spectroscopy. *Holz als Roh- und Werkst.* **61**, 216–220 (2003).
112. Heigenmoser, A., Liebner, F., Windeisen, E. & Richter, K. Investigation of thermally treated beech (*Fagus sylvatica*) and spruce (*Picea abies*) by means of multifunctional analytical pyrolysis-GC/MS. *J. Anal. Appl. Pyrolysis* **100**, 117–126 (2013).
113. Nonier, M. F. *et al.* Pyrolysis-gas chromatography/mass spectrometry of *Quercus* sp. wood: Application to structural elucidation of macromolecules and aromatic profiles of different species. *J. Anal. Appl. Pyrolysis* **75**, 181–193 (2006).
114. Pouwels, A. D., Tom, A., Eijkel, G. B. & Boon, J. J. Characterisation of beech wood and its holocellulose and xylan fractions by pyrolysis-gas chromatography-mass spectrometry. *J. Anal. Appl. Pyrolysis* **11**, 417–436 (1987).
115. Grinins, J., Andersons, B., Biziks, V., Andersone, I. & Dobeles, G. Analytical pyrolysis as an instrument to study the chemical transformations of hydrothermally modified wood. in *Journal of Analytical and Applied Pyrolysis* **103**, 36–41 (2013).
116. Arias, M. E. *et al.* Thermal transformations of pine wood components under pyrolysis/gas chromatography/mass spectrometry conditions. *J. Anal. Appl. Pyrolysis* **77**, 63–67 (2006).

117. Schwarzing, C. & List, M. Identification of marker compounds in pyrolysis-GC/MS of various acetylated wood types. *J. Anal. Appl. Pyrolysis* **87**, 144–153 (2010).
118. Prins, M. J., Ptasincki, K. J. & Janssen, F. J. J. G. Torrefaction of wood. Part 2. Analysis of products. *J. Anal. Appl. Pyrolysis* **77**, 35–40 (2006).
119. Esteves, B., Velez Marques, A., Domingos, I. & Pereira, H. Chemical changes of heat treated pine and eucalypt wood monitored by FTIR. *Maderas. Cienc. y Tecnol.* 0–0 (2013). doi:10.4067/S0718-221X2013005000020
120. Pandey, K. K. A study of chemical structure of soft and hardwood and wood polymers by FTIR spectrscopy. *J. Appl. Polym. Sci.* **71**, 1969–1975 (1999).
121. Tjeerdsma, B. F. & Militz, H. Chemical changes in hydrothermal treated wood: FTIR analysis of combined hydrothermal and dry heat-treated wood. *Holz als Roh - und Werkst.* **63**, 102–111 (2005).
122. Zhao, J. *et al.* Thermal degradation of softwood lignin and hardwood lignin by TG-FTIR and Py-GC/MS. *Polym. Degrad. Stab.* **108**, 133–138 (2014).
123. Shen, D. K., Gu, S. & Bridgwater, A. V. The thermal performance of the polysaccharides extracted from hardwood: Cellulose and hemicellulose. *Carbohydr. Polym.* **82**, 39–45 (2010).
124. Kaboorani, A. Thermal Properties of Composites Made of Heat-treated Wood and Polypropylene. *J. Compos. Mater.* **43**, 2599–2607 (2009).
125. Burhenne, L., Messmer, J., Aicher, T. & Laborie, M. P. The effect of the biomass components lignin, cellulose and hemicellulose on TGA and fixed bed pyrolysis. *J. Anal. Appl. Pyrolysis* **101**, 177–184 (2013).
126. Gašparovič, L., Koreňová, Z. & Jelemenský, L'. Kinetic study of wood chips decomposition by TGA. *Chem. Pap.* **64**, (2010).
127. Wang, W., Cao, J. Z., Cui, F. T. & Wang, X. Effect of pH on chemical components and mechanical properties of thermally modified wood. *Wood Fiber Sci.* **44**, 46–53 (2012).
128. Petrič, M. *et al.* Wettability of waterborne coatings on chemically and thermally modified pine wood. *J. Coatings Technol. Res.* **4**, 203–206 (2007).
129. Welzbacher, C. R., Brischke, C. & Rapp, A. O. Influence of treatment temperature and duration on selected biological, mechanical, physical and optical properties of thermally modified timber. *Wood Mater. Sci. Eng.* **2**, 66–76 (2007).

130. Niemz, P. & Hofmann, T. Thermally Modified Wood. *Maderas. Cienc. y Tecnol.* **12**, 69–78 (2010).
131. Awoyemi, L. & Jones, I. P. Anatomical explanations for the changes in properties of western red cedar (*Thuja plicata*) wood during heat treatment. *Wood Sci. Technol.* **45**, 261–267 (2011).
132. Pétrissans, M., Gérardin, P., El Bakali, I. & Serraj, M. Wettability of heat-treated wood. *Holzforschung* **57**, 301–307 (2003).
133. Metsä-Kortelainen, S. & Viitanen, H. Wettability of sapwood and heartwood of thermally modified Norway spruce and Scots pine. *Eur. J. Wood Wood Prod.* **70**, 135–139 (2012).
134. Hakkou, M., Pétrissans, M., El Bakali, I., Gérardin, P. & Zoulalian, A. Wettability changes and mass loss during heat treatment of wood. *Holzforschung* **59**, 35–37 (2005).
135. Hakkou, M., Pétrissans, M., Zoulalian, A. & Gérardin, P. Investigation of wood wettability changes during heat treatment on the basis of chemical analysis. *Polym. Degrad. Stab.* **89**, 1–5 (2005).
136. Vázquez, M. C. T. Madera modificada : nuevas posibilidades constructivas en madera. (2012).
137. Balkis, B. F., Hiziroglu, S. & Md Tahir, P. Properties of some thermally modified wood species. *Mater. Des.* **43**, 348–355 (2013).
138. Leitch, M. A. Hardness Values for Thermally Treated Black Ash. *Wood Fiber Sci.* **41**, 440–446 (2009).
139. Militz, H. & Altgen, M. Processes and properties of thermally modified wood manufactured in Europe. Chapter 16 pp 269–285 in book "Deterioration and Protection of Sustainable Biomaterials". ACS Symposium Series, Vol. 1158 (2014).
140. Michielsen, S., Pourdeyhimi, B. & Desai, P. Review of thermally point-bonded nonwovens: Materials, processes, and properties. *Journal of Applied Polymer Science* **99**, 2489–2496 (2006).
141. Bryden, K. M., Ragland, K. W. & Rutland, C. J. Modeling thermally thick pyrolysis of wood. *Biomass and Bioenergy* **22**, 41–53 (2002).
142. Welzbacher, C. R. & Rapp, A. O. Durability of thermally modified timber from industrial-scale processes in different use classes: Results from laboratory and field tests. *Wood Mater. Sci. Eng.* **2**, 4–14 (2007).
143. Xu, G. & Goodell, B. Mechanisms of wood degradation by brown-rot fungi: Chelator-mediated cellulose degradation and binding of iron by cellulose. *J. Biotechnol.* **87**, 43–57 (2001).

144. Goodell, B. Brown-rot fungal degradation of wood: Our evolving view. in *Wood Deterioration and Preservation* **845**, 97–118 (2003).
145. Aust, S. D. Mechanisms of degradation by white rot fungi. in *Environmental Health Perspectives* **103**, 59–61 (1995).
146. Blanchette, R. A. Delignification by Wood-Decay Fungi. *Annu. Rev. Phytopathol.* **29**, 381–403 (1991).
147. Fackler, K. *et al.* Biotechnological wood modification with selective white-rot fungi and its molecular mechanisms. *Food Technol. Biotechnol.* **45**, 269–276 (2007).
148. Arantes, V., Milagres, A. M. F., Filley, T. R. & Goodell, B. Lignocellulosic polysaccharides and lignin degradation by wood decay fungi: The relevance of nonenzymatic Fenton-based reactions. *J. Ind. Microbiol. Biotechnol.* **38**, 541–555 (2011).
149. Giles, R. L., Galloway, E. R., Elliott, G. D. & Parrow, M. W. Two-stage fungal biopulping for improved enzymatic hydrolysis of wood. *Bioresour. Technol.* **102**, 8011–8016 (2011).
150. Kumar, R. & Wyman, C. E. Effects of cellulase and xylanase enzymes on the deconstruction of solids from pretreatment of poplar by leading technologies. *Biotechnol. Prog.* **25**, 302–314 (2009).
151. Ringman, R., Pilgard, A., Brischke, C. & Richter, K. Mode of action of brown rot decay resistance in modified wood: A review. *Holzforschung* **68**, 239–246 (2014).
152. Espejo, E. & Agosin, E. Production and degradation of oxalic acid by brown rot fungi. *Appl. Environ. Microbiol.* **57**, 1980–1986 (1991).
153. Fackler, K., Schwanninger, M., Gradinger, C., Hinterstoisser, B. & Messner, K. Qualitative and quantitative changes of beech wood degraded by wood-rotting basidiomycetes monitored by Fourier transform infrared spectroscopic methods and multivariate data analysis. *FEMS Microbiol. Lett.* **271**, 162–169 (2007).
154. Pandey, K. K. & Pitman, A. J. FTIR studies of the changes in wood chemistry following decay by brown-rot and white-rot fungi. *Int. Biodeterior. Biodegrad.* **52**, 151–160 (2003).
155. Boonstra, M. J., Acker, J. Van, Tjeerdsma, B. F. & Kegel, E. V. Strength properties of thermally modified softwoods and its relation to polymeric structural wood constituents. *Ann. For. Sci.* **64**, 679–690 (2007).
156. Kránitz, K., Sonderegger, W., Bues, C. T. & Niemz, P. Effects of aging on wood: a literature review. *Wood Sci. Technol.* **50**, 7–22 (2016).
157. Žlahtič, M. & Humar, M. Influence of Artificial and Natural Weathering on

- the Moisture Dynamic of Wood. *BioResources* **12**, 117–142 (2017).
158. Yildiz, S., Tomak, E. D., Yildiz, U. C. & Ustaomer, D. Effect of artificial weathering on the properties of heat treated wood. *Polym. Degrad. Stab.* **98**, 1419–1427 (2013).
 159. Huang, X., Kocaefe, D., Kocaefe, Y., Boluk, Y. & Krause, C. Structural analysis of heat-treated birch (*Betule papyrifera*) surface during artificial weathering. *Appl. Surf. Sci.* **264**, 117–127 (2013).
 160. Tomak, E. D., Ustaomer, D., Yildiz, S. & Pesman, E. Changes in surface and mechanical properties of heat treated wood during natural weathering. *Measurement* **53**, 30–39 (2014).
 161. Xie, Y., Fu, Q., Wang, Q., Xiao, Z. & Militz, H. Effects of chemical modification on the mechanical properties of wood. *Eur. J. Wood Wood Prod.* **71**, 401–416 (2013).
 162. Cavalli, A., Cibecchini, D., Togni, M. & Sousa, H. S. A review on the mechanical properties of aged wood and salvaged timber. *Construction and Building Materials* **114**, 681–687 (2016).
 163. Salca, E. A. & Hiziroglu, S. Evaluation of hardness and surface quality of different wood species as function of heat treatment. *Mater. Des.* **62**, 416–423 (2014).
 164. Lowden, L. & Hull, T. Flammability behaviour of wood and a review of the methods for its reduction. *Fire Sci. Rev.* **2**, 4 (2013).
 165. Ivanović-Šekularac, J., Čikić-Tovarović, J. & Šekularac, N. Application of wood as an element of façade cladding in construction and reconstruction of architectural objects to improve their energy efficiency. *Energy Build.* **115**, 85–93 (2016).
 166. Tolvaj, L. & Mitsui, K. Correlation between hue angle and lightness of light irradiated wood. *Polym. Degrad. Stab.* **95**, 638–642 (2010).
 167. Brischke, C., Welzbacher, C. R., Brandt, K. & Rapp, A. O. Quality control of thermally modified timber: Interrelationship between heat treatment intensities and CIE L*a*b* color data on homogenized wood samples. *Holzforschung* **61**, 19–22 (2007).
 168. Evans, P. D., Michell, A. J. & Schmalzl, K. J. Studies of the degradation and protection of wood surfaces. *Wood Sci. Technol.* **26**, 151–163 (1992).
 169. Sundqvist, B., Karlsson, O. & Westermark, U. Determination of formic-acid and acetic acid concentrations formed during hydrothermal treatment of birch wood and its relation to colour, strength and hardness. *Wood Sci. Technol.* **40**, 549–561 (2006).
 170. Effect of artificial weathering on the properties of heat treated wood.

- Polym. Degrad. Stab.* **98**, 1419–1427 (2013).
171. Ayadi, N., Lejeune, F., Charrier El Bouhtoury, F., Charrier, B. & Merlin, A. Color stability of heat-treated wood during artificial weathering. *Eur. J. Wood Wood Prod.* **61**, 221–226 (2003).
 172. Tsuchikawa, S. A review of recent near infrared research for wood and paper. *Applied Spectroscopy Reviews* **42**, 43–71 (2007).
 173. Brunner, M., Eugster, R., Trenka, E. & Bergamin-Strotz, L. FT-NIR spectroscopy and wood identification. *Holzforschung* **50**, 130–134 (1996).
 174. Chen, H. *et al.* Qualitative and quantitative analysis of wood samples by Fourier transform infrared spectroscopy and multivariate analysis. *Carbohydr. Polym.* **82**, 772–778 (2010).
 175. Abdi, H. & Williams, L. J. Principal component analysis. *Wiley Interdisciplinary Reviews: Computational Statistics* **2**, 433–459 (2010).
 176. De Meijer, M. & Miltz, H. Wet adhesion of low-VOC coatings on wood. A quantitative analysis. *Prog. Org. Coatings* **38**, 223–240 (2000).
 177. Proszyk, S., Lis, B., Krystofiak, T. & Terakowska, K. Influence of caring agent on utility properties of ash wood surfaces finished with oil-waxes products. Part IV. Resistance to some thermal and chemical factors. *Ann. Warsaw Univ. Life Sci. For. Wood Technol.* **69**, 203–206 (2009).
 178. Nejad, M., Shafaghi, R., Ali, H. & Cooper, P. Coating performance on oil-heat treated wood for flooring. *BioResources* **8**, 1881–1892 (2013).
 179. Collett, B. M. A review of surface and interfacial adhesion in wood science and related fields. *Wood Science and Technology* **6**, 1–42 (1972).
 180. Korkut, D. S. & Guller, B. The effects of heat treatment on physical properties and surface roughness of red-bud maple (*Acer trautvetteri* Medw.) wood. *Bioresour. Technol.* **99**, 2846–2851 (2008).
 181. Unsal, O. & Ayrilmis, N. Variations in compression strength and surface roughness of heat-treated Turkish river red gum (*Eucalyptus camaldulensis*) wood. *J. Wood Sci.* **51**, 405–409 (2005).
 182. Gérardin, P., Petrič, M., Petrissans, M., Lambert, J. & Ehrhardt, J. J. Evolution of wood surface free energy after heat treatment. *Polym. Degrad. Stab.* **92**, 653–657 (2007).
 183. Hochmańska, P., Mazela, B. & Krystofiak, T. Hydrophobicity and weathering resistance of wood treated with silane-modified protective systems. *Drewno* **57**, (2014).
 184. Scrinzi, E., Rossi, S., Deflorian, F. & Zanella, C. Evaluation of aesthetic durability of waterborne polyurethane coatings applied on wood for

- interior applications. in *Progress in Organic Coatings* **72**, 81–87 (2011).
185. Faga, M. G. & Settineri, L. Innovative anti-wear coatings on cutting tools for wood machining. *Surf. Coatings Technol.* **201**, 3002–3007 (2006).
 186. Richter, K., Feist, W. & Knaebe, M. The effect of surface roughness on the performance of finishes. Part 1: Roughness characterization and stain performance. *For. Prod. J.* **45**, 91–97 (1995).
 187. De Meijer, M. A review of interfacial aspects in wood coatings: wetting, surface energy, substrate penetration and adhesion. *COST E18, High Perform. Wood Coating. Final Semin.* 1–16 (2004).
 188. Bulian, F. & Graystone, J. *Wood Coatings. Wood Coatings* (2009). doi:10.1016/B978-0-444-52840-7.X0001-X
 189. Saha, S., Kocaefer, D., Boluk, Y. & Pichette, A. Surface degradation of CeO₂ stabilized acrylic polyurethane coated thermally treated jack pine during accelerated weathering. *Appl. Surf. Sci.* **276**, 86–94 (2013).
 190. Van Den Bulcke, J., Van Acker, J. & Stevens, M. Experimental and theoretical behavior of exterior wood coatings subjected to artificial weathering. *J. Coatings Technol. Res.* **5**, 221–231 (2008).
 191. Zenkiewicz, M. Comparative study on the surface free energy of a solid calculated by different methods. *Polym. Test.* **26**, 14–19 (2007).
 192. Moura, L. De & Hernandez, R. Evaluation of varnish coating performance for three surfacing methods on sugar maple wood. *For. Prod. J.* **56**, 130–136 (2006).
 193. Liptáková, E. & Kúdela, J. Study of the system wood-coating material. Part 2. Wood-solid coating material. *Holzforschung* **56**, 547–557 (2002).
 194. Deka, M. & Petrič, M. Photo-degradation of water borne acrylic coated modified and non-modified wood during artificial light exposure. *BioResources* **3**, 346–362 (2008).
 195. Kúdela, J. & Liptáková, E. Adhesion of coating materials to wood. *J. Adhes. Sci. Technol.* **20**, 875–895 (2006).
 196. Ahola, P. Adhesion between paints and wooden substrates: effects of pre-treatments and weathering of wood. *Mater. Struct.* **28**, 350–356 (1995).
 197. Fouquet, M. *et al.* Methodological challenges and developments in LCA of low energy buildings: Application to biogenic carbon and global warming assessment. *Build. Environ.* **90**, 51–59 (2015).
 198. Klein, D., Wolf, C., Schulz, C. & Weber-Blaschke, G. 20 years of life cycle assessment (LCA) in the forestry sector: state of the art and a methodical proposal for the LCA of forest production. *Int. J. Life Cycle Assess.* **20**,

- 556–575 (2015).
199. Hirschier, R., Althaus, H.-J. & Werner, F. Developments in Wood and Packaging Materials Life Cycle Inventories inecoinvent. *Int. J. Life Cycle Assess.* **10**, 50–58 (2005).
 200. Jungmeier, G., Werner, F., Jarnehammar, A., Hohenthal, C. & Richter, K. Allocation in LCA of Wood-based Products: Experiences of Cost Action E9, Part I. Methodology. *Int. J. Life Cycle Assess.* **7**, 369–375 (2002).
 201. Ohtani, Y., Mazumder, B. B. & Sameshima, K. Influence of the chemical composition of kenaf bast and core on the alkaline pulping response. *J. Wood Sci.* **47**, 30–35 (2001).
 202. Mészáros, E., Jakab, E. & Várhegyi, G. TG/MS, Py-GC/MS and THM-GC/MS study of the composition and thermal behavior of extractive components of Robinia pseudoacacia. *J. Anal. Appl. Pyrolysis* **79**, 61–70 (2007).
 203. Shebani, A. N., van Reenen, A. J. & Meincken, M. The effect of wood extractives on the thermal stability of different wood species. *Thermochim. Acta* **471**, 43–50 (2008).
 204. Tenorio, C. & Moya, R. Thermogravimetric characteristics, its relation with extractives and chemical properties and combustion characteristics of ten fast-growth species in Costa Rica. *Thermochim. Acta* **563**, 12–21 (2013).
 205. Kim, H. S., Kim, S., Kim, H. J. & Yang, H. S. Thermal properties of bio-flour-filled polyolefin composites with different compatibilizing agent type and content. *Thermochim. Acta* **451**, 181–188 (2006).
 206. Guillén, M. D. & Manzanos, M. J. Study of the volatile composition of an aqueous oak smoke preparation. *Food Chem.* **79**, 283–292 (2002).
 207. Ajuong, E. M. A. & Redington, M. Fourier transform infrared analyses of Bog and modern oak wood (*Quercus petraea*) extractives. *Wood Sci. Technol.* **38**, 181–190 (2004).
 208. Boonstra, M. J. & Tjeerdsma, B. Chemical analysis of heat treated softwoods. *Holz als Roh - und Werkst.* **64**, 204–211 (2006).
 209. Liu, H., Shang, J., Chen, X., Kamke, F. A. & Guo, K. The influence of thermal-hydro-mechanical processing on chemical characterization of *Tsuga heterophylla*. *Wood Sci. Technol.* **48**, 373–392 (2014).
 210. Beall, F. C. & Eickner, H. W. THERMAL DEGRADATION OF WOOD COMPONENTS : a review of the literature. *Agriculture* **26** (1970).
 211. Ponder, G. R. & Richards, G. N. A Review of Some Recent Studies on Mechanisms of Pyrolysis of Polysaccharides. *Biomass and Bioenergy* **7**, 1–24 (1994).

212. Alén, R., Oesch, P. & Kuoppala, E. Py-GC/AED studies on the thermochemical behavior of softwood. *J. Anal. Appl. Pyrolysis* **35**, 259–265 (1995).
213. Conde, E. *et al.* Antioxidant activity of the phenolic compounds released by hydrothermal treatments of olive tree pruning. *Food Chem.* **114**, 806–812 (2009).
214. Esteves, B., Graça, J. & Pereira, H. Extractive composition and summative chemical analysis of thermally treated eucalypt wood. *Holzforschung* **62**, 344–351 (2008).
215. Natali, N., Chinnici, F. & Riponi, C. Characterization of volatiles in extracts from oak chips obtained by Accelerated Solvent Extraction (ASE). *J. Agric. Food Chem.* **54**, 8190–8198 (2006).
216. Melzer, M., Blin, J., Bensakhria, A., Valette, J. & Broust, F. Pyrolysis of extractive rich agroindustrial residues. *J. Anal. Appl. Pyrolysis* **104**, 448–460 (2013).
217. Nanda, S., Mohanty, P., Kozinski, J. A. & Dalai, A. K. Physico-Chemical Properties of Bio-Oils from Pyrolysis of Lignocellulosic Biomass with High and Slow Heating Rate. *Energy Environ. Res.* **4**, (2014).
218. Pakdel, H., Zhang, H. G. & Roy, C. Production and characterization of carboxylic acids from wood, part II: High molecular weight fatty and resin acids. *Bioresour. Technol.* **47**, 45–53 (1994).
219. Hudy, J. A. Resin Acids: Gas Chromatography of Their Methyl Esters. *Anal. Chem.* **31**, 1754–1756 (1959).
220. Oasmaa, A., Kuoppala, E. & Solantausta, Y. Fast pyrolysis of forestry residue. 2. Physicochemical composition of product liquid. *Energy and Fuels* **17**, 433–443 (2003).
221. Leppälähti, J. & Koljonen, T. Nitrogen evolution from coal, peat and wood during gasification: Literature review. *Fuel Processing Technology* **43**, 1–45 (1995).
222. Dizhbite, T., Telysheva, G., Jurkjane, V. & Viesturs, U. Characterization of the radical scavenging activity of lignins - Natural antioxidants. *Bioresour. Technol.* **95**, 309–317 (2004).
223. Vinardell, M. P., Ugartondo, V. & Mitjans, M. Potential applications of antioxidant lignins from different sources. *Ind. Crops Prod.* **27**, 220–223 (2008).
224. Velioglu, Y. S., Mazza, G., Gao, L. & Oomah, B. D. Antioxidant Activity and Total Phenolics in Selected Fruits, Vegetables, and Grain Products. *J. Agric. Food Chem.* **46**, 4113–4117 (1998).

225. Campbell, W. G. & Booth, J. The effect of partial decay on the alkali solubility of wood. *Biochem. J.* **23**, 566–572 (1929).
226. Rowell, R. *The Chemistry of Solid Wood*. (American Chemical Society, 1984). doi:<https://doi.org/10.1021/ba-1984-0207>

APPENDIX I

PROCEDURES

Chemical composition

I-1.1 Lignin

Procedure TAPPI T222 om-98. Acid-insoluble lignin in wood and pulp.

I-1.2 Extractives

Procedure T 204 om-97. Solvent extractives of wood and pulp.

I-1.3 Ashes

Procedure T 211 om-93. Ash in wood, pulp, paper and paperboard: combustion at 525°C.

I-1.4 Holocellulose

Wood holocellulose is commonly characterized according to the method propose by Campbell and Booth, 1929 ²²⁵, which was normalized in the procedure NREL/TP-510-42618-12, determination of Structural Carbohydrates and Lignin in Biomass. Then, from the obtainted fraction was analyzed the carbohydrates composition by HPLC techniques detailed in Appendix II-1.1-2.

I-1.5 Cellulose

The procedure to obtain the wood cellulose is referred as the "Rowell method" from the book: The Chemistry of Solid Wood, 1984, edited by Professor R. Rowell²²⁶.

I-1.6 Acidity

To determine the total acid of wood samples, the process applied was the acid-base titration, in which small quantities of a strong base are added until the pH reaches a predetermined value, the so-called equivalence point where the amount of added base equals the amount of total acid in the solution. The base is added in the form of a dilute solution of known concentration. Sometimes the term neutralization is used but the equivalence point is not necessarily pH 7. The equivalence point is defined as the pH at which the amount of base added is equal to the amount of proton-donating molecules. The amount required to reach the equivalence point was determined and used as a measure for the acidity of dry wood; then the following equation was obtained:

$$A = \frac{meq}{g \text{ drywood}} = \frac{(V - V_0) \times 10^2}{m}$$

Where v is the volume (mL) titration solution used for a wood sample, v_0 the volume (mL) solution used for neutralizing the sample and m the sample mass (g) used for titration.

For the determination of pH, 1.25 g of sawdust was suspended in 25 mL of distilled water and stirred for 24 h. Then the pH of the suspension was measured with a CRISON- Basic 20 pH meter.

Physical properties

I-2.1 Density

The dry density (ρ_0) was determined in accordance with UNE-EN 408:2011 Timber structures - Structural timber and glued laminated timber - Determination of some physical and mechanical properties.

I-2.2 Moisture content

The equilibrium moisture content was determined in accordance with UNE-EN 13183-1:2002 Moisture content of a piece of sawn timber - Part 1: Determination by oven dry method. The parameters for the EMC must be determined at 20 °C and 65% RH.

I-2.3 Volumetric shrinkage

The volumetric shrinkage was determined in agreement with UNE 56533-77 Physical-mechanical characteristics of wood. Determination of lineal and volumetric contraction. In addition, the coefficient of anisotropy was determined as the ratio between the tangential and radial shrinkage.

I-2.4 Water uptake

Water uptake test was performed calculating the weight of water absorbed (% WWA) of samples, which were submitted first to a vacuum of 7 mbars for 15 minutes, and then introduced in a vessel filled with deionized water and maintained fully submerged during 96 h. The weight of samples was measured in the beginning and after submersion at oven-dry state and in different times (4, 8, 24, 48, 72 and 96 h) of the experiment. WWA was calculated as shown in the following equation:

$$WWA = \frac{w_f - w_i}{w_i} [\%]$$

Where w_i is the initial weight and w_f is the weight of the sample impregnated after each period of time.

I-2.5 Surface Energy

Surface free energy on wood γ_{S1} , as well as these disperse γ_{S^d} and polar shares γ_{S^p} were measured by means of a sessile drop technique, which is explained in the

Appendix II-2.1. The free surface energy was calculated from the contributions of the liquid and the solid states, following the routine proposed by Owens, Wendt, Rabel and Kaelble:

$$\gamma_L(1 + \cos \theta) = 2\sqrt{\gamma_S^d \gamma_L^d} + 2\sqrt{\gamma_S^p \gamma_L^p}$$

Where γ_L , γ_L^p , γ_L^d are the surface free energy, polar and disperse shares of the testing liquids, γ_S^p , γ_S^d are the polar and disperse shares of the substrates free surface energy, respectively. It is possible to determine γ_S^p and γ_S^d by deriving the geometric mean from the equation and implementing values of γ_L^p , γ_L^d following the literature references:

$$\gamma_S^L = \gamma_S + \gamma_L \frac{2\sqrt{\gamma_S^d \gamma_L^d} + 2\sqrt{\gamma_S^p \gamma_L^p}}{1 + \cos \theta}$$

Accordingly, the linear solution of transformed equation leads to the conclusion that γ_S^p corresponds to the slope of the linear function and γ_S^d to its intercept. The mathematical presentation of such relation is presented as follows:

$$y = ax + b = \frac{1 + \cos \theta}{2} \cdot x + \frac{\gamma_L}{\sqrt{\gamma_L^d}}$$

Where:

$$x = \frac{\gamma_L^p}{\sqrt{\gamma_L^d}} ; a = \sqrt{\gamma_S^p} ; b = \sqrt{\gamma_S^d}$$

It was assumed that measurement of wetting with three diverse liquids was sufficient to accurately determine the linear function. The work of cohesion (W_{cl}) can be determined according to the following equations:

$$W_{C1} = 2\gamma_{S1}$$

The interactions between unsaturated force fields of the wood-solid coating system were determined by applying valid relations in a common solid-liquid system by the free surface energy at the phase boundary of the wood-solid coating (γ_{S1S2}). The work of adhesion of the solid coating to wood (W_a) and work of cohesion (W_{C1} =uncoated surface; W_{C2} =coated surface) were determined according to the following equations:

$$\gamma_{S1S2} = \left(\sqrt{\gamma_{S1}^d} - \sqrt{\gamma_{S2}^d} \right)^2 + \left(\sqrt{\gamma_{S1}^p} - \sqrt{\gamma_{S2}^p} \right)^2$$

$$W_a = 2\sqrt{\gamma_{S1}^d \gamma_{S2}^d} + 2\sqrt{\gamma_{S1}^p \gamma_{S2}^p}$$

$$W_{C1} = 2\gamma_{S1} ; W_{C2} = 2\gamma_{S2}$$

Mechanical properties

I-2.6 Bending strength

Three-point bending, according to EN 408:2010+A1-2012 Timber structures - Structural timber and glued laminated timber-Determination of some physical and mechanical properties, determined this property.

The modulus of rupture or bending strength (σ) at three points was calculated as follows:

$$\sigma = \frac{3P_{max}L}{2wh^2}$$

In which P_{max} is the maximum load (N) and the bending load was applied on two symmetrical points with a span equal to 18 ± 2 thickness. The crosshead speed was calculated for each sample. The load was fixed in the tangential direction of the replicates.

I-2.7 Flexural modulus

This property was determined by three-point bending, and two different values of flexural modulus (MOE) were calculated. Firstly, the standard MOE according to EN 408:2010+A1:2012, but correcting the effects of the equipment used as explained below: The system stiffness (k_{sys}) was calculated for each set of samples to correct the effects of the supporting pins and the loading head, thus obtaining values not influenced by the equipment used (Fig.1). Each set of samples were disposed over a solid flat bar supported by the pins at the minimum span. The universal test system (MTS Insight 10) with 10 kN load cell and three-point bending method was used to calculate the k_{sys} with a load at 25% of slope.

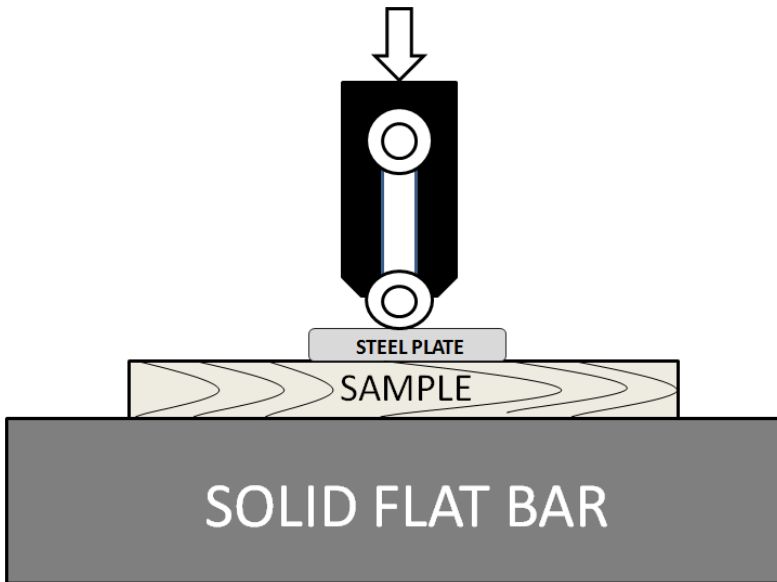


Fig. 1 Model used to determine system stiffness.

The system stiffness (k_{sys}) measured to correct the MOE is in the following table:

Table 1. System stiffness for each set of samples

Sample	k_{sys} [MPa]
<i>Fraxinus excelsior</i>	8784±86
T-Ash210	10189±105
<i>Pinus radiata</i>	7114±92
T-Pine210	9690±110

I-2.8 Flexural modulus model

The experimental MOE was measured from five different spans considering the shear effect and local deformations, in order to create a linear regression model to finally indicate an adjusted value. To correct the experimental values, the following equations were used:

$$\delta_{exp} = \delta_S + \delta_M + \delta_Q = \begin{cases} \delta_M = PL^3 / 4E_f wh^3 \\ \delta_S = P / K_{sys} \\ \delta_Q = 3PL / 10Gwh \end{cases}$$

Where δ_{exp} is the experimental displacement, δ_S is the system displacement, δ_M is flexural displacement, δ_Q is the shear displacement. P is the applied load, L is the span, E_f is the MOE, w is the sample width, h is sample thickness and G is the shear modulus. Then, describing the equations as a function of two tested points (δ_1 ; δ_2) according to following equations:

$$\delta = \begin{cases} \delta_2 = \frac{P_2 L^3}{4E_f w h^3} \left[1 + \frac{6E_f}{5G} \left(\frac{h}{L} \right)^2 \right] \\ \delta_1 = \frac{P_1 L^3}{4E_f w h^3} \left[1 + \frac{6E_f}{5G} \left(\frac{h}{L} \right)^2 \right] \\ \delta = \delta_{exp} - P/K_{sys} ; m = \frac{P_2 - P_1}{\delta_2 - \delta_1} \end{cases}$$

The MOE was calculated using the corrected values from the spans to finally create a linear regression model:

$$E_f = \frac{mL^3}{4wh^3} \left[1 + \frac{6E_f}{5G} \left(\frac{h}{L} \right)^2 \right]$$

I-2.9 Hardness

The hardness of samples was measured based on UNE-EN1534=2011 Wood flooring-Determination of resistance to indentation-Test method. The test was carried out using a Rockwell equipment (HR-150A) with conical indenters. The machine was loaded at 100 Kg on the surface during 5 s., then, the indentation width was measured and the hardness Brinell (HB) calculated according with the following equation:

$$HB = \frac{2F}{g \times \pi \times D [D - \sqrt{D^2 - d^2}]} \left(N/mm^2 \right)$$

In which, F is the maximum strength applied, g is the acceleration of gravity, D is the ball diameter and d is the average print of penetration. All samples were conditioned at 20 °C and 65% relative humidity.

Biological durability

I-3.1 Wood leaching procedure

The samples were ageing before the inoculation of rot fungi. The test was performed according to UNE-EN 84:1997 Wood preservatives. Accelerated ageing of treated wood prior to biological testing. Leaching procedure. Ten samples free of defects of treated and untreated wood were leached (dimensions = 40 × 25 × 10 mm³) and then used for the durability test.

I-3.2 Determination of biological durability by basidiomycetes test

The test of resistance to basidiomycetes was carried out according to EN113:1996/A1:2004 Wood preservatives-Test method for determining the protective effectiveness against wood destroying basidiomycetes-Determination of the toxic values.

The decay test was performed with the brown-rot fungus *Gloeophyllum trabeum* (Pers.) Murril (MB356811) and the white-rot fungus *Trametes versicolor* (L.) Lloyd (TR489). The incubation periods were 8 weeks and 24 weeks at 23±2 °C and at relative humidity of 60%±5 to allow the colonization by mycelium. After this period, colonized wood blocks were carefully removed from agar plates, taking away the surrounding mycelia of the samples. Finally, the samples were conditioned in a climatic chamber at temperature of 23±2 °C and relative humidity of 50%±5 until they achieved a stable mass.

In order to assess the grade of durability, the initial dry mass (m_i) and the final dry mass after incubation (m_f) were determined by oven drying the specimens at 103±1 °C. The mass loss (ML) due to fungal attack of each specimen was calculated as a percentage of the initial dry mass according to the following formula:

$$ML[\%] = \frac{m_i - m_f}{m_i} \times 100$$

Moreover, the durability classification was according to UNE-EN 350:2016 Durability of wood and wood-based products-Testing and classification of the durability to biological agents of wood and wood-based materials, where is introduced the following X-value:

$$X = \frac{\textit{Average mass loss of test sample}}{\textit{Average mass loss of control sample}}$$

I-3.3 Enzymatic activity

Wood specimens from the test I-3.2 were cleaned, milled, screened through a 4–6 mm mesh sieve and then oven dried at 103 ± 1 °C. The obtained ground wood was used for enzymatic tests performed in triplicate using decayed and control samples. Enzymatic hydrolysis was carried out with two different enzymes, cellulase from *T. reesei* (EC 3.2.1.4) and endo-1,4-β- xylanase derived from *T. longibrachiatum* (EC 3.2.1.8) provided by Sigma-Aldrich. Experiments were performed using 1 g of groundwood (m_i) into 50 mL centrifuge flasks containing a working volume 25 mL of citrate buffer solution (0.05 M; pH 4.8) and an enzyme dosage of 15 FPU/g and 500 nkat/g; respectively. The flasks were centrifuged at 150 rpm and 50 °C for 72 h.

The hydrolysis was terminated by boiling for 10 min to inactivate the enzymes and the supernatants were subsequently filtered through a 0.22 μm syringe filter to determine the amounts of sugars generated by high performance liquid chromatography (HPLC) procedure (appendix II-2.1 and II-2.2). Besides, after enzymatic hydrolysis the solid residue was filtered, washed with distilled water, oven dried at 103 ± 1 °C and finally weighed (m_f). Weight loss (WL) due to enzyme activity was calculated according to the following formula:

$$WL[\%] = \frac{m_i - m_f}{m_i} \times 100$$

Weathering test

I-4.1 Natural weathering test

The sets of samples were exposed twelve months to natural weathering in a location with oceanic climate (San Sebastian, Spain: 43°18'33.054"Latitude N; 2°0'34.817"Length W) facing south direction at 45 degrees of inclination. The following picture show how the samples were disposed.



Fig. 2 Set of samples facing south direction at 45 degrees of inclination.

After weathering test, samples were conditioned (20 °C; 65% RH) to measure the obtained properties.

I-4.2 Artificial weathering test

Samples were subjected to accelerated aging cycles based on a modified EN 927-6:2007 Paints, varnishes-Coating materials, and coating systems for exterior wood-Part 6: Exposure of wood coatings to artificial weathering using fluorescent UV lamps and water. Each cycle consists of the following steps: water submersion at approximately 20 kPa for 15 hours, drying at 75 °C for 9 hours in a convection oven, intervals of 2.5 hours of UV-A light (80 cycles, 2120 hours).

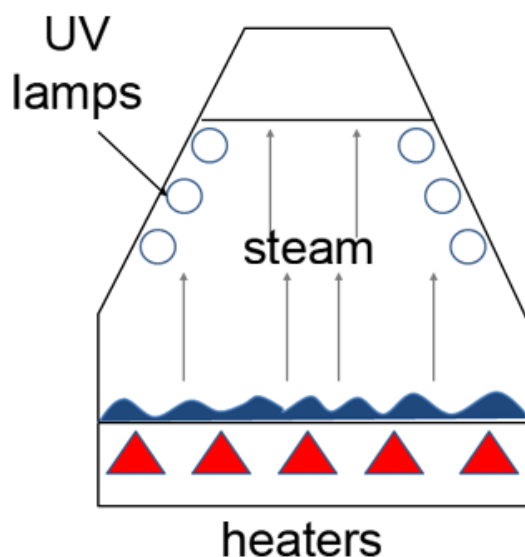


Fig. 3 Schematic of factors applied in artificial weathering test.

Afterwards, samples were conditioned (20 °C; 65% RH) to measure the obtained properties.

Surface evaluations

I-5.1 Identity test

The chemical differences between uncoated samples were tracked by NIR spectrometry (Appendix II-1.10), to visualize the heterogeneity or homogeneity of the material according to the general trends. The preliminary analysis of variables on NIR spectra integrates the data set using algorithms for clustering data. Principal components analysis (PCA) and Identity test were additionally performed on the obtained spectra in order to evidence the capability of NIR measurement system to discriminate the differences between samples.

I-5.2 Surface adhesion pull-off test

The adherence was determined by the pull-off method performed according to EN 4624: 2003 Paints and varnishes-Pull-off test for adhesion. The samples were adhered to aluminum test dollies (20 mm in diameter; 6 per sample) glued to the coated surface with 2K silane-epoxy adhesive for 24 hours and then detached from the surface in a perpendicular direction to the substrate. The force required to delaminate the sample (MPa) was recorded and the surface was evaluated in visual mode.

I-5.3 Surface adhesion cross - cut method

The cross-cut test was performed as specified in EN ISO 2409:1994 Paints and varnishes. Cross-cut test. A right angle lattice was cut into the coating at 45° to the direction of the grain with a sharp blade with a distance of 2 mm between the cuts. The cross-cut area was examined and classified from 0 (very good adhesion) to 5 (weak adhesion) by a visual comparison with the illustrations in the standard, depending on the amount of flaked coating.

I-5.4 Coating hardness

The coating hardness was measured in accordance to ASTM D2134-93(2012) Standard Test Method for Determining the Hardness of Organic Coatings with a Sward-Type Hardness Rocker.

I-5.5 Abrasion test

The abrasion test was measured in accordance to UNE-EN 13696:2009 Wood flooring-Test methods to determine elasticity and resistance to wear and impact resistance. For the test was used a Taber® Abraser 352G (type 5130) weighing

samples after each 50 rotations to calculate the wear index (weight loss by the number of cycles).

I-5.6 Impact test

The impact test according to EN 13696:2008 standard, using a prototype device PUD-6 (Dozafil Polifarb, Wroclaw) testing at increased drop-ball heights (10, 25, 50, 100, 200, 400 mm) and peel strength test assessing failures.

Statistical analysis

The results of measurements were analyzed according to the characteristics values of normality and homogeneity of variances UNE-EN 1435815. In addition, a multiple comparison procedure was used in some tests to determine which means were significantly different from others and its confidence levels according to the Bonferroni correction (BSD). The software used for the statistical and graphing analysis was Origin 9.1.

APPENDIX II

TECHNIQUES

Chemical identification

II-1.1 Carbohydrates

An aliquot of each obtained fraction (Appendix I-1.4) was neutralized with CaCO_3 , and then determined the monosaccharides (glucose, xylose, arabinose, galactose, and mannose) with a Transgenomic CARBOsep CHO-682 column; the mobile phase was H_2O at a flow rate of $0.4 \text{ cm}^3 \text{ min}^{-1}$ at $80 \text{ }^\circ\text{C}$.

The analysis was carried out by means of High Performance Liquid Chromatography (HPLC) with a Jasco LC Net II/ADC chromatograph equipped with a refractive index detector and a photodiode array detector MD-2018Plus.

II-1.2 Degradation products

An aliquot of each obtained fraction (Appendix I-1.1) was used for the analysis of acetic acid, galacturonic acid and the degradation products (furfural and hydroxymethylfurfural) using a Phenomenex Rezex ROA Organic Acid H+ (8%) column; the mobile phase ($0.005 \text{ N H}_2\text{SO}_4$) was eluted at a flow rate of $0.35 \text{ cm}^3 \text{ min}^{-1}$ at $60 \text{ }^\circ\text{C}$.

The analysis was carried out by means of High Performance Liquid Chromatography (HPLC) with a Jasco LC Net II/ADC chromatograph equipped with a refractive index detector and a photodiode array detector MD-2018Plus.

II-1.3 Fourier-transform infrared spectroscopy (FT-IR)

Fourier Transform Infrared (FTIR) spectra were recorded on a Perkin Elmer spectrophotometer equipped with a Universal Attenuated Total Reflectance accessory (ATR) with internal reflection diamond crystal lens. The first step was to

collect a background spectrum to subtract from the sample spectrum. Next, few milligrams of sample were analyzed using the module for eight scans in a range from 750 to 4000 cm^{-1} at a resolution 4 cm^{-1} . After scanning, the baseline was corrected and the bands of the FTIR profile were used to obtain the qualitative information regarding functional groups present on each sample. For each one, the measurements were recorded in triplicate.

II-1.4 Gas chromatography-mass spectrometry (GC-MS)

The chemical composition of samples analyzed by GC-MS technique requires 0.5 g L^{-1} of sample dissolved in ethyl acetate. Then, the samples are analyzed using a GC coupled with an Agilent 5975C mass spectrometry detector. Ionization voltage of mass spectrometer in the EI-mode was equal to 70 eV and ionization source temperature was 250 °C. The additional operating conditions were split inlet mode (10:1); carrier gas helium at a flow rate 0.7 $\text{cm}^3 \text{min}^{-1}$; injection at 280 °C with a sample volume of 0.001 cm^3 .

The identification of the obtained compounds was accomplished using a National Institute of Standards Library version 2.0 Mass Spectral Search Program (Agilent Techn.). Mass spectra and retention time of compounds were compared with available library data and the percentage of peaks was calculated by the area normalization method.

II-1.5 Pyrolysis-Gas chromatography-mass spectrometry (Py-GC-MS)

In order to separate and identify the pyrolysis volatiles, pyrolysis-gas chromatography-mass spectrometry (Py-GC-MS) system was used. A commercial pyrolyzer (Pyroprobe model 5150, CDS Analytical Inc., Oxford, PA) was connected to gas chromatography-mass spectrometry (7890GC/5975MSD, Agilent). Samples (in the μg range) were pyrolyzed in a quartz boat at 230 °C for 15 s with a heating rate of 2 $^\circ\text{C ms}^{-1}$ (ramp-off) with the interface kept at 250 °C. Then, the pyrolyzates

were purged from the pyrolysis interface into the GC using helium gas. The fused-silica capillary column used was an HP-5MS (30 m x 0.25 mm x 0.25 μm). The GC oven was programmed at 50 °C as an initial temperature holding for 2 min, with 10 °C increases per minute to 120 °C, followed by a temperature enhancement of 10 °C min^{-1} to 280 °C and keeping at the mentioned temperature for 8 min. Finally, the temperature was elevated to 300 °C at 10 °C min^{-1} and held for 10 min.

The identification of the obtained compounds was accomplished using a National Institute of Standards Library version 2.0 Mass Spectral Search Program (Agilent Techn.). Mass spectra and retention time of compounds were compared with available library data and the percentage of peaks was calculated by the area normalization method.

Thermal behavior

II-1.6 Thermal decomposition

Dynamic thermo-gravimetric measurements were carried out in order to observe the decomposition of samples with increasing the temperature. The thermo-gravimetric analysis (TGA) was conducted in a nitrogen atmosphere using a Mettler Toledo TGA/SDTA RSI analyzer. The samples (5-10 mg) are scanned from 25 to 700 °C at a heating rate of 10 °C min^{-1} . The gas flow rate was 10 $\text{cm}^3 \text{min}^{-1}$. For the quantitative calculations, the response factors between the weight gain (TG) and the mass loss rate (DTG) were determined.

II-1.7 Thermal resistance

Thermal resistance of samples were performed on a TA instruments TGA Q5000 IR equipment, under dynamic nitrogen flow with a flow rate of 40 mL min^{-1} . Temperature range was from 30 to 1000 °C at a constant heating rate of 20 °C/min under O_2 atmosphere (airflow rate 60 mL min^{-1}). Approximately 10-15 mg of sample were placed in a platinum crucible. For the quantitative calculations, the

response factors between the weight gain (TG) and the mass loss rate (DTG) were determined.

Phenolics and antioxidants

II-1.8 Total phenolic content

The total phenolic content (TPC) of the residual extracts was spectrophotometrically measured according to the Folin-Ciocalteu's method. The samples were solubilized with methanol at final concentration of 2 mg cm⁻³. Aliquots of these samples (0.25 cm³) were mixed with 2.5 cm³ of distilled water and 0.25 cm³ of the Folin-Ciocalteu reagent (previously diluted 1:10 with distilled water). After 5 min, 0.25 cm³ of aqueous solution was mixed with sodium carbonate (75 mg cm⁻³) and distilled water (10 cm³). The mixtures were kept at room temperature for 60 min and calculated the absorbance at 725 nm. The absorbance was measured using a visible ultraviolet spectrophotometer (Jasco V-630 instrument). TPC was calculated as a gallic acid equivalent from the calibration curve (0-0.2 mg cm⁻³; R²=0.990) and expressed as gram gallic acid per kilogram of dried extract (g kg⁻¹).

II-1.9 Antioxidant activity

The antioxidant activity of the residual extracts was determined according to the D1, 1-diphenyl-2-picrylhydrazyl (DPPH) free radical method. . An aliquot (0.04 cm³) of the samples was added to DPPH methanolic solution 0.06 mM (2 mg cm⁻³ in methanol) and kept at room temperature for 30 min. The scavenging activity on DPPH radical was determined by measuring the absorbance at 517 nm and using Trolox as positive control. Inhibition rate (%) on DPPH radical was calculated by the following equation:

$$\text{Inhibition rate\%} = \frac{A_{\text{control } t=30} - A_{\text{sample } t=30}}{A_{\text{DPPH } t=0}} \times 100$$

In which A_{control} is the absorbance value of the control (2 cm³ of DPPH solution plus 0.04 cm³ of the solvent); A_{sample} is the absorbance of the extract sample; t is the time (min) at which absorbance was read and A_{DPPH} is the absorbance of the blank at time zero. The absorbance was measured using a visible ultraviolet spectrophotometer (Jasco V-630 instrument). All experiments were triplicated and results are the average of measurements.

Sample discrimination

II-1.10 Near infrared spectroscopy

NIR spectroscopy was used for analysis of the chemical composition in order to discriminate investigated samples. The main objective was to create database of NIR spectra that might be used for future discrimination of thermal treatments with similar appearance, but of different technological properties. Samples were measured with VECTOR 22-N produced by Bruker Optics GmbH. The spectral range measured was between 4000 and 7500 cm⁻¹. Each spectrum was computed as an average of 20 successive measurements per sample, in order to minimize the measurement error. As a result, a database of 800 spectra (200 of each treatment) was created. The PCA model (appendix I-5.1) was built on the base of raw NIR spectra.

Physical properties

II-2.1 Surface wettability

Surface wettability was evaluated by means of sessile drop technique at the state of equilibrium contact angle θ . It was assumed that measurement of wetting the experimental samples with three diverse liquids was sufficient to accurately determine the linear function. The equipment used is a goniometer OCA20 (DataPhysics) and the components of the liquids used are as follows: Deionized water ($\gamma_L = 72.8 \text{ mJm}^{-2}$, $\gamma_L^d = 21.8 \text{ mJm}^{-2}$, $\gamma_L^p = 51.0 \text{ mJm}^{-2}$). Ethylene glycol ($\gamma_L = 48.0 \text{ mJm}^{-2}$, $\gamma_L^d = 29.0 \text{ mJm}^{-2}$, $\gamma_L^p = 19.0 \text{ mJm}^{-2}$). Diiodomethane ($\gamma_L = 50.8 \text{ mJm}^{-2}$, $\gamma_L^d = 50.8 \text{ mJm}^{-2}$, $\gamma_L^p = 0.0 \text{ mJm}^{-2}$). A CCD camera recorded the contour of the sessile drop for 90 seconds after wetting the surface.

II-2.2 Three-dimensional surface topography

The coated surface roughness map was generated by means of a depth-of-field scanner developed at CNR-IVALSA (Italy). The surfaces of experimental samples were photographed using a high resolution CCD camera (PL-A782, Pixelink), zero distortion multi-configuration macro lens (MC3-03X, Optoengineering) and a diffused white light illuminator. The sequence of images was acquired by the camera while was changing the distance between the measured surface and the focusing lenses, with a resolution of 3000 x 2208 pixels. A stack of 40 images was collected from each sample as the measurement depth range was $\pm 0.5 \text{ mm}$ and images were taken with a step of 25 μm . Helicon Focus (www.heliconsoft.com) software was used for reconstruction of the depth map images and Helicon 3D viewer to visualize the resulting images (Fig 1).

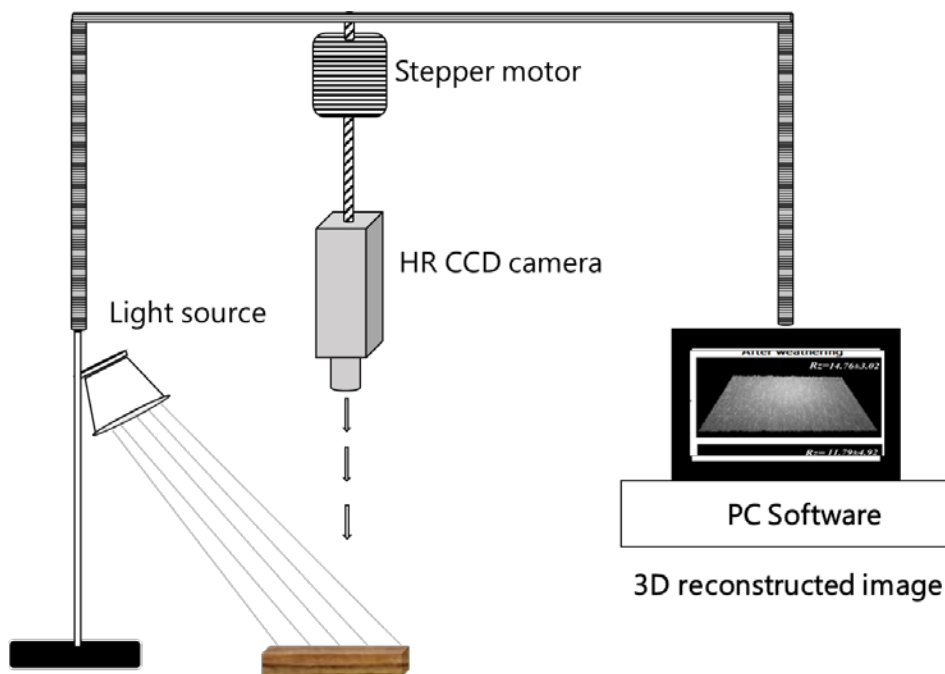


Fig. 1 schematic of 3D reconstructed images.

II-2.3 Surface roughness

Surface roughness was assessed with a stylus profilometer (Surftest SJ-301, Mitutoyo). Each sample was measured ten times in random locations over the surface in perpendicular to the fibers direction, considering these as a representative surface roughness indicator. The length of scan and cut-off wavelength was 12.5 mm and 2.5 mm respectively. Measurement speed of the stylus was 0.5 mm/s. The average distances between the highest peak and lowest valley R_z were calculated in order to quantify the surface roughness.

Optical measurements

II-2.4 Color measurements by colorimeter

The color and color changes were monitored at the end of weathering tests by the CIE-Lab color space coordinate system, measuring in ten different points on the

surfaces using a Konica Minolta CM-2600d device and expressing the results according to the following equation:

$$\Delta E^* = \sqrt{\Delta L^{*2} + \Delta a^{*2} + \Delta b^{*2}}$$

Where ΔE^* is the total color difference between lightness (ΔL^*), red–green axis (Δa^*), and yellow–blue axis (Δb^*) before and after test. The evaluation criteria of overall color changes was as follow: $0.2 < \Delta E^*$ (invisible difference); $0.2 < \Delta E^* < 2$ (small difference); $2 < \Delta E^* < 3$ (color change visible with high-quality filter); $3 < \Delta E^* < 6$ (color change visible with medium-quality filter); $6 < \Delta E^* < 12$ (high color changes); $\Delta E^* > 12$ (different color).

In addition, the hue angle (h^*) and chroma (C^*) were computed on the base of CIE Lab parameters:

$$h^* = \tan^{-1}(b^*/a^*)$$

$$C^* = \sqrt{a^{*2} + b^{*2}}$$

II-2.5 Hyperspectral images

In addition to the CIE Lab color parameters (L^* , a^* , b^*) by colorimeter technique, the color were computed based on the hyperspectral images covering the visible range of the electromagnetic spectra. The hyperspectral imaging scanner was developed at CNR-IVALSA (Italy) and included high resolution monochromatic camera (ORCA-O5G, Hamamatsu) equipped with an imaging spectrograph Inspector V10 (Specim) and semi-telecentric lenses (TEC-55, Computar). Halogen light source was used to uniformly illuminate the assessed surface profile. The spectral range of the instrument was 400 to 1000 nm with a spectral resolution of 9 nm. However, only visible part of the spectra (400 to 700 nm) was extracted in order to determine color coordinates independently for each pixel on the hyperspectral image. The sensor calibration included collection of black

and white references. Ten spectral images corresponding to spatially distributed sections of the surface were collected from each sample assuring optimal focus of the camera. Three independent two-dimensional matrixes corresponding to L^* , a^* and b^* surface color distribution map was scrutinized as a result of the hyperspectral image analysis.

The images were captured and the hyperspectral information was processed by using custom software algorithms (developed at IVALSA/CNR, Italy) to transform the data pixels to a profile map of CIE Lab color space. The spectra were processed with a dedicated software tools developed in LabView 2013 (National Instruments) and included computation of the reflectance spectra, interpolation, computation of color coordinates (CIE L^* , CIE a^* , CIE b^*) as well as statistical representation of results in a form of histograms.

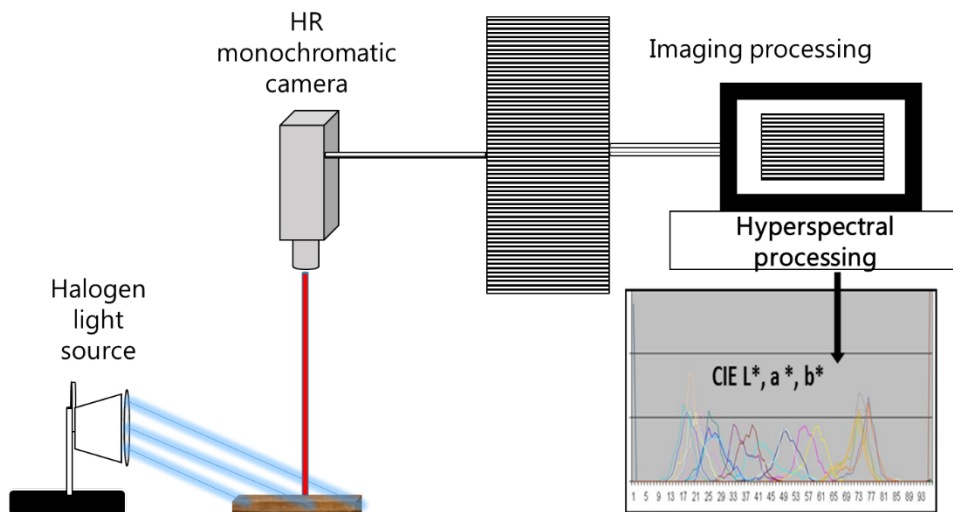


Fig.2 Schematic of hyperspectral data processing to CIE $L^*a^*b^*$.

II-2.6 Gloss measurements

The surface gloss units were evaluated according to ASTM D523 standard with a Multi Gloss 268+ (Konika-Minolta) gloss meter, assuring at least ten measurements on each sample in different locations. Specular reflectance was

assessed with incidence angles of 65° and 85°, assuring the incident ray direction being parallel to the fiber direction.

Environmental profile

II-3.1 Life cycle assessment

The life cycle assessment is well defined in the section 3.3.6.1 and the principal techniques are summarized below:

The LCA study of thermally modified boards was performed based on ISO 14040 (ISO 2006a) and ISO 14044 (ISO 2006b) standards.

The impact analysis were performed using the LCA software SimaPro 8.1.0.60 (Pré 2015) and associated databases and methods.

The method chosen for environmental impact assessment was ReCiPe Midpoint and Endpoint (H), version V1.12 / Europe ReCIPE H/A and for energy use was the Cumulative Energy Demand V1.09 (Pré 2015).

LIST OF FIGURES

Figure I-1 Global forest density and production of industrial roundwood.

Figure I-2 Wood processing steps and possible paths of use of industrial byproducts, residues and used wood.

Figure I-3 Processing sequence of engineering wood products.

Figure I-4 Tree trunk cross-section anatomy with the characteristic parts.

Figure I-5 Three-dimensional representation of the wood microscopic structure (*Pinus sylvestris*, left; *Quercus robur*, right). Images of the Transverse Section (TrS), Radial Section (RS) and Tangential Section (TgS).

Figure I-6 Schematic diagram of cell wall structural models and its subdivisions.

Figure I-7 Components and interactions of the wood polymer in its secondary cell wall.

Figure I-8 Representation of bonding between monolignols of wood.

Figure I-9 Water in wood at different drying points and the relation between shrinkage and MC.

Figure I-10 Wood-water interactions. Left: EMC as function of RH-Temp. Center: MC-RH relations under adsorption and various desorption conditions. Right: Sorption isotherms for wood cell wall components.

Figure I-11 Representation of accepted models of wood adhesion.

Figure I-12 Representative samples of deteriorating agents.

Figure I-13 Wood color changes by UV degradation (Kulch, Austria).

Figure I-14 Possible Mechanism of free radical formation from lignin degradation.

Figure I-15 Principal axes of wood with respect to fiber direction and growth rings.

Figure I-16 Strength plotted against Young's modulus for selected plant materials. Adapted from L.J. Gibson.

Figure I-27 Acetylated wood used in civil engineering project, Cincinnati (USA), 2016.

Figure I-28 Stages of Belmadur process (BASF pilot plant, Gottingen, Germany).

Figure I-29 The Biological House, Middelfart (Denmark), using Kebony for the exterior cladding.

Figure I-30 Thermally modified façades, Leioa and San Sebastian, Spain.

Figure I-31 Examples of tall wood buildings: (A) Kizhi Pogost-37.5m, Russia, 1862; (B) WIDC-30m, Vancouver, Canada, 2014; (C) Oakwood tower-300m, London, conceptual stage

Figure II-1 Schematic of the different sections of study and the experimental procedures performed in each of them.

Figure II-2 Scheme of the chemical analysis performed on wood.

Figure II-3 Scheme of depolymerization and degradation of polysaccharides during wood modification.

Figure II-4 Py-GC/MS chromatograms of modified and control specimens. Peak labels are listed in Table II-4.

Figure II-5 FT-IR chromatograms of modified and control specimens. Peak labels are listed in Table II-5.

Figure II-6 Thermo-gravimetric curves and their derivatives (DTG) of Pine, Oak and Ash and modified samples

Figure II-7 Correlation between acidity and pH of wood samples.

Figure II-8 Scheme of the physical and mechanical properties performed on wood.

Figure II-9 Dimensional stability in dry wood and thermally modified wood.

Figure II-10 Correlations between weight loss and MOR, MOE after heat-treatment.

Figure II-11 Thermal degradation performance of wood in inert and oxidative conditions.

Figure II-12 Scheme of the experimental procedure and measurements of the section.

Fig. II-13 Performance over time of wood samples after fungal inoculation.

Figure II-14 Evolution of soluble carbohydrates in wood with rotting-fungi.

Figure II-15 FT-IR spectra of wood before 8 and 24 weeks of fungal attack.

Figure II-16 Schematic of weathering tests on wood and properties analyzed.

Figure II-17 Variations on density and moisture content after natural or artificial weathering test.

Figure II-18 Reduction of mechanical properties after weathering tests.

Figure II-19. Correlation between MOR-density and wood groups association.

- Figure II-20.** Thermo-gravimetric curves of unweather and weathered wood.
- Figure II-21** Percentage of variations in parameters L^*, a^*, b^* after artificial (Aw) or natural weathering (Nw).
- Figure II-22** Schematic of tests on coated surfaces of thermally modified wood.
- Figure I-23** NIR band assignments for wood and its components
- Figure I-24** Cluster analysis (A) and PCA scores discrimination (B) of samples.
- Figure II-25** Appearance of wood surfaces after pull-off test.
- Figure II-26** 3D surface topography maps and roughness (R_z) values of wood coated with *100%UV-curable* coating before and after aging test.
- Figure II-27** 3D surface topography maps and roughness (R_z) values of wood coated with *waterborne* coating before and after aging test.
- Figure II-28** Scanned images of wood with coating product.
- Figure II-29** Histograms of CIE $L^*a^*b^*$ color parameters after (a) and before (b) artificial weathering test obtained by hyperspectral image. T-Ash: (190,200,210). Control: C0.
- Figure II-30** Schematic of methodology used and experimental process for the analysis of residues generated.
- Figure II-31** System boundary for the product system.
- Figure II-32** Prototype of industrial thermal treatment kiln and location of solid (A) and liquid (B) residues.
- Figure II-33** TGA/DTG profiles of wood solid (A) and liquid (B) residual extracts of heat treatment of *Pinus radiata*
- Figure II-34** FTIR spectra of wood residual extracts of heat treatment of *Pinus radiata*. Peak numbers were classified according to Table II-29.
- Figure II-35** Chromatograms obtained by Py-GC-MS (SRE) and GC-MS (fLE). Peak labels are listed in Table II-31.

LIST OF TABLES

Table I-1 Global production and trade of forest products in 2015.

Table I-2 Common monosaccharides and disaccharides present in wood cell wall.

Table I-3 Common polysaccharides present in the chemical structure of wood.

Table I-4 Composition of monolignols in different wood types.

Table I-5 Names and structures of the most common fatty acids present in wood.

Table I-6 Most relevant analytic techniques used in wood surfaces.

Table I-7 Biotic factor causing deterioration of wood.

Table I-8 Bond dissociation energies and radiation wavelength.

Table I-9 Production of thermally modified wood in Europe (Adapted).

Table II-1 Treatment temperatures, classes and wood species.

Table II-2 Changes in chemical composition after heat treatment of wood.

Table II-3 Carbohydrates content and changes after heat treatment of wood.

Table II-4 Peak assignment for the pyrograms obtained. Relative intensity of the products (%) and retention time (RT) are showed.

Table II-5 FT-IR bands present in wood and its assignment.

Table II-6 Acidity and pH values in modified and control samples.

Table II-7 Changes in physical properties of wood after modification.

Table II-8 Liquid-solid interactions and values of work of cohesion.

Table II-9 Changes in mechanical properties of thermally modified samples.

Table II-10 Ranges of thermal degradation of wood and their temperatures.

Table II-11 Results of biological durability test of thermally modified wood.

Table II-12 Changes in chemical composition of wood after durability test.

Table II-13 Soluble carbohydrates released after acid hydrolysis (w/w).

Table II-14 Soluble compounds released after enzymatic hydrolysis (w/w).

Table II-15 Changes of physical properties after weathering tests.

Table II-16 Changes in mechanical properties after weathering tests.

Table II-17 Thermal degradation parameters extracted from the TG analysis.

Table II-18 Changes in optical parameters after weathering tests.

Table II-19 Technical details of finishing process on wood.

Table II-20 Chemical composition and features of wood coatings systems.

Table II-21 Coating adhesion on wood by pull-off test.

Table II-22 Values of contact angle, surface energy and work of adhesion and cohesion of coated surfaces.

Table II-23 Measurements of wood surface-coating resistance.

Table II-24 Changes in optical parameters after weathering test.

Table II-25 Liquid-solid interactions before and after weathering test.

Table II-26 Surface free energy, work of adhesion and work of cohesion at the boundary phase of wood-solid coating.

Table II-27 Datasets for production of 1 m³ of Spanish thermally treated radiata pine boards.

Table II-28 Datasets for the background system.

Table II-29 Impact assessment results associated with the production of 1 m³ of thermally modified pine boards.

Table II-30 Mass allocation results of thermally treated boards.

Table II-31 Peaks and assignments of FTIR spectra from residues generated during heat treatment of pine.

Table II-32 Relative amounts of monosaccharides and degradation products in *Pinus radiata* (untreated and heat-treated) and in the residues generated during treatment.

Table II-33 Chemical composition of the residues generated.

Table II-34 Phenolic content and antioxidant activity of the residues generated during the heat-treatment.

The industrial application of new wood technologies open the door to the development of a forest bioeconomy, especially in regions with this important renewable biological resource. This doctoral dissertation describes the specific changes that occurs in solid wood at chemical and physical level by heat treatments, in order to recognize the characteristics of the treated products, as well as to investigate the evolution of the material over time, to obtain a comprehensive study of the material and its commercialization. Finally, the assessing the environmental aspects and potential impacts associated with their industrial production may help to identify processes or stages in the wood chain with a high environmental impact.



**This work was carried out thanks to the financial support of
the Basque Government, Department of Economic
Development and Competitiveness**

